Gold Complexes and Cages with Aroylthioureas

Inaugural-Dissertation
to obtain the academic degree
Doctor rerum naturalium (Dr. rer. nat.)

submitted to the Department of Biology, Chemistry and Pharmacy
of Freie Universität Berlin

by

SUELEN FERREIRA SUCENA

From Caldas (Brazil)

2018

1. Supervisor: Prof. Dr. Ulrich Abram

2. Supervisor: Prof. Dr. Christian Müller

Date of defense: 16.05.2018

Acknowledgment

I would like to thank my supervisor Prof. Dr. Ulrich Abram for giving me the opportunity to work in his research group. His important contribution to this study along to this $4^{1/2}$ years, providing all support, giving advices, suggestions and great ideas. Beyond the work, his support and special care on my personal issues.

I gratefully thank Prof. Dr. Christian Müller for being the second reviewer of this thesis.

I would like to express my gratitude to Dr. Adelheid Hagenbach for her technical support and meticulous care in X-ray data collections and structures validation. Besides that, I appreciate your kind attention during my stay in Germany. I will never forget her words and the way I felt comfortable to speak about my pregnancy for the first time.

I appreciate all the members of the Prof. Abram group both past and present. Jacqueline and Detlef for support with the organization stuffs, the internship and master students Richard, Max and Ilgin. Thank you all to be my hands when I was unable to work. I thank Dr. Juliane März from the Helmholtz-Zentrum Dresden-Rossendorf for her collaboration in the fluorescence measurements.

Very special thanks go to Clemens for his dedication in the corrections of my thesis and being available to help me anytime. Beyond the work, I thank for his friendship and for being my co-worker. I also thank Christelle for her patience and many talks. It was a pleasure sharing the working place with you both.

I thank the Brazilian students, Thomaz, for the great conversations. Cassia, what a pleasure to meet you, a friendship that did not only stay in Berlin, and Bruno thank you for being my flatmate. Thank you all for a great time we spent together.

I also want to thank Arantxa for our intense and instant friendship. Thank you for allowing us to meet your family and share moments that will never be forgotten.

Abdullah, thank you for teaching me to be a better person. It is special your way of seeing life and your kind way of dealing to everyone around you.

My gratitude goes to my husband André, who made himself available to take care of our daughter Elis so that I could finish the thesis. I admire you for being this lovely father and husband and how important you are in our lives. My thanks are extended to my family and friends, my mother Mariza, my sister Patricia, my mother-in-law Thais, who came and

overcame the fear of traveling alone to help us take care of Elis. I thank my friend Bruna, who even so far, her love and friendship made the distance to became small.

Finally, I really appreciate the financial support from Coordenação de Aperfeiçoamento de Pessoal de Nível Superior (CAPES) and the Dahlem Research School (DRS).

I dedicate this thesis to my little princess Elis. Becoming her mom is the sweetest part of my life. Also the memory of my lovely aunt Marilda.

Table of Contents

Abbreviations

AuSR	Gold thiolate
Bu_4N^+	Tetrabutylammonium
Calcd.	Calculated
C.N.	Coordination number
$Damp^-$	2-(*N,N*-[(dimethylamino)methyl]phenyl)
DFT	Density Functional Theory
DMSO	Dimethyl sulfoxide
EtOH	Ethanol
Et_2O	Diethylether
Et_3N	Triethylamine
EPR	Electron Paramagnetic Resonance
ESI^+	Positive Electrospray Ionization
HOMO	Highest Occupied Molecular Orbital
Im	Imidazole
IR	Infrared
LMCT	Ligand to Metal Charge Transfer
Ln	Lanthanide
LUMO	Lowest Unoccupied Molecular Orbital
MeOH	Methanol
Me	Methyl
MOFs	Metal-Organic Frameworks
MS	Mass Spectrometry
NHC	*N*-heterocyclic carbene
NMR	Nuclear Magnetic Resonance
OAc^-	Acetate
Hpdc	Pyridine-2,6-dicarboxylic acid
PPh_3	Triphenylphosphine
r.t.	Room temperature
Terpy	Terpyridyl

	THF	Tetrahydrofuran
	THT	Tetrahydrothiophene
	TRLFS	Time-Resolved Laser Fluorescence
	tu	Thiourea
	UV-Vis	Ultraviolet visible
IR	ν	Stretching vibration
	δ	Bending vibration
	s	Strong
	w	Weak
	m	Medium
NMR	br	Broad
	s	Singlet
	d	Doublet
	t	Triplet
	m	Multiplet
	J	Coupling constant
	ppm	Parts per million
	δ	Chemical shift
ESI^+	M^+	Molecular ion
	m/z	Mass/charge ratio
UV-vis	ε	Molar Absorptivity

Abstract

This thesis comprises the synthesis, spectroscopic and structural characterization of novel gold(I) and gold(III) complexes with benzoylthioureas (e.g. HL1) and its benzamidine derivatives (e.g. H_2L2 or H_2L3). In addition to these compounds, heterometallic cage-like gold(I) complexes with the bipodal 2,6-dipicolinoylbis(*N,N*-diethylthiourea) (H_2L4) in the main scaffold have been obtained by self-assembly with alkaline earth, lanthanide or transition metal ions. H_2L4 shows a flexible coordination behaviour with gold atoms being coordinated by the sulfur donor atoms, This results in the tridentate donor sets {*O,N,O*}, {*N,N,O*} or {*N,N,N*}, which are provided for the coordination of the host metal ions. A selective exchange of the metal ions in such assemblies is possible.

1. Introduction

Gold is one of the most noble metals, which does not oxidize on exposure to the air or even to most other reagents. Gold is a good conductor of electricity and heat. It has the lowest electrochemical potential compared to any metal [1]. Gold shows exceptional properties, such as the ability to form M···M contacts, also called as aurophilic interactions [2, 3].

The chemistry of gold has been developed much later than those of the other coinage metals. Up to the 20th century, the potential of gold chemistry was widely unexplored due to its chemical inertness [4]. Nowadays, the gold chemistry has become one of the most popular areas of research and technology [5]. An almost complete review covering various aspects of gold chemistry is summarized in a themed issue of "Chemical Society Reviews". Excellent reviews describe the role of gold in quantum chemistry [6], homogeneous and heterogeneous catalysis [7, 8, 9], metal clusters [10], surface science [11], nanotechnology [12, 13], medical sciences [14, 15, 16], and supramolecular chemistry [17].

In general, gold forms compounds in a broad range of oxidation states and coordination numbers [18]. For a long time, chemists had known only three oxidation states of gold (Au^0, Au^{1+}, Au^{3+}). Nowadays, in the modern gold chemistry the range has been extended from Au^{1-} to Au^{5+} compounds, often with unusual stereochemistry [1].

Nevertheless, the coordination chemistry of gold is dominated by linear gold(I) and square-planar gold(III) compounds [18]. The chemistry of gold(I) is by far the most developed. Gold(I) has a d^{10} closed-shell configuration, which (due to relativistic effects) strongly stabilizes the 6s level, more than 6p and destabilizes the 5d levels. The large 6s → 6p energy separation favours the formation of complexes with linear geometry [14, 19]. Beyond that, there are two more coordination geometries: trigonal, and tetragonal. However, Puddephatt pointed out in the first comprehensive book on "*The Chemistry of Gold*" published at 1978 [20], that some gold structures can not be explained by standard valence rules. The nature of gold-gold interactions, which is an unpredicted phenomenon in the chemistry of gold(I), was proposed by Schmidbaur as "*aurophilic effect*" [2, 3].

The chemistry of gold(III) is comparatively less developed. The electron configuration of Au^{3+} is $[Xe]4f^{14}5d^8$ and all known gold(III) complexes are diamagnetic with low-spin configuration. Most of the complexes have square-planar geometry, although, evidence of compounds with coordination number 5 and 6 is also given. They have trigonal pyramidal or octahedral structures [18, 19, 21].

Organogold derivatives have been known for more than 100 years [22]. They belong to an important class of compounds in gold chemistry [1] and have at least one Au—C σ or π bond. Such bonds are predominantly covalent, and their stability depends on the type of ligands chosen [23].

Due to the remarkable oxidizing character of the gold(III) compounds and the pronounced tendency to get reduced to gold(I) species, different families of organometallic gold(III) complexes have been synthesized, since the presence of Au—C bonds frequently stabilizes the gold(III) oxidation state [24]. A convenient method for the formation of metal-carbon bond is cyclometallation [25].

A remarkable progress has been made during the recent decades in the organometallic chemistry of gold(I). The stability of organogold(I) compounds increases in the following order of ligands: carbonyl ≤ π-bonded ligands ≪ alkyl < aryl < ylide < methanide < carbenes ≤ alkynyl [1]. The latter two families of gold(I) compounds have been shown to be important in the biological medicinal sciences and supramolecular chemistry, respectively. Carbenes are neutral ligands displaying formally a divalent carbon atom with six electrons in its valence shell. Gold-carbenes have been known since the early 1970`s [1]. A considerable number of reports is related to cytotoxic gold(I/III) complexes with *N*-heterocyclic carbenes [26, 27]. In addition, the preference of gold(I) for a linear coordination, together with the linearity of C≡C bond have made the alkynyl gold(I) complexes attractive building blocks for the formation of polynuclear complexes. Such ligands led to the discovery of the organometallic catenanes by self-assembly [17, 23].

The pioneering work by Lehn [28] and Sauvage [29] in the field of supramolecular self-assembly of helicates, grids, racks, knots, catenanes, rotaxanes and metal-organic frameworks (MOFs) was followed by several researchers such as Stang [30], Raymond [31], Fujita [32], Cotton [33], and Yaghi [34], who have developed novel systems in self-assembly with well-defined shapes and sizes, which are able to accommodate guest molecules. Molecular networks with gold building blocks are frequently stabilized by weak $Au^{I}\cdots Au^{I}$ interactions [35 - 37]. Linear gold(I) units are particularly suitable for the formation of polymers, with gold···gold secondary bonding or gold-heterometal interactions [2, 38 - 40]. In most of the gold(I) compounds, the metal prefers to bind with soft donor atoms [41]. A strategy for the synthesis of such systems is the use of simple building blocks, which form larger aggregates, such as polymers, rings, oligomers, catenanes, helicates or macrocycles by self-assembly [42, 43]. A few examples are shown in Figure 1. A complete review about macromolecules involving gold in their structures is found in references 17 and 35.

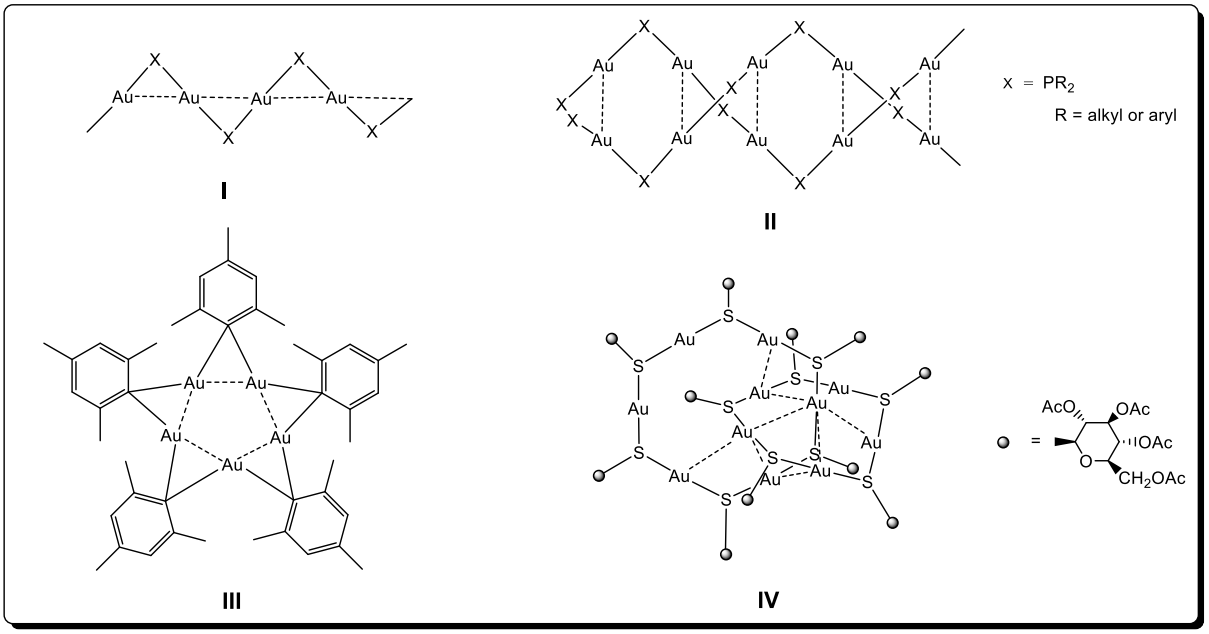

Figure 1: Structures of gold-containing polymeric chains **(I)**, helicates with (X = PR_2; R = alkyl or aryl) **(II)**, macrocyclic star-shaped molecules **(III)**, and [2]catenane with interlocked rings of $[Au_6(SR)_6]$ and $[Au_5(SR)_5]$ subunits (spheres represent R = 2,3,4,6-tetra-O-acetyl-glucopyranose rings). All the structures are supported by Au···Au contacts represented by dashed lines. The structures were taken from references 17 and 35.

1.1. Aspects of Gold Chemistry with Sulfur and Nitrogen Containing Ligands

Gold compounds have attracted increasing attention within the bioinorganic and medicinal chemistry for their antiproliferative and antitumor properties [44]. Gold(I) compounds are commonly stabilized by "soft" ligands [45]. A large number of examples with several types of ligands have been reported. This includes ligands containing phosphines, thiolates, organometallic gold complexes or species with chalcogenolato ligands [46]. Gold(III) complexes are stabilized by carbon, nitrogen, phosphorus, sulfur and even oxygen donors [1]. They were among the first, which have been studied for anti-tumour activity due to the resemblance to *Cisplatin*. However, gold(III) ions are oxidizing and in biological environments, they are frequently reduced to gold(I) or elemental gold [47]. Nevertheless, an appropriate selection of donor sets, and donor atom arrangements protect gold(III) compounds against reduction. Particularly, chelating ligands are well suitable for the stabilization of Au(III).

Thiourea gives a very stable, water soluble gold(I) complex $[Au\{S=C(NH_2)_2\}_2]^+$, which is useful for the extraction of gold from ores [48]. Important gold(I) compounds for medicinal purposes are thiolate and phosphine complexes. Sodium aurothiomalate (Myocrisin™, **V**), aurothioglucose (Solganol™, **VI**), and auranofin (Ridaura™, **VII**) (Fig. 2) are some

representatives of gold(I) thiolates, which have applications in the treatment of rheumatoid arthritis [15].

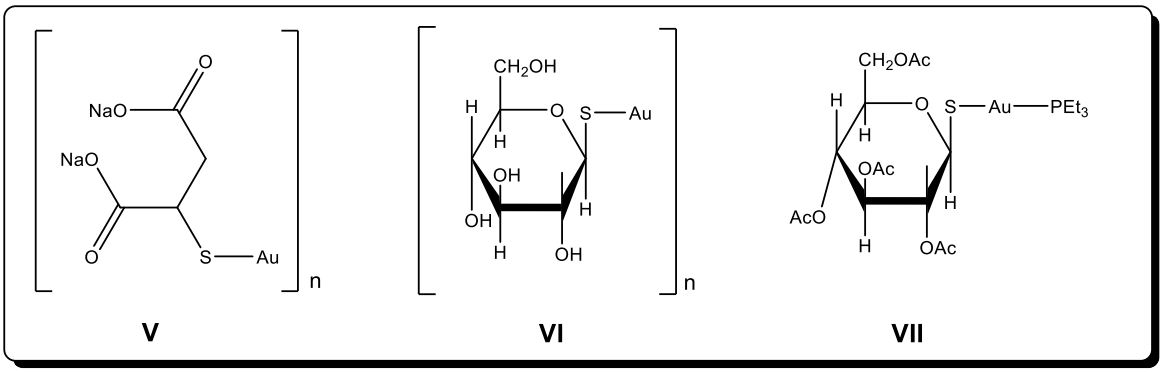

Figure 2: Structures of gold(I) thiolates used in the treatment of rheumatoid arthritis: *Myocrisin* **(V)**, *Solganol* **(VI)** and *Auranofin* **(VII)**.

Derivatives related to the structure of auranofin proved also to be promising with regard to their antitumor activity [45, 49]. Fregona investigated the cytotoxicity scores of gold(I) dithiocarbamates **(VIII)** and the results are encouraging [50].

Gold(III) is isoelectronic to Pt(II) and the complexes of both ions adopt a square-planar geometry. These similarities open the opportunity that gold(III) complexes might have anticancer activity similar to *Cisplatin* [51, 52]. A number of gold dithiocarbamates (Fig. 3) was studied and some representatives show significant inhibition of the growth of cancer cell [53].

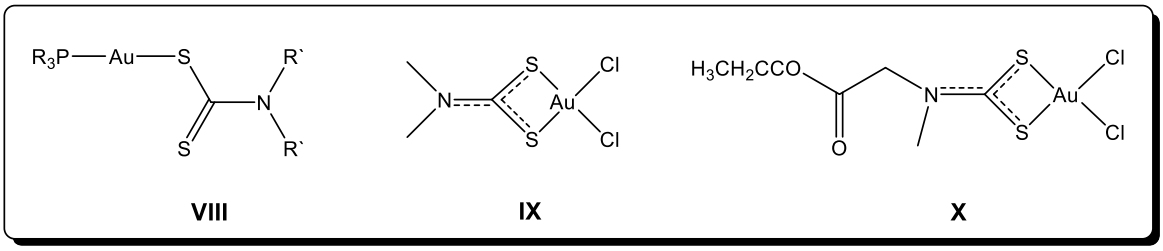

Figure 3: Examples of gold(I) and gold(III) compounds with dithiocarbamate ligands having antitumor activity.

A large number of neutral and charged gold(I) complexes with heterocyclic *N*-donor ligands have been reported [54 - 56]. Also, Au(III) compounds with nitrogen donors are common [57]. Most of them are derived from diimine donors like bipyridine or phenanthroline. Compounds containing polypyridyl-type molecules show activity against lung carcinoma [58]. Gold(III) porphyrins show *in vitro* and *in vivo* anticancer activity against a range of human cancer cell

lines. The use of porphyrinato ligands might protect Au(III) ions against reduction in biological medium [59].

In the last few years, antitumor activity has also been reported for linear Au(I) complexes with *N*-heterocyclic carbenes (NHC) [60]. Cationic Au(I) NHC complexes $[(R_2Im)_2Au]^+$ **(XI)** show a selective toxicity against breast cancer cell lines, but do not interfer to normal breast cells [61]. Recently, Che *et al*. have reported that cyclometallated Au(III) NHC complexes of the type $[Au(C^N^C)(NHC)]^+$ **(XII)** suppress tumour growth in a nude mice model [62]. The discovery of anti-tumour properties of the complex $[Au(damp\text{-}\kappa C^1,N)Cl_2]$ ($damp^-$ = 2-(*N,N*-[(dimethylamino)methyl]phenyl) **(XIII)** by Parish caused a renaissance of interest in gold(III) complexes as anticancer agents [63]. Figure 4 summarizes some gold complexes with antitumor activity.

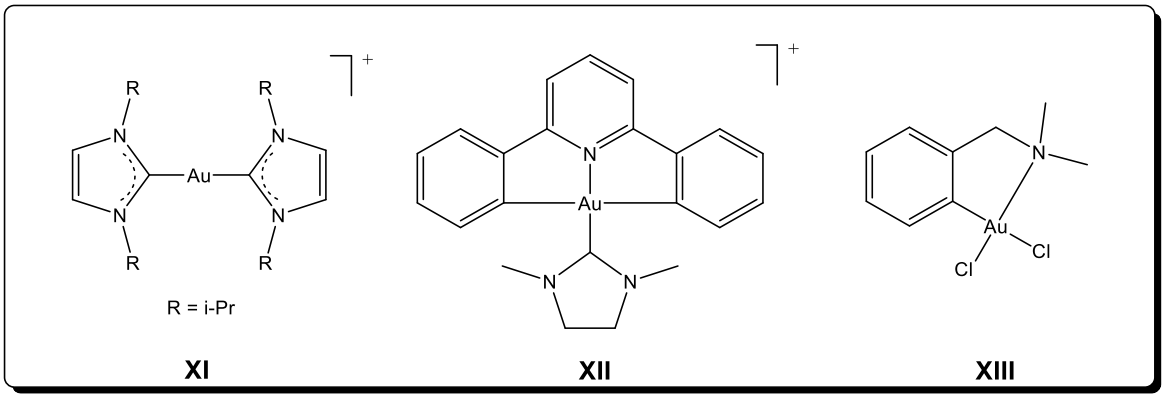

Figure 4: Examples of gold(I) and gold(III) complexes with antitumor activity.

1.2. Self-assembly of Metallamacrocyclic Arrays

The metal-directed self-assembly of supramolecular arrangements has become a field of intense research, starting over the last 50 years with Lehn, who described it as the "chemistry beyond the molecule". Highly complex, functional chemical systems, are held together by intermolecular forces [64]. Based on such interactions supramolecular chemistry can be classified into three main branches: i) compounds with predominating hydrogen bonds, ii) compounds with non-covalent interactions, such as ion-ion, ion-dipole, π-π stacking or van der Waals forces, and iii) complexes with strong and directional metal-ligands bonds [65, 66].

The spontaneous organization of a variable number of molecules into a discrete and well-defined supramolecular aggregate is designated self-assembly [67, 68]. Inorganic self-assembly refers to the formation of well-defined metallo-supramolecular structures from organic ligands and metal ions [69]. A great variety of self-assembled metallamacrocycles was introduced by

Lehn [70, 71], as well as by Fujita, Raymond and Stang who have developed self-assemblies of threaded rings (rotaxanes) [72], interlocking ring systems (catenane) [73], and molecular polyhedra with triangular and square shapes [74] (Fig. 5). The inclusion of metal centers into such macromolecules gives access to chemical and physical properties, which are not present in entirely organic compounds [75].

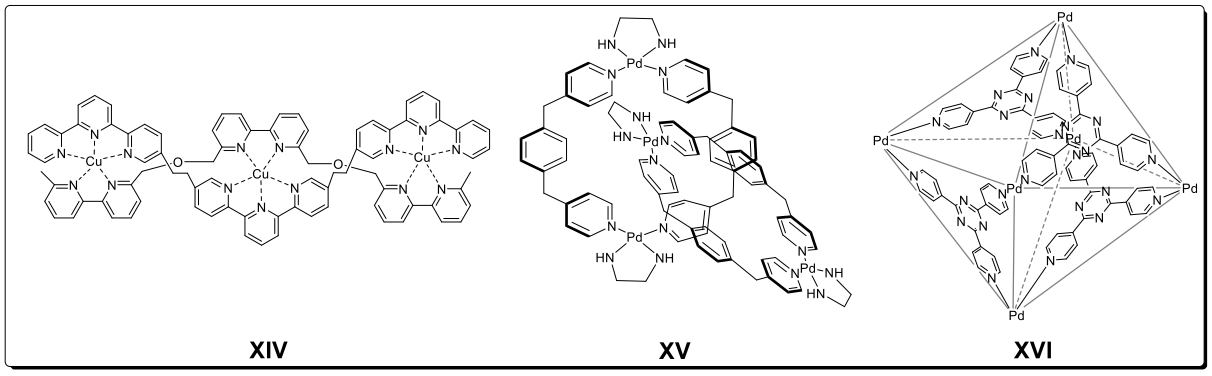

Figure 5: Examples of molecular structures of double-heterostranded helicates **(XIV)**, interlocked rings (catenane) **(XV)**, and polyhedral cage **(XVI)** obtained from self-assembly. Images taken from ref. 70, 76.

Moreover, the metal ions may play an important role in the self-assembly process itself. They provide i) a defined coordination environment and, thus, determine the stereochemistry, ii) a range of binding strengths, from weak to very strong and iii) a variety of chemical properties, which can be used to increase the dimensionality of self-assembled structures [69, 77]. The control of the formation of complex arrangements using transition metal ions has evolved into one of the mostly used strategies for the pre-organization of molecular building blocks into supramolecular assemblies as seen in the example of Figure 6 [78]. Such structures are spontaneously generated by simply mixing ligand(s) and metal ion(s) in one-pot reactions, affording efficient templates in high yield [79, 80].

Self-assembly templated by metal ions has been used as a strategy to build up compounds containing closed and large cavities [81, 82]. The synthesis of polynuclear complexes with defined three-dimensional building blocks results in cage-like structures [83]. These complexes play an important role in supramolecular chemistry and may exhibit interesting host-guest properties.

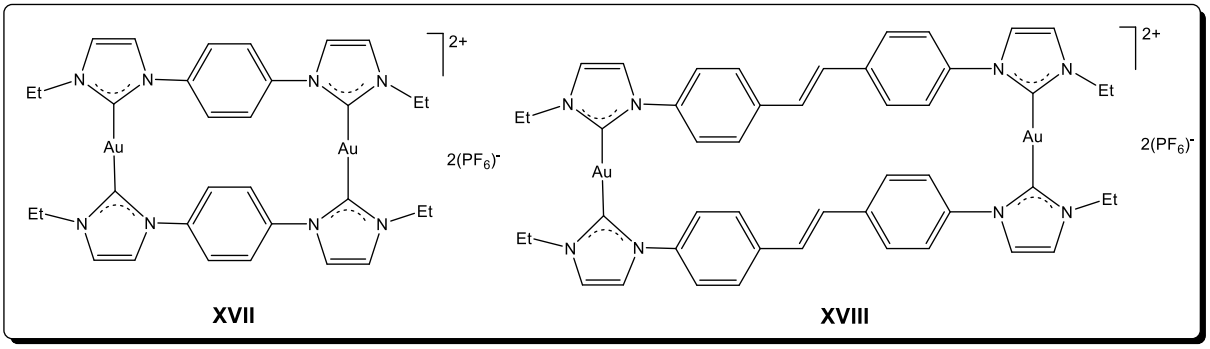

Figure 6: Examples of rectangular forms of gold complexes obtained by self-assembly. Examples are taken from ref. 80.

Host-guest chemistry is one of the focus of supramolecular chemistry [84]. There are selective interactions between host and guest molecules, *i.e.* the host recognizes the guest molecule, which contains binding sites and/or steric features that complement those of the host [85]. The host usually contains a large cavity and the guests have both a complementary shape and interactions with the host [86, 87]. Examples of these class include crown ethers [88], cryptands [89], cyclodextrins [90] and others.

1.3. Aspects of *N,N*-Diethyl-*N´*-benzoylthioureas and Derivatives

N-Dialkyl/aryl-*N´*-acylthiourea derivatives of the type R-C(O)NHC(S)NR´$_2$ have received a considerable attention over the decades because of their coordination properties, applications in catalysis and pharmacological activities [91, 92]. Acylthiourea ligands have hard (O), borderline (N), and soft (S) donor atoms and exhibit several coordination modes as is shown in Scheme 1, i) as monoanionic *S,O* bidentate [93], ii) as neutral only *S* bonded [94].

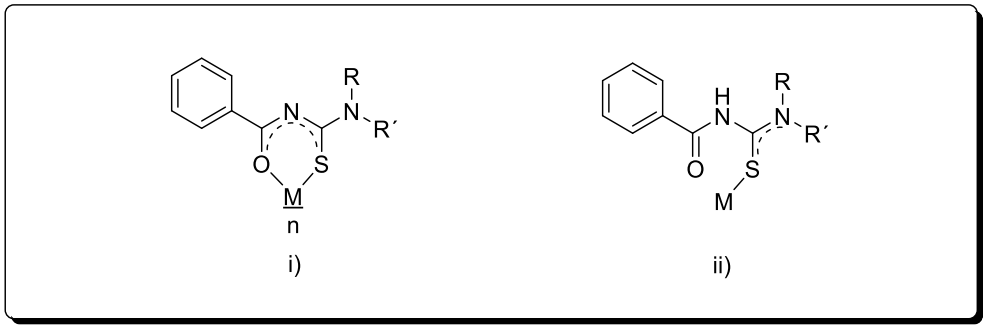

Scheme 1: Coordination modes of benzoylthioureas.

In most of the structurally characterized complexes they act as monoanionic *S,O* chelators. There are many compounds of this type of coordination with metal ions such as Re^{+}, Re^{3+}, Re^{5+}, Ru^{3+}, Ru^{2+}; Ni^{2+}, Cu^{2+}, Co^{2+} Zn^{2+}, Pd^{2+}, Pt^{2+}, Tc^{3+}, Tc^{5+}, Re^{5+}, Fe^{3+}, Co^{3+}, Rh^{3+} or Tc^{3+} [95 - 101]. *S*-Bonded complexes are formed with Hg^{2+}, Cu^{+}, Re^{+} or Au^{+} ions [100, 102, 103].

In recent years, there has been an increased interest in the development of thiourea-based ligands. With the synthesis of *N*-[(dialkylamino)(thiocarbonyl)]benzimidoyl chloride, a novel building block was developed, which enables a ready synthesis of related benzamidines [104]. Such ligands coordinate to a huge number of metals ions [105, 106]. *N,N*-[(Dialkylamino)(thiocarbonyl)]-substituted benzamidines, can be prepared from reactions of *N,N*-[(dialkylamino)(thiocarbonyl)]benzimidoyl chlorides with ammonia or functionalized amines [107]. This synthetic route gives access to bi- or multidentate organic ligands with different donor atoms with a wide variety of steric and electronic environments [106, 108, 109]. The coordination of the *N,N*-[dialkylamino)(thiocarbonyl)]benzamidines can be done in different ways: monoanionic and bidentate with *S,N* chelate formation with Ni^{2+}, Cu^{2+}, Pd^{2+}, Co^{3+} [110], Tc^{5+} [111] or Re^{+} ions [95], or monodentate as neutral *S*-bonded ligands to Ag^{+} [112] or Au^{+} [113]. Occasionally, the formation of heterocyclic rings is observed as in the reaction with $[AuCl_4]^{-}$, which lead to the thiadiazolium dichloroaurate(I) [114], as is shown in Figure 7. Substituted benzamidine ligands display many coordination modes and form stable chelate complexes. Tridentate benzamidines having *S,N,N* [109 - 117], *S,N,O* [108, 109, 118, 119], *S,N,S* [120 - 122] and *P,N,S* donor atoms [123], and a few examples of tetradentate benzamidines with *S,N,N,S* donor sets are reported [124, 125].

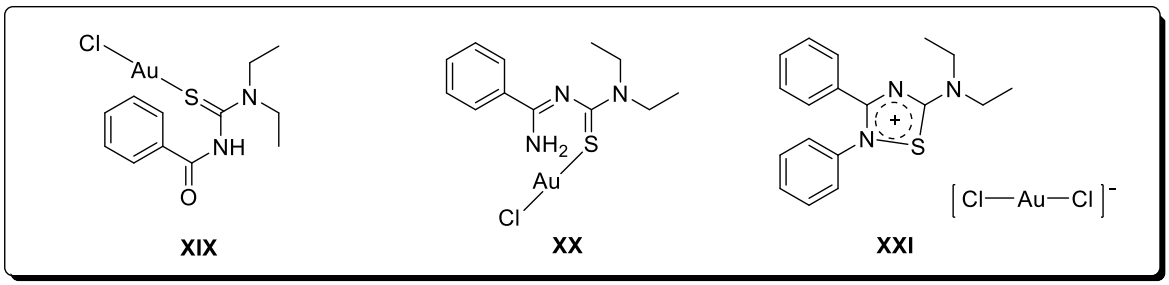

Figure 7: Neutral *S*-bonded complexes of gold(I) with *N,N*-diethyl-*N*`-benzoylthiourea **(XIX)**, a *N*-thiocarbamoylbenzamidine **(XX)** and a thiadiazolium cation **(XXI)**, which was formed during the reaction of $[AuCl_4]^{-}$ with a thiocarbamoyl benzamidine. Examples are taken from ref. 103, 113 and 114.

1.4. Aspects of the Chemistry of 2,6-Dipicolinoylbis(*N,N*-dialkythioureas)

The coordination chemistry of bipodal aroylthiourea derivatives clearly extends the complex formation properties of the simple bidentate derivatives. Some recent results suggest that the bipodal ligands are well suitable for the synthesis of metallamacrocycle complexes by self-assembly. A significant number of complexes has been reported with tetraalkylisophtaloylbis-(thioureas) in binuclear bis-chelates with Ni^{2+}, Cu^{2+}, Co^{2+}, Zn^{2+}, Cd^{2+}, Pd^{2+}, Pt^{2+} and Pt^{4+} ions [126 - 130] and in tris-chelates of In^{3+} and Fe^{3+} [131, 132].

The simple introduction of a heterocyclic spacer such as a pyridine or a pyrrole ring may result in a ligand system, which can coordinate additional metal ions. Recent attempts with a pyrrole-centered ligand failed, since the pyrrole ring did not deprotonate, and the central NH functionalities only established hydrogen bonds to guest solvent molecules [133]. A recent report about the pyridine-type ligand however, confirms the versatility of such ligands. They can act as building blocks for oligo- and polynuclear architectures. The ligand system gives access to a novel class of heterometallic host-guest complexes [134]. It possesses a structural flexibility originated from the facile rotation of the thiourea groups attached to the carboxamide group. This allows the possibility of several conformational isomers. The pincers formed by {*O,N,O*}; {*N,N,N*}; and {*O,N,N*} chelates (Scheme 2) provide another coordination versatility of the ligand and, thus, offer the possibility to predetermine the shape and the size of the desired complexes.

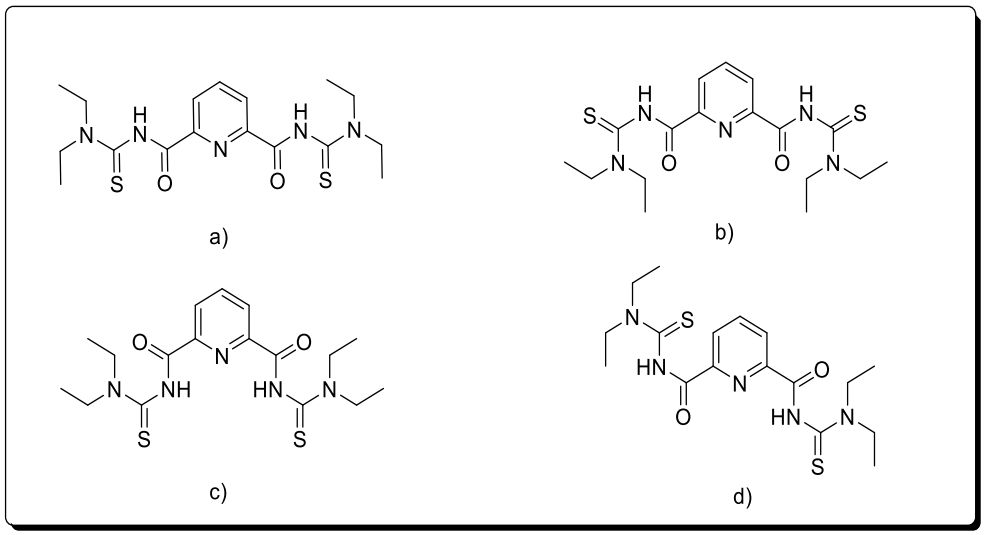

Scheme 2: Possible conformations of dipicolinoylbis(*N,N*-diethylthiourea).

1.5. Goal of the Present Thesis

This thesis addresses the rational design of gold complexes with benzoylthioureas (HL1, H_2L4) and their derivatives (H_2L2, H_2L3). The research also covers the synthesis of mixed-metal complexes and host-guest chemistry with the symmetrical bipodal 2,6-dipicolinoylbis-(*N,N*-diethylthiourea). A summary of the ligands used is given in Scheme 3. [Au(THT)Cl] (THT = tetrahydrothiophene), [Au(PPh_3)Cl] and [Au(damp-κC^1,*N*)Cl_2] have been used as gold starting materials.

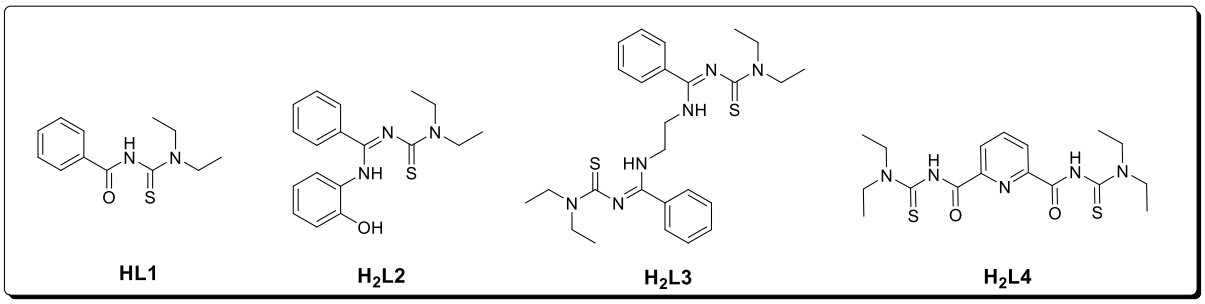

Scheme 3: Ligands used in this thesis.

2. Results and Discussion

2.1. Organometallic Gold(III) Complexes with *N,N*-Diethyl-*N´*-benzoylthiourea (HL1) and its *O,N,S*-Donating Derivative (H_2L2)

Despite the fact that *N,N*-diethyl-*N´*-benzoylthiourea **(HL1)** has been reported as a powerful *S,O*-chelating ligand with many metals of the periodic table, gold complexes remain almost unexplored. HL1 has been synthesized from the reaction of benzoyl chloride with isothiocyanate and diethylamine [102]. In order to extend the denticity of such chelating systems, a substituted *N,N*-[(diethylamino)(thiocarbonyl)]benzamidine ligand **(H_2L2)** was synthesized from the reaction of *N,N*-[(diethylamino)(thiocarbonyl)]benzimidoyl chloride with 2-aminophenol [119]. Since frequently cyclometallated *C,N*- ligands stabilize the gold(III) centre towards reduction to gold(I) [24], also the organometallic Au(III) compound [Au(damp-κC^1,*N*)Cl_2] was used as starting material [135].

2.1.1. Synthesis and Spectroscopy

A reaction of HL1 with [Au(damp-κC^1,*N*)Cl_2] in a 1:1 molar ratio in THF, using Et_3N as a supporting base, and subsequent workup with $(Bu_4N)PF_6$ as a source for a counter-ion, afforded the complex **1** of the composition [Au(damp-κC^1,*N*)(L1)](PF_6). The reaction of H_2L2 with [Au(damp-κC^1,*N*)Cl_2] in a 1:1 molar ration in MeOH, without a supporting base, but workup with KPF_6 afforded the complex **2** of the composition [Au(Hdamp-κC^1)(L2)](PF_6) (Scheme 4).

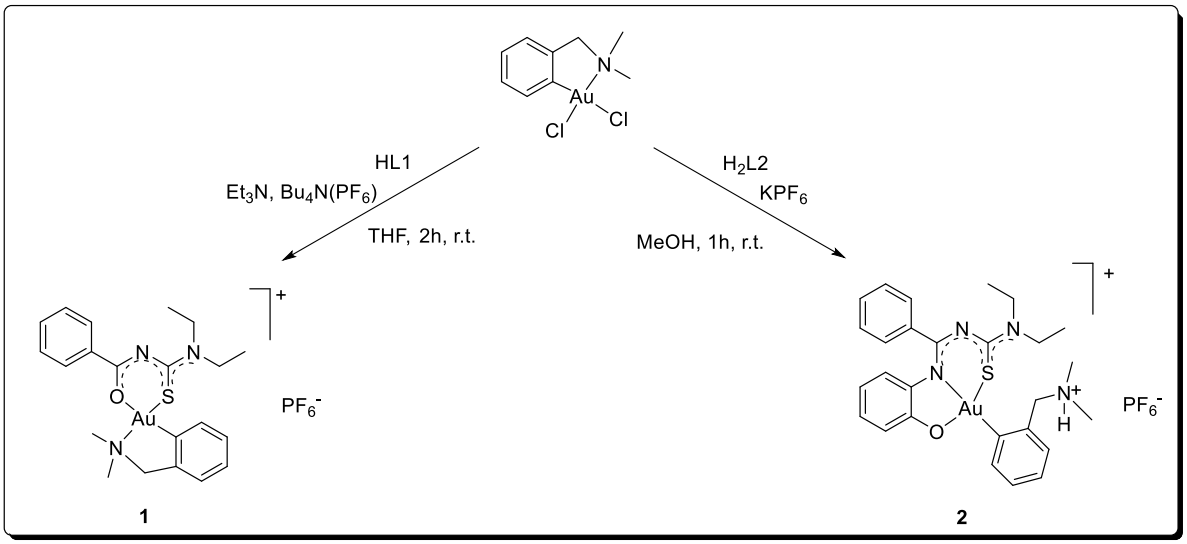

Scheme 4: Synthesis of [Au(damp-κC^1,*N*)(L1)](PF_6) **1** and [Au(Hdamp-κC^1)(L2)](PF_6) **2**.

Single crystals suitable for X-ray diffraction analysis were obtained from slow diffusion of MeOH into the solution of **1** in CH_2Cl_2 and from slow evaporation of the MeOH solution of complex **2**. The composition of the complexes was confirmed by elemental analysis and mass spectrometry.

The IR spectra of the ligands reveal broad, medium absorption bands in the range of 3420 - 3260 cm^{-1} due to the ν(N-H) stretching vibrations. As expected, they are absent in the IR spectrum of compound **1**, while in complex **2** an NH band is observed at 2605 cm^{-1} [136]. It is due to the protonation of the -NMe_2 group of the Hdamp-C^1 moiety and has been observed for a number of gold complexes before [117, 137 - 141]. The ^{1}H-NMR spectrum supports the protonation of the NMe_2 group with a broad signal at δ(NH) 8.7 ppm. A strong IR band associated with the ν(C=O) stretch is observed at 1510 cm^{-1} in complex **1**. This corresponds to a bathochromic shift of about 150 cm^{-1} with respect to the value in the non-coordinated HL1 and indicates chelate formation with a large degree of π-electron delocalization within the chelate rings. The C=N band present in the IR spectrum of complex **2** is observed at 1595 cm^{-1}. It is also shifted to lower wavenumbers with respect to H_2L2, which indicates that the nitrogen atom of the benzamidine group participates in the coordination of the metal ion. The strong absorption frequencies between 839 and 752 cm^{-1} are associated with the hexafluorophosphate counterions.

The NH singlet of the ^{1}H-NMR spectrum of **HL1** is absent in the ^{1}H-NMR spectrum of complex **1**. This suggests coordination of the ligand in its deprotonated form. The coordination of the damp$^-$ ligand is supported by the presence of two singlet signals at 3.31 and 4.51 ppm, which can be assigned to the CH_3 and CH_2 group. In the ^{1}H-NMR spectrum of compound **2**, there are new singlets at 2.79 and 3.48 ppm. They belong to the non-equivalent hydrogen atoms of the methyl groups, and one singlet at 4.15 ppm supports the presence of the damp group in the complex. The ^{13}C-NMR spectrum of **1** displays signals of C=S and C=O carbon atoms, which are shifted to higher field by around 10 and 3 ppm in comparison to the uncoordinated **HL1**. It suggests the coordination of {L1}$^-$ by S and O atoms. The ^{13}C-NMR spectrum of **2** shows the signals in the expected regions. The signal of the C=S group shifts 14 ppm upfield while the C=N signal shifts 8.3 ppm downfield upon coordination.

Further support for the composition of the compound is given by the ESI$^+$ (Electrospray Ionization) mass spectrum of **1**, which contains one intense signal corresponding to the molecular ion peak of [Au(damp-κC^1,N)(L1)]$^+$ at *m/z* = 566.1731 (calc. 566.1540). The signal of [Au(Hdamp-κC^1)(L2)]$^+$ at *m/z* = 657.1934 (calc. 657.1957) is much less intense. The low intensity reveals the instability of compound **2**.

2.1.2. Crystal and Molecular Structures

Single X-ray diffraction analysis reveals the formation of cationic chelates. Complexes **1** and **2** crystallize in the monoclinic space groups $P2_1/c$ and $P2_1/n$, respectively. The coordination environment around the gold atoms is square-planar with some distortions.

Figure 8 illustrates the molecular structure of the cation of compound **1,** showing the atomic numbering scheme. Selected bond lengths and angles are given in Table 1. The benzoyl thiourea acts as a monoanionic bidentate *O,S*-chelator, which is coordinated with the sulfur atom *trans* to the *N*-dimethylamino group of the damp$^-$ ligand.

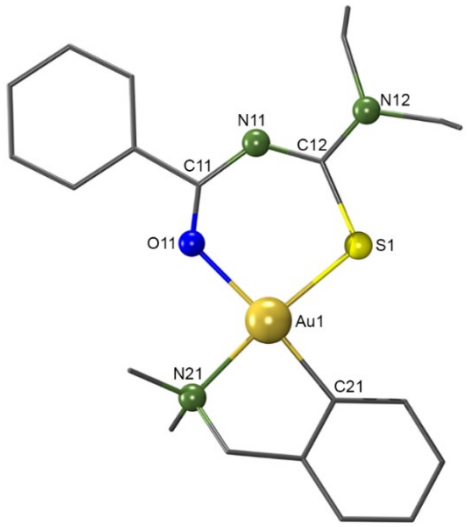

Figure 8: Molecular structure of the complex [Au(damp-κC^1,N)(L1)]$^+$. Hydrogen atoms are omitted for clarity.

Table 1: Selected bond lengths and angles in [Au(damp-κC^1,N)(L1)](PF_6).

Bond lengths (Å)					
Au1-S1	2.266(1)	Au1-O11	2.111(3)	N11-C12	1.343(6)
Au1-C21	2.007(4)	O11-C11	1.181(5)	C12-N12	1.317(6)
Au1-N21	2.116(4)	C11-N11	1.360(5)	C12-S1	1.763(4)
Angles (°)					
C21-Au1-N21	82.9(2)	S1-Au1-C21	91.1(1)	O11-Au1-C21	174.7(2)
O11-Au1-S1	93.97(8)	O11-Au1-N21	92.0(1)	S1-Au1-N21	173.5(1)

In complex **1**, the C11-N11 and thioamide C12-N11 bond lengths are between 1.360(5) and 1.343(6) Å. They show partial double bond character, similar to the C12-N12 bond (1.317(6) Å). The C12-S1 bond length is 1.763(4) Å, which is longer than the C-S bonds in thiourea complexes [96]. The amide C11-O11 bond in the complex is surprisingly shorter

(1.181(5) Å) than in the uncoordinated benzoylthiourea (1.219(2) Å) [142]. This suggests an unusual bonding situation and manifests a high degree of delocalization of electron density within the thiourea unit, which also includes the exocyclic C12-N12 bond. The six-membered chelate ring, however, is not included. Slightly distorted square-planar coordination geometry is formed by the O, S, N and C donor atoms. The angles around the gold atom deviate slightly from 90° which is due to the formation of the chelate rings.

The structure of compound **2** is shown in Figure 9. Selected bond lengths and bond angles are summarized in Table 2. H_2L2 acts as a tridentate *S,N,O* ligand in its double deprotonated form. This results in a coordination environment similar to that in Au(III) complexes with *S,N,S* thiocarbonyl benzamidines [121]. The tridentate coordination mode of $\{L2\}^{2-}$ is also reported for tridentate complexes of Re^{V}, Tc^{V} [119] and Ru^{II} [143].

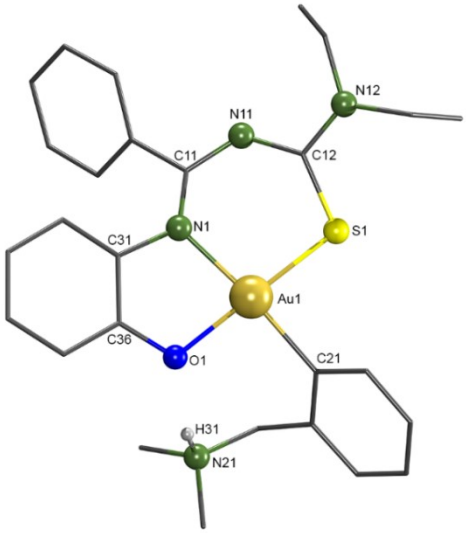

Figure 9: Molecular structure of the complex [Au(Hdamp-κC^{I})(L2)]$^{+}$. Hydrogen atoms bonded to carbon atoms are omitted for clarity.

A crystallographic study of compound **2** confirms the cleavage of the Au-N bond of [Au(damp-κC^{I},*N*)Cl_2] and the protonation of the released dimethyl amino group. Cleavage of the Au-N bond has been observed before for reactions of [Au(damp-κC^{I},*N*)Cl_2] with thiosemicarbazone derivatives and other ligands [117, 141, 144].

Table 2: Selected bond lengths and angles in [Au(Hdamp-κC^1)(L2)](PF_6).

Bond lengths (Å)					
Au1-S1	2.259(2)	O1-C36	1.364(7)	N11-C12	1.354(8)
Au1-C21	2.040(6)	C31-N1	1.438(8)	C12-N12	1.344(7)
Au1-N1	2.053(5)	C11-N1	1.329(8)	C12-S1	1.736(6)
Au1-O1	2.030(4)	C11-N11	1.336(8)		
Angles (°)					
O1-Au1-N1	82.6(2)	S1-Au1-C21	86.9(2)	O1-Au1-S1	179.3(1)
S1-Au1-N1	98.02(1)	O1-Au1-C21	92.5(2)	C21-Au1-N1	174.7(2)

Expectedly, a square-planar geometry around of the gold(III) ion is established. Although the low affinity of gold oxygen is known, the chelating effect of the tridentate ligand prevails over the formation of a *C,N*-coordination of the damp$^-$ ligand as is seen in **1**. A considerable delocalization of π-electron density is indicated by the observed bond lengths inside the chelate rings.

2.2. H_2L3 and its Gold(I) Complexes

Interestingly, less is known about the coordination behaviour of tetradentate thiocarbamoyl benzamidine ligands of the type **H_2L3** [145], which can be synthesized following the general procedure described for H_2L2 in the previous section. There is hitherto only one complex reported with H_2L3, a neutral Ni(II) chelate [145].

2.2.1. Synthesis and Structural Characterization of H_2L3

The ligand H_2L3 was prepared from the corresponding benzimidoyl chloride and ethylenediamine in THF following the procedure described previously (Scheme 5).

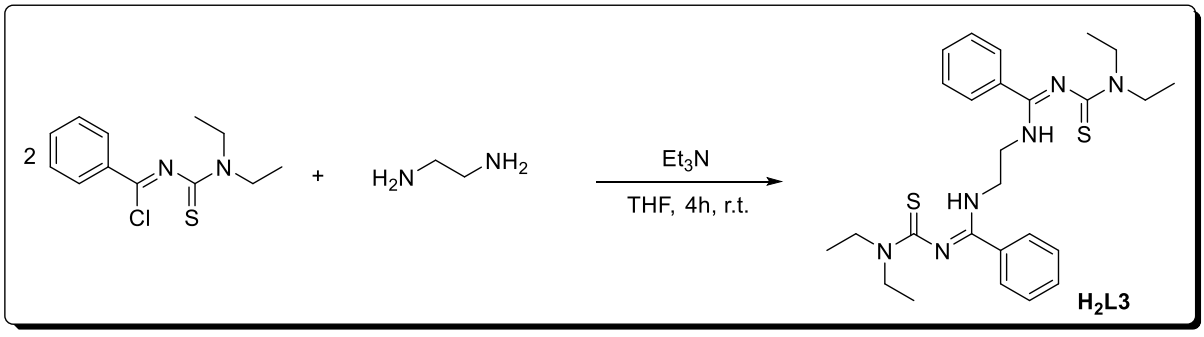

Scheme 5: Synthesis of the ligand H_2L3 [145].

The ligand was characterized by elemental analysis, spectroscopic methods and X-ray crystallography, since the original report contains no structural and crystallographic information. The IR spectrum of H_2L3 exhibits a medium absorption at 3250 cm^{-1} related to the ν(N-H) stretch. A medium broad absorption band at 1255 cm^{-1} is related to the ν(C=N) vibrations, two bands at 1138 and 1076 cm^{-1} are assigned as ν(C=S) and ν(C-N) frequencies respectively. The ^{1}H-NMR spectrum of H_2L3 confirms its symmetric structure. The resonances of the aromatic protons appear as a multiplet in the region between 7.45 - 7.35 ppm. Three signals corresponding to the alkyl groups are observed at 3.88 ppm, 3.71 ppm and 1.22 ppm, although they are less resolved due to the hindered rotation of the thiourea units. The proton of the amine is observed at 2.2 ppm in the spectrum as a broad singlet. Further support for the composition of H_2L3 is given by its ESI^+ mass spectrum. It shows two intense signals at *m/z* = 519.2335 (calc. 519.2335) and *m/z* = 535.2074 (calc. 535.2074), which are assigned to the cations $[M + Na]^+$ and $[M + K]^+$, respectively.

2.2.2. Crystal and Molecular Structure

Single crystals of **H_2L3** suitable for X-ray analysis were obtained by slow diffusion of Et_2O into the EtOH solution (3:1; v:v). Figure 10 illustrates the molecular structure of H_2L3. Selected bond lengths and bond angles are summarized in Table 3.

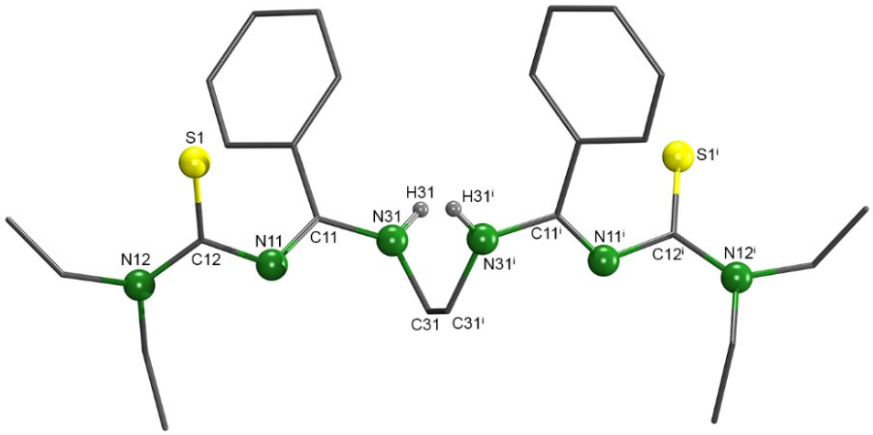

Figure 10: Molecular structure of H_2L3. The hydrogen atoms bonded to carbon atoms are omitted for clarity. Symmetry transformations used to generate equivalent atoms: ^{i} y,x,-z.

Table 3: Selected bond lengths and angles in H_2L3.

Bond lengths (Å)					
C11-N11	1.293(4)	C11-N31	1.344(4)	C12-N12	1.334(3)
N11-C12	1.373(4)	N31-C31	1.439(4)	C12-S1	1.696(3)
Angles (°)					
N31-C11-N11	119.1(3)	N11-C12-S1	122.6(2)	N12-C12-S1	121.7(2)
C11-N11-C12	122.2(2)	N11-C12-N12	115.4(3)	C11-N31-C31	125.7(3)

The compound crystallizes in the tetragonal space group $P4_212$. While the C12-S1 and C11-N11 bonds lengths of 1.696(3) and 1.293(4) Å fit with values expected for C=S and C=N double bonds, the C11-N31, C12-N11 and C12-N12 bonds reflect partial double bond character. This is also found in a similar ligand [146], which has a central phenylenediamine group. The atoms N31 and $N31^i$ are protonated.

2.2.3. Synthesis and Characterization of Gold(I) Complexes with H_2L3

Reactions of H_2L3 with common gold(I) starting materials such as [AuCl(THT)] or [AuCl(PPh_3)] give colourless solids of the compositions [{AuCl}$_2$(H_2L3-κS)] **3**, [{Au(SCN)}$_2$(H_2L3-κS)] **4** and [{Au(PPh_3}$_2$(H_2L3-κS)](PF_6)$_2$ **5**. The syntheses of complexes **3** and **5** were performed in MeOH by stirring the reactants for 2 hours at room temperature. The synthesis of **4** proceeds at room temperature in a mixture of CH_2Cl_2 and MeOH. Complexes **3** and **4** show low solubility in organic solvents, while complex **5** dissolves in CH_2Cl_2 and $CHCl_3$. Therefore, the ^{1}H-NMR and ^{13}C-NMR acquisitions for complexes **3** and **4** could not be performed. Attempts to dissolve the compounds in hot DMSO failed and greyish powders deposited after a few minutes in the NMR tubes. For the synthesis of complex **4**, an excess of KSCN was necessary, and the addition of (Bu_4N)PF_6 was necessary for the isolation of compound **5** (Scheme 6).

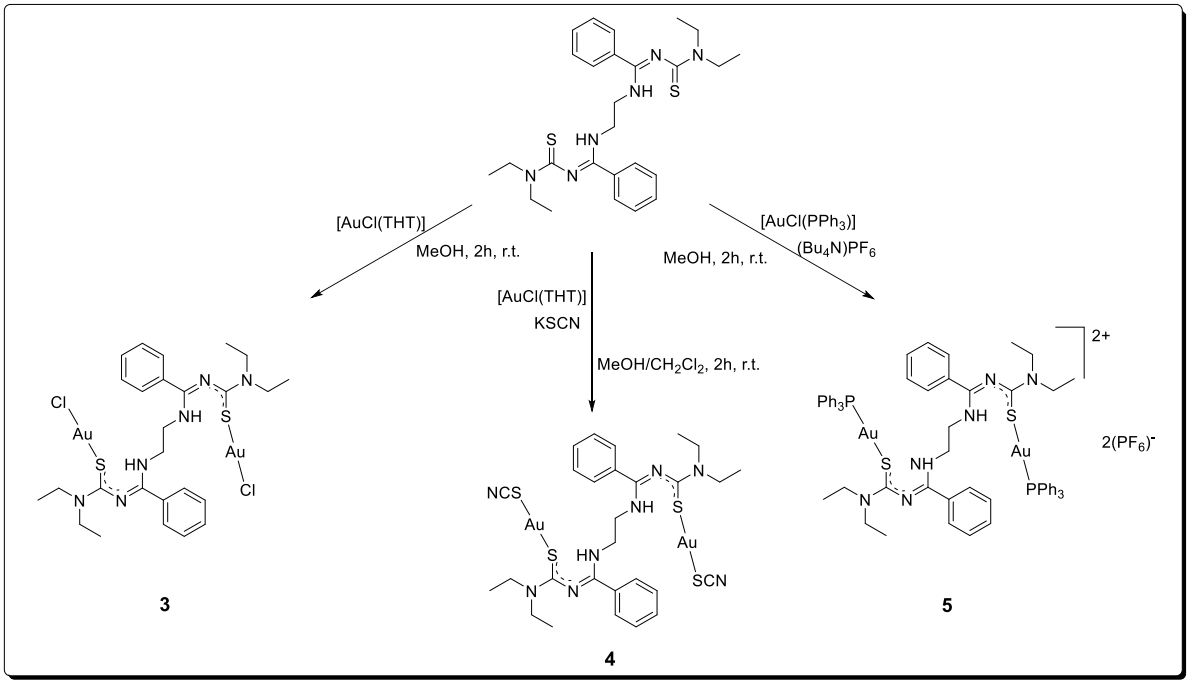

Scheme 6: Synthesis of the complexes $[\{AuCl\}_2(H_2L3\text{-}\kappa S)]$ **3**, $[\{Au(SCN)\}_2(H_2L3\text{-}\kappa S)]$ **4**, and $[\{Au(PPh_3)\}_2(H_2L3\text{-}\kappa S)](PF_6)_2$ **5**.

IR spectra of the compounds depict medium bands in the region between 3268 and 3406 cm^{-1}, which indicate that the ligands remain protonated during the complex formation. The band assigned to ν(C=S) at 1138 cm^{-1} in the spectrum of H_2L3 shifts 40 cm^{-1} to lower wavelengths after complex formation, suggesting a lower C-S bond order. Two other bands present in the IR spectrum of H_2L3 at 1597 cm^{-1} and 1076 cm^{-1} remain almost unchanged. The presence of SCN^- in compound **4** is supported by a very strong band at 2123 cm^{-1}. A broad band at 839 cm^{-1} in the spectrum of **5** is related to the ν(PF_6) stretch of the counterion.

The NMR spectra of complex **5** were acquired in CD_2Cl_2. They show the signals in the expected regions. The ^{1}H-NMR spectrum shows broad signals. That at 7.20 ppm is related to the two NH groups. The ^{13}C-NMR spectrum shows the C=S signal 8 ppm upfield shifted upon coordination. ESI^+ mass spectrometry has been used for the characterization of the gold(I) complexes. The spectrum of compound **5** shows the signal of $[Au(PPh_3)_2]^+$ at *m/z* = 721.1573 as the base peak. The spectra of compounds **3** and **4** both show signals at *m/z* = 693.2165. They can be assigned to an ion of the composition $[Au(H_2L3)]^+$ (calcd. *m/z:* 693.2103) (Fig. 11).

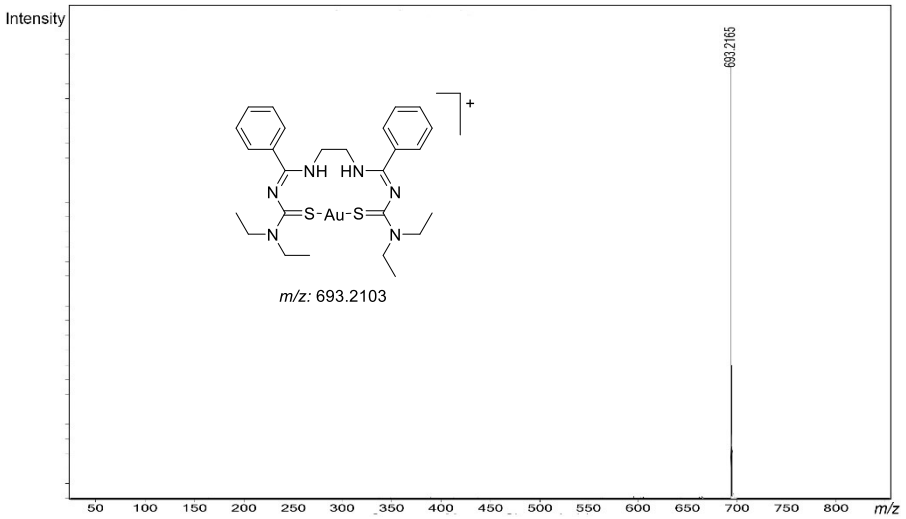

Figure 11: ESI$^+$ mass spectrum of compound **3**, which show exclusively a cation of the composition $[Au(H_2L3)]^+$.

2.2.4. Crystal and Molecular Structures

The isolated gold(I) complexes were studied by X-ray crystallography. Figure 12 depicts the molecular structures of the neutral complexes **3** and **4**. Selected bond lengths and angles are summarized in Table 4 along with the values found for compound **5**.

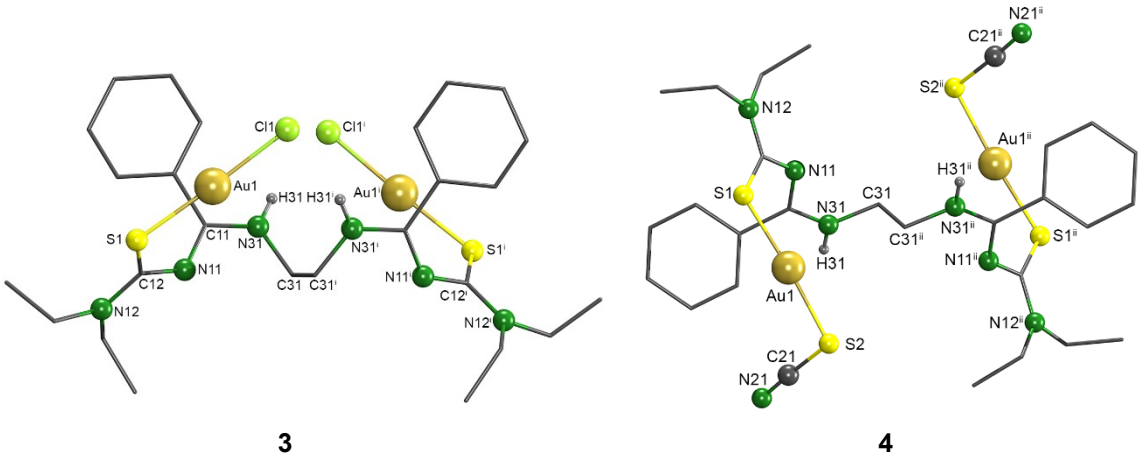

Figure 12: Molecular structures of the neutral complexes $[\{AuCl\}_2(H_2L3\text{-}\kappa S)]$ **3** and $[\{Au(SCN)\}_2(H_2L3\text{-}\kappa S)]$ **4**. The hydrogen atoms bonded to the carbon atoms are omitted for clarity. Symmetry transformations used to generate equivalent atoms: ^{i} -x+1,y,-z+3/2 and ^{ii} -x,-y,-z+1.

The structure of the latter complex is shown in Figure 13. H_2L3 acts as a neutral ligand in all three complexes. The gold atoms are coordinated by the sulfur donor atom. The environments of the gold atoms are almost linear with X-Au-S bond angles between 175.77(2) and 177.89(5)°. It is noteworthy that the C-N bonds next to the thiocarbonyl groups show partial double bond

character after the complexation. Also a lengthening of the C12-S1 bonds in the complexes is observed, in comparison to the value in the uncoordinated H_2L3 (1.696(3) Å).

Table 4: Selected bond lengths, distances and angles in **3**, **4**, and **5**.

Bond lengths (Å)

	3	**4**	**5**		**3**	**4**	**5**
C11-N11	1.306(6)	1.301(4)	1.308(3)	Au1-S1	2.259(1)	2.274(1)	2.322(7)
C11-N31	1.339(6)	1.334(4)	1.341(3)	Au1-X	2.281(1)	2.293(1)	2.270(7)
N11-C12	1.338(6)	1.351(4)	1.344(3)	Au···Au	-	3.520(1)	3.231(3)
C12-N12	1.325(6)	1.328(5)	1.330(3)	S2-C21	-	1.675(5)	-
C12-S1	1.746(5)	1.743(3)	1.747(3)	C21-N21	-	1.145(6)	-

Angles (°)

	3	**4**	**5**
S1-Au1-Cl1	177.89(5)	-	-
S1-Au1-S2	-	176.08(4)	-
S1-Au1-P1	-	-	175.77(2)
C12-S1-Au1	106.0(2)	107.2(1)	105.21(9)
C21-S2-Au1	-	99.2(2)	-

X = Cl, S or P in complexes **3**, **4**, or **5** respectively.

Compound **3** crystallizes in the monoclinic space group C2/c. The linear coordination of the gold atoms in **3** is completed by a chlorido ligand. Compound **4** crystallizes in the triclinic space group $P\bar{1}$. The linear coordination of the gold atom is completed by a *S*-bonded thiocyanato ligand. The Au1-S2 bond length of 2.293(1) Å is slightly longer than the Au1-S1 bond. The linear SCN^- ligand is coordinated with an Au1-S2-C21 angle of 99.2(2)°.

The structure of the cationic complex of **5** is shown in Figure 13. The compound crystallizes in the monoclinic space group C2/c. Similar to compound **4**, H_2L3 crystallizes in anti-configuration, minimizing the repulsion between the bulky PPh_3 ligands. Also, in complex **5**, there is evidence for some delocalization of π-electron density over the thiourea group. As expected, a lengthening of the Au1-S1 bond in complex **5** is observed when compared to the related bonds in **3** and **4**. This is due to the structural *trans*-influence of PPh_3 and has been observed earlier [147, 148]. The lengthening of Au-S bond lengths in the following sequence $Cl^- < SCN^- < PPh_3$ is due to the σ-donor and π-acceptor behaviour of the ligands.

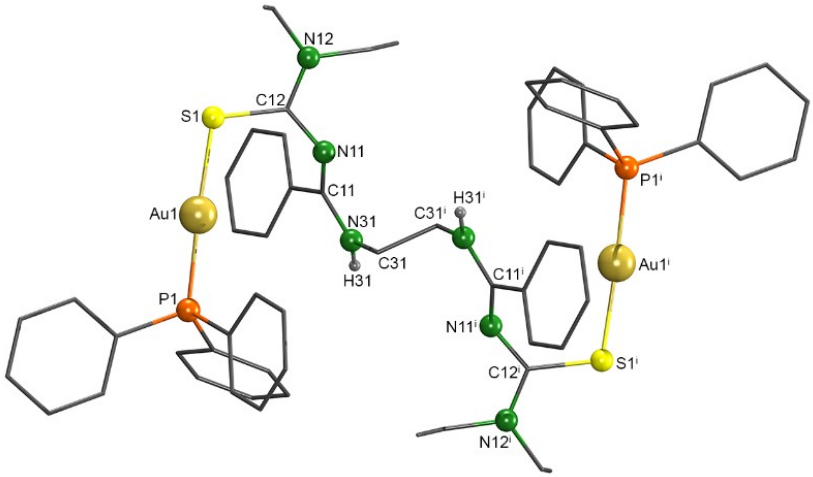

Figure 13: Molecular structure of the complex cation $[\{Au(PPh_3)\}_2(H_2L3\text{-}\kappa S)]^{2+}$ **5**. The hydrogen atoms bonded to carbon atoms are omitted for clarity. Symmetry transformations used to generate equivalent atoms: ^{i} -x+1, -y+1, -z+2.

The solid-state structures of compounds **4** and **5** show intermolecular interactions. They are dominated by aurophilic interactions with Au···Au distances between 3.2 and 3.5 Å, which are supported by additional Au···S contacts of about 3.3 Å. The resulting bonding situations are shown in Figure 14. Compound **4** forms linear polymeric chains and compound **5** helical chains. The *syn*-conformation of the two coordination sites in compound **3** prevent from the formation of similar polymers. The shortest Au···Au distance found in **3** is 6.739(4) Å.

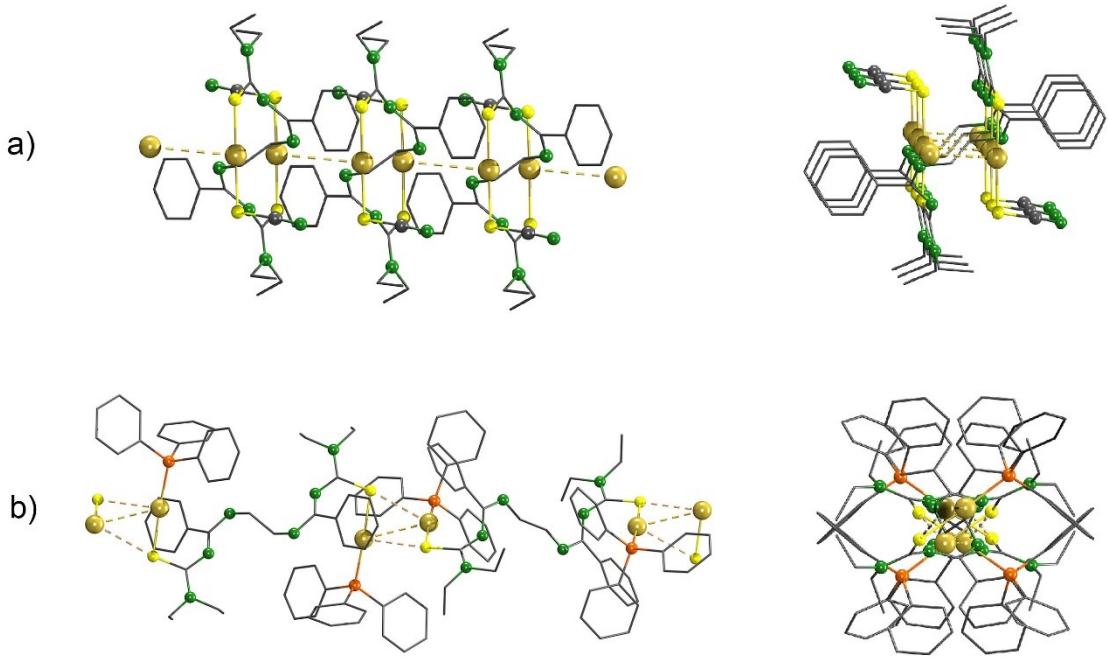

Figure 14: Supramolecular aggregation of the complex molecules in compounds **4** (a) and **5** (b).

2.3. Gold(I) Complexes with 2,6-Dipicolinoylbis(*N,N*-diethylthiourea) – H_2L4

H_2L4 offers a high structural flexibility for the formation of metal complexes. It originates from the possible rotation of the *N,N*-diethylthiourea building blocks attached to the amide group. To the best of my knowledge, there are hitherto no gold compound known with this ligand.

2.3.1. Synthesis and Spectroscopy

The reaction between one equivalent of H_2L4 with two equivalents of [AuCl(THT)] in 5 mL of THF gave a colourless precipitate without the addition of a supporting base. The product is insoluble in alcohols and hydrocarbons, and slightly soluble in CH_2Cl_2. Recrystallization from a hot mixture of CH_2Cl_2/MeOH gave a pure, crystalline product of the composition $[\{AuCl\}_2(H_2L4\text{-}\kappa S)]$ **6**. In contrast to the previous reaction, the reaction between $[AuCl(PPh_3)]$ and H_2L4 in 5 mL of MeOH did not result in the formation of a precipitate but resulted in a suspension. A clear solution was observed after the addition of Et_3N. Colourless crystals of a complex of the composition $[\{Au(PPh_3)\}_2(L4\text{-}\kappa S)]$ **7** were obtained from slow evaporation of the solvent (Scheme 7). The product is slightly soluble in polar solvents and alcohols and practically insoluble in hydrocarbons.

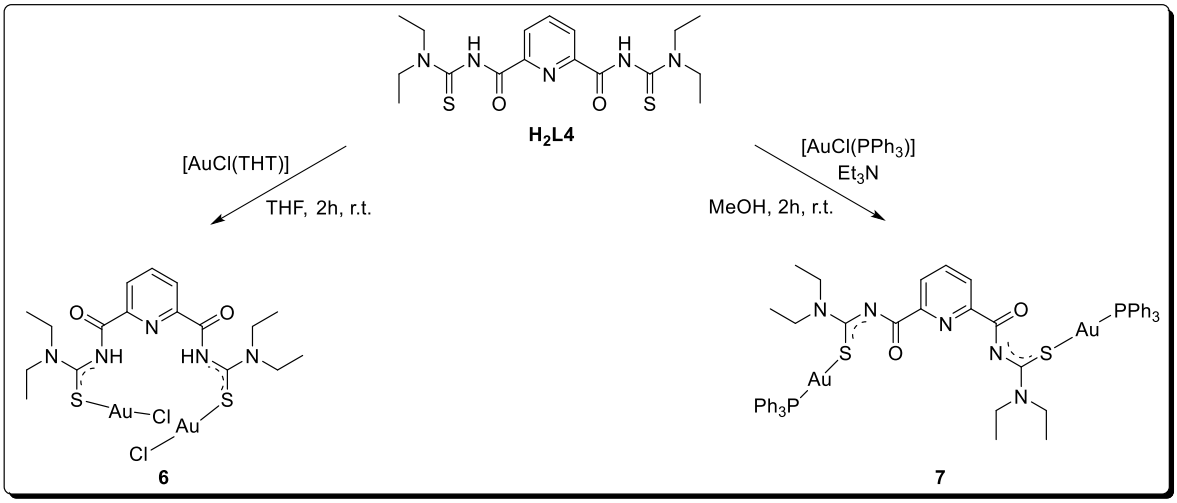

Scheme 7: Synthesis of complexes $[\{AuCl\}_2(H_2L4\text{-}\kappa S)]$ **6** and $[\{Au(PPh_3)\}_2(L4\text{-}\kappa S)]$ **7**.

The IR spectrum of compound **6** shows a medium absorption band referring to the ν(N-H) stretch at 3302 cm^{-1}. It is absent in the spectrum of compound **7**. This suggests that the thiourea ligand in **6** remains protonated, while deprotonation is observed in compound **7**. The carbonyl absorption for compound **6** is observed at 1707 cm^{-1}, which means a shift about 25 cm^{-1} to higher frequencies after complex formation.

The NMR spectra of complex **6** provide additional evidence for the proposed composition and molecular structure. The ^{1}H-NMR spectrum shows a singlet related to the (NH) proton at 10.83 ppm. One doublet and one triplet at 8.42 and 8.20 ppm are related to the protons of the pyridine ring. Two quartets related to the CH_2 protons at 4.0 and 3.75 ppm, and two triplets related to CH_3 groups at 1.49 and 1.42 ppm show that the ethyl groups are magnetically not equivalent. The ^{13}C-NMR spectrum exhibits a pattern similar to that of the uncoordinated ligand. The acquisition of ^{1}H-NMR and ^{13}C-NMR spectra for complex **7** was not possible due to the low solubility in any solvent. Attempt to obtain the spectra in hot deuterated DMSO lead to decomposition of the compound.

The ESI^{+} mass spectrum of **6** does not exhibit the molecular ion, but the most intense peak belongs to the $[Au(H_2L4)]^{+}$ cation at *m/z* = 592.1175 (calcd. 592.1110). The ESI^{+} mass spectrum of **7** shows the molecular ion, by the detection of a signal at *m/z* = 1334.2305 (calcd. 1334.2339), which can be assigned to the $[M + Na]^{+}$ ion.

2.3.2. Crystal and Molecular Structures

Compound **6** crystallizes in the monoclinic space group $P2_1/c$. The gold atoms are exclusively coordinated by the sulfur atoms of H_2L4 and chloride ligands. This results in a linear S-Au-Cl coordination. Figure 15 shows the molecular structure of **6**. Table 5 summarizes selected bonds lengths and bond angles. The coordination of the sulfur atoms to gold results in some bond lengths modifications in the skeleton of the ligand with regard to its non-coordinated form.

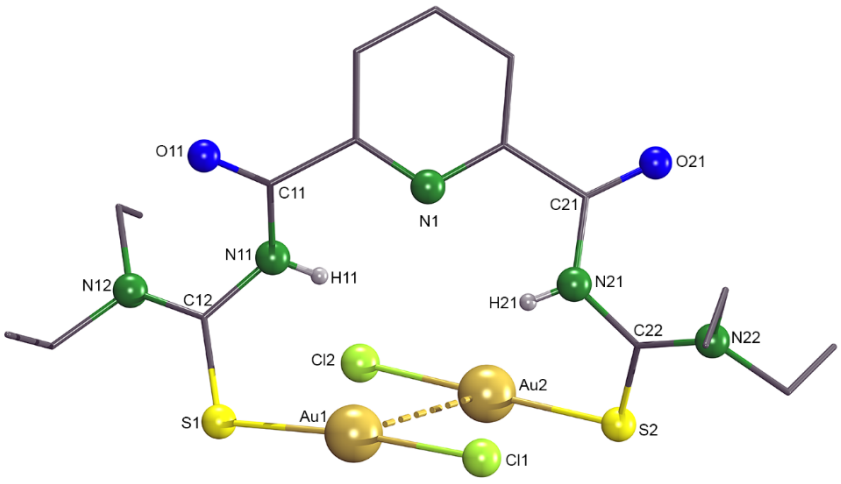

Figure 15: Molecular structure of the complex $[\{AuCl\}_2(H_2L4\text{-}\kappa S)]$, showing the atomic numbering scheme and aurophilic interactions between gold atoms. Hydrogen atoms bonded to carbon atoms are omitted for clarity.

The C=S bond lengths in the complex are in the range between 1.710(4) - 1.717(4) Å. They are slightly longer than in the uncoordinated ligand (1.662(5) Å) [149]. The C-N bond lengths next to the thiocarbonyl groups are in the range 1.398(5) - 1.408(5) Å. Thus, they are slightly shorter than in the uncoordinated ligand (1.427(5) Å) [149]. These values correspond to the partial single and double bond character of the C=S and C-N bonds and reflect the delocalization of π-electron density over the thiourea fragment.

Table 5: Selected bond lengths and angles in [{AuCl}$_2$(H$_2$L4-κS)].

Bond lengths (Å)							
Au1-S1	2.266(1)	C11-N11	1.375(5)	C21-N21	1.382(5)	N11-C12	1.408(5)
Au1-Cl1	2.285(1)	C11-O11	1.218(5)	C21-O21	1.212(5)	N21-C22	1.398(5)
Au2-S2	2.270(1)	Au2-Cl2	2.276(1)	C12-S1	1.710(4)	C22-S2	1.717(4)
Au1···Au2	3.5493(5)						

Angles (°)					
S1-Au1-Cl1	172.55(4)	C12-S1-Au1	108.8(2)	C11-N11-C12	123.9(3)
S2-Au2-Cl2	175.16(4)	C22-S2-Au2	106.1(1)	C21-N21-C22	122.9(3)

The Au-Cl and Au-S distances are very similar to those observed in the structure of *N,N*-diethyl-*N′*-camphanylthioureatogold(I) chloride obtained by Koch [150] and *N,N*-diethyl-*N′*-benzoylthioureatogold(I) chloride reported by Bensch [103]. Weak Au···Au interactions of 3.5493(5) Å are established in the solid-state structure of **6**. They are accompanied by π-π interactions between pyridine rings of 3.709(1) Å as shown in Figure 16. These values of Au···Au as well as the offset parallel orientation π-π interactions are consistent with the values determined by Pathaneni [151] and Janiak [152], respectively.

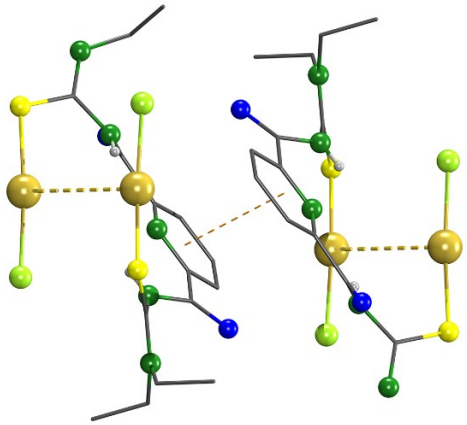

Figure 16: Crystal packing in the solid-state structure of [{AuCl}$_2$(H$_2$L4-κS)]. Intramolecular aurophilic interactions and parallel orientation of two molecules held together by π-π interactions.

Complex **7** crystallizes in the monoclinic space group $P2_1/n$. Figure 17 shows the molecular structure of [{Au(PPh$_3$)}$_2$(L4-κS)]. Selected bonds lengths and angles are shown in Table 6. The solid state structure of this compound contains a perfect disorder of the carbonyl groups and pyridine ring over two positions. Similar disorder is observed to another gold(I) complex with isophtaloylbis(thiourea) ligand [131].

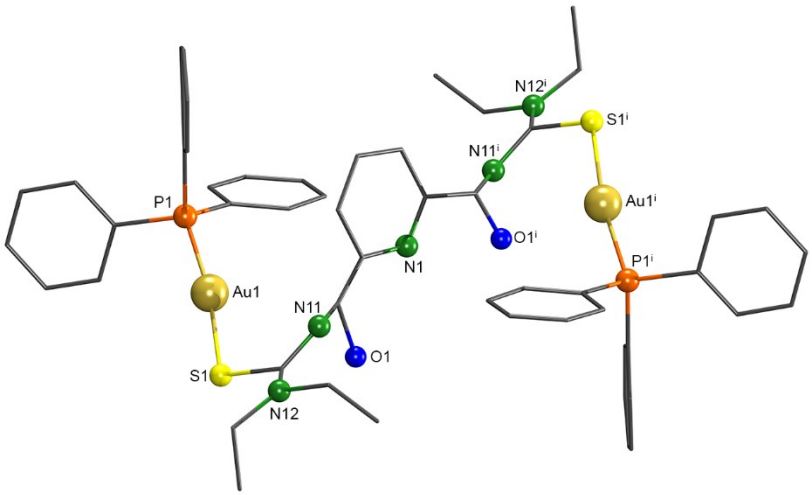

Figure 17: Structure of the complex [{Au(PPh$_3$)}$_2$(L4-κS)]. Hydrogen atoms are omitted for clarity.

Table 6: Selected bond lengths and angles in [{Au(PPh$_3$)}$_2$(L4-κS)].

Bond lengths (Å)					
Au1-S1	2.296(3)	C11-O1	1.63(3)	N11-C12	1.33(2)
Au1-P1	2.267(3)	C11-N11	1.22(3)	C12-S1	1.73(1)*
Angles (°)					
S1-Au1-P1	171.4(1)				

* average of the bond length of the disordered part of the structure.

The gold atoms are in an almost linear environment, with a P-Au-S angle of 171.4(1)°. The Au-P distances of 2.267(3) Å and the Au-S bond lengths of 2.296(3) Å are similar to the values in structures published by Schwade [131] and Gimeno [153]. The C=S bond length in the complex is 1.73(1) Å. It is longer than in the uncoordinated ligand (1.662(5) Å) [149]. The C-N bonds next to the thiocarbonyl groups (1.33(2) Å) are shorter compared with the same bonds in the uncoordinated ligand (1.427(5) Å). These values also correspond to the partial single and double bond character of the C=S and C-N bonds. In compound **7** is no evidence for supramolecular aggregation. The shortest Au···Au distance found is 9.535(8) Å.

2.4. M^{2+} Complexes (M^{2+} = Ca^{2+}, Sr^{2+} or Ba^{2+}) with a Tetranuclear Gold(I) Coronand

2.4.1. Synthesis and Spectroscopy

The reaction between two equivalents of [AuCl(THT)], two equivalents of H_2L4 and one equivalent of $Ca(NO_3)_2{\cdot}4H_2O$, $Sr(NO_3)_2{\cdot}4H_2O$ or $Ba(NO_3)_2$ in 5 mL of MeOH gave clear solutions within 30 minutes of stirring at room temperature. Colourless precipitates of the compositions [{Ca_2(MeOH)$_3$(H_2O)}{Au(L4-κS)}$_4$] **8**, [{Sr_2(MeOH)$_2$(H_2O)$_2$}{Au(L4-κS)}$_4$] **9**, and [{Ba_2(μ-OH_2)}{Au(L4-κS)}$_4$] **10** were obtained after addition of four drops of Et_3N. The complexes were isolated as analytically pure compounds directly from MeOH after 1 hour of stirring at room temperature in good yields. The complexes are soluble in CH_2Cl_2 and $CHCl_3$. Single crystals of the complexes were obtained by slow diffusion of MeOH into the CH_2Cl_2 solutions (Scheme 8).

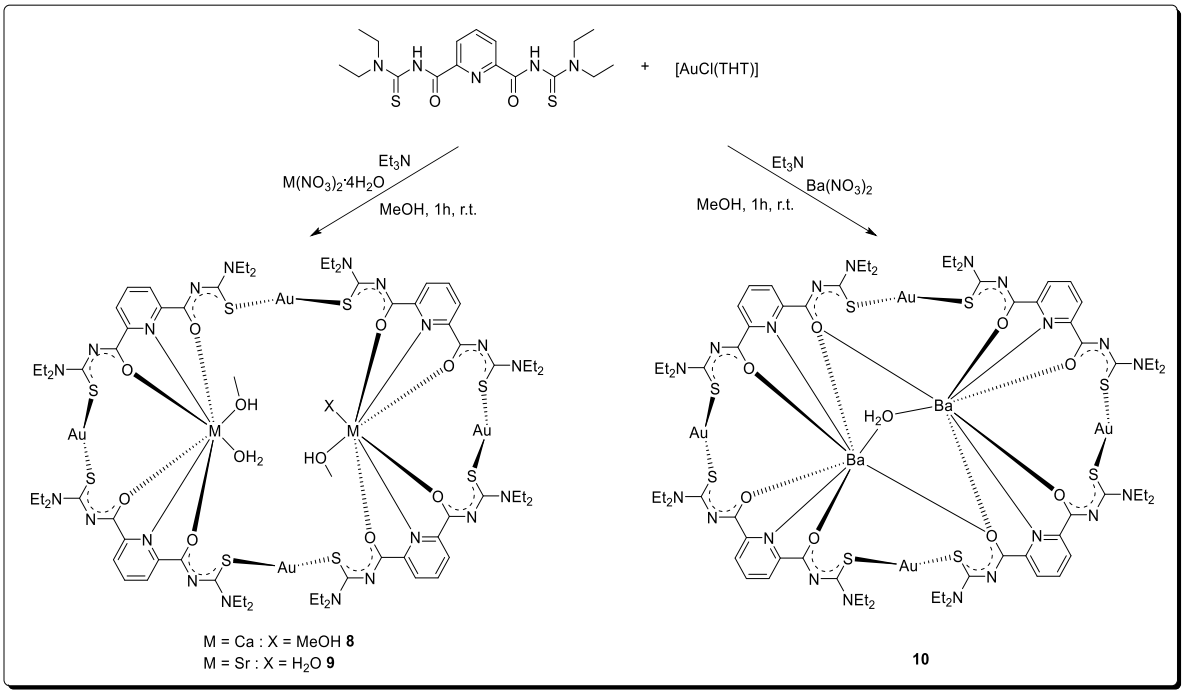

Scheme 8: Synthesis of [{Ca_2(MeOH)$_3$(H_2O)}{Au(L4-κS)}$_4$] **8**, [{Sr_2(MeOH)$_2$(H_2O)$_2$}{Au(L4-κS)}$_4$] **9**, and [{Ba_2(μ-OH_2)}{Au(L4-κS)}$_4$] **10**.

The products were characterized by elemental analysis, IR, ^{1}H-NMR and ^{13}C-NMR spectroscopy as well as by ESI mass spectrometry. The IR spectra confirm the double deprotonation of H_2L4 during the complex formation by the absence of ν(NH) bands around 3300 cm^{-1} and a typical bathochromic shift of the ν(C=O) absorption band by approximately

85 cm^{-1}. This shift indicates that the oxygen atoms of the carboxamide groups are involved in the coordination of the metal ions. The ν(C=S) stretching vibrations appear at 750, 748 and 746 cm^{-1} in the IR spectra of complexes **8**, **9**, and **10** respectively. This indicates a slight weakening of the C=S bonds.

The ^{1}H-NMR spectra of complexes **8** and **10** confirm the presence of $\{L4\}^{2-}$ and show the signals in the expected regions. In both spectra, broad signals at 1.15 ppm instead of well resolved triplets can be assigned to the methyl protons. Also, broad signals around 3.6 ppm instead of well resolved quartets can be assigned to the methylene protons. This is a sign for the hindered rotation of the -NEt_2 group in the $\{R_2N\text{-}C(S)\text{-}\}$ fragment. Such a phenomenon was previously reported by Hoyer et al., where the authors have elucidated this hindered rotation for *N,N*-dialkyl-*N′*benzoylthioureas and their complexes [154]. The authors also describe that exclusively *S*-bonded complexes show the same effect [154]. The ^{13}C-NMR spectra show the signals in the expected regions. The signals in the spectrum of compound **8** are duplicated, which shows the non-equivalence of the carbon atoms in the complex. The signals of the C=O and C=S carbon atoms of H_2L4 appear at 178.3 and 159.3 ppm respectively, while upon coordination and formation of complexes **8** and **10**, the signals appear downfield shifted by 4 and 2.5 ppm for the C=O groups and by 8.5 and 9.5 ppm for the C=S groups, respectively. Complex **9** is unstable in solution and a grey powder deposits in the NMR tube after some minutes. Thus, the acquisition of NMR spectra of reasonable quality was not possible for this compound.

Further information about the composition of the complexes is given by their ESI mass spectra. That of compound **8** shows the base peak at *m/z* = 1243.1665 (calcd. 1243.1441). It corresponds to a cation of the composition $[\{Au(L4)\}_2\{Ca\} + Na]^+$. A second, less intense peak at *m/z* = 2463.3379 (calcd. 2463.2979) is related to the molecular ion of the tetrameric compound. In both ions, no solvent molecules are coordinated. Similar signals could also be measured for compounds **9** and **10**.

2.4.2. Crystal and Molecular Structures

Single crystal X-ray diffraction of the colourless single crystals reveals neutral complexes of Ca^{2+}, Sr^{2+} and Ba^{2+} and confirms the conclusion drawn from the spectroscopic studies. The complexes host two alkaline earth metal ions in the void of a metallamacrocycle, which is formed by four gold(I) ions and four ligands $\{L4\}^{2-}$. The gold ions are exclusively coordinated by the sulfur atoms of the organic ligands in a linear fashion. The molecular structure of **8** and

9 are shown in Figure 18. Selected bonding parameters of the two complexes **8** and **9** are summarized in Table 7.

The Ca^{2+} ions in compound **8** are coordinated by four chelating $\{L4\}^{2-}$ molecules, three molecules of methanol and one water molecule. Compound **9** shows the same general structure of four chelating $\{L4\}^{2-}$ molecules. In contrast to compound **8**, two molecules of methanol and two water molecules complete the coordination environments of the Sr^{2+} ions. This leads to a coordination number of eight for each metal(II) ion in both compounds, and results in a distorted dodecahedral coordination geometry around the alkaline earth metals ions [155] (Fig. 18.c).

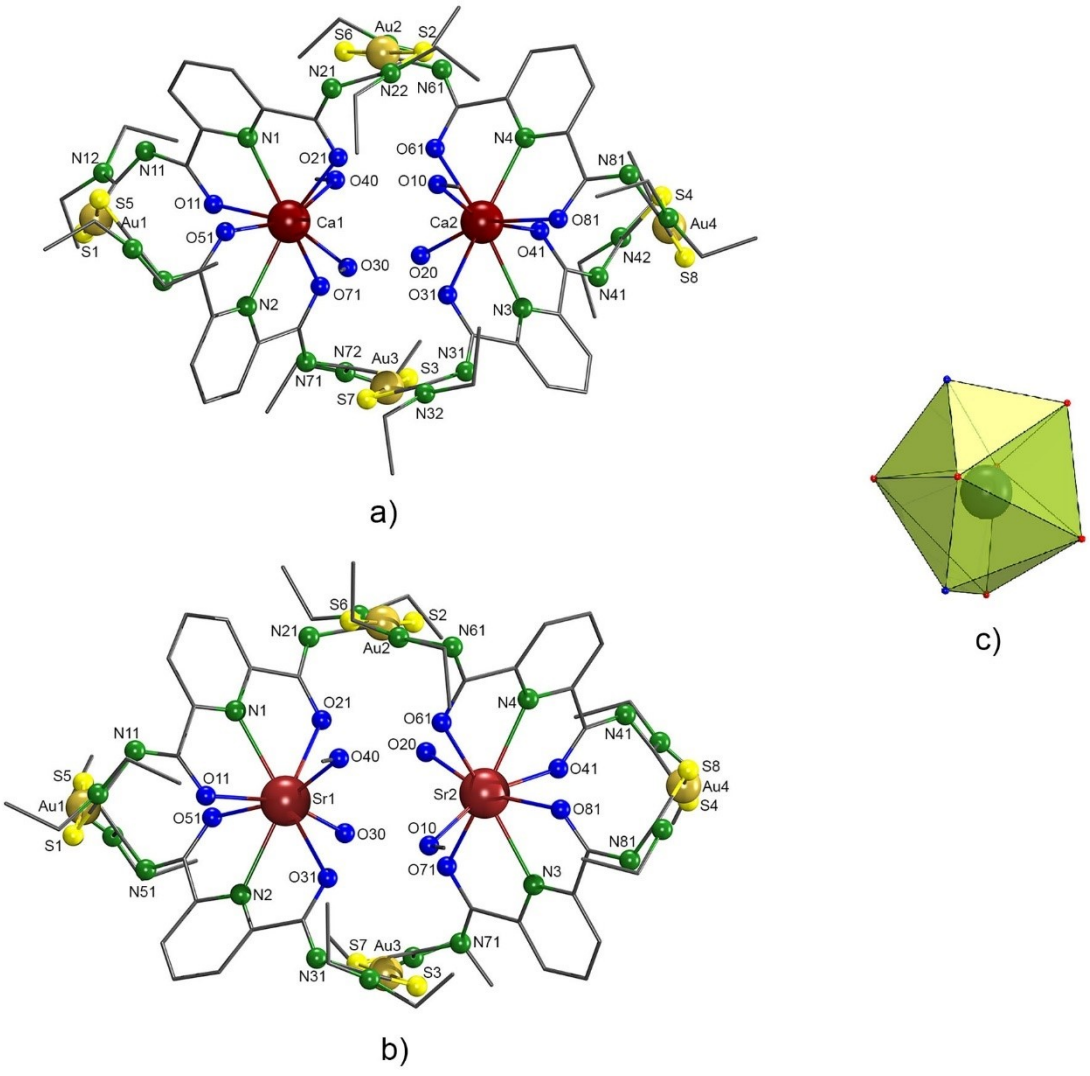

Figure 18: Molecular structures of the complexes a) $[\{Ca_2(MeOH)_3(H_2O)\}\{Au(L4\text{-}\kappa S)\}_4]$ and b) $[\{Sr_2(MeOH)_2(H_2O)_2\}\{Au(L4\text{-}\kappa S)\}_4]$. Hydrogen atoms are omitted for clarity. c) Polyhedron of the coordination environment of the alkaline earth metal ions in these two compounds.

Table 7: Selected bond lengths and angles at the complexes **8** and **9**.

Bond lengths (Å)							
[{$Ca_2(MeOH)_3(H_2O)$}{Au(L4-κS)}$_4$]				[{$Sr_2(MeOH)_2(H_2O)_2$}{Au(L4-κS)}$_4$]			
Au1-S1	2.280(2)	Au1-S5	2.275(2)	Au1-S1	2.269(3)	Au1-S5	2.268(4)
Au2-S2	2.273(2)	Au2-S6	2.283(2)	Au2-S2	2.301(3)	Au2-S6	2.275(3)
Au3-S3	2.288(2)	Au3-S7	2.296(2)	Au3-S3	2.283(3)	Au3-S7	2.278(3)
Au4-S4	2.287(2)	Au4-S8	2.285(2)	Au4-S4	2.278(4)	Au4-S8	2.292(4)
Ca1-N1	2.490(6)	Ca2-N3	2.506(7)	Sr1-N1	2.62(1)	Sr2-N3	2.645(9)
Ca1-N2	2.489(5)	Ca2-N4	2.490(6)	Sr1-N2	2.64(1)	Sr2-N4	2.65(1)
Ca1-O11	2.486(5)	Ca2-O41	2.586(5)	Sr1-O11	2.561(8)	Sr2-O41	2.563(9)
Ca1-O21	2.538(4)	Ca2-O61	2.435(5)	Sr1-O21	2.622(8)	Sr2-O61	2.656(8)
Ca1-O31	2.445(4)	Ca2-O71	2.586(5)	Sr1-O31	2.623(7)	Sr2-O71	2.650(9)
Ca1-O51	2.522(5)	Ca2-O81	2.413(5)	Sr1-O51	2.609(9)	Sr2-O81	2.553(9)
Ca1-O30	2.404(5)	Ca2-O10	2.392(5)	Sr1-O30	2.57(1)	Sr2-O10	2.540(9)
Ca1-O40	2.405(5)	Ca2-O20	2.397(5)	Sr1-O40	2.547(8)	Sr2-O20	2.55(1)
O11-C11	1.250(8)	O51-C51	1.239(8)	O11-C11	1.24(1)	O51-C51	1.27(2)
C11-N11	1.341(8)	C51-N51	1.334(8)	C11-N11	1.33(1)	C51-N51	1.32(2)
N11-C12	1.335(8)	N51-C52	1.326(8)	N11-C12	1.33(1)	N51-C52	1.38(2)
C12-S1	1.725(7)	C52-S5	1.746(7)	C12-S1	1.73(1)	C52-S5	1.71(1)
O21-C21	1.269(8)	O61-C61	1.258(9)	O21-C21	1.25(1)	O61-C61	1.26(1)
C21-N21	1.311(8)	C61-N61	1.343(9)	C21-N21	1.33(1)	C61-N61	1.32(1)
N21-C22	1.329(8)	N61-C62	1.32(1)	N21-C22	1.32(1)	N61-C62	1.33(1)
C22-S2	1.757(7)	C62-S6	1.72(1)	C22-S2	1.75(1)	C62-S6	1.74(1)
O31-C31	1.254(8)	O71-C71	1.246(7)	O31-C31	1.27(1)	O71-C71	1.27(2)
C31-N31	1.316(8)	C71-N71	1.327(8)	C31-N31	1.33(1)	C71-N71	1.33(2)
N31-C32	1.325(9)	N71-C72	1.316(8)	N31-C32	1.33(1)	N71-C72	1.33(2)
C32-S3	1.732(7)	C72-S7	1.760(6)	C32-S3	1.75(1)	C72-S7	1.72(2)
O41-C41	1.247(9)	O81-C81	1.266(8)	O41-C41	1.24(2)	O81-C81	1.26(2)
C41-N41	1.321(9)	C81-N81	1.311(9)	C41-N41	1.33(2)	C81-N81	1.30(2)
N41-C42	1.340(9)	N81-C82	1.33(1)	N41-C42	1.33(2)	N81-C82	1.36(2)
C42-S4	1.744(7)	C82-S8	1.746(9)	C42-S4	1.74(1)	C82-S8	1.72(2)
Angles (°)							
S1-Au1-S5	173.25(7)	S2-Au2-S6	177.67(7)	S1-Au1-S5	173.1(2)	S2-Au2-S6	178.1(1)
S3-Au3-S7	178.64(7)	S4-Au4-S8	174.53(8)	S3-Au3-S7	177.3(1)	S4-Au4-S8	174.3(2)

Both complexes crystallize in the monoclinic space group Cc. In compound **8** and **9** the bond lengths between Ca^{2+} or Sr^{2+} and the donor atoms are in the expected region. The C=S bond lengths in the complexes are in the range between 1.72(1) - 1.760(6) Å and 1.71(1) - 1.75(5) Å, respectively. The C=O distances in the complexes are in the range between 1.239(8) - 1.269(8) Å and 1.24(1) - 1.27(2) Å, respectively. In the uncoordinated ligand these bonds are with 1.662(5) Å and 1.209(5) Å slightly shorter [149]. The C-N bonds next to the thiocarbonyl groups in complexes **8** and **9** are in the range of 1.316(8) - 1.340(9) Å and 1.32(1) - 1.38(2) Å, respectively. Thus, they are shorter than in the uncoordinated ligand (1.427(5) Å) [149]. These values correspond to the partial double bond characters of the C=S, C=O and C-N bonds and reflect the delocalization of electron density throughout of thiourea fragment in the complex. In complex **9**, the distances between the alkaline earth metal ions and the donor atoms are slightly larger than in complex **8**.

Compound **10** crystallizes in the monoclinic space group P2/n. Figure 19 depicts the molecular structure of **10**. Selected bond lengths and angles are shown in Table 8. Different to the coordination environments found in **8** and **9**, each barium ion is 9-coordinate. Two nitrogen donor atoms from the pyridine rings, five oxygen atoms from carbonyl groups, one bridging water molecule and one sulfur donor atom form a distorted tricapped trigonal prism as is shown in Figure 19. The distances between Ba^{2+} and the donor atoms are in the expected regions. A delocalized π-electron system within the organic ligands as is described for compounds **8** and **9** can also be observed in complex **10**.

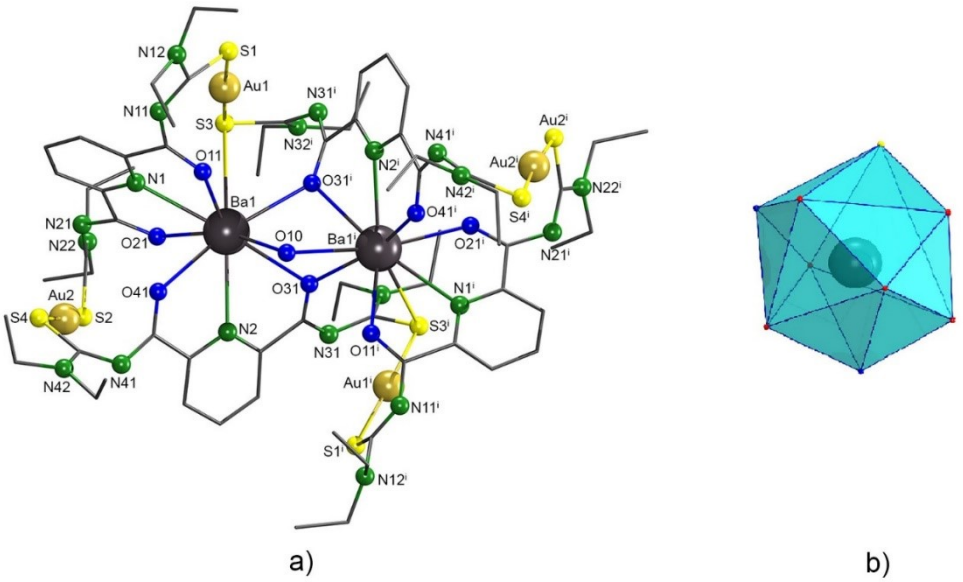

Figure 19: a) Molecular structure of the complex $[\{Ba_2(\mu\text{-}OH_2)\}\{Au(L4\text{-}\kappa S)\}_4]$. Hydrogen atoms are omitted for clarity. b) Polyhedron of the coordination environment of Ba^{2+}. Symmetry transformation used to generate equivalent atoms: ^{i} -x+3/2,y,-z+3/2.

Table 8: Selected bond lengths, angles and hydrogen interactions in [{$Ba_2(\mu\text{-}OH_2)$}{$Au(L4\text{-}\kappa S)$}$_4$].

Bond lengths (Å)							
Au1-S1	2.277(4)	Ba1-O11	2.781(7)	Ba1-O31	2.775(6)	Ba1-N1	2.917(7)
Au1-S3	2.304(3)	Ba1-O21	2.737(7)	Ba1-O31^{i}	2.854(6)	Ba1-N2	2.856(9)
Au2-S2	2.285(3)	Ba1···Ba1^{i}	4.429(1)	Ba1-O41	2.789(7)	Ba1-O10	2.896(7)
Au2-S4	2.272(3)	Au1···Ba1	4.086(8)	Ba1-S3	3.536(3)		
C11-O11	1.26(1)	C21-O21	1.24(1)	C31-O31	1.26(1)	C41-O41	1.25(1)
C11-N11	1.30(1)	C21-N21	1.36(1)	C31-N31	1.31(1)	C41-N41	1.34(1)
N11-C12	1.29(1)	N21-C22	1.33(1)	N31-C32	1.37(1)	N41-C42	1.32(1)
C12-S1	1.73(1)	C22-S2	1.73(1)	C32-S3	1.74(1)	C42-S4	1.73(1)

Angles (°)					
S1-Au1-S3	177.2(1)	S4-Au4-S2	174.3(1)	Ba1-O10-Ba1^{i}	99.8(3)

D-H…A	d(D…A) (Å)	<(DHA) (°)
O10-H10B...O20	2.77(1)	156(2)
O20-H20...O11	2.70(1)	156.3(1)
O30-H30...O41	2.91(2)	137.8(1)

Symmetry transformations used to generate equivalent atoms: ^{i} -x+3/2,y,-z+3/2.

In the solid state structure of **10**, a network of hydrogen bonds with OH···O distances ranging from 2.70(1) - 2.91(2) Å is stablished as is shown in Figure 20. The main interactions occur between the oxygen atoms of carboxamido groups with molecules of methanol, and the metal-bound water molecule and methanol. Theses hydrogen interactions are listed in Table 8.

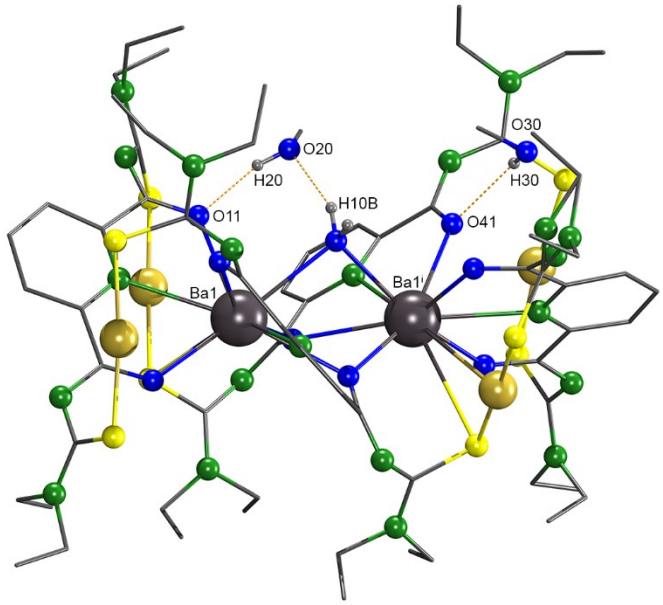

Figure 20: Hydrogen interactions in complex **10**.

2.5. Lanthanide Complexes with Trinuclear Gold(I) Coronand

Following the previous approach to implement metal ions into the cavity of the framework formed by Au^{+} ions and $\{L4\}^{2-}$ ligands, lanthanide ions have been included into the study. They usually occur in the oxidation state "+III". Trivalent lanthanide ions form stable complexes with a large variety of chelating ligands [156]. Bonding is preferable done via oxygen or nitrogen donor atoms [157]. H_2L4 shows a flexible coordination behaviour as is shown in Scheme 2. Depending on the coordination preferences of the metals, different donor atoms can be provided. Assuming that the sulfur donor will be occupied by the gold(I) ions, different tridentate donor sets can be provided by the host lanthanide ions: ONO, NNN or ONN [158].

2.5.1. Synthesis and Spectroscopy

The synthesis of the heteronuclear complexes was carried out in one-pot reactions. The neutral $[Ln\{Au(L4\text{-}\kappa S)\}_3]$ complexes (Ln = La, Ce, Nd, Sm, Eu, Gd, Tb, Dy, Ho, Er, Tm, Yb, Lu) were obtained by the reaction of lanthanide chlorides or nitrates with H_2L4 and [AuCl(THT)] in MeOH at room temperature in a ratio of 1:3:3. A clear solution was observed after approximately 30 minutes, except for the reaction containing Tm, Yb and Lu, which formed a colourless suspension. Then, Et_3N was added as a supporting base, and the reaction mixtures were stirred for two hours as is shown in Scheme 9. Most of the products could be isolated as colourless solids, except for the Ce^{3+} and Ho^{3+} compounds, which showed orange and light pink colours.

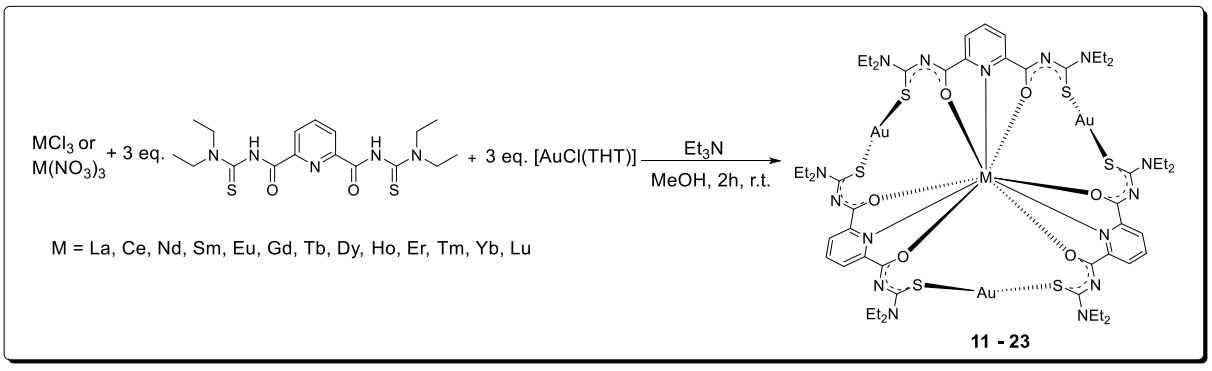

Scheme 9: Synthesis of lanthanide(III) complexes with the $[\{Au(L4\text{-}\kappa S)\}_3]^{3-}$ coronand.

The complexes have a uniform composition of $[Ln\{Au(L4\text{-}\kappa S)\}_3]$ (Ln = La: **11**, Ln = Ce: **12**, Ln = Nd: **13**, Ln = Sm: **14**, Ln = Eu: **15**, Ln = Gd: **16**, Ln = Tb: **17**, Ln = Dy: **18**, Ln = Ho: **19**, Ln = Er: **20**, Ln = Tm: **21**, Ln = Yb: **22**, and Ln = Lu: **23**). The complexes were characterized

by elemental analysis, IR and UV-vis spectroscopy, and ESI mass spectrometry. Complex **11** was additionally characterized by NMR spectroscopy.

The IR spectra of the complexes reveal a shift of the carbonyl stretching frequency ν(C=O) of H_2L4 by 100 cm^{-1} to lower frequencies to about 1685 cm^{-1}. This is again due to the delocalized π-electron system in the chelate rings. The absence of typical ν(NH) stretching vibrations in the region above 3200 cm^{-1} strongly suggests the double deprotonation of H_2L4.

The ^{1}H-NMR spectrum of complex **11** is characterized by the absence of an NH signal around 9 ppm. This indicates its deprotonation upon coordination. The protons of the methylene groups are non-equivalent, since they show three multiplets at 3.7, 3.5 and 3.4 ppm. This is due to the hindered rotation around the C-N bond, which has already been discussed for the alkaline earth metal complexes. The ^{13}C-NMR spectrum shows the signals in the expected region. The C=O and C=S signals in the complex appear at 185.7 and 166.7 ppm, while in the spectrum of H_2L4 they are found at 177.3 and 159.3 ppm, respectively. Thus, a downfield of approximately 8 ppm is observed upon coordination.

ESI mass spectra of the complexes were measured in order to provide additional evidence for the formation of compounds having a $[\{Au(L4\text{-}\kappa S)\}_3]^{3-}$ skeleton. The ESI^+ spectrum of **15** is clearly dominated by the molecular ion peak $[M + H]^+$ at *m/z* = 1924.2145 (calcd. 1924.2161). Figure 21 shows the ion molecular ion peak of this compound together with the calculated isotopic pattern. The experimental spectrum clearly reflects the natural isotope distribution of europium: ^{151}Eu (47.8%), ^{153}Eu (52.2%).

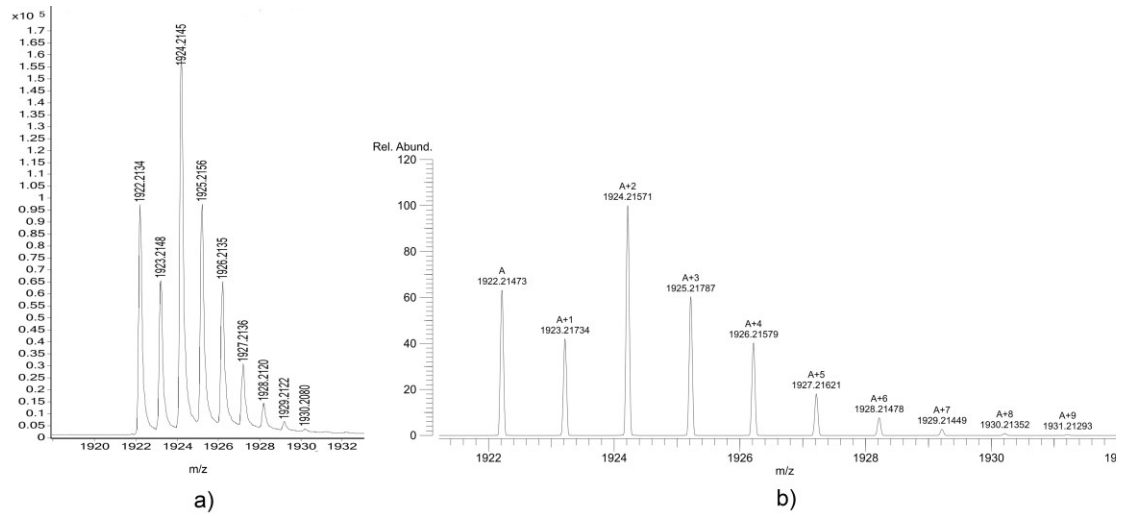

Figure 21: a) Molecular ion part of the experimental ESI^+ mass spectrum of $[Eu\{Au(L4\text{-}\kappa S)\}_3 + H]^+$ with peaks belonging to the natural isotope distribution of europium. b) Calculated spectrum for $[Eu\{Au(L4\text{-}\kappa S)\}_3 + H]^+$.

UV-vis spectra of the ligand and its gold(I) lanthanide complexes were recorded in CH_2Cl_2 at room temperature. The UV absorption for H_2L4 exhibits a broad and asymmetrical band at 256 nm. It can be assigned to a combination of $\pi \rightarrow \pi^*$ and $n \rightarrow \pi^*$ transitions (HOMO → LUMO) in the pyridine-dicarboxamide units [159]. The absorption spectra of [Ln{Au(L4-κS)}$_3$] complexes are similar for all studied Ln(III) ions, they reflect a nine-coordinate environment around the central atom [160]. The transitions appear at 309 nm and 264 nm, a LMCT band is localized at 226 nm. The complexes show higher molar absorption coefficients in comparison to the ligand due to the presence of three coordinated ligands (Table 9).

Table 9: Maximum absorption (λ_{max}) and molar absorption coefficients (ε) for H_2L4 and its [Ln{Au(L4-κS)}$_3$] complexes measured in CH_2Cl_2.

Compound	λ_{max}/nm (ε/10^{-4} M^{-1} cm^{-1})	Electron Configuration
H_2L4	230 (2.3); 256 (3.4); 360 (0.2)	—
[La{Au(L4-κS)}$_3$]	227 (15.6); 264 (10.4); 309 (8.3)	[Xe]4f^0
[Ce{Au(L4-κS)}$_3$]	228 (9.3); 265 (6.7); 308 (5.2)	[Xe]4f^1
[Nd{Au(L4-κS)}$_3$]	227 (7.2); 264 (4.9); 309 (3.8)	[Xe]4f^3
[Sm{Au(L4-κS)}$_3$]	228 (5.5); 264 (3.7); 310 (2.8)	[Xe]4f^5
[Eu{Au(L4-κS)}$_3$]	227 (8.8); 264 (5.9); 309 (4.4)	[Xe]4f^6
[Gd{Au(L4-κS)}$_3$]	227 (9.8); 263 (6.8); 309 (5.0)	[Xe]4f^7
[Tb{Au(L4-κS)}$_3$]	265 (7.9); 310(4.5)	[Xe]4f^8
[Dy{Au(L4-κS)}$_3$]	276 (7.3); 312 (6.1)	[Xe]4f^9
[Ho{Au(L4-κS)}$_3$]	265(5.3); 310 (3.4)	[Xe]4f^{10}
[Er{Au(L4-κS)}$_3$]	227 (5.8); 264 (3.9); 309 (2.7)	[Xe]4f^{11}
[Tm{Au(L4-κS)}$_3$]	265 (6.3); 310 (4.6)	[Xe]4f^{12}
[Yb{Au(L4-κS)}$_3$]	227 (12.8), 264 (8.5); 309 (6.0)	[Xe]4f^{13}
[Lu{Au(L4-κS)}$_3$]	274 (1.8); 310 (1.4)	[Xe]4f^{14}

2.5.2. Crystal and Molecular Structures

The molecular structures of the [Ln{Au(L4-κS)}$_3$] complexes have been determined by X-ray diffraction analysis. Most of the complexes crystallize in the trigonal space group $P\bar{3}$, while the [Tm{Au(L4-κS)}$_3$] complex crystallizes in the monoclinic space group C2/c and [Lu{Au(L4-κS)}$_3$] in the triclinic space group $P\bar{1}$. The asymmetric units of the trigonal

structures contain one third of the lanthanide complexes and disordered solvent molecule (CH_2Cl_2 or $CHCl_3$). Figure 22 shows the molecular structure of the europium complex **15** as a representative for this class of complexes and relevant bond lengths and angles are given in Table 10. The Eu(III) ion is situated on a 3-fold axis, three gold atoms occupy the corners of the "virtual" triangle and three ligands $\{L4\}^{2-}$ are positioned along the edges. The lanthanide ion is coordinated by the nitrogen atom of the pyridine ring and two oxygen atoms of the carboxamide groups of each deprotonated $\{L4\}^{2-}$ ligand. This leads to a coordination number of 9. No coordinated solvent molecules are observed in the lanthanide complexes. All of these complexes contain three linear coordinated gold atoms comprising six Au-S bonds.

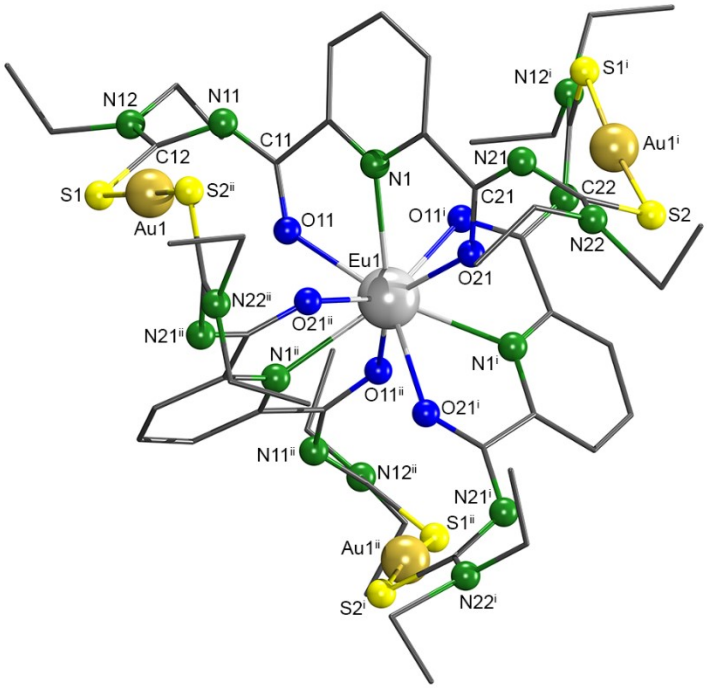

Figure 22: Molecular structure of the complex [Eu{Au(L4-κS)}$_3$]. The hydrogen atoms are omitted for clarity. Symmetry transformations used to generate equivalent atoms: ^{i} -x+y+1,-x+1,z ^{ii} -y+1,x-y,z.

A considerable lengthening of the C=O and C=S bonds upon coordination to the metal ions is observed in all [Ln{Au(L4-κS)}$_3$] complexes. The averages of C=O and C=S bond lengths are 1.259 Å and 1.742 Å, while in the uncoordinated ligand these values are 1.209(5) Å and 1.662(5) Å [149]. On the other hand, a shortening of the C-N bonds next to the thiocarbonyl moieties is observed. The average for these C-N bonds is 1.336 Å in the complexes, whereas the mean value of the same bonds in H_2L4 is 1.425 Å [149]. The bond values range between

typical carbon-nitrogen single and double bonds and the bond lengths reflect considerable delocalization of electron density in the $\{L4\}^{2-}$ ligand.

The coordination polyhedron around the lanthanide(III) ions can be described as a distorted tricapped trigonal prism. Three ligand molecules are arranged in a helical fashion with six oxygen donor atoms from the carboxamide groups occupying the vertices of the trigonal prism. The three nitrogen atoms occupy the equatorial plane as is seen in Figure 23. Analogous helical complexes with similar coordination evironment have already been reported [161 - 164].

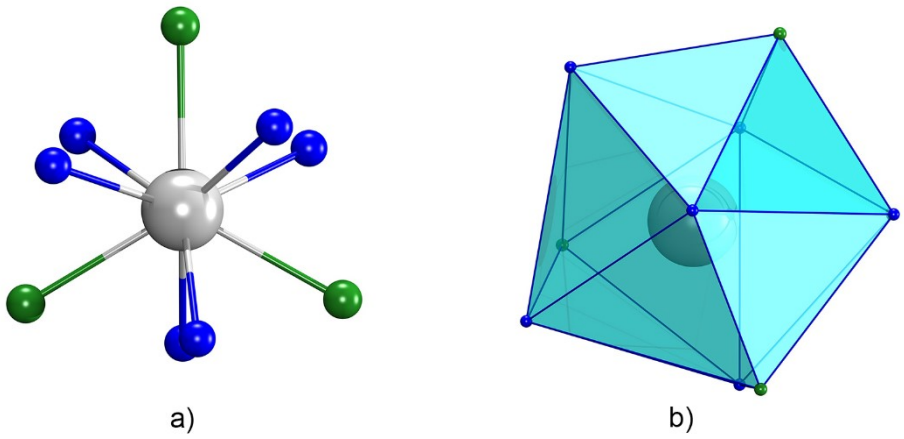

Figure 23: a) Nitrogen atoms (green) are in the vertices of a triangle. b) The coordination polyhedron around the lanthanide(III) ions that forms a distorted tricapped trigonal prism.

Moving from compound **11** to compound **23**, the Ln-N bond lengths decrease from 2.661(5) Å to 2.437 Å, respectively, and the average Ln-O bond lengths decreases from 2.537 Å for compound **11** to 2.356 Å for compound **23**. These bond lengths are in accordance with previously reported Ln-pyridine-dicarboxamide compound [165, 166]. In the lanthanide series, the ionic radii are determined by the nuclear charge and by the number of electrons in the electronic shells, that also affect the atomic size. There is a trend that the size decreases from La to Lu with coordination number 9, they have ionic radii of 1.216 and 1.032 Å, respectively. This is due to the lanthanide contraction effect [167].

Table 10: Selected bond lengths, angles and intermetallic separations between Ln-Au, Au-Au in Å.

	Bond lengths (Å)											
	11 (La)	**12** (Ce)	**13**(Nd)	**14** (Sm)	**15** (Eu)	**16** (Gd)	**17** (Tb)	**18** (Dy)	**19** (Ho)	**21** (Tm)	**22** (Yb)	**23** (Lu)
Ln-N1	2.661(5)	2.629(5)	2.594(5)	2.550(7)	2.542(9)	2.532(6)	2.513(3)	2.496(9)	2.488(4)	2.455(4)	2.46(1)	2.448(6)
Ln-O11	2.559(4)	2.524(5)	2.503(5)	2.469(6)	2.416(8)	2.408(5)	2.436(3)	2.417(7)	2.418(3)	2.342(3)	2.372(9)	2.393(5)
Ln-O21	2.514(5)	2.477(5)	2.460(5)	2.430(6)	2.454(7)	2.449(5)	2.391(3)	2.381(8)	2.371(4)	2.378(3)	2.343(9)	2.364(5)
Au1-S1	2.272(2)	2.273(2)	2.279(2)	2.274(2)	2.289(3)	2.291(2)	2.277(1)	2.279(3)	2.281(1)	2.287(2)	2.274(3)	2.268(2)
Au1-S2	2.280(2)	2.285(2)	2.290(2)	2.285(3)	2.278(3)	2.277(2)	2.288(1)	2.292(3)	2.294(2)	2.284(1)	2.291(4)	2.282(2)
C11-O11	1.259(7)	1.268(8)	1.268(8)	1.26(1)	1.26(1)	1.253(9)	1.256(4)	1.25(1)	1.255(6)	1.261(5)	1.26(2)	1.239(9)
C11-N11	1.312(8)	1.309(8)	1.315(8)	1.32(1)	1.32(1)	1.329(9)	1.319(5)	1.32(1)	1.317(6)	1.313(6)	1.30(2)	1.333(1)
N11-C12	1.347(8)	1.336(9)	1.335(8)	1.32(1)	1.34(2)	1.34(1)	1.333(5)	1.34(1)	1.338(6)	1.356(6)	1.33(2)	1.282(1)
C12-S1	1.741(6)	1.746(7)	1.746(7)	1.754(9)	1.74(1)	1.739(9)	1.740(4)	1.74(1)	1.741(5)	1.729(6)	1.76(2)	1.773(9)
C21-O21	1.273(8)	1.261(8)	1.265(8)	1.26(1)	1.27(1)	1.256(8)	1.255(5)	1.25(1)	1.256(7)	1.251(6)	1.25(2)	1.255(9)
C21-N21	1.319(8)	1.312(9)	1.333(9)	1.32(1)	1.32(1)	1.316(9)	1.321(5)	1.33(2)	1.320(7)	1.323(6)	1.32(2)	1.338(9)
N21-C22	1.34(1)	1.34(1)	1.35(1)	1.34(1)	1.34(1)	1.329(9)	1.340(6)	1.32(2)	1.337(8)	1.325(6)	1.33(3)	1.327(1)
C22-S2	1.746(8)	1.734(9)	1.744(9)	1.73(1)	1.74(1)	1.749(7)	1.742(5)	1.74(1)	1.748(7)	1.748(5)	1.73(2)	1.737(9)
Au···Ln	5.069(5)	5.012(3)	5.011(7)	4.969(6)	4.950(7)	4.940(4)	4.920(5)	4.906(8)	4.895(4)	4.784(5)	4.857(7)	4.869(3)
Au···Au	8.776(8)	8.678(4)	8.675(7)	8.605(9)	8.572(1)	8.550(5)	8.516(5)	8.495(1)	8.473(5)	8.578(7)	8.407(8)	8.203(1)
	Angles (°)											
S1-Au1-S2	172.8(9)	173.86(9)	173.61(9)	173.9(1)	174.2(1)	174.1(1)	173.98(5)	174.4(2)	174.26(7)	176.82(6)	174.4(2)	175.8(1)

2.5.3. Luminescence Properties of the Eu Compound

The Eu^{3+} compound shows fluorescence under UV light at 365 nm. Thus, a more detailed study has been performed. The fluorescence of rare earth complexes is a known phenomenon. Binnemans [157], Görrler-Walrand [168], Bünzli [169, 170], Carnall [171, 172], Judd [173], and Ofelt [174] are the main contributors to the understanding of the emission spectra of lanthanide complexes. In a recent paper, Binnemans [175] has published a detailed report entitled "Interpretation of europium(III) spectra". Herein, the fluorescence properties of Eu^{3+} will be discussed regarding the influence of site symmetry in the compounds.

As seen in Figure 24.a, the [Eu{Au(L4-κS)}$_3$] complex was measured in CH_2Cl_2 at room temperature with 300 mm^{-1} of grating. The europium(III) spectrum is composed of the red luminescence of the Eu^{3+} ion, which is a result of transitions from the first excited state ($^5D_0$) to all the lower J levels of the ground term ^7F_J (J = 0-4) [176]. Emission bands can be observed at 16835, 16207, 15290 and 14205 cm^{-1}, which are attributed to the f-f transitions $^5D_0 \rightarrow {}^7F_1$, $^5D_0 \rightarrow {}^7F_2$, $^5D_0 \rightarrow {}^7F_3$ and $^5D_0 \rightarrow {}^7F_4$, respectively. Transitions arising from $^5D_1$ are not observed or they are too week for a detailed study.

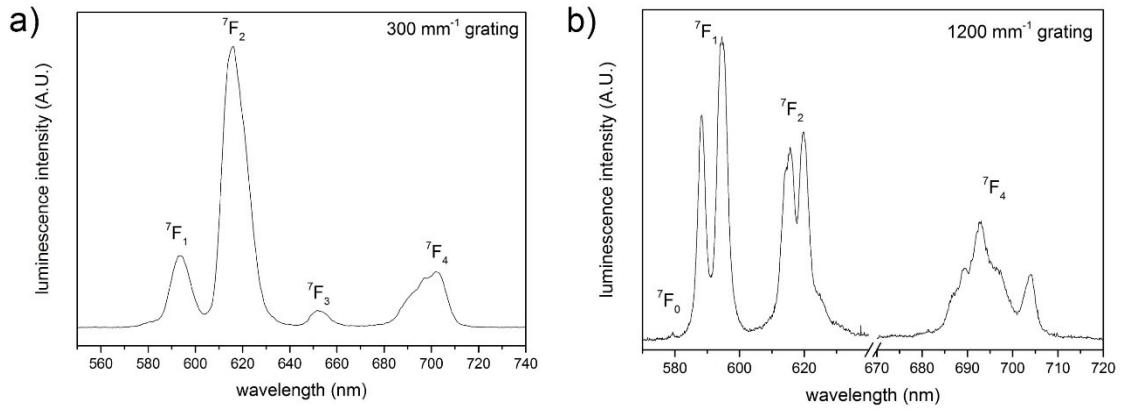

Figure 24: Emission spectrum of [Eu{Au(L4-κS)}$_3$]; excitation with λ_{ex} = 396 nm radiation with a) 300 mm^{-1} and b) 1200 mm^{-1} grating.

In the first transition, $^5D_0 \rightarrow {}^7F_1$, the selection rules forbid an electric-dipole, but allow a magnetic-dipole transition [171]. The $^5D_0 \rightarrow {}^7F_2$ transition is a so-called "*hypersensitive transition*", which indicates that the intensity is influenced by the environment of the europium(III) ion and the nature of the ligand [161]. This means, the high intensity is attributed to a low symmetry around the Eu^{3+} ion. The explanation for the high intensity of

this transition is the presence of highly polarizable ligands, especially in compounds with chelating rings, such as ß-diketonates or DPA (2,6-pyridinedicarboxylate = dipicolinate) ligands, which are similar to H_2L4 [177]. An extremely weak absorption at 15290 cm^{-1} is attributed to a forbidden $^5D_0 \rightarrow {}^7F_3$ transition. The intensity of the $^5D_0 \rightarrow {}^7F_4$ transition can be compared to the $^5D_0 \rightarrow {}^7F_1$. It is determined by the chemical composition of the host matrix, however it is not hypersensitive.

According to Binnemans [157, 175], the spectroscopic data provide information about the point group symmetry of the Eu^{3+} ion. The absorption and emission spectroscopy have been used for the determination of the coordination number, the nature of bonding, and the symmetry around the lanthanide ions [178, 179]. Thus, the site symmetry determination is an important tool to corroborate with single crystal X-ray studies. With the increasing of the resolution of the emission spectrum to 1200 mm^{-1} grating, as is seen in Figure 23.b, a band is observed in the region of the $^5D_0 \rightarrow {}^7F_0$ transition, but its intensity is very low and, thus, this transition can be regarded as forbidden. The $^5D_0 \rightarrow {}^7F_1$ transition is the most intense one. It consists of two strong lines, where the lower frequency is splitted into two components. The $^5D_0 \rightarrow {}^7F_2$ transition consists of a relatively intense band, with the higher frequency being splitted into two lines. A shoulder is observed in the second one. No band is observed in the region of $^5D_0 \rightarrow {}^7F_3$ transitions, while two broad bands of medium intensity appear in the region of the $^5D_0 \rightarrow {}^7F_4$ transition. The highest frequency band is split into 5 lines, although it is quite difficult to determine their exact positions, and the second one is split into two lines. The same conclusions can be drawn from the luminescence spectrum.

2.6. Sc^{3+}, In^{3+} and Ga^{3+} Complexes with Gold(I) Coronands

Following the same approach as for the lanthanide compounds, the use of other trivalent metal ions might give an idea what the driving force for the formation of the structure of these multinuclear products is. Scandium(III), indium(III) and gallium(III) were chosen because of the differences in size (Ga^{3+}: 0.62 Å; Sc^{3+}: 0.74 Å, In^{3+}: 0.80 Å for C.N. = 6 each) and their preferred coordination numbers [180].

A few structures with ligands containing pyridine-2,6-dicarboxylic acid with group 13 metal ions have been reported, and nothing has been described with Sc(III) so far [181]. In this section, the complexation of the metal ions Sc^{3+}, In^{3+} and Ga^{3+} with $\{Au(L4\text{-}\kappa S)\}^-$ assemblies will be discussed. For gallium(III), coordination numbers of 4, 5 or 6 have been reported, while indium(III) adopts coordination number between 4 and 12 in its complexes

[181, 182]. Scandium(III) frequently exhibits coordination numbers such as 6, 7, 8 and 9 [183 - 187].

2.6.1. Synthesis and Spectroscopy

The syntheses of the complexes were carried out in one-pot reactions of H_2L4 with Sc^{3+}, In^{+3} or Ga^{3+} salts and [AuCl(THT)] in methanol at room temperature. They resulted in colourless solutions, except for the synthesis of $[Ga\{Au(L4\text{-}\kappa S)\}_2](NO_3)$, which gave colourless suspensions. The reactions have been performed first with a {3:1:3} molar ratio of the reactants. Later, the ratio for the gallium compound was optimized with respect to the composition of the product obtained from the first reaction. The addition of Et_3N gave colourless solids. The low solubility of the gallium-containing product in MeOH is a strong hint for the formation of an ionic compound. Attempts to force the precipitation with PF_6^- as counterion failed. Finally, the product was crystallized as NO_3^- salt with 63 % yield, while the other compounds were obtained with approximately 80 % yield (Scheme 10). Single crystals suitable for X-ray diffraction analysis were obtained by slow diffusion of MeOH into CH_2Cl_2 solutions.

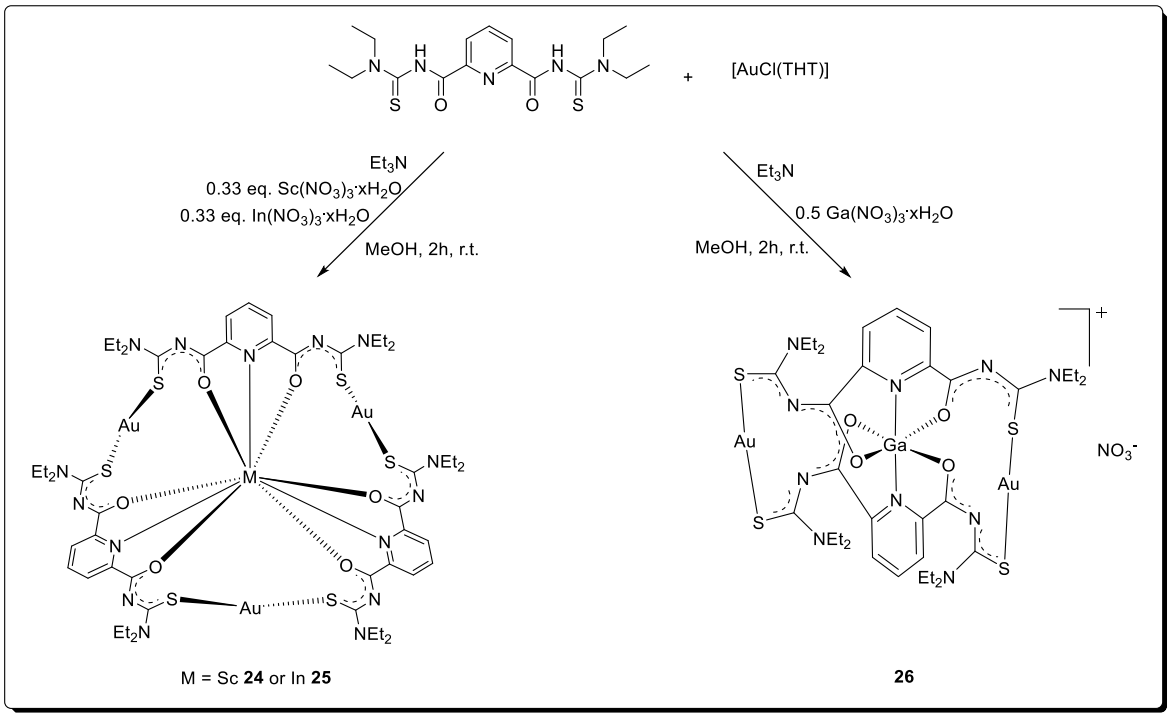

Scheme 10: Synthesis of coronand complexes with Sc^{3+}, Ga^{3+} and In^{3+} ions.

The complexes were characterized by elemental analysis, IR, NMR spectroscopy and ESI mass spectrometry. X-ray structural analysis revealed the trimeric complexes, [Sc{Au(L4-κS)}$_3$] **24** and [In{Au(L4-κS)}$_3$] **25**, while the dimeric, cationic complex [Ga{Au(L4-κS)}$_2$](NO$_3$) **26** is formed from the reaction with gallium nitrate.

The IR spectra of compounds **24**, **25,** and **26** show a strong band in the 1590 - 1595 cm^{-1} region due to the ν(C=O) stretches. A bathochromic shift of 80 - 95 cm^{-1} with respect to the uncoordinated ligand indicates a delocalized π-electron system and, thus, the involvement of the oxygen atom of amide in the coordination to the central metal ions. No absorption bands for typical ν(NH) stretches in the region above 3200 cm^{-1} are observed. This indicates the double deprotonation of H$_2$L4 during the complex formation. A broad, strong band at 845 - 833 cm^{-1} in the spectrum of compound **26** can be assigned to the stretching vibrations of the NO$_3^-$ counterion.

The ^{1}H-NMR spectra of complexes are consistent with the presence of {L4}$^{2-}$ and shows the signals in the expected regions. A broad signal at 1.10 ppm is assigned to the methyl protons, and two multiplet signals at 3.45 and 3.73 ppm are assigned to the methylene protons. This indicates the hindered rotation of the terminal C-NR$_2$ bond of the {R$_2$N-C(S)-} fragment. This phenomenon was previously reported by Hoyer and co-workers, where the authors have elucidated this hindered rotation for *N,N*-dialkylbenzoyl-thiourea and its complexes [154]. The ^{13}C-NMR spectra of complexes show signals in the expected regions. The C=O and C=S signals are downfield shifted by 6 and 3 ppm in the spectra of complexes **25** and **26**, respectively, and about 7 ppm in the spectrum of complex **24** in comparison with H$_2$L4. The ^{45}Sc-NMR spectrum of complex **24** shows a chemical shift at 7.2 ppm, which is downfield shifted in comparison with chemical shift of the Sc(NO$_3$)$_3$·nH$_2$O starting material (-18.5 ppm) [188]. This might be explained by the change of the coordination number from 6 to 9 in the resulting complex.

The ESI$^+$ mass spectrum of **24** is dominated by the molecular ion peak [M + H]$^+$ at *m/z* = 1816.2544 (calcd. 1816.2508). The spectrum of complex **25** shows the main peak at *m/z* = 1295.1023 (calcd. 1295.0956), which indicates the formation of a dimeric [M - {Au(L4)}]$^+$ ion. This reflects that the compound **25** in solution resembles with its family neighbour Ga^{3+} [182]. The ESI$^+$ MS spectrometry of **26** shows the signal of the molecular cation [M]$^+$ at *m/z* = 1249.1341 (calcd. 1249.1168).

2.6.2. Crystal and Molecular Structures

The X-ray diffraction analysis reveals that the compounds **24** and **25** are neutral and isostructural. The molecular structure of **24** is presented in Figure 25. A summary of the selected bond lengths and bond angles is presented in Table 11. In both complexes, the three potentially pentadentate ligands bind to the central M^{3+} ion by their $\{O,N,O\}$ donor atom sets. This brings the metal ions inside the cavity, comprising three M-N and six M-O bonds. The coordination mode is the same as for the lanthanide complexes.

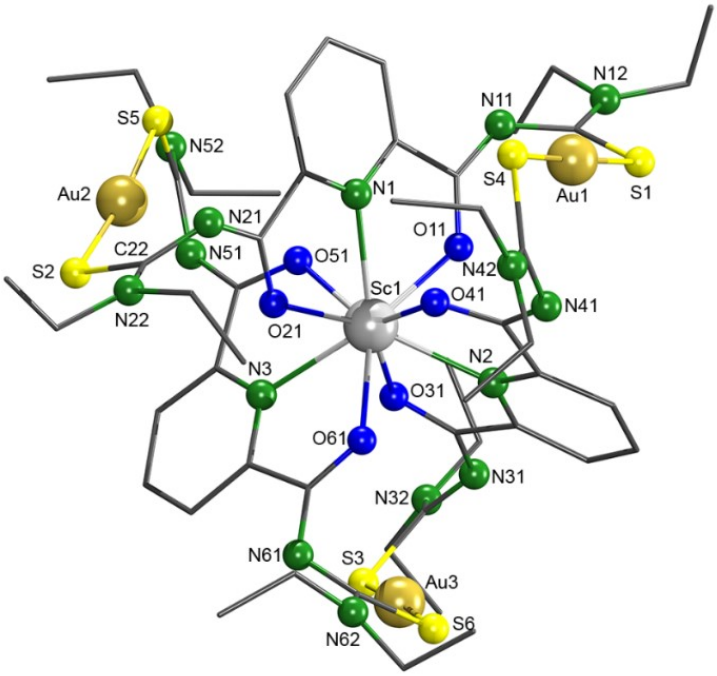

Figure 25: Molecular structure of $[Sc\{Au(L4\text{-}\kappa S)\}_3]$. Hydrogen atoms are omitted for clarity.

The chemistry of scandium is often reported to be similar to that of the lanthanides, particularly to the Lu^{3+} ion [189]. Thus, it is not surprising that the Sc^{3+} complex of this work well resembles the structural chemistry of the previously discussed lanthanide compounds. The complexes additionally contain three gold atoms in a linear coordination by sulfur atoms of the $\{L4\}^{2-}$, comprising six S-Au bonds. The ligands are arranged helically producing pseudo-D_3 triple helical structures. The scandium and indium metal ions are nine-coordinate and possess distorted tricapped trigonal prismatic coordination polyhedra as is shown in Figure 26.

Table 11: Selected bond length and angles in [Sc{Au(L4-κS)}$_3$] and [In{Au(L4-κS)}$_3$].

Bond lengths (Å)							
Au1-S1	2.289(6)	Au1-S4	2.284(6)	Au1-S1	2.287(1)	Au1-S3*	2.412(6)
Au2-S2	2.281(6)	Au2-S5	2.292(6)	Au2-S2	2.288(1)	Au2-S2^{i}	2.288(1)
Au3-S3	2.292(6)	Au3-S6	2.277(6)				
Sc1-O21	2.291(2)	Sc1-O31	2.221(2)	In1-O21	2.353(2)	In1-O31	2.389(3)
Sc1-N1	2.350(2)	Sc1-O41	2.292(2)	In1-N1	2.334(3)	In1-O11^{i}	2.321(2)
Sc1-N2	2.350(2)	Sc1-O51	2.294(2)	In1-N2	2.327(5)	In1-O21^{i}	2.353(2)
Sc1-N3	2.366(2)	Sc1-O61	2.316(2)	In1-N1^{i}	2.334(3)	In1-O31^{i}	2.389(3)
Sc1-O11	2.248(2)			In1-O11	2.321(2)		
C11-O11	1.260(3)	C41-O41	1.260(2)	C11-O11	1.259(4)		
C11-N11	1.320(3)	C41-N41	1.321(3)	C11-N11	1.317(4)		
N11-C12	1.348(3)	N41-C42	1.336(3)	N11-C12	1.360(5)		
C12-S1	1.736(2)	C42-S4	1.750(2)	C12-S1	1.733(4)		
C21-O21	1.253(3)	C51-O51	1.257(2)	C21-O21	1.253(4)		
C21-N21	1.323(3)	C51-N51	1.326(3)	C21-N21	1.322(5)		
N21-C22	1.327(3)	N51-C52	1.339(3)	N21-C22	1.321(5)		
C22-S2	1.749(2)	C52-S5	1.754(2)	C22-S2	1.760(4)		
C31-O31	1.264(2)	C61-O61	1.248(2)	C31-O31	1.253(5)		
C31-N31	1.315(3)	C61-N61	1.327(3)	C31-N31	1.312*		
N31-C32	1.351(3)	N61-C62	1.315(3)	N31-C32	1.36*		
C32-S3	1.742(2)	C62-S6	1.761(2)	C32-S3	1.747*		
Angles (°)							
S1-Au1-S4		176.61(2)		S1-Au1-S3		174.95*	
S2-Au2-S5		174.16(2)		S2-Au2-S2^{i}		168.44(6)	
S3-Au3-S6		175.91(2)					

Symmetry transformations used to generate equivalent atoms: ^{i} -x,y,-z+1/2.
* Average of values taken from the disordered part of the structure.

The average values of the Sc-O and Sc-N distances are 2.277 Å and 2.355 Å, which agrees with the values found in the nine-coordinate complex [Sc(terpy)(NO$_3$)$_3$] with the tridentate ligand terpyridyl (terpy) [184]. The C=S and C=O distances in [Sc{Au(L4-κS}$_3$] are in the range of 1.736(2) - 1.761(2) Å and 1.248(2) - 1.264(2) Å, respectively. The same lengthening of the C=S and C=O bonds and shortening of the C-N bonds due to the electron delocalization as described for the lanthanide complexes can be observed here. The average of the In-O bond lengths is 2.354 Å and that of the In-N bonds 2.331 Å. Both In-O and In-N

distances are in good agreement with the values found in $[Hg_2In(L4)_3]Cl$ [165]. This compound also shows a tricapped trigonal prismatic coordination geometry around the indium ion.

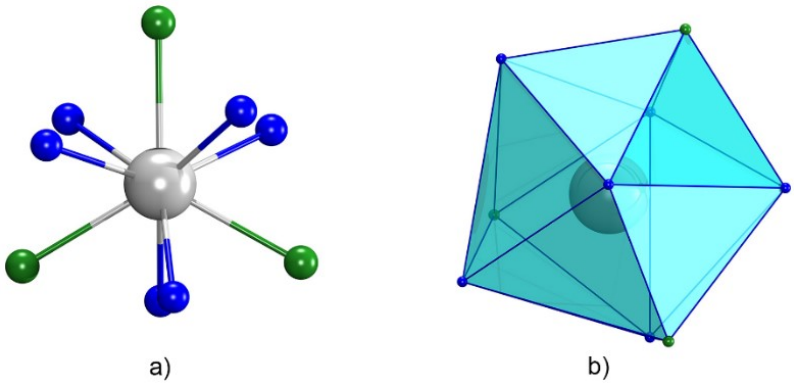

Figure 26: a) Nitrogen atoms (green) are in the vertices of a triangle. b) The coordination polyhedron around the Sc(III) or In(III) ions in [M{Au(L4-κS)] complexes, which form tricapped trigonal prism.

In contrast to the reactions with Sc^{3+} and In^{3+} ions, the reaction with $Ga(NO_3)_3$ gave a complex with only two $\{Au(L4\text{-}\kappa S)\}^-$ units. The difference to compounds **24** and **25** is most probably due to the smaller ionic radius of Ga(III) of 0.62 Å in comparison to Sc(III) and In(III) (0.74 and 0.80 Å) [180]. Suitable single crystals for X-ray diffraction have been obtained by slow diffusion MeOH into a $CHCl_3/CH_2Cl_2$ solution of the gallium complex. The structure of the complex **26** is shown in Figure 27.

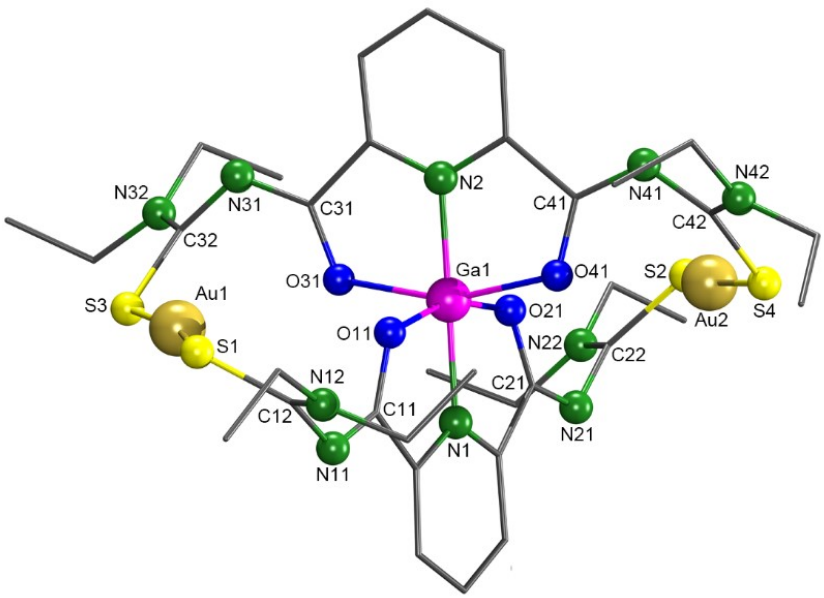

Figure 27: Molecular structure of the complex cation $[Ga\{Au(L4\text{-}\kappa S)\}_2]^+$. Hydrogen atoms are omitted for clarity.

The compound crystallizes in the monoclinic space group $P2_1/c$. The gallium(III) ion is coordinated by the oxygen and nitrogen donor atoms of two $\{L4\}^{2-}$ ligands. This results in an octahedral coordination environment around the gallium ion. Due to its small size and high charge, Ga^{3+} can be regarded as a hard Lewis acid and preferably binds to oxygen donor atoms [190].

The ligands are coordinated to the Ga(III) ion in a conformation which provides the maximum of oxygen donor sites to form a cationic $[Ga\{Au(L4\text{-}\kappa S)\}_2]^+$ complex. The coordination environment of the Ga(III) ion comprises two pyridine nitrogen atoms in *trans* position to each other and four oxygen donors. The cationic complex has additionally two gold atoms in a linear coordination by sulfur atoms of the $\{L4\}^{2-}$ ligands. Table 12 lists selected bond lengths and angles of complex **26**.

Table 12: Selected bond lengths and angles in $[Ga\{Au(L4\text{-}\kappa S)\}_2](NO_3)$.

Bond lengths (Å)							
Au1-S1	2.276(1)	Au1-S3	2.268(1)	Au2-S2	2.278(1)	Au2-S4	2.281(1)
Ga1-N1	1.955(3)	Ga1-N2	1.953(3)				
Ga1-O11	1.990(3)	Ga1-O21	1.979(3)	Ga1-O31	1.988(3)	Ga1-O41	2.014(3)
C11-O11	1.296(5)	C21-O21	1.283(5)	C31-O31	1.287(5)	C41-O41	1.282(5)
C11-N11	1.289(5)	C21-N21	1.296(6)	C31-N31	1.290(5)	C41-N41	1.285(5)
N11-C12	1.370(5)	N21-C22	1.380(5)	N31-C32	1.377(5)	N41-C42	1.373(5)
C12-S1	1.730(4)	C22-S2	1.733(5)	C32-S3	1.722(4)	C42-S4	1.732(5)

Angles (°)					
S1-Au1-S3	167.29(4)	N1-Ga1-O11	80.2(1)	N1-Ga1-O31	100.2(1)
S2-Au2-S4	166.76(4)	N1-Ga1-O21	79.9(1)	N1-Ga1-O41	100.4(1)
N1-Ga1-N2	178.4(1)	N2-Ga1-O11	98.3(1)	N2-Ga1-O31	80.2(1)
O11-Ga1-O41	92.6(2)	N2-Ga1-O21	101.7(1)	N2-Ga1-O41	79.3(1)
O21-Ga1-O31	93.2(1)	O11-Ga1-O21	160.0(1)	O31-Ga1-O41	159.4(1)
		O11-Ga1-O31	90.5(1)	O21-Ga1-O41	90.8(1)

The average of the bond lengths between Ga-O and Ga-N atoms are 1.995 and 1.954 Å, respectively. These values are very close to those found in $[Ga(pydc)_2]^-$ (Hpydc = pyridine-2,6-dicarboxylic acid) [191].

The C=S and C=O bonds are lengthened upon coordination of $\{L4\}^{2-}$ to the metal ion. They range between 1.722(4) and 1.733(5) Å (C=S) and 1.282(5) - 1.296(5) Å (C=O),

respectively. The same bonds in the uncoordinated H_2L4 are 1.662(2) and 1.216(2) Å [149]. The C-N bond lengths next to the thiocarbonyl groups are in the range of 1.370(5) - 1.380(5) Å. Thus, they are shorter than in the uncoordinated ligand (1.427(5) Å) [149]. These values correspond to the partial single and double bond character of the C=S, C=O and C-N bonds, which can readily be explained by the delocalization of electron density throughout the thiourea fragment of the complex.

2.7. Gold(I) Complexes with Six-coordinate M^{II} ions (M = Mn, Fe, Co, Ni, Cu, Zn, Hg)

Concluding the results of the experiments undertaken with Sc^{3+}, In^{3+} and Ga^{3+} ions, reactions with mixtures of transition metal (M = Mn, Fe, Co, Ni, Cu, Zn, or Hg) and gold(I) ions were expected to give similar mixed-metal complexes with $\{Au(L4\text{-}\kappa S)\}^-$ coronands.

2.7.1. Synthesis and Spectroscopy

The complexes were synthesized by reactions of one equivalent of $Fe(SO_4)_2 \cdot 7H_2O$, $Fe(acac)_3$, $HgCl_2$, $Cu(OAc)_2 \cdot H_2O$, $Zn(OAc)_2 \cdot 2H_2O$, or $M(OAc)_2 \cdot 4H_2O$ (M = Mn, Co or Ni) with two equivalents of H_2L4 and an equimolar amount of [AuCl(THT)] in 5 mL of MeOH. The reactions could be followed by the change of the colours of the reaction mixtures. After 30 minutes of stirring at room temperature, clear solutions were obtained. Et_3N was then added as a supporting base, affording the precipitation of the respective compounds. The only exception was the $[Hg\{Au(L4\text{-}\kappa S)\}_2]$ complex, which stayed in solution and was crystallized by slow evaporation of the solvent. The other compounds were recrystallized by slow diffusion of MeOH into the corresponding CH_2Cl_2 solutions.

In the synthesis, which was carried out with $Fe(acac)_3$, the reduction of Fe^{3+} to Fe^{2+} is observed, that might be caused by the ligand. The reaction starting from Fe(II) sulfate and Fe(III) acetylacetonate both result in blue precipitates. The solids were recrystallized and the X-ray crystal analysis diffraction confirmed the formation of identical, dimeric structures.

Scheme 11 shows the three coordination modes of the ligand $\{L4\}^{2-}$, which were observed in the obtained transition metal complexes. Type **I** is the preferred coordination mode for the most of the used transition metals. The obtained transition metal complexes are composed of a $\{Au_2(L4\text{-}\kappa S)_2\}^{2-}$ metallacycle, which accommodates the transition metal ion in its cavity. The products have the compositions $[Mn\{Au(L4\text{-}\kappa S)\}_2]$ **27**, $[Fe\{Au(L4\text{-}\kappa S)\}_2]$ **28**, $[Co\{Au(L4\text{-}\kappa S)\}_2]$ **29**, $[Ni\{Au(L4\text{-}\kappa S)\}_2]$ **30**, $[Cu\{Au(L4\text{-}\kappa S)\}_2]$ **31**, $[Zn\{Au(L4\text{-}\kappa S)\}_2]$ **32**,

and [Hg{Au(L4-κS)}$_2$] **33**. They were characterized and analysed by elemental analysis, IR and UV-vis spectroscopy and ESI mass spectrometry. Additionally, complex **31** was characterized by EPR spectroscopy, and complex **33** was characterized by NMR spectroscopy. All the complexes were structurally characterized by single crystal X-ray diffraction analysis.

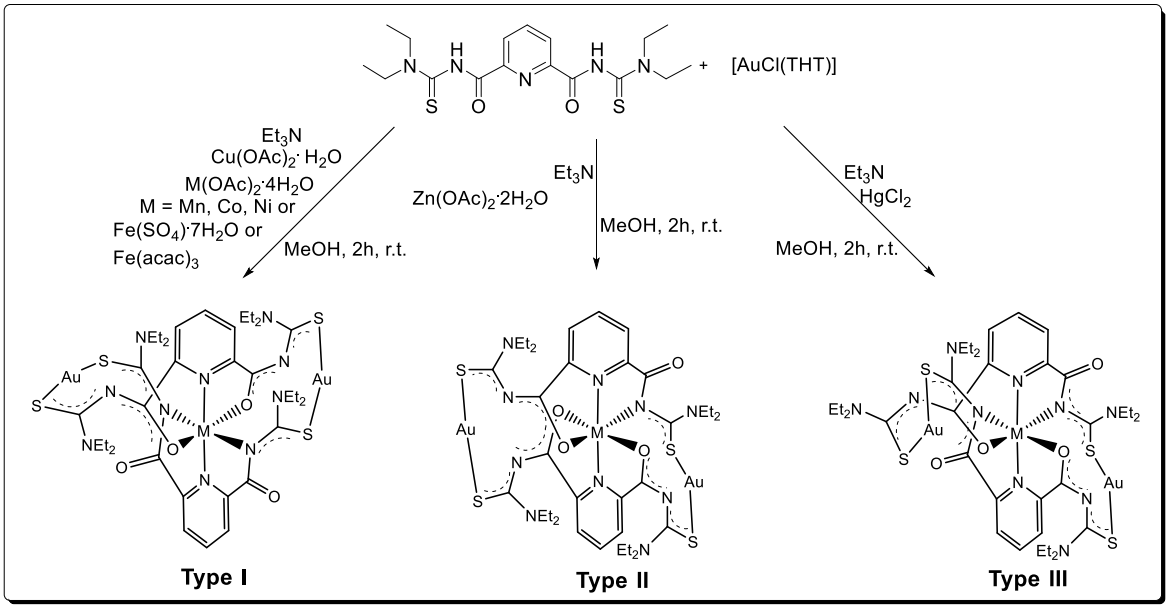

Scheme 11: Synthesis of $\{Au_2(L4\text{-}\kappa S)_2\}^{2+}$ metallacycles with divalent transition metal ions.

The IR spectra of the complexes **27** - **33** do not show ν(N-H) stretches in the region above 3200 cm^{-1}. This is a clear indication for the deprotonation of the amide group of H_2L4. Moreover, the ν(C=O) stretching vibrations of the carboxamide groups in the complexes displays two bands around 1630 and 1590 cm^{-1}, the later one represents a shift of about 100 cm^{-1} to lower wavenumbers in comparison to the uncoordinated ligand. The IR spectrum of complex **33** shows a splitting of the ν(C-N) stretch at 1577 and 1554 cm^{-1}. This may be due to a distorted coordination polyhedron around Hg^{2+} affording different Hg-O and Hg-N distances and consequently two different C=O and C-N bonds.

In the ^{1}H-NMR spectrum of compound **33**, the methylene and methyl groups give broad signals, which is a consequence of hindered rotation around the C(S)-NEt_2 bonds. This is often observed for benzoyl thioureas and their complexes [154].

ESI$^+$ mass spectrometry shows the molecular ion peaks $[M + H]^+$ for the complexes **29**, **31**, **32** or **33** and $[M + Na]^+$ species for complexes **27**, **28**, or **30**. They are consistent with the expected mass values. Figure 28 shows the isotopic pattern of complex **31**. The correct

isotopic patterns for the naturally abundant $^{63}Cu/^{65}Cu$ isotope distribution are clearly resolved for the $[M + H]^+$, $[M + Na]^+$ and $[M + K]^+$ signals.

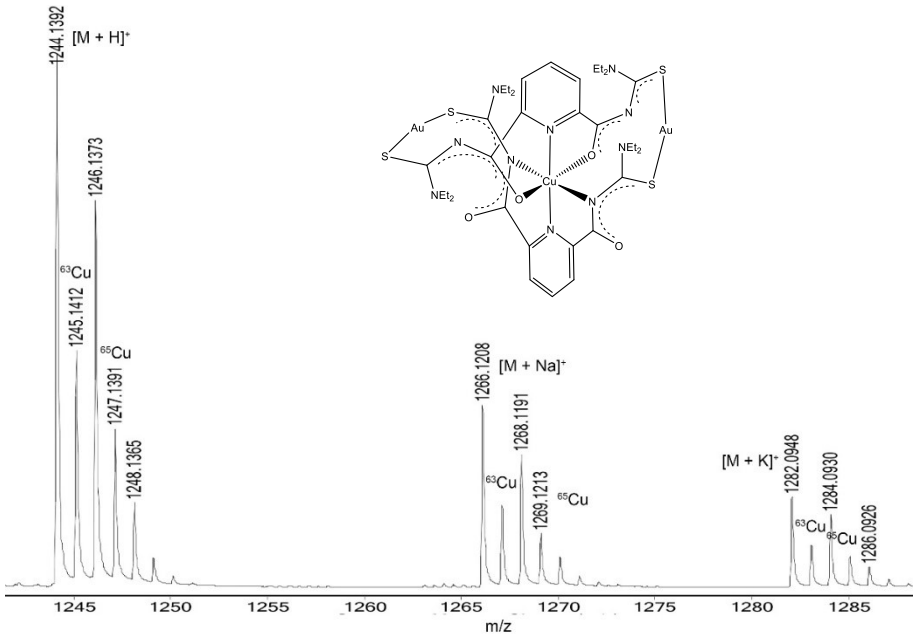

Figure 28: ESI^+ spectrum of complex **31** showing the correct $^{63/65}Cu$ isotopic pattern for the molecular ion and its cluster ions.

The electronic spectra of the ligand and the complexes were recorded in CH_2Cl_2. The transition metal complexes display three distinct absorption bands at 300, 250 and 230 nm. The extinction coefficients have high values between $30 \cdot 10^4$ - $72 \cdot 10^4$ mol^{-1} cm^{-1} L. Such high values suggest a ligand to metal charge transfer (LMCT) transition from the low-lying filled ligand orbitals to empty metal orbitals.

The forbidden d-d transitions of the Mn(II), Zn(II) and Hg(II) complexes were not observed. In contrast to the UV-vis spectrum of the uncoordinated ligand (see Section 2.5.1), the intensity of both intraligand bands is increased in the complexes due to sulfur → gold(I), oxygen → metal(II) and nitrogen → metal(II) charge transfer transitions. Other charge transfer bands contribute to the increase in intensity of the band in the region around 250 nm. The red-shift of this band which owes some of its intensity to intraligand π→π* transitions, is due to the conjugation of the deprotonated ligands [192 - 194].

The EPR spectra of compound **31** were performed in CH_2Cl_2 at room temperature and at -196 °C (frozen solution) (Fig. 29). Surprisingly, no $^{63,65}Cu$ hyperfine structural could be resolved in the room temperature spectrum. Thus, only g_0 (2.135) could be derived from the spectrum. Line width considerations suggest the $^{63,65}Cu$ coupling constant being around $70 \cdot 10^{-4}$ cm^{-1}. This fits approximately with the g_{av} value of $99 \cdot 10^{-4}$ cm^{-1}, which can be

derived from the anisotropic spectrum in frozen solution. In the frozen solution spectrum, the values for the coupling constants in the parallel and perpendicular part could be determined as $A_{\parallel} = 129.0$ and $A_{\perp} = 35.0 \cdot 10^{-4}$ cm^{-1}. The respective g values are $g_{\parallel} = 2.249$ and $g_{\perp} = 2.095$. The measurement in frozen solution shows an almost axially symmetrical anisotropic spectrum. The ratio $g_{\parallel} > g_{\perp} > 2.0023$ calculated for Cu(II) complexes suggests that the unpaired electron is mainly located in the d_{x2-y2} orbital [195].

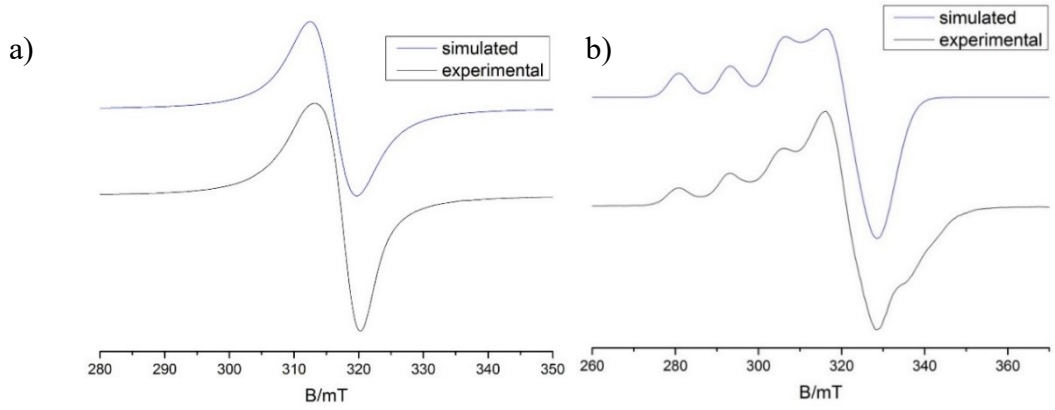

Figure 29: Simulated and experimental X-band EPR spectra of [Cu{Au(L4-κS)}$_2$] at a) r.t. and b) -196 °C. (solvent: CH_2Cl_2).

2.7.2. Crystal and Molecular Structures

Heterobimetallic complexes of type I: The complexes **27**, **28**, **29**, **30** and **31** are isostructural and crystallize in the monoclinic space groups C2/c (**27**, **30**) or P2$_1$/n (**28**, **29**, **31**). The structures of the nickel **30** and copper **31** complexes are shown in Figure 30 as representative for this class of compounds.

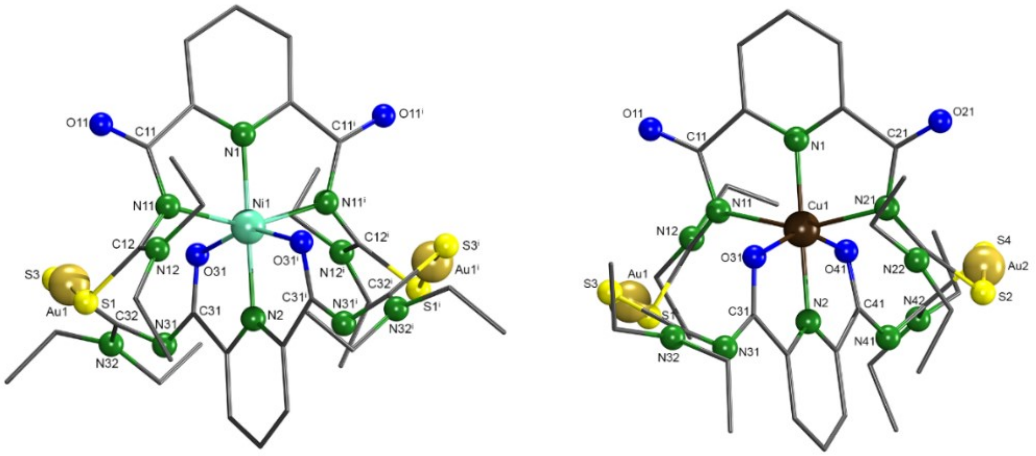

Figure 30: Molecular structures of complexes **30** and **31**. Hydrogen atoms are omitted for clarity. Symmetry transformations used to generate equivalent atoms -x+1,y,-z+1/2.

Two ligands coordinate the M^{2+} ions tridentate in a meridional fashion. The ligands adopt two different coordination modes: {*O,N,O*} and {*N,N,N*}. The coordination environments around the transition metal ions can be described as distorted octahedral with two ligands arranged almost perpendicular to each other. Two pyridine nitrogen atoms are in the axial positions and the oxygen and nitrogen atoms of the carboxamide groups form the equatorial plane. Additionally, the complexes contain two linearly coordinated gold(I) ions comprising four S-Au bonds. Selected bond lengths and bond angles of the complexes are summarized in Table 13.

Table 13: Selected bond lengths and angles in the complexes of type I. For atom labelling see Figure 30.

Bond lengths (Å)				
	27 (Mn)	**29 (Co)**	**30 (Ni)**	**31 (Cu)**
Au1-S1	2.262(2)	2.273(2)	2.267(2)	2.264(2)
Au1-S3	2.281(2)	2.291(2)	2.283(6)	2.294(2)
$Au1^{i}$-$S1^{i}$	2.262(2)	2.287(2)	2.267(2)	2.274(2)
$Au1^{i}$-$S3^{i}$	2.281(2)	2.299(2)	2.283(6)	2.289(2)
M1-N1	2.169(8)	2.040(5)	1.987(3)	1.925(5)
M1-N2	2.171(7)	2.054(5)	1.975(2)	1.972(5)
M1-N11	2.298(5)	2.220(5)	2.141(2)	2.153(5)
M1-$N11^{i}$	2.298(5)	2.178(5)	2.141(2)	2.128(5)
M1-O31	2.244(5)	2.139(5)	2.150(2)	2.281(4)
M1-$O31^{i}$	2.244(5)	2.143(4)	2.150(2)	2.292(4)
C11-O11	1.230(8)	1.248(8)	1.244(3)	1.225(8)
$C11^{i}$-$O11^{i}$	1.230(8)	1.233(8)	1.244(3)	1.230(7)
C31-O31	1.265(7)	1.268(8)	1.264(3)	1.251(7)
$C31^{i}$-$O31^{i}$	1.265(7)	1.269(7)	1.264(3)	1.244(8)
C11-N11	1.345(8)	1.335(9)	1.337(3)	1.327(9)
$C11^{i}$-$N11^{i}$	1.345(8)	1.338(8)	1.337(3)	1.338(8)
C31-N31	1.314(8)	1.318(8)	1.326(3)	1.328(8)
$C31^{i}$-$N31^{i}$	1.314(8)	1.325(8)	1.326(3)	1.336(9)
N11-C12	1.380(8)	1.377(9)	1.383(3)	1.383(8)
$N11^{i}$-$C12^{i}$	1.380(8)	1.382(8)	1.383(3)	1.376(9)
N31-C32	1.378(8)	1.369(9)	1.343(3)	1.342(9)
$N31^{i}$-$C32^{i}$	1.378(8)	1.336(8)	1.343(3)	1.332(9)
C12-S1	1.718(6)	1.723(7)	1.724(2)	1.716(7)

Continuation of Table13

C12^{i}-S1^{i}	1.718(6)	1.722(6)	1.724(2)	1.731(7)
C32-S3	1.748(7)	1.746(7)	1.757(2)	1.750(7)
C32^{i}-S3^{i}	1.748(7)	1.747(7)	1.757(2)	1.752(6)
Angles (°)				
S1-Au1-S3	171.30(7)	172.43(7)	173.38(2)	172.76(8)
S1^{i}-Au1^{i}-S2^{i}	171.30(7)	178.41(6)	173.38(2)	176.95(7)
N1-M1-N2	180.0	172.0(2)	180.0	175.3(2)
N11-M1-O31^{i}	92.6(2)	93.0(2)	89.97(6)	89.08(19)
N11^{i}-M1-O31	92.6(2)	87.6(2)	89.97(6)	85.3(1)
N1-M1-N11	72.3(1)	75.4(2)	76.96(5)	78.7(2)
N1-M1-N11^{i}	72.3(1)	75.2(2)	76.96(5)	78.8(2)
N1-M1-O31	107.7(1)	112.3(2)	102.45(4)	107.0(2)
N1-M1-O31^{i}	107.7(1)	96.8(2)	102.45(4)	99.8(2)
N2-M1-N11	107.7(1)	102.0(2)	103.04(5)	98.4(2)
N2-M1-N11^{i}	107.7(1)	107.7(2)	103.04(5)	104.2(2)
N2-M1-O31	72.3(1)	75.5(2)	77.55(4)	77.0(2)
N2-M1-O31^{i}	72.3(1)	75.8(2)	77.55(4)	76.4(2)
N11-M1-N11^{i}	144.6(3)	150.3(2)	153.9(1)	157.3(2)
N11-M1-O31	98.0(2)	99.8(2)	95.62(6)	98.4(2)
N11^{i}-M1-O31^{i}	98.0(2)	94.4(2)	95.62(6)	97.7(2)
O31-M1-O31^{i}	144.7(2)	150.4(2)	155.10(8)	153.1(2)

Symmetry transformations used to generate equivalent atoms: ^{i} -x+2,y,-z+3/2 **27** ; -x+1,y,-z+1/2 **30**.

The average of the C=O bond lengths of the non-coordinated carbonyl groups (C11-O11 and C21-O21) is 1.236 Å. This is only slightly longer compared to the carbonyl groups of the uncoordinated ligand (1.216 Å), but shorter than the coordinated carbonyl groups (C31-O31 and C41-O41), which have an average bond length of 1.263 Å. The average of the C=S bond lengths is 1.736 Å, while the average in the uncoordinated ligand is 1.666 Å [149]. Thus, they are lengthened as a consequence of the coordination of the ligand.

The average of C-N bond lengths of carboxamide groups C31-N31 and C41-N41 are 1.322 Å. They are shorter than in the uncoordinated ligand (1.35 Å), and also shorter than the C11-N11 and C21-N21 bonds in the complexes. The N11-C12, N21-C22, N31-C32 and N41-C42 bonds in the complexes are considerably shorter than the corresponding bonds in

the uncoordinated ligand, (1.425 Å) [149]. The observed bond lengths reflect delocalization of electron density over the picolinoyl moiety as well as over the thiourea moiety, which is induced by the coordination to the gold atoms.

The heterobimetallic complex of type II: Another coordination mode is observed for the complex [Zn{Au(L4-κS)}$_2$] **32**. The molecular structure of **32** is shown in Figure 31. Selected bond lengths and angles are listed in Table 14. The compound crystallizes in the monoclinic space group P2$_1$/c. The Zn^{2+} ion is meridionally coordinated by two tridentate $\{L4\}^{2-}$ ligands in the coordination fashions $\{O,N,O\}$ and $\{N,N,O\}$. This leads to a distorted octahedral coordination environment. The Zn^{2+} metal ion is bonded by one deprotonated carboxamide nitrogen (N11) atom and three carbonyl oxygen atoms (O21, O31, and O41), which form the equatorial plane and to two pyridine nitrogen atoms (N1 and N2), which are in axial positions. Additionally, the complex contains two linearly coordinated gold(I) ions, comprising four S-Au bonds.

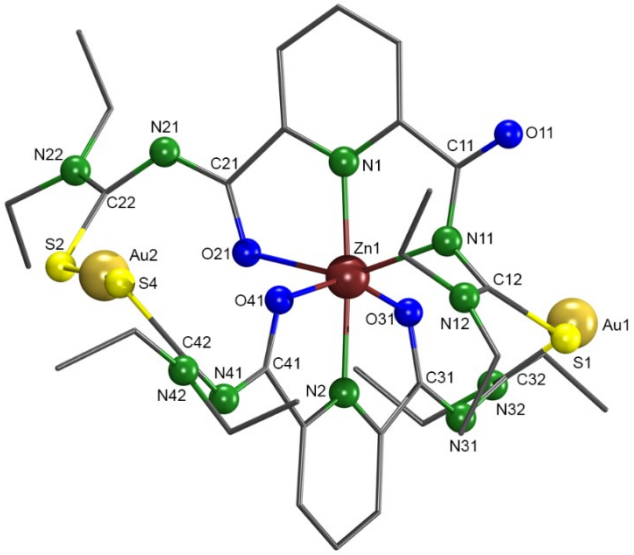

Figure 31: Molecular structure of [Zn{Au(L4-κS)}$_2$]. Hydrogen atoms are omitted for clarity.

The C11-O11 bond length of 1.243(6) Å is slightly shorter than the average value of the C-O bonds of the coordinated carbonyl bonds (1.266 Å), but it is longer than the C-O bonds in the uncoordinated H_2L4 (1.21 Å) [149]. This indicates that, even though the atom O11 does not participate in the coordination of the metal ion, the C11-O11 bond is slightly influenced by the shift of electron density upon complexation. The C=S bond lengths range between 1.724(5) and 1.745(5) Å. They are also longer than in the uncoordinated ligand (1.666 Å).

The C-N bond lengths next to the thiocarbonyl groups range from 1.351(6) Å to 1.372(6) Å. They are shorter compared with the values in the uncoordinated ligand (1.425 Å) [149].

Table 14: Selected bond lengths and angles in [Zn{Au(L4-κS)}$_2$].

Bond lengths (Å)							
Au1-S1	2.289	Au1-S3	2.293(1)	Au2-S2	2.290(1)	Au2-S4	2.289(1)
Zn1-N1	2.035(4)	Zn1-N11	2.222(4)	Zn1-O21	2.156(3)	Zn1-O31	2.118(3)
Zn1-N2	2.047(4)	Zn1-O41	2.183(3)				
C11-O11	1.243(6)	C21-O21	1.263(6)	C31-O31	1.272(6)	C41-O41	1.254(6)
C11-N11	1.337(6)	C21-N21	1.316(6)	C31-N31	1.312(6)	C41-N41	1.322(6)
N11-C12	1.372(6)	N21-C22	1.351(7)	N31-C32	1.360(6)	N41-C42	1.353(6)
C12-S1	1.724(5)	C22-S2	1.745(5)	C32-S3	1.735(6)	C42-S4	1.737(5)

Angles (°)					
S1-Au1-S3	173.24(5)	N1-Zn1-N11	75.0(2)	N1-Zn1-O31	108.4(1)
S2-Au2-S4	167.00(5)	N1-Zn1-O21	77.1(2)	N1-Zn1-O41	99.4(1)
N1-Zn1-N2	175.0(2)	N2-Zn1-N11	105.9(2)	N2-Zn1-O31	76.5(1)
N11-Zn1-O41	92.6(1)	N2-Zn1-O21	101.8(1)	N2-Zn1-O41	75.6(1)
O21-Zn1-O31	92.8(1)	N11-Zn1-O21	152.0(1)	O31-Zn1-O41	152.0(1)
		N11-Zn1-O31	97.3(1)	O21-Zn1-O41	90.5(1)

The observed bond lengths fit between C-N, C=O and C=S single and double bonds. The delocalization of π-electron density over the ligand backbone as described for the complexes of type I, can also be observed for the zinc complex. In comparison to the uncoordinated ligand, the C=O and C=S bonds are lengthened, whereas the C-N bonds are shortened.

The heterobimetallic complex of type III: The molecular structure of [Hg{Au(L4-κS)}$_2$] **33** is shown in Figure 32. Selected bond lengths and bond angles are listed in Table 15. The compound crystallizes in the monoclinic space group $P2_1/n$ with two molecules in the asymmetric unit. As in the complexes of type I and II, two $\{L4\}^{2-}$ ligands coordinate to the Hg^{2+} ion tridentate in a meridional fashion. But here, both ligands adopt the same coordination mode $\{N,N,O\}$. This results in a distorted octahedral coordination environment around the Hg^{2+} cation. The N-Hg-N bond angles strongly deviate from 180° (145.5(2)° and 150.20(2)°). This leads to a pseudo-octahedral coordination geometry around the mercury

atom. The pyridine nitrogen atoms are in the axial positions, while the oxygen and nitrogen atoms of the carboxamide groups form the equatorial planes. Additionally, two gold(I) atoms are linearly coordinated by the thiourea fragments, resulting in four Au-S bonds in each of the complex molecules.

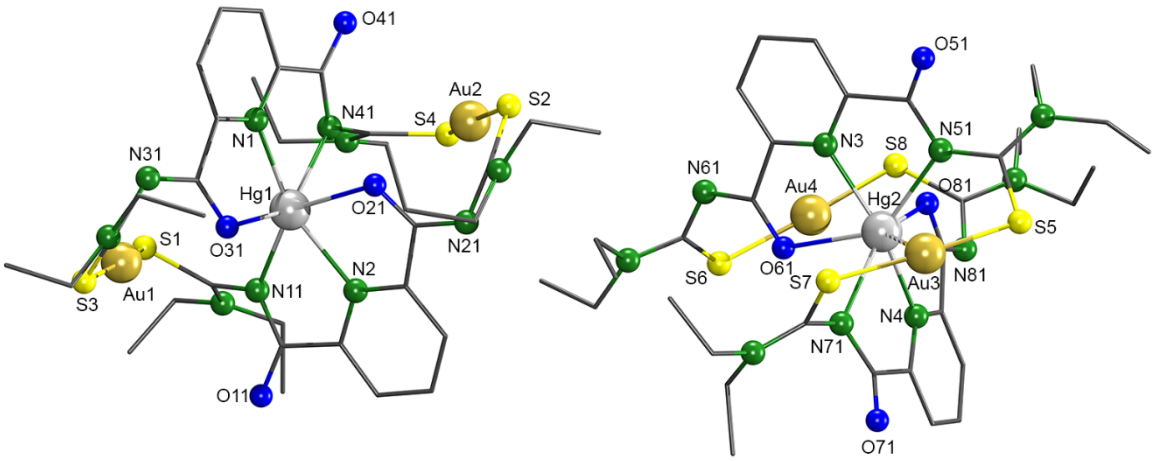

Figure 32: Molecular structures of [Hg{Au(L4-κS)}$_2$]. Two symmetry-independent species are shown. Hydrogen atoms are omitted for clarity.

Table 15: Selected bond lengths and angles of [Hg{Au(L4-κS)}$_2$]. (Values for two crystallographically independent species).

Bond lengths (Å)							
Au1-S1	2.277(2)	Au1-S3	2.282(1)	Au2-S2	2.288(2)	Au2-S4	2.268(2)
Au3-S5	2.286(2)	Au3-S7	2.292(2)	Au4-S6	2.280(2)	Au4-S8	2.279(2)
Hg1-N1	2.299(4)	Hg1-N2	2.247(4)	Hg2-N3	2.258(4)	Hg2-N4	2.245(4)
Hg1-N11	2.299(4)	Hg1-O21	2.542(4)	Hg1-O31	2.465(4)	Hg1-N41	2.429(4)
Hg2-N51	2.391(4)	Hg2-O61	2.516(4)	Hg2-N71	2.462(5)	Hg2-O81	2.508(4)
C11-O11	1.228(6)	C21-O21	1.250(6)	C31-O31	1.260(6)	C41-O41	1.248(7)
C11-N11	1.356(6)	C21-N21	1.322(7)	C31-N31	1.316(7)	C41-N41	1.333(7)
N11-C12	1.365(7)	N21-C22	1.338(7)	N31-C32	1.351(7)	N41-C42	1.366(7)
C12-S1	1.733(5)	C22-S2	1.740(5)	C32-S3	1.746(6)	C42-S4	1.729(6)
C51-O51	1.240(7)	C61-O61	1.255(7)	C71-O71	1.236(7)	C81-O81	1.251(6)
C51-N51	1.351(7)	C61-N61	1.297(8)	C71-N71	1.322(7)	C81-N81	1.321(7)
N51-C52	1.375(8)	N61-C62	1.343(8)	N71-C72	1.374(7)	N81-C82	1.329(7)
C52-S5	1.733(6)	C62-S6	1.739(6)	C72-S7	1.725(6)	C82-S8	1.732(6)

Continuation of Table 15

Angles (°)					
S1-Au1-S3	171.33(6)	N1-Hg1-N11	72.1(2)	N1-Hg1-O31	96.1(1)
S2-Au2-S4	170.74(5)	N1-Hg1-O21	67.2(1)	N1-Hg1-N41	115.7(2)
N1-Hg1-N2	145.5(2)	N2-Hg1-N11	140.0(2)	N2-Hg1-O31	70.2(1)
N11-Hg1-N41	110.7(2)	N2-Hg1-O21	79.7(1)	N2-Hg1-N41	70.7(2)
O21-Hg1-O31	84.5(1)	N11-Hg1-O21	139.3(1)	O31-Hg1-N41	140.8(1)
		N11-Hg1-O31	100.1(1)	O21-Hg1-N41	87.4(1)
S5-Au3-S7	176.98(7)	N3-Hg2-N51	71.0(2)	N4-Hg2-O81	70.2(1)
S8-Au4-S6	167.63(5)	N3-Hg2-O71	119.3(2)	N3-Hg2-O81	90.2(1)
N3-Hg2-N4	150.2(2)	N4-Hg2-N51	128.1(2)	N4-Hg2-O61	86.5(1)
N51-Hg2-N71	127.9(2)	N4-Hg2-N71	70.1(2)	N3-Hg2-O61	69.4(2)
O61-Hg2-O81	85.9(1)	N71-Hg2-O61	78.8(2)	N51-Hg2-O81	88.0(2)
		N51-Hg2-O61	139.8(1)	N71-Hg2-O81	138.1(1)

Interestingly, in one of the molecules of the asymmetric unit, a weak gold-mercury interaction is observed. The Au···Hg distance of 3.1698(3) Å is very close to the sum of van der Waals radii of the corresponding atoms (3.2 Å) [196].

Delocalization of π-electron density within the organic ligand as was described for the complexes of types I and II, can also be observed for the mercury compound of type III.

2.8. The Formation of [Ni{Au(L4-κS)}$_2$] *via* Metal Exchange Starting from [{Ca$_2$(MeOH)$_3$(H$_2$O)}{Au(L4-κS)}$_4$]

The synthesis of heterometallic complexes with $\{Au(L4)\}^-_n$ (n = 2-4) metallacyclic rings as host structures via one-pot reactions is straightforward and the self-assembled products are obtained in high yields. The ready formation of such complexes with various metal ions (main group/transition metal/lanthanide, M^{2+}/M^{3+} ions) leads to the question of metal exchange reactions. A particularly interesting point is the formation of tetranuclear ring structures with Ca^{2+}, Sr^{2+} and Ba^{2+} ions, while divalent transition metal ions are hosted in binuclear metallacycles. Thus, some metal-exchange reactions were undertaken.

2.8.1. Synthesis and Spectroscopy

The tetrameric complex **8** ([{$Ca_2(MeOH)_3(H_2O)$}{Au(L4-κS)}$_4$]) was used as starting material in a reaction with nickel acetate. The addition of $Ni(OAc)_2 \cdot 4H_2O$ to a solution of compound **8** immediately resulted in a colour change from colourless to green (Scheme 12). The product was isolated as green single crystals by slow evaporation of the solvent with a yield of 65 %. The complex was characterized by elemental analysis and spectroscopic methods such as IR and UV-vis spectroscopy and ESI mass spectrometry and single crystal X-ray diffraction analysis.

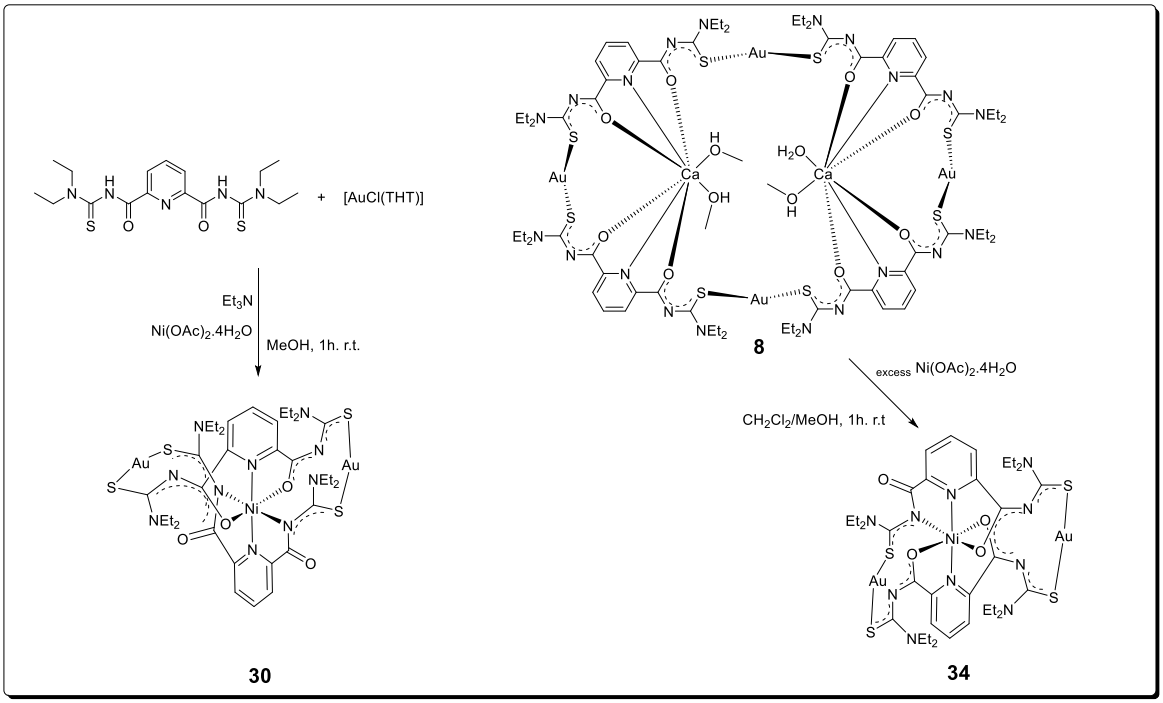

Scheme 12: Syntheses of the isomeric nickel complexes **30** and **34** by one-pot synthesis **(30)** or by a metal-exchange procedure from compound **8**.

The IR and UV-vis spectra of complex **34** are very similar to those of the nickel(II) compound, which was isolated from the one-pot approach (complex **30**). Further support for the composition of complex **34** as [Ni{Au(L4-κS)}$_2$] complex is provided by ESI^+ mass spectrometry. The ESI^+ spectrum shows the molecular ion peak $[M + Na]^+$ at *m/z* = 1261.1214 (calcd. 1261.1169). This is a strong hint that not just a simple replacement of Ca^{2+} ions in the compound **8** by Ni^{2+} ions resulted, but a complete re-organization of the metallacycle and the formation of a complex with only two gold atoms in the periphery.

2.8.2. Crystal and Molecular Structure

The X-ray diffraction analysis confirms the observations of the spectroscopic studies. Figure 33 shows the molecular structure of complex **34**. Selected bond lengths and angles are given in Table 16. Compound **34** crystallizes in the monoclinic space group $P2_1/c$.

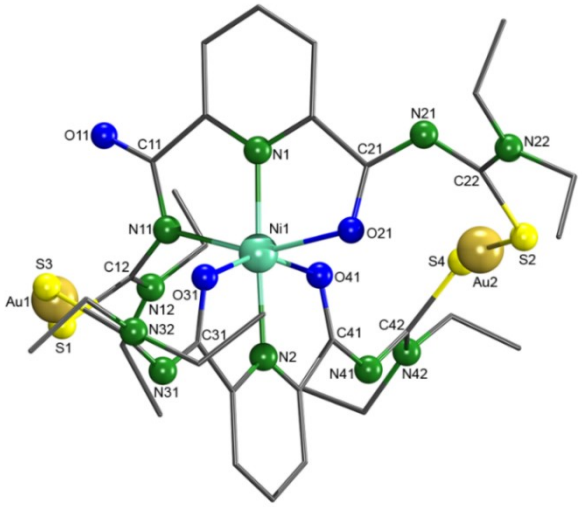

Figure 33: Molecular structure of [Ni{Au(L4-κS)}$_2$] **34**. The hydrogens atoms were omitted for clarity.

Table 16: Selected bond lengths and angles and hydrogen bonds in compound **34** [Ni{Au(L4-κS)}$_2$].

Bond lengths (Å)							
Au1-S1	2.283(2)	Au1-S3	2.291(2)	Au2-S2	2.286(2)	Au2-S4	2.294(2)
		Ni1-N1	1.965(5)	Ni1-N11	2.138(6)	Ni1-O31	2.088(5)
		Ni1-N2	1.978(5)	Ni1-O21	2.108(5)	Ni1-O41	2.125(5)
C11-O11	1.235(9)	C21-O21	1.269(8)	C31-O31	1.273(8)	C41-O41	1.261(8)
C11-N11	1.348(9)	C21-N21	1.312(9)	C31-N31	1.310(9)	C41-N41	1.316(9)
N11-C12	1.383(9)	N21-C22	1.36(1)	N31-C32	1.35(1)	N41-C42	1.34(1)
C12-S1	1.717(8)	C22-S2	1.749(7)	C32-S3	1.747(9)	C42-S4	1.751(8)

Angles (°)					
S1-Au1-S3	173.58(8)	N1-Ni1-N11	77.1(2)	N1-Ni1-O31	103.3(2)
S2-Au2-S4	167.50(8)	N1-Ni1-O21	78.7(2)	N1-Ni1-O41	100.9(2)
N1-Ni1-N2	177.5(2)	N2-Ni1-N11	105.0(2)	N2-Ni1-O31	77.9(2)
N11-Ni1-O41	92.8(2)	N2-Ni1-O21	99.1(2)	N2-Ni1-O41	77.8(2)
O21-Ni1-O31	91.9(2)	N11-Ni1-O21	155.7(2)	O31-Ni1-O41	155.5(2)
		N11-Ni1-O31	95.9(2)	O21-Ni1-O41	89.4(2)

D-H…A	d(D…A) (Å)	<(DHA) (°)
O20-H20A...O21	2.97(3)	147.3

The Ni^{2+} ion is coordinated by two meridionally arranged $\{L4\}^{2-}$ molecules. In contrast to compound **30**, which was obtained by a one-pot synthesis (Scheme 12), the coordination sphere of the metal ion in **34** is not formed by two {*N,N,N*} and {*O,N,O*} coordinated $\{L4\}^{2-}$ ligands, but the donor atom constellation in **34** follows the {*N,N,O*} and {*O,N,O*} coordination pattern (type II). This arrangement is the same found in the zinc complex **32**. The coordination geometry around the Ni^{2+} ion can be described as a distorted octahedron. The pyridine nitrogen atoms are in the axial positions while one nitrogen and three oxygen atoms from the carboxamide groups form the equatorial plane. In addition, the complex contains two gold(I) atoms linearly coordinated by sulfur atoms, resulting in four Au-S bonds.

The C=O bond of the non-coordinating carbonyl group (C11-O11) is the shortest (1.235(9) Å) when compared with the C21-O21, C31-O31, C41-O41 bonds. The C-N bonds next to thiocarbonyl groups range from 1.34(1) to 1.383(9) Å . They are shorter compared with the values in the uncoordinated ligand 1.425(Å) [149].

The crystal packing of complex **34** contains O-H···O hydrogen bonds between O21 and water molecules (see Fig. 34 and Table 16).

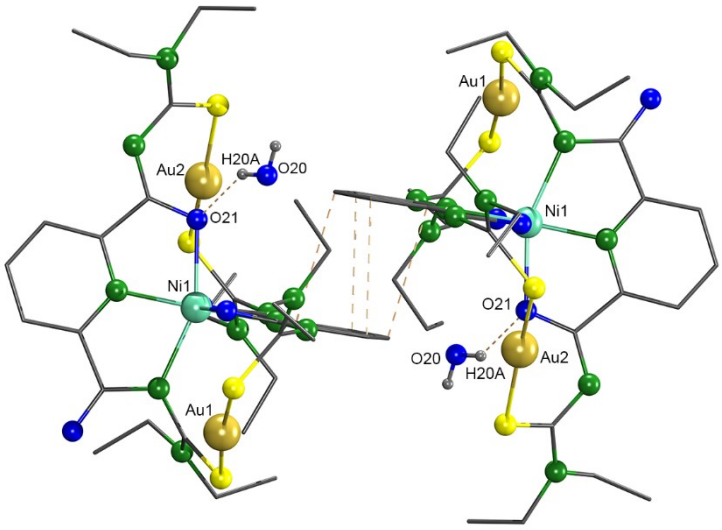

Figure 34: Hydrogen bonds and π···π stacking interactions in the crystal structure of complex **34**. Hydrogen atom bonded to carbon atoms are omitted for clarity.

Also, π···π stacking interactions between the pyridine rings of the $\{L4\}^{2-}$ ligands are observed, with a centroid-centroid distance of approximately 3.26 Å. Such intermolecular interactions are not observed in the analogous complex **30**.

In order to estimate the reason for the formation of two different structural isomers of [Ni{Au(L4-κS)}$_2$] complexes, DFT (Density Functional Theory) calculations were performed by Jungfer, FU Berlin. The input coordinates were taken from X-ray data and included with Gauss View [197]. The compounds were calculated without any symmetry constraints at the density functional B3LYP level of theory. The geometry optimization of the two [Ni{Au(L4-κS)}$_2$] isomers shows that the isomer **34** is thermodynamically slightly more stable than **30**. The energy difference is 26.0 kJ/mol. This small energy difference found in the DFT calculations indicates that the isolation of the individual conformers is mainly determined by the solubility of the products in the reaction media and/or crystallographic packing effects.

3. Summary

This thesis describes the synthesis and characterization of gold complexes and heteronuclear cage-like compounds with the aroylthiourea derivatives HL1, H_2L2, H_2L3 and H_2L4. These multidentate ligands offer hard (*O*), borderline (*N*) and soft (*S*) donor atoms, which make them capable to coordinate to "hard" and "soft" metal ion simultaneously.

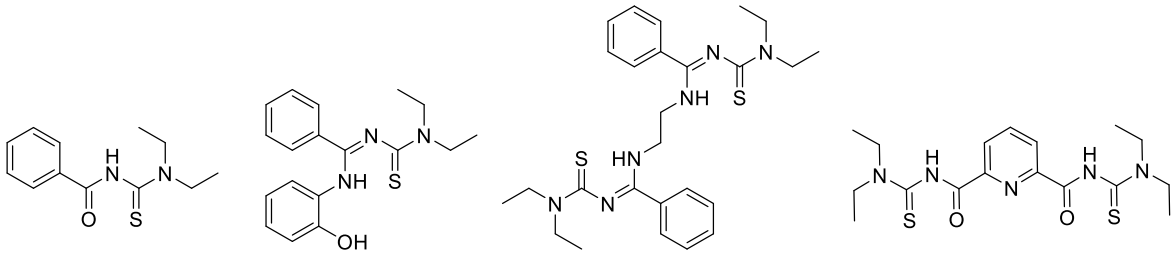

HL1 **H_2L2** **H_2L3** **H_2L4**

The first part of the thesis describes the synthesis and characterization of gold(III) complexes with the ligands HL1 and H_2L2. The common gold(III) starting material [Au(damp-κC^1,N^1)Cl_2] was used in order to stabilize the gold(III) against reduction. The ligands HL1 and H_2L2 exhibit *O,S*-bidentate and *O,N,S*-tridentate coordination modes for complexes **1** and **2**, respectively. The coordination environment is governed by the formation of chelate rings. The main structural feature of the resulting gold(III) complex with $\{L2\}^{2-}$ in complex **2** is the formation of an ammonium functionality from the liberated dimethylamino group, which is not observed for compound **1**. The bonding situation within the chelate rings is dominated by delocalization of electron density, which is extended to the exocyclic parts the ligands in both complexes.

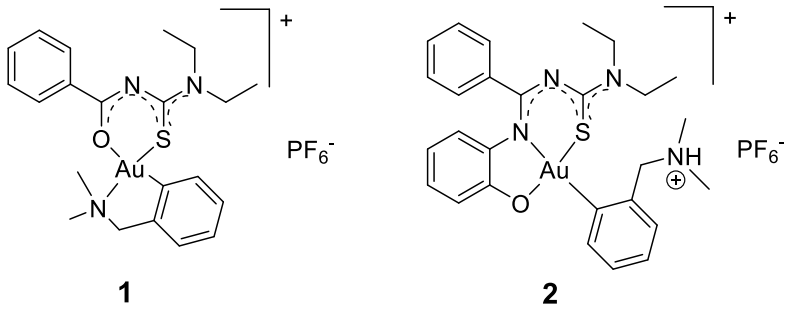

1 **2**

The second part of the thesis describes H_2L3 as a model building block for oligometallic structures. It has a remarkable flexibility and can accommodate two-coordinate gold(I) ions with different ligands. Different conformations are adopted in the complexes **4**, **5**, and **6**. A lengthening of the X-Au-S is observed in the complexes **4**, **5**, and **6**, which increases in the

following $Cl^- < SCN^- < PPh_3$. This correlates well with the π-acceptor properties of the ligands, which can decrease the excess of negative charge on the metal through π-back bonding.

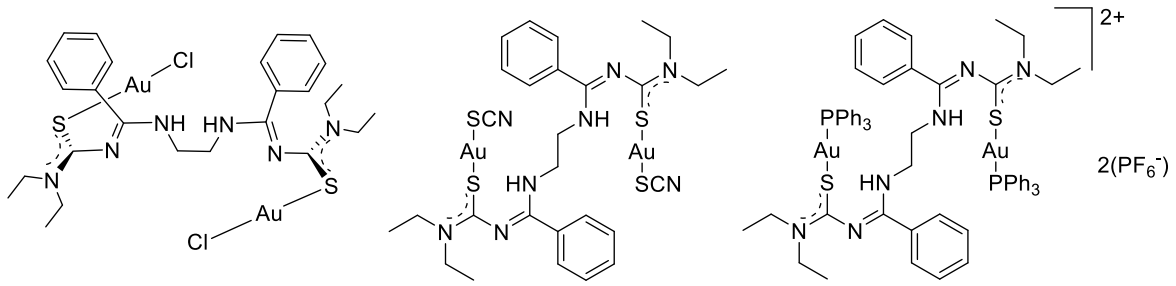

3 **4** **5**

The ligand H_2L4 proved to be very versatile. When it reacts with [AuCl(PPh_3)] the bulky triphenylphosphine remains coordinated and the ligand arranges in a way that these two bulky groups are in opposite side to each other (see **7**). When the ligand reacts with [AuCl(THT)], however, the chlorido ligand remains coordinated and aurophilic interactions are observed in the complex **6**. The solid-state structure of the later complex shows an interesting feature by the formation of a cavity formed by nitrogen and oxygen donor atoms, which remain uncoordinated.

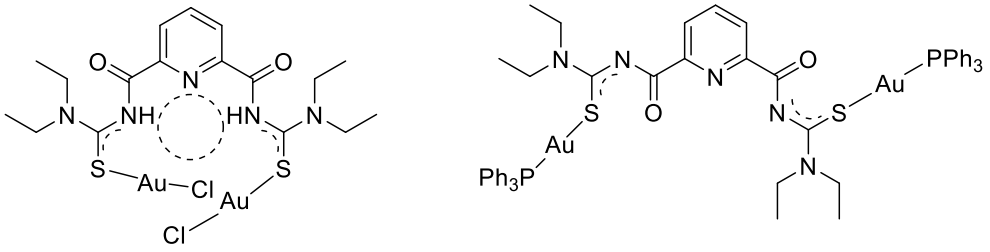

6 **7**

The third part of the thesis describes the synthesis and characterization of multinuclear complexes developed from the 2,6-dipicolinoylbis(*N,N*-diethylthiourea) ligand (H_2L4). The syntheses of the complexes were carried out as one-pot reactions of stoichiometric ratios of H_2L4 and mixtures of soft and hard metal ions, in the presence of a supporting base. They result in the formation of neutral and cationic heterometallic host-guest complexes by self-assembly. The structural variety of the obtained products is shown in Figure 35.

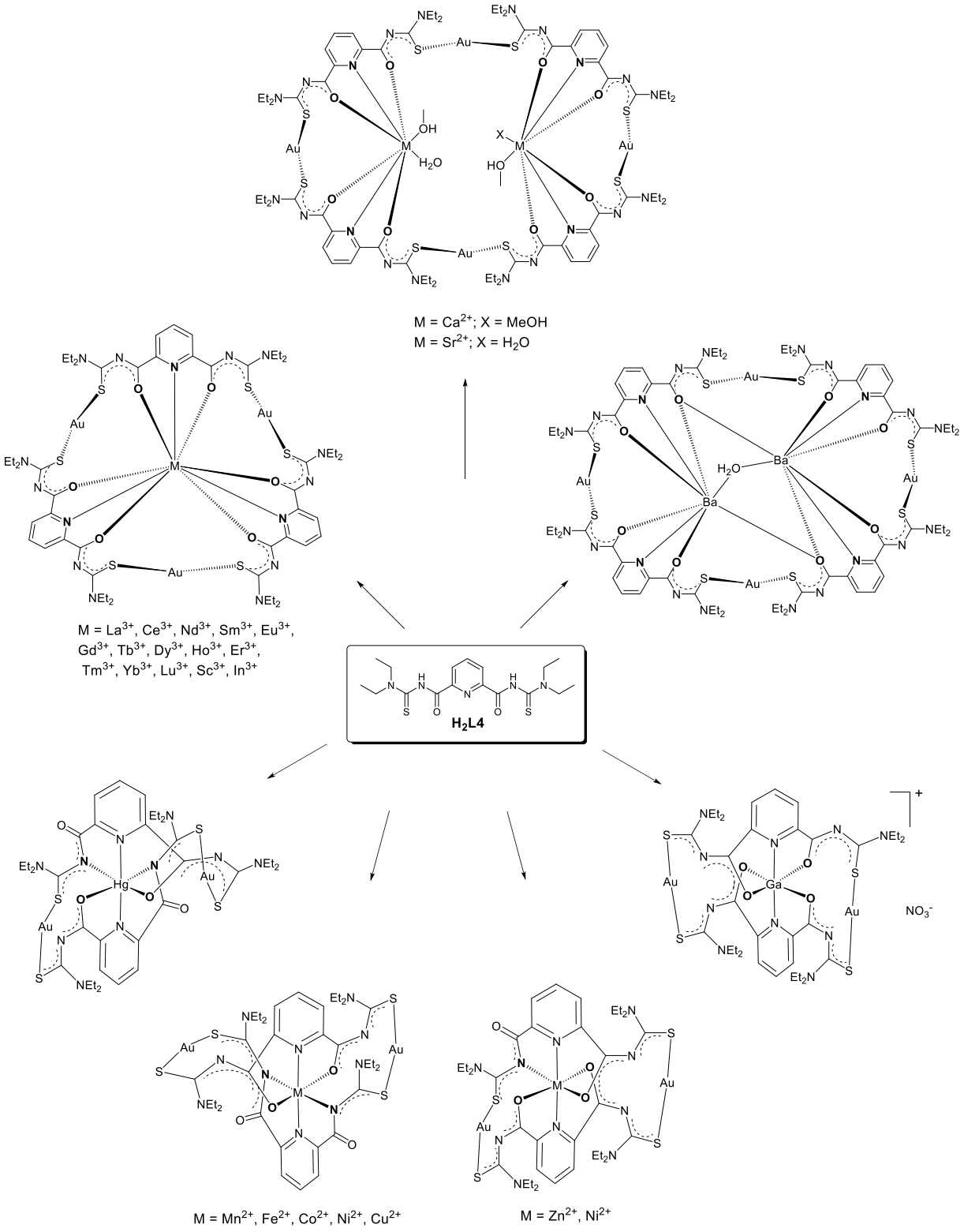

Figure 35: Molecular structures of the heterometallic complexes derived from H_2L4.

The different donor atoms of H_2L4 are selective for the coordination of divalent alkaline earth metals, transition metal ions as well as for trivalent lanthanides and others trivalent metal ions such as Sc^{3+}, In^{3+}, and Ga^{3+}. The ionic radii, charge of the metal ion, the coordination geometry, the coordination number, and the formed ring cavity are fundamental for the structures of the formed complexes.

Depending on the hosted metal ions, tetrameric, trimeric and dimeric metallacycles are formed consisting of $\{Au(L4)\}^-$ building blocks. The tetrameric complexes host two alkaline earth metal ions, the trimeric coronands host one lanthanide ion, one scandium, or one indium ion, and the dimeric units host one divalent transition metal ion, or in an exceptional case one trivalent gallium ion. The obtained complexes were characterized by elemental analysis, IR and UV-vis spectroscopy, ESI mass spectrometry and X-ray diffraction.

The coordination mode *{O,N,O}* of the deprotonated $\{L4\}^{2-}$ ligands around the divalent alkaline earth ions or the trivalent Ln^{3+}, Sc^{3+}, and In^{3+} ions result in complexes with $[\{Au(L4\text{-}\kappa S)\}_4]^{4-}$ or $[\{Au(L4\text{-}\kappa S)\}_3]^{3-}$ coronands. In the product with Ga^{3+} ions, the smallest and hardest trivalent ion, also *{O,N,O}* coordination is established. The divalent transition metal ions are coordinated by *{O,N,N}* or *{N,N,N}* or *{O,N,O}* pincers. The heterometallic complexes show a delocalization of π-electron density in the C-N bond next to the thiourea groups, as well as in the C=S and C=O bonds.

The replacement of Ca^{2+} ions in the compound $[\{Ca_2(MeOH)_3(H_2O)\}\{Au(L4\text{-}\kappa S)\}_4]$ by Ni^{2+} ions results in the formation of a compound of the composition $[Ni\{Au(L4\text{-}\kappa S)\}_2]$. Thus, Au-S bonds have been cleaved and new ones have been formed. This indicates that the metal in the cavity strictly determines the composition of host-guest assemblies. This knowledge can be used for the construction of new host-guest compounds with almost freely adjustable host metal ions.

Zusammenfassung

Diese Arbeit beschreibt die Synthese und Charakterisierung von Goldkomplexen und heteronuklearen, käfigartigen Verbindungen mit den Aroylthioharnstoffen HL1, H_2L2, H_2L3 und H_2L4. Diese mehrzähnigen Liganden besitzen harte (*O*), mittlere (*N*) und weiche (*S*) Donoratome, so dass sie gleichzeitig an „harte“ und „weiche“ Metallionen koordinieren können.

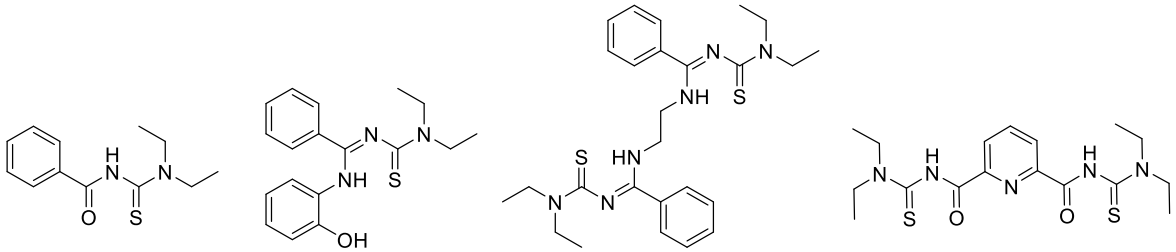

Der erste Teil der Arbeit beschreibt die Synthese und Charakterisierung von Gold(III)-Komplexen mit den Liganden HL1 und H_2L2. Die gängige Gold(III)-Startverbindung [Au(damp-κC^1,N^2)Cl_2] wurde verwendet, um Gold(III) gegen Reduktion zu stabilisieren. In den Komplexen **1** und **2** koordinieren die Liganden HL1 und H_2L2 in einem zweizähnigen *O,S*-Modus bzw. einem dreizähnigen *O,N,S*-Modus. Die Koordinationsumgebung wird durch die Bildung von Chelatringen geprägt. Ein zentrales Strukturelement in Komplex **2** ist die Bildung eine Ammoniumfunktion aus der vom Gold(III)-Ion dissoziierten Dimethylamingruppe. Dies wird für Komplex **1** nicht beobachtet.

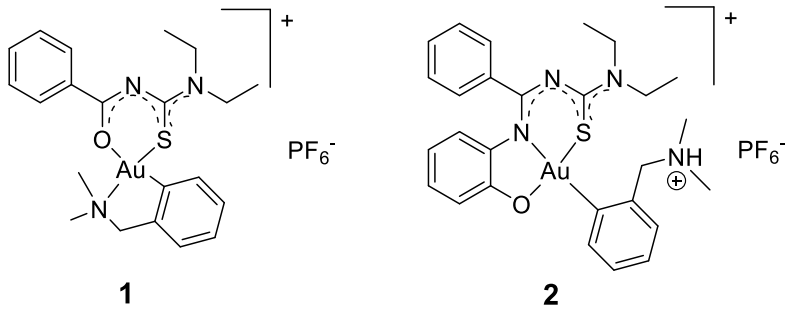

Der zweite Teil der Arbeit beschreibt H_2L3 als Modellbaustein für oligometallische Strukturen. Der Ligand besitzt eine bemerkenswerte Flexibilität und kann zweifach koordinierte Gold(I)-Ionen mit verschiedenen Liganden komplexieren. In den Komplexen **4, 5** und **6** werden unterschiedliche Konformationen angenommen. Eine Verlängerung der X-Au-S-Bindung kann in den Komplexen **4, 5** und **6** beobachtet werden. Sie steigt in

folgender Reihenfolge an: Cl^- < SCN^- < PPh_3. Das korreliert mit den p-Akzeptoreigenschaften der Liganden, wodurch die Elektronendichte am Metall durch p-Rückbindung verringert wird.

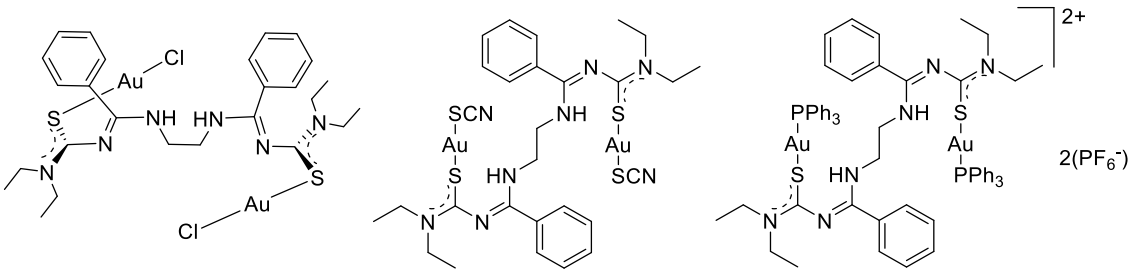

3 **4** **5**

Ligand H_2L4 stellte sich als sehr vielseitig heraus. Bei der Reaktion mit [AuCl(PPh_3)] bleibt der sperrige Triphenylphosphanligand am Gold koordiniert und H_2L4 nimmt eine Konformation ein, in der sich die beiden sterisch anspruchsvollen Gruppen auf gegenüberliegenden Seiten befinden (siehe **7**). Bei der Reaktion mit [AuCl(THT)] hingegen, bleibt der Chloridoligand koordiniert und innerhalb des Komplexes können aurophile Wechselwirkungen beobachtet werden **6**. In der Festkörperstruktur von Komplex **6** bildet sich ein von unkoordinierten Stickstoffatomen umgebener Hohlraum.

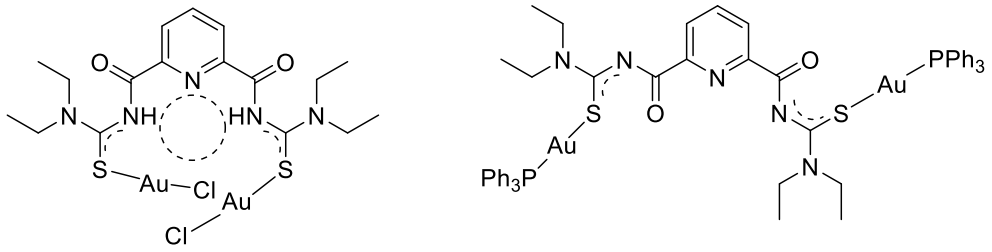

6 **7**

Der dritte Teil der Arbeit beschreibt die Synthese und Charakterisierung von mehrkernigen Komplexen, die mit dem 2,6-Dipicolinoylbis(*N,N*-diethylthioharnstoff)-Liganden H_2L4 erhalten wurden. Die Synthesen der Komplexe wurden als Eintopfreaktionen von H_2L4 mit Gemischen von weichen und harten Metallionen im entsprechenden stöchiometrischen Verhältnis und unter Zugabe einer Hilfsbase durchgeführt. Dabei entstanden durch Selbstorganisation neutrale oder kationische, heterometallische Wirts-Gast-Komplexe. Die strukturelle Vielfalt der erhaltenen Produkte ist in Abbildung 35 dargestellt.

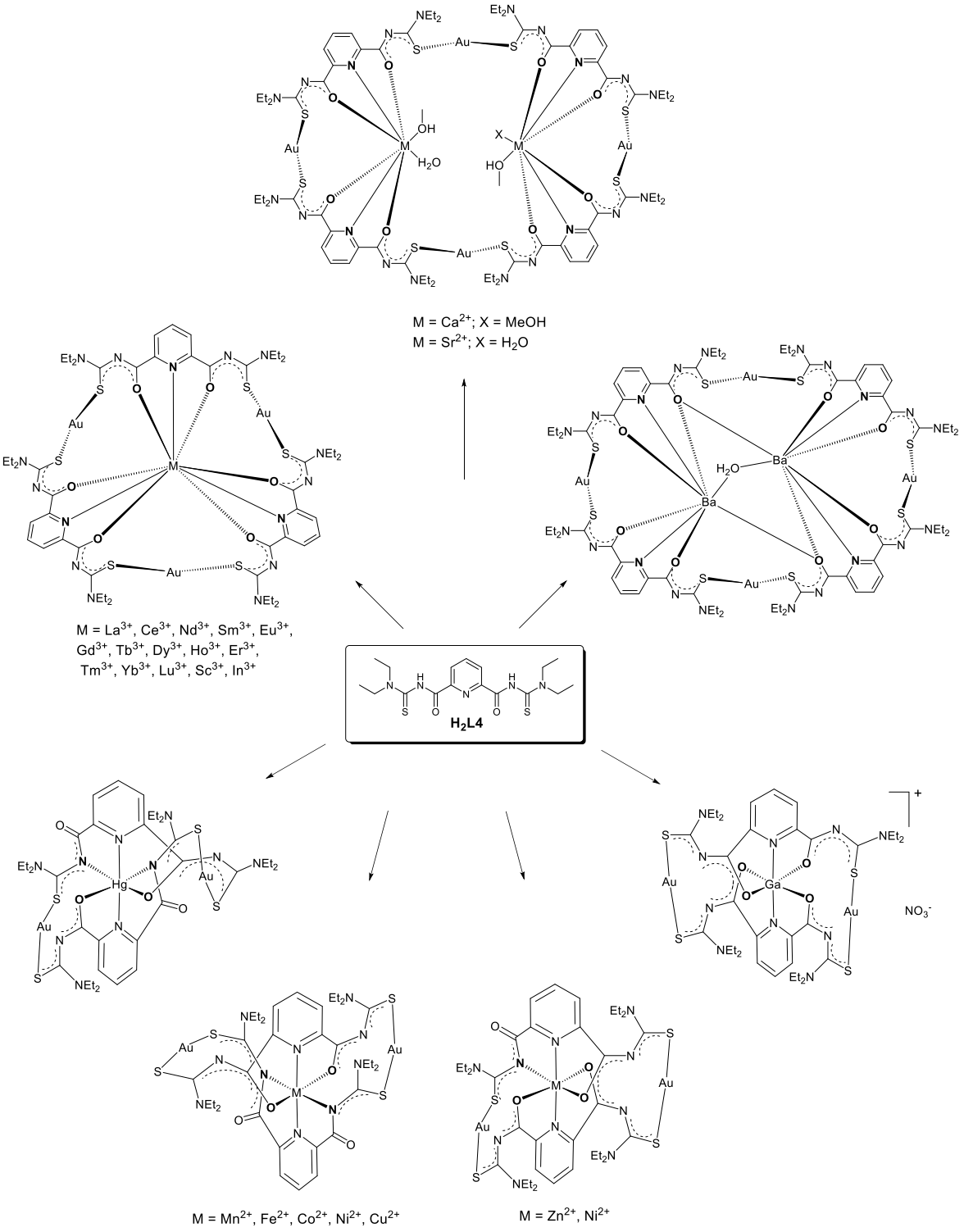

Abbildung 35: Molekülstrukturen der heterometallischen Komplexe mit H_2L4.

Die unterschiedlichen Donoratome von H_2L4 koordinieren selektiv an zweiwertige Erdalkalimetall- und Übergangsmetall-Ionen, sowie an dreiwertige Lanthanoid-Ionen oder Sc^{3+}, In^{3+} und Ga^{3+}. Die Strukturen der gebildeten Komplexe hängen maßgeblich von den Ionenradien, der Ladung der Metallionen, deren bevorzugter Koordinationsgeometrie, der Koordinationszahl und der Größe des gebildeten Hohlraums ab.

Abhängig vom Gastmetall-Ion, bilden sich tetramere, trimere oder dimere Metallacyclen, die aus $\{Au(L4)\}^-$-Einheiten bestehen. Kronenetherartige Strukturen mit vier $\{Au(L4)\}^-$-Einheiten koordinieren zwei Erdalkalimetallionen, die trimeren Coronanden ein Lanthanoid-Ion, ein Scandium-Ion oder ein Indium-Ion, und die dimeren Käfigstrukturen enthalten jeweils ein zweiwertiges Übergangsmetall-Ion oder in einem Spezialfall ein dreiwertiges Ga^{3+}-Ion. Die Komplexe wurden mittels Elementaranalyse, IR- und UV/Vis-Spektroskopie, ESI-Massenspektrometrie und Röntgendiffraktometrie charakterisiert.

Der Koordinationsmodus $\{O,N,O\}$ des deprotonierten Liganden $\{L4\}^{2-}$ an die Zentralionen führt zur Bildung von Coronanden der Zusammensetzungen $[\{Au(L4\text{-}\kappa S)\}_4]^{4-}$ bzw. $[\{Au(L4\text{-}\kappa S)\}_3]^{3-}$, die zweiwertigen Erdalkalimetall-Ionen oder die dreiwertigen Ln^{3+}, Sc^{3+}, In^{3+}-Ionen koordinieren. In den Produkten mit Ga^{3+}-Ionen, dem kleinsten und härtesten dreiwertigen Ion, liegt ebenfalls der Koordinationsmodus $\{O,N,O\}$ vor. Die zweiwertigen Übergangsmetall-Ionen werden in den Koordinationsmodi $\{O,N,N\}$, $\{N,N,N\}$ oder $\{O,N,O\}$ komplexiert. Die heterometallischen Komplexe zeigen eine Delokalisierung der π-Elektronendichte in den den Thioharnstoffgruppen benachbarten C-N-Bindungen, sowie in den C=S- und C=O-Bindungen.

Der Austausch von Ca^{2+}-Ionen in der Verbindung $[\{Ca_2(MeOH)_3(H_2O)\}\{Au(L4\text{-}\kappa S)\}_4]$ durch Ni^{2+}-Ionen führt zur Bildung eines Komplexes der Zusammensetzung $[Ni\{Au(L4\text{-}kS)\}_2]$. Die vorhandenen Au-S-Bindungen wurden dementsprechend gespalten und neue ausgebildet. Daraus lässt sich schließen, dass das Gastmetall-Ion die Zusammensetzung der Komplexe bestimmt. Diese Erkenntnis kann für die Konstruktion neuer Wirts-Gast-Verbindungen mit beinahe frei anpassbaren Gastmetall-Ionen angewendet werden.

4. Experimental Section

4.1. Physical Measurements

Elemental analyses of carbon, hydrogen, nitrogen, and sulfur were determined using a *Heraeus vario EL* elemental analyzer.

IR spectra were measured as KBr pellets on a *Shimadzu IR Affinity-1* spectrometer between 400 and 4000 cm^{-1} or a *Thermo Scientific Nicolet iS10* ATR spectrometer.

The NMR spectra were recorded on a *JEOL 400 MHz* spectrometer. ESI-TOF mass spectra were measured with an *Agilent 6210 ESI-TOF* (Agilent Technologies, Santa Clara, CA, USA). All MS results are given in the form: *m/z*, assignment.

UV-vis spectra were recorded on a *Specord 40 (Analytik Jena)* spectrophotometer in the wavelength range 200-700 nm.

The X-band EPR spectra were recorded on a *Miniscope MS400 Magnettech* spectrometer with a Rectangular TE102 microwave generator at 300 K and 77 K. The simulated spectra were taken with the program WinEPR SimFonia [198].

Time-Resolved Laser Fluorescence (TRLFS) was performed at < 20 K using a pulsed Nd:YAG (*Spectra Physics*) pumped dye laser system (*Radiant Dyes Narrow Scan K*). The detection was done with a spectrograph (*Shamrock 303i*) equipped with a polychromator with 300, 600, and 1200 lines/mm gratings and an ICCD camera system (*Andor iStar*).

Chemdraw Professional 15.1 was used to determine the calculated values for elemental analysis and mass spectra.

DFT calculations were performed with the high-performance computing system of the ZEDAT (SOROBAN) [199] using the program packages GAUSSIAN 09 [200, 201] and GAUSSIAN 16. The gas phase geometry optimizations were performed using coordinates derived from the X-ray crystal data. The calculations of the isomeric complexes **30** and **34** were undertaken using the hybrid density functional B3LYP [202 - 204] together with the pseudopotential LANL2DZ obtained from EMSL database [205, 206].

4.2. Crystal Structure Determination

The intensities for the X-ray determinations were collected on STOE IPDS-2T or Bruker D8 Venture instruments with Mo/Kα radiation. The space groups were determined using CHECK-HKL [207]. Semi-empirical or numerical absorption corrections were carried out by SADABS or X-RED32 programs [208, 209]. Structure solution and refinement were performed with the SHELXS 97 [210], SHELXS 86 [210], and SHELXL 2014/7 programs included in the WinGX program package [211, 212]. Hydrogen atoms were calculated for the idealized positions and treated with the 'riding model' option of SHELXL. The lanthanide compounds crystallized with dichloromethane or chloroform as solvent molecule, in a special position and highly disordered. The refinements of the structures were undertaken with removal of the disordered solvents molecule using the SQUEEZE option installed in the program PLATON. Besides that, the compound $[Ga\{Au(L4\text{-}\kappa S)\}_2](NO_3) \cdot 0.5CHCl_3 \cdot CH_2Cl_2 \cdot 0.5MeOH$ crystallized with highly disordered solvent molecules. The SQUEEZE option was required to remove the solvent molecules as well. The representation of molecular structures was done using the programs DIAMOND 4 [213] and POV-Ray V.3.6 [214]. Tables containing more information about crystal data, refinement, positional parameter and ORTEP [212] ellipsoid drawings are given as Supplementary material.
Table 17 compares the refinement parameters with and without SQUEEZE for some lanthanide compounds and $[Ga\{Au(L4\text{-}\kappa S)\}_2](NO_3) \cdot 0.5CHCl_3 \cdot CH_2Cl_2 \cdot 0.5MeOH$.

Table 17: Comparison of the structures refinement parameters for the compounds, **11**, **13** - **19**, **22** and $[Ga\{Au(L4\text{-}\kappa S)\}_2]^+$ **26**, with and without the SQUEEZE calculations.

Solvents	$[La\{Au(L4\text{-}\kappa S)\}_3]$		$[Nd\{Au(L4\text{-}\kappa S)\}_3]$	
	$0.5CH_2Cl_2$	SQUEEZE	$0.5CH_2Cl_2$	SQUEEZE
S. A. V. [Å^3]	205.9		190.6	
# of removed electrons	49		51	
Solvent per Unit Cell	CH_2Cl_2	ca. CH_2Cl_2	CH_2Cl_2	ca. CH_2Cl_2
Goof	1.057	1.055	1.033	1.098
R1(I>2σ)	0.0473	0.0428	0.0490	0.0470
R1(all data)	0.0602	0.0513	0.0840	0.0633
wR2(I>2σ)	0.1224	0.1034	0.0835	0.0792
wR2(all data)	0.1331	0.1079	0.0954	0.0835
Largest diff. peak [e. Å^{-3}]	2.953	2.360	2.778	2.695
Largest diff. hole [e. Å^{-3}]	-3.661	-3.519	-2.384	-2.596

Continuation of Table 17

Solvents	[Sm{Au(L4-κS)}$_3$]		[Eu{Au(L4-κS)}$_3$]	
	0.5CH_2Cl_2	SQUEEZE	0.5CH_2Cl_2	SQUEEZE
S. A. V. [Å^3]	140.0		138.1	
# of removed electrons	50		42	
Solvent per Unit Cell	CH_2Cl_2	ca. CH_2Cl_2	CH_2Cl_2	ca. CH_2Cl_2
Goof	1.153	1.032	1.006	0.847
R1(I>2σ)	0.0661	0.0469	0.0600	0.0535
R1(all data)	0.0847	0.0542	0.0708	0.0609
wR2(I>2σ)	0.1380	0.0944	0.1337	0.1168
wR2(all data)	0.1457	0.0972	0.1437	0.1208
Largest diff. peak [e. Å^{-3}]	4.356	2.643	3.243	2.724
Largest diff. peak [e. Å^{-3}]	-3.997	-2.540	-3.044	-2.809

Solvents	[Gd{Au(L4-κS)}$_3$]		[Tb{Au(L4-κS)}$_3$]	
	0.5CH_2Cl_2	SQUEEZE	0.5$CHCl_3$	SQUEEZE
S. A. V. [Å^3]	140.5		290.6	
# of removed electrons	52		47	
Solvent per Unit Cell	CH_2Cl_2	ca. CH_2Cl_2	$CHCl_3$	ca. $CHCl_3$
Goof	1.089	1.249	1.041	1.101
R1(I>2σ)	0.0524	0.0490	0.0309	0.0265
R1(all data)	0.0590	0.0528	0.0371	0.0283
wR2(I>2σ)	0.1269	0.0921	0.0631	0.0543
wR2(all data)	0.1309	0.0935	0.0659	0.0550
Largest diff. peak [e. Å^{-3}]	4.390	3.112	2.027	1.688
Largest diff. peak [e. Å^{-3}]	-3.582	-3.246	-2.514	-2.863

Solvents	[Dy{Au(L4κ-S)}$_3$]		[Ho{Au(L4κ-S)}$_3$]	
	0.5CH_2Cl_2	SQUEEZE	0.5$CHCl_3$	SQUEEZE
S. A. V. [Å^3]	137.8		142.9	
# of removed electrons	47		52	
Solvent per Unit Cell	CH_2Cl_2	CH_2Cl_2	$CHCl_3$	$CHCl_3$
Goof	1.200	1.124	1.122	1.226
R1(I>2σ)	0.0730	0.0634	0.0437	0.0345
R1(all data)	0.0933	0.0762	0.0498	0.0391
wR2(I>2σ)	0.1583	0.1362	0.1096	0.0691
wR2(all data)	0.1658	0.1420	0.1128	0.0705
Largest diff. peak [e. Å^{-3}]	4.134	3.208	6.153	1.605

Continuation of Table 17

Largest diff. peak [e. Å^{-3}]	-3.919	-3.146	-2.454	-2.400
Solvents	[Yb{Au(L4κ-S)}$_3$]		[Ga{Au(L4κ-S)}$_2$]	
	0.5CH_2Cl_2	SQUEEZE	0.5$CHCl_3$, CH_2Cl_2 0.5MeOH	SQUEEZE
S. A. V. [Å^3]	146.9		1899.2	
# of removed electrons	46		538	
Solvent per Unit Cell	CH_2Cl_2	ca. CH_2Cl_2	2$CHCl_3$, 2MeOH 4CH_2Cl_2	4.5$CHCl_3$, 5MeOH 4.5CH_2Cl_2
Goof	1.083	1.073	1.037	1.057
R1(I>2σ)	0.0718	0.0653	0.0405	0.0334
R1(all data)	0.0836	0.0759	0.465	0.0383
wR2(I>2σ)	0.1568	0.1402	0.1045	0.0847
wR2(all data)	0.1634	0.1450	0.1077	0.0865
Largest diff. peak [e. Å^{-3}]	4.734	4.251	2.671	2.576
Largest diff. peak [e. Å^{-3}]	-4.055	-3.782	-1.615	-1.774

4.3. Synthetic Procedures

Chloro(tetrahydrothiophene)gold(I) ([AuCl(THT)]) [215], chloro(triphenylphosphine) gold(I), ([AuCl(PPh_3)]) [216], sodium tetrachloroaurate(III) hydrate, (Na[$AuCl_4$]·xH_2O) [217], and dichloro[2-(dimethylaminomethyl)phenyl-C^1,N^1]gold(III), ([Au(damp-κC^1,N)Cl_2]) [135], *N*,*N*-diethyl-*N*′-benzoylthiourea (HL1) [95], *N*-(3,3-diethylamino-thiocarbonyl)-*N*′-(2-hydroxyphenyl)benzamidine (H_2L2) [119], 2,6-dipicolinoylbis(*N*,*N*-diethylthiourea) (H_2L4) [218] were synthesized according to literature procedures. *N*,*N*-diethylthiourea was synthesized according to the procedure of Yokohama [219].

4.3.1. Synthesis of H_2L3

H_2L3 was synthesized following the procedure published by Castillo Gomez et al. [146] with some modifications. 3,3-Diethylamino(thiocarbamoyl)benzimidoyl chloride (2.54 g, 10 mmol) dissolved in 25 mL of dry THF was added dropwise to a stirred mixture of ethylenediamine (0.33 mL, 5 mmol) and Et_3N (1.67 mL, 12 mmol) in 10 mL of dry THF. The mixture was stirred for 4 hours at room temperature. During this time, a colourless precipitate of $Et_3N{\cdot}HCl$ was formed. It was filtered off and the filtrate was evaporated to dryness under reduced pressure. The oily residue was dissolved in ethanol (3 mL) and overlayed with diethyl ether (9 mL), which was carefully added on the border of flask. The mixture was stored in the refrigerator overnight, the pale yellow crystalline compound of H_2L3 obtained from the solution was filtered off, washed with diethyl ether and dried in vacuum.

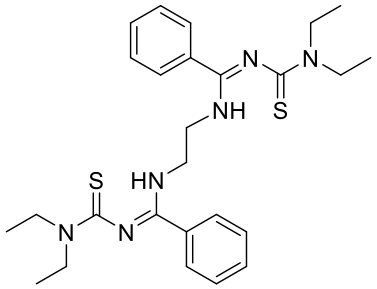

Yield: 1.97 g (79 %).

Elemental analysis: Calcd. for $C_{26}H_{36}N_6S_2{\cdot}2C_2H_6O$: C, 61.2; H, 8.2; N, 14.3; S, 10.9 %. Found: C, 61.3; H, 7.9; N, 13.7; S, 11.3 %.

IR (KBr, cm^{-1}): 3250 (m), 2970 (m), 2929 (m), 2870 (w), 1587 (s), 1560 (m), 1438 (s), 1419 (s), 1375 (m), 1313 (m), 1255 (m), 1138 (s), 1076 (m), 881 (w), 777 (s), 698 (m).

^{1}H NMR (400 MHz, CD_2Cl_2, ppm): 7.45 - 7.35 (m, 10H, Ph); 3.8 (m, 4H, CH_2); 3.58 - 3.52 (m, 8H, CH_2); 1.17 (t, J = 8.0 Hz, 6H, CH_3); 1.09 (t, J = 8.0 Hz, 6H, CH_3).

^{13}C{^{1}H} NMR ($CDCl_3$, ppm): 188.4 (C=S); 159.3 (C=N); 134.1 (Ph), 130.4 (Ph); 128.3 (Ph); 57.8 (CH_2); 46.0 (CH_2); 44.6 (CH_2); 18.2 (CH_2); 12.8 (CH_3); 11.8 (CH_3).

ESI$^+$ MS (*m/z*): 519.2335, 100 % $[M + Na]^+$ (Calcd. 519.2335), 535.2074, 41 % $[M + K]^+$ (Calcd. 535.2074).

4.3.2. Organometallic Gold(III) Complexes with Thiourea Derivatives

[Au(damp-κC^1,N)(L1)](PF$_6$)

[Au(damp-κC^1,N)Cl$_2$] (120 mg, 0.3 mmol) dissolved in 3 mL of THF was added dropwise to a stirred solution of HL1 (71 mg, 0.3 mmol) in 2 mL of THF, and three drops of Et_3N were added. The colour of the solution immediately turned yellow and a colourless solid of Et_3N·HCl was formed. The suspension was stirred for 2 hours at room temperature and filtered. The solvent was removed in vacuum and the residue was dissolved in 3 mL of EtOH. $(Bu_4N)PF_6$ (116 mg, 0.3 mmol) was added and the suspension was stirred for 20 minutes. A pale-yellow precipitate was formed. It was filtered off and washed with EtOH. The precipitate was recrystallized from a mixture of CH_2Cl_2/MeOH.

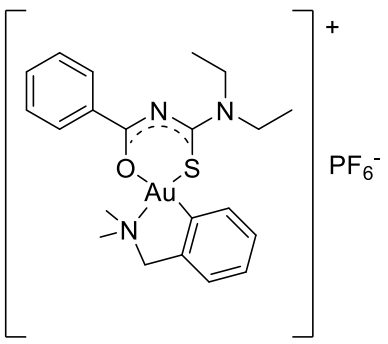

Yield: 159 mg (75 %).

Elemental analysis: Calcd. for $C_{21}H_{27}AuN_3OSPF_6$: C, 35.5; H, 3.8; N, 5.9; S, 4.5 %. Found: C, 35.3; H, 3.2; N, 5.9; S, 4.7 %.

IR (KBr, cm^{-1}): 3070 (w), 2980 (w), 2940 (w), 1510 (s), 1448 (m), 1408 (s), 1356 (m), 1254 (m), 1200 (w), 1076 (w), 839 (s), 752 (m), 715 (m), 557 (s).

^{1}H NMR (400 MHz, CD_2Cl_2, ppm): 8.21- 8.06 (m, 2H, Ph); 7.61 (t, J = 7.3 Hz, 2H, Ph); 7.55-7.46 (m, 2H, Ph); 7.40-7.15 (m, 4H, Ph); 4.51 (s, 2H, NCH_2); 3.95 (m, 4H, CH_2); 3.31 (s, 6H, CH_3); 1.43 (t, J = 7.1 Hz, 3H); 1.34 (t, J = 7.1 Hz, 3H).

^{13}C{^{1}H} NMR (CD_2Cl_2, ppm): 169.4 (C=S); 161.5 (C=O); 144.8 (C-Au), 135.5 (Ph-CH_2), 134.0 (Ph-damp); 132.6 (Ph); 129.0 (Ph); 127.9 (Ph); 127.5 (Ph), 124.4 (Ph-damp); 71.6 ($\underline{C}H_2$-N(CH_3)$_2$); 50.6 ((CH_3)$_2$-N)); 47.6, 47.2 (CH_2); 11.9 (CH_3) 11.7 (CH_3).

ESI$^+$ MS (*m/z*): 566.1731, 100 % $[M]^+$ (Calcd. 566.1535).

[Au(Hdamp-κ*C*^{1})(L2)](PF$_6$)

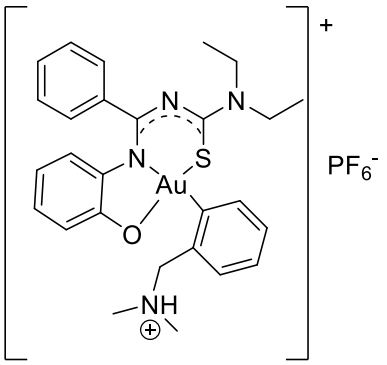

[Au(κC^1,N-damp)Cl$_2$] (80 mg, 0.2 mmol) was suspended in 1 mL of MeOH and H$_2$L2 (64 mg, 0.2 mmol) dissolved in 4 mL of MeOH was added dropwise. After one hour of stirring at room temperature, KPF$_6$ (38 mg, 0.2 mmol) was added giving a dark-yellow solution, which was filtered *via* celite. The resulting solution was left for slow evaporation, which resulted in the formation of orange crystals.

Yield: 83 mg (52 %).

Elemental analysis: Calcd. for $C_{27}H_{32}AuN_4OSPF_6$: C, 40.4; H, 4.0; N, 7.0; S, 4.0 %. Found: C, 38.0; H, 4.4; N, 6.4; S, 3.9 %.

IR (KBr, cm^{-1}): 3302 (m), 3064 (w), 2980 (w), 2937 (w), 2877 (w), 2847 (w), 1610 (m), 1560 (s), 1529 (s), 1458 (m), 1384 (m), 1363 (m), 1254 (m), 1141 (m), 1028 (w), 981 (w), 960 (w), 943 (w), 839 (s), 763 (m), 710 (m), 557 (s).

^{1}H NMR (400 MHz, $CDCl_3$, ppm): 8.66 (br, 1H, NH^+); 8.17- 8.0 (br, 1H, Ph); 7.62-7.41 (m, 2H, Ph); 7.41-7.27 (m, 3H, Ph); 7.22-6.99 (m, 5H, Ph); 6.88-6.70 (m, 2H, Ph); 4.15 (s, 2H, NCH_2); 3.98 (q, J=7.12 Hz, 2H, CH_2); 3.80 (q, J=7.1, 2H, CH_2); 3.48 (s, 3H, NCH_3); 2.79 (s, 3H, NCH_3); 1.42 (m, 6H, CH_3).

^{13}C{^{1}H} NMR ($CDCl_3$, ppm): 173.0 (C=S); 157.7 (N-C=N); 147.8 (C-O), 146.9 (Ph), 145.4 (C-CH_2); 133.3 (Ph-N), 132.0 (Ph); 130.5 (Ph), 129.7 (2C (Ph)); 129.3 (C-Au); 127.9 (2C (Ph)); 127.3 (Ph); 125.1 (2C (Ph)); 124.9 (Ph); 121.5 (Ph); 120.9 (Ph); 116.3 (Ph); 74.2 ($\underline{C}H_2$-NH(CH_3)$_2$); 52.2 ((CH_3)$_2$-N); 48.9 (CH_2); 47.3 (CH_2); 13.5 (CH_3); 12.6 (CH_3).

ESI$^+$ MS (*m/z*): 657.1934, 4 % $[M]^+$ (Calcd. 657.1957).

4.3.3. Gold(I) Complexes with H$_2$L3

[{AuCl}$_2$(H$_2$L3-κS)]: A solution of H$_2$L3 (49.6 mg, 0.1 mmol) in 2 mL of MeOH was added dropwise to a suspension of [AuCl(THT)] (65 mg, 0.2 mmol) in 1 mL of MeOH. The mixture was stirred for 2 hours at room temperature. The formed colourless precipitate was filtered off and washed with a small amount of MeOH. Colourless single crystals suitable for X-ray diffraction were obtained dissolving the compound

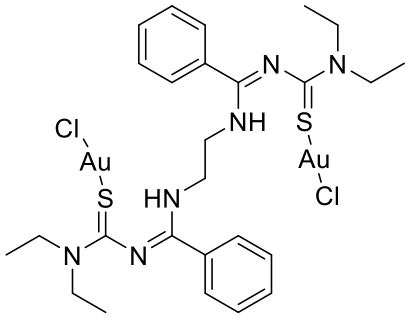

in hot CH_2Cl_2 (3mL) and overlayering it with MeOH (3mL) which was added carefully on the border of the vial and stored in the refrigerator overnight.

Yield: 72 mg (75 %).

Elemental analysis: Calcd. for $C_{26}H_{36}Au_2Cl_2N_6S_2$: C, 32.5; H, 3.8; N, 8.7; S, 6.7 %. Found: C, 32.3; H, 4.0; N, 8.5; S, 6.7 %.

IR (KBr, cm^{-1}): 3288 (br, s), 3057 (w), 2978 (m), 2931 (m), 2870 (w), 1604 (s), 1595 (s), 1575 (s), 1552 (s), 1508 (s), 1436 (s), 1379 (m), 1359 (m), 1296 (s), 1232 (m), 1143 (m), 1078 (m), 943 (w), 900 (w), 869 (w), 773 (s), 696 (m), 650 (w), 613 (w), 594 (w), 495 (w), 420 (w).

^{1}H-NMR and **^{13}C-NMR:** The acquisition of NMR spectra was not possible due to the low solubility of the compound in organic solvents.

ESI$^+$ MS (*m/z*): 693.2165, 100 % $[M\text{-}Au\text{-}2Cl)]^+$ (Calcd. 693.2108).

[{Au(SCN)}$_2$(H$_2$L3κ-S)]: A solution of KSCN (9.6 mg, 0,1 mmol) dissolved in 1 mL of MeOH was added dropwise to a solution containing [AuCl(THT)] (32.5 mg, 0.1 mmol) and H_2L3 (24.8 mg, 0.05 mmol) dissolved in 5 mL of CH_2Cl_2. The resulting solution was stirred for 2 hours at room temperature. Colourless single crystals suitable for X-ray diffraction were obtained by slow evaporation of the solvents.

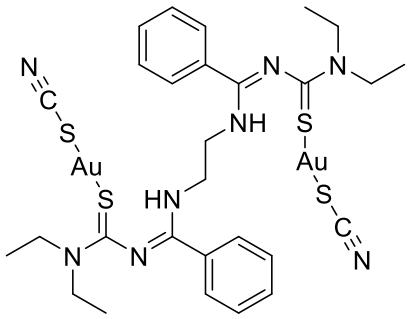

Yield: 26.0 mg (49 %).

Elemental analysis: Calcd. For $C_{30}H_{44}Au_2N_8O_2S_4$ [{Au(SCN)}$_2$(H_2L3-κS)]·2MeOH, 33.7; H, 4.1; N, 10.5; S, 12.0 %. Found: C, 33.2; H, 4.3; N, 10.5; S, 12.0 %.

IR (KBr, cm^{-1}): 3390 (br, w), 3346 (br, w), 3267 (br, m), 3126 (w), 3064 (w), 2978 (m), 2931 (m), 2870 (w), 2123 (vs), 1593 (s), 1560 (s), 1508 (s), 1436 (s), 1379 (m), 1357 (m), 1309 (m), 1292 (m), 1230 (m), 1145 (m), 1118 (m), 1076 (m), 1020 (m), 885 (m), 777 (vs), 694 (vs), 673 (w), 586 (w), 495 (w), 426 (w).

^{1}H-NMR and **^{13}C-NMR:** The acquisition of NMR spectra was not possible due to the low solubility of the compound in organic solvents.

ESI$^+$ MS (*m/z*): 693.2195, 100 % $[M\text{-}Au\text{-}2(SCN)]^+$ (Calcd. 693.2108).

[{Au(PPh$_3$)}$_2$(H$_2$L3κ-S)](PF$_6$)$_2$: A solution of H$_2$L3 (49.6 mg, 0.1 mmol) in 3 mL of MeOH was added to a suspension of [AuCl(PPh$_3$)] (100 mg, 0.2 mmol) in 5 mL of MeOH. The suspension became a clear yellow solution. The mixture was stirred for 2 hours at room temperature. (Bu$_4$N)(PF$_6$) (77.0 mg, 0.2 mmol) was added at once and the suspension was stirred for more 15 minutes. During this time, a colourless precipitate was formed, which was filtered off and dried in the air. The solid was dissolved in 2 mL of CH_2Cl_2 and overlayered with 3 mL of MeOH. Single crystals suitable for X-ray diffraction were obtained from slow diffusion of the MeOH into the CH_2Cl_2 solution.

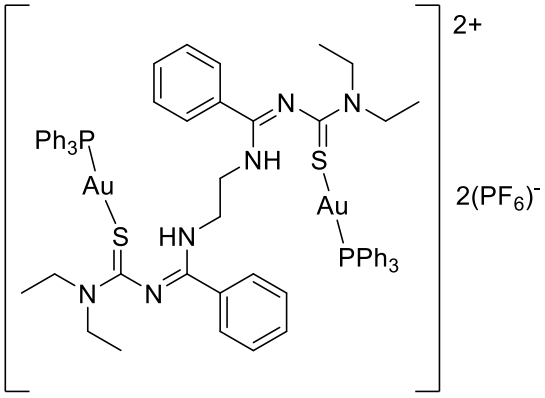

Yield: 72.0 mg (70 %).

Elemental analysis: Calcd. for $C_{62}H_{66}Au_2N_6S_2P_4F_{12}$: C, 43.7; H, 3.7; N, 4.9; S, 3.8 %. Found: C, 44.0; H, 4.3; N, 4.9; S, 3.9 %.

IR (KBr, cm^{-1}): 34060 (m), 2981 (w), 2937 (w), 1591 (m), 1558 (m), 1508 (s), 1436 (s), 1375 (w), 1307 (m), 1269 (w), 1234 (w), 1147 (w), 1099 (m), 839 (vs), 754 (m), 696 (s), 557 (s), 540 (s), 499 (m).

^{1}H NMR (400 MHz, CD_2Cl_2, ppm): 8.0 - 7.0 (m, 40H, Ph); 6.7 (br, 2H, NH); 3.8 (br, 4H, N-CH_2-CH_2-N); 3.60 (br, 2H, CH_2); 3.45 (br, 2H, CH_2); 1.33 (m, 12H, CH_3).

^{13}C{^{1}H} NMR (CD_2Cl_2, ppm): 180.5 (C=S); 161.0 (N-C=N); 134.0, 132.5, 129.7, 129.6, 128.1, 127.5 (Ph); 47.9 (HN-$\underline{C}H_2$-CH_2-NH); 46.9 (CH_2); 41.4 (CH_2); 12.1 (CH_3).

^{31}P{^{1}H} NMR (CD_2Cl_2, ppm): 38.3

ESI$^+$ MS (*m/z*): 721.1573, 100 % $[Au(PPh_3)_2]^+$ (Calcd. 721.1483).

4.3.4. Gold(I) Complexes with H$_2$L4

[{AuCl}$_2$(H$_2$L4-κS)]: [AuCl(THT)] (64 mg, 0.2 mmol) was added to a solution of H$_2$L4 (40 mg, 0.1 mmol) in 3 mL of hot THF. After a few minutes, the suspension became clear and a colourless solid precipitated. The suspension was stirred for 2 hours at room temperature and the precipitate was filtered off and washed with THF. The solid was dissolved in 2 mL of

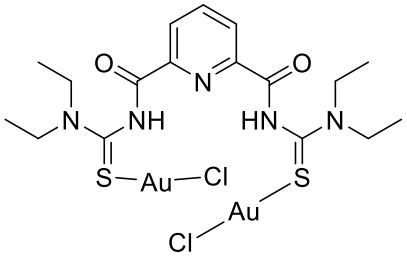

CH_2Cl_2 and overlayered with 2 mL of MeOH. Single crystals suitable for X-ray diffraction were obtained from slow diffusion of the MeOH into the CH_2Cl_2 solution.

Yield: 55 mg (64 %).

Elemental analysis: Calcd. for $C_{17}H_{25}Au_2Cl_2N_5O_2S_2$: C, 23.7; H, 2.9; N, 8.1; S, 7.5 %. Found: C, 23.7; H, 2.9; N, 8.2; S, 7.8 %.

IR (KBr, cm^{-1}): 3302 (s), 2976 (w), 2930 (w), 1707 (s), 1560 (s), 1446 (s), 1290 (m), 1224 (m), 1076 (w), 999 (w), 842 (w), 750 (m).

^{1}H NMR (400 MHz, $CDCl_3$, ppm): 10.83 (s, 2H, NH); 8.42 (d, J = 7.8 Hz, 2H, Ph); 8.20 (t, J = 8 Hz, 1H, Ph); 4.02 (q, J = 7 Hz, 4H, CH_2); 3.75 (q, J = 7.2 Hz, 4H, CH_2); 1.49 (t, J = 7.2 Hz, 3H); 1.42 (t, J = 7.2 Hz, 3H).

^{13}C{^{1}H} NMR ($CDCl_3$, ppm): 177.4 (C=O); 157.3 (C=S); 147.4, 140.2, 127.5 (Py); 51.4, 48.9 (CH_2); 12.8, 11.6 (CH_3).

ESI$^+$ MS (*m/z*): 592.1175, 100 % $[M - Au - 2Cl]^+$ (Calcd. 592.1110).

[{Au(PPh$_3$)}$_2$(L4-κS)]: A solution of H_2L3 (40 mg, 0.1 mmol) in 3 mL of MeOH was added to a suspension of [AuCl(PPh_3)] (100 mg, 0.2 mmol) in 5 mL of MeOH. After addition of 2 drops of Et_3N, the suspension became a clear yellow solution. The mixture was stirred for 2 hours at room temperature and kept in a freezer for crystallization. Colourless crystals were obtained after one week.

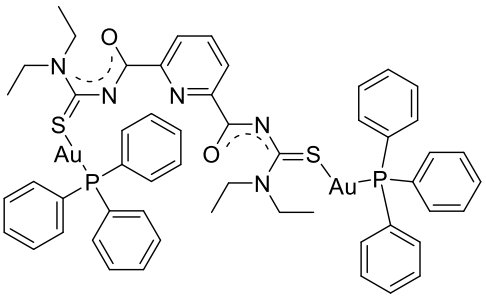

Yield: 60 mg (46 %).

Elemental analysis: Calcd. for $C_{53}H_{53}Au_2N_5O_2P_2S_2$: C, 48.5; H, 4.1; N, 5.3; S, 4.9 %. Found: C, 48.4; H, 4.2; N, 5.6; S, 4.9 %.

IR (KBr, cm^{-1}): 3069 (w), 3049 (w), 2976 (w), 2932 (w), 2870 (w), 1610 (m), 1558 (m), 1500 (s), 1435 (s), 1355 (s), 1240 (s), 1101 (s), 997 (m), 900 (m), 848 (m), 746 (s), 692 (s), 538 (s), 503 (s), 401 (m).

^{1}H-NMR and **^{13}C-NMR:** The acquisition of NMR spectra was not possible due to the low solubility of the compound in organic solvents.

ESI$^+$ MS (*m/z*): 1334.2305, 26 % $[M + Na]^+$ (Calcd. 1334.2339).

4.4. M^{2+} Complexes (M^{2+} = Ca^{2+}, Sr^{2+} or Ba^{2+}) with a Tetranuclear Gold(I) Coronand

H_2L4 (40 mg, 0.1 mmol) was added to a suspension of [AuCl(THT)] (32.5 mg, 0.1 mmol) and $Ca(NO_3)\cdot 4H_2O$, $Sr(NO_3)\cdot 4H_2O$ or $Ba(NO_3)\cdot 2H_2O$ (0.05 mmol) in 3 mL of MeOH and 2 drops of water. The mixture was stirred for 30 minutes before the addition of 4 drops of Et_3N. The mixture was stirred at room temperature for 1 hour. During this process, a white precipitate was obtained. This was filtered off, washed with MeOH and dried in the air. The solid was dissolved in CH_2Cl_2 (1 mL) and overlayered with MeOH (1 mL), the mixture was kept in the refrigerator overnight. Single crystals suitable for X-ray diffraction were obtained from slow diffusion of MeOH into the CH_2Cl_2 solution.

[{$Ca_2(MeOH)_3(H_2O)$}{Au(L4-κS)}$_4$]

Yield: 62 mg (48 %).

Elemental analysis: Calcd. for $C_{73.5}H_{115}Au_4N_{20}O_{14}S_8Ca_2Cl$: ($[C_{71}H_{106}Au_4N_{20}O_{12}S_8Ca_2] \cdot 0.5CH_2Cl_2 \cdot 2MeOH$): C, 33.1; H, 4.3; N, 10.6; S, 9.6 %. Found: C, 32.1; H, 4.1; N, 10.8; S, 10.1 %.

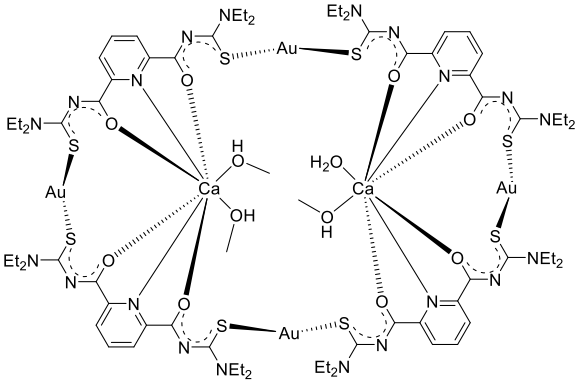

IR (KBr, cm^{-1}): 3431 (br, m), 2974 (m), 2931 (m), 2870 (w), 1602 (w), 1550 (m), 1585 (w), 1554 (w), 1508 (s), 1458 (m) 1431 (m), 1406 (m), 1357 (s), 1315 (w), 1244 (s), 1201 (w), 1122 (s), 1076 (m), 1012 (w), 906 (w), 858 (w), 750 (m), 669 (w), 655 (w), 482 (w), 420 (w).

^{1}H NMR (400 MHz, $CDCl_3$, ppm): 8.02 (d, J = 8.0 Hz, 1H, Py); 7.96 (d, J = 8.0 Hz, 1H, Py); 7.78 (t, J = 7.6 Hz, 1H, Py); 3.72 (m, 8H, CH_2); 1.14 (m, 12H, CH_3).

^{13}C{^{1}H} NMR ($CDCl_3$,ppm): 181.3 (C=O); 179.8 (C=O); 167.7 (C=S); 165.6 (C=S); 153.0 (C1-Py); 152.4 (C5-Py); 137.9 (C3-Py); 125.8 (C2-Py); 125.6 (C4-Py); 46.6 (CH_2), 46.3 (CH_2); 46.1 (CH_2); 45.6 (CH_2); 12.7 (CH_3).

ESI$^+$ MS (*m/z*): 2463.3379, 27 % $[M - 3MeOH - H_2O + Na]^+$ (Calcd. 2463.2979), 1243.1665, 100 % $[M - 2Au - 2(L4) - Ca + Na]^+$ (Calcd. 1243.1435).

[{Sr$_2$(MeOH)$_2$(H$_2$O)$_2$}{Au(L4-κS)}$_4$]

Yield: 59.6 mg (43 %).

Elemental analysis: Calcd. for $C_{71}H_{111}Au_4N_{20}O_{14.5}S_8Sr_2$: ([$C_{70}H_{104}Au_4N_{20}O_{12}S_8Sr_2$] · MeOH · 1.5$H_2O$): C, 31.6; H, 4.2; N, 10.4; S, 9.5 %. Found: C, 31.5; H, 4.0; N, 10.3; S, 9.7 %.

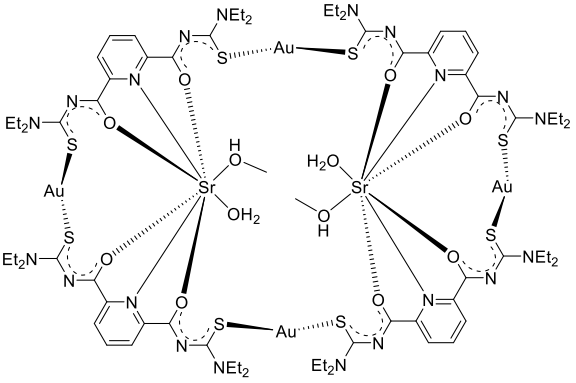

IR (KBr, cm^{-1}): 3431 (br, m), 2974 (m), 2931 (m), 2870 (w), 1602 (w), 1583 (w), 1554 (m), 1508 (s), 1458 (s), 1431 (s), 1406 (s), 1356 (s), 1315 (w), 1244 (s), 1122 (m), 1076 (w), 1008 (w), 906 (w), 841 (w), 748 (m), 678 (w), 654 (w), 480 (w), 420 (w).

^{1}H-NMR and **^{13}C-NMR:** The acquisition of NMR spectra was not possible due to the low stability of the compound in organic solvents.

ESI$^+$ MS (*m/z*): 2537.2070, 14 % [M – 2MeOH – 2H_2O +H]$^+$ (Calcd. 2537.2020).

[{Ba$_2$(μ-H$_2$O)}{Au(L4-κS)}$_4$]

Yield: 62 mg (47 %).

Elemental analysis: Calcd. for $C_{75}H_{120}Au_4Ba_2Cl_2N_{20}O_{15}S_8$: ([$C_{68}H_{94}Au_4Ba_2N_{20}O_8S_8$] · CH_2Cl_2 · 6MeOH) C, 30.7; H, 4.1; N, 9.6; S, 8.8 %. Found: C, 29.3; H, 3.90; N, 9.9; S, 9.3 %.

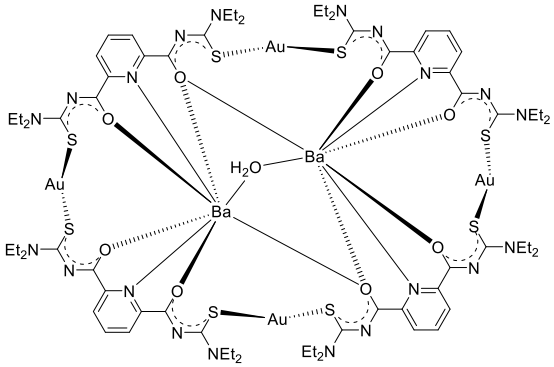

IR (KBr, cm^{-1}): 3431 (br, m), 2974 (m), 2931 (m), 2870 (w), 1600 (w), 1550 (m), 1508 (s), 1431 (s), 1356 (s), 1315 (w), 1244 (s), 1120 (m), 1076 (m), 1005 (w), 906 (w), 841 (w), 746 (m), 680 (w), 653 (w), 480 (w), 420 (w).

^{1}H NMR (400 MHz, $CDCl_3$, ppm): 8.03 (br, 1H, Py); 7.76 (t, J = 7.6 Hz, 2H, Py); 3.62 (br, 8H, CH_2); 1.15 (t, J = 6.7 Hz, 12H, CH_3).

^{13}C{^{1}H} NMR ($CDCl_3$, ppm): 179.7 (C=O); 168.6 (C=S); 154.3 (Py), 137.6 (Py), 126.5 (Py); 46.5 (CH_2), 46.0 (CH_2); 13.0 (CH_3).

ESI$^+$ MS (*m/z*): 2659.1751, 58 % [M - H_2O + Na]$^+$ (calcd. 2659.1832), 1341.0823, 86 % [M - 2Au - 2(L4) - H_2O + Na]$^+$ (calcd. 1341.0862).

4.4.1. Ln^{3+} Complexes with a Trinuclear Gold(I) Coronand

H_2L4 (59.3 mg, 0.15 mmol) was added to a suspension of [AuCl(THT)] (48.0 mg, 0.15 mmol) and the respective lanthanides salts (MCl_3 for M = Gd or Dy, $MCl_3 \cdot 6H_2O$ for M = Nd, Sm, Eu, Er, or Yb, $M(NO_3)_3$ for M = La, Ho, or Tm, $Tb(NO_3)_3 \cdot 5H_2O$, $Ce(NO_3)_3 \cdot 6H_2O$ and $Lu(NO_3)_3 \cdot H_2O$ (0.05 mmol) in 3 mL of MeOH. Most of the mixtures formed a solution after 30 minutes, with the exception of the reactions with Er^{3+}, Tm^{3+}, Yb^{3+}, and Lu^{3+}, which formed suspensions. The addition of 6 drops of triethylamine resulted in an immediate precipitation of the complexes from the reaction mixtures as colourless solids. The complex **12** was formed as an orange-red solid. The mixture was stirred for 1.5 hour at room temperature. The solids were filtered off, washed with small amount of MeOH and dried in the air. The complexes were dissolved in 1 mL of CH_2Cl_2 or $CHCl_3$ and overlayered with 1 mL of MeOH, which was added carefully on the wall of the vial. Single crystals suitable for X-ray diffraction were obtained overnight by slow diffusion of MeOH into CH_2Cl_2 or $CHCl_3$ solutions, that were stored in the refrigerator.

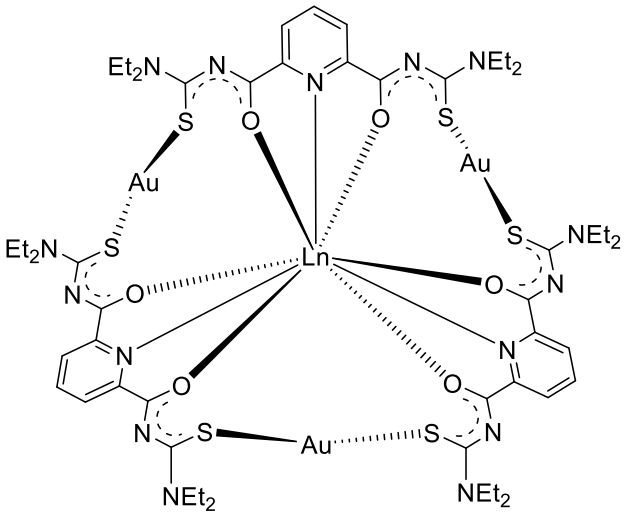

M = La, Ce, Nd, Sm, Eu, Gd, Tb, Dy, Ho, Er, Tm, Yb, Lu

The elemental analyses for all lanthanide complexes were performed from finely powdered and carefully dried samples.

[La{Au(L4-κS)}$_3$]

Yield: 90.0 mg (94 %).

Elemental analysis: Calcd. for $C_{51}H_{69}N_{15}O_6S_6Au_3La$: C, 32.1; H, 3.6; N, 11.0; S, 10.1 %. Found: C, 32.0; H, 3.7; N, 10.7; S, 10.3 %.

IR (KBr, cm^{-1}): 3066 (vw), 2970 (w), 2933 (w), 2870 (w), 1583 (m), 1558 (vs), 1512 (vs), 1436 (m), 1357 (s), 1244 (s), 1124 (s), 1072 (m), 912 (m), 750 (m), 669 (m), 632 (m), 482 (w), 430 (w), 410 (w).

^{1}H NMR (400 MHz, $CDCl_3$, ppm): 8.02 (d, J = 8.0 Hz, 2H, Py); 7.83 (t, J = 8.0 Hz, 1H, Py); 3.68 (m, 2H, CH_2); 3.50 - 3.40 (m, 6H, CH_2); 1.07 (s, br, 12H, CH_3).

^{13}C{^{1}H} NMR ($CDCl_3$, ppm): 185.7 (C=O); 162.7 (C=S); 153.3, 138.2, 125.2 (Py); 46.9, 46.3 (CH_2); 12.8, 12.5 (CH_3).

ESI$^+$ MS (*m/z*): 1910.2003, 100 % $[M + H]^+$ (calcd. 1910.2012).

UV-vis: (CH_2Cl_2), 227 nm (ε = 156 x10^3 M^{-1} cm^{-1}), 264 nm (ε = 104 x10^3 M^{-1} cm^{-1}), 309 nm (ε = 83 x10^3 M^{-1} cm^{-1}).

[Ce{Au(L4-κS)}$_3$]

Yield: 80.0 mg (84 %).

Elemental analysis: Calcd. for $C_{51}H_{69}N_{15}O_6S_6Au_3Ce$: C, 32.0; H, 3.6; N, 11.0; S, 10.1 %. Found: C, 32.1; H, 3.7; N, 11.0; S, 10.2 %.

IR (KBr, cm^{-1}): 3066 (vw), 2972 (w), 2933 (w), 2870 (vw), 1583 (m), 1556 (vs), 1512 (vs), 1438 (m), 1398 (m), 1357 (s), 1315 (m), 1244 (s), 1201 (m), 1124 (s), 1070 (m), 1016 (m), 912 (s), 860 (w), 752 (s), 667 (s), 632 (m), 482 (w), 432 (w), 410 (w).

ESI$^+$ MS (*m/z*): 1911.2008, 100 % $[M + H]^+$ (calcd. 1911.2003); 1933.5769 61 % $[M + Na]^+$ (calcd. 1933.1823).

UV-vis: (CH_2Cl_2), 228 nm (ε = 93 x10^3 M^{-1} cm^{-1}), 265 nm (ε = 67 x10^3 M^{-1} cm^{-1}), 308 nm (ε = 52 x10^3 M^{-1} cm^{-1}).

[Nd{Au(L4-κS)}$_3$]

Yield: 81.4 mg (85 %).

Elemental analysis: Calcd. for $C_{51}H_{69}N_{15}O_6S_6Au_3Nd$: C, 32.0; H, 3.6; N, 11.0; S, 10.0 %. Found: C, 31.8; H, 3.6; N, 10.4; S, 9.7 %.

IR (KBr, cm^{-1}): 3066 (vw), 2972 (w), 2931 (w), 2870 (w), 1585 (m), 1558 (vs), 1512 (vs), 1438 (m), 1400 (m), 1357 (s), 1315 (m), 1246 (s), 1201 (m), 1124 (s), 1070 (m), 1016 (m), 912 (s), 860 (w), 752 (s), 665 (s), 632 (m), 482 (w), 432 (w), 410 (w).
ESI$^+$ MS (*m/z*): 1913.2135, 55 % $[M + H]^+$ (calcd. 1913.2026); 1935.1957, 52 % $[M + Na]^+$ (calcd. 1935.1851).
UV-vis (CH_2Cl_2): 227 nm ($\varepsilon = 72 \times 10^3$ M^{-1} cm^{-1}), 264 nm ($\varepsilon = 49 \times 10^3$ M^{-1} cm^{-1}), 309 nm ($\varepsilon = 58 \times 10^3$ M^{-1} cm^{-1}).

[Sm{Au(L4-κS)}$_3$]

Yield: 88.7 mg (92 %).
Elemental analysis: Calcd. for $C_{51}H_{69}N_{15}O_6S_6Au_3Sm$: C, 31.9; H, 3.6; N, 10.9; S, 10.0 %. Found: C, 31.8; H, 3.6; N, 10.5; S, 10.0 %.
IR (KBr, cm^{-1}): 3066 (vw), 2972 (w), 2931 (w), 2870 (w), 1585 (m), 1560 (vs), 1512 (vs), 1438 (m), 1400 (m), 1357 (s), 1315 (m), 1246 (s), 1203 (m), 1124 (s), 1070 (m), 1018 (w), 912 (s), 860 (w), 752 (s), 663 (m), 632 (m), 484 (w), 432 (w), 412 (w).
ESI$^+$ MS (*m/z*): 1923.2432, 44 % $[M + H]^+$ (calcd. 1923.2146).
UV-vis (CH_2Cl_2): 228 nm ($\varepsilon = 55 \times 10^3$ M^{-1} cm^{-1}), 264 nm ($\varepsilon = 37 \times 10^3$ M^{-1} cm^{-1}), 310 nm ($\varepsilon = 28 \times 10^3$ M^{-1} cm^{-1}).

[Eu{Au(L4-κS)}$_3$]

Yield: 90.2 mg (94 %).
Elemental analysis: Calcd. for $C_{51}H_{69}N_{15}O_6S_6Au_3Eu$: C, 31.9; H, 3.6; N, 10.9; S, 10.0 %. Found: C, 31.9; H, 3.7; N, 10.6; S, 10.2 %.
IR (KBr, cm^{-1}): 3066 (vw), 2970 (w), 2931 (w), 2870 (w), 1587 (m), 1560 (vs), 1508 (vs), 1456 (m), 1357 (m), 1246 (s), 1124 (s), 1070 (m), 912 (m), 750 (m), 663 (m), 634 (m), 484 (w), 432 (w), 412 (w).
ESI$^+$ MS (*m/z*): 1924.2145, 100 % $[M + H]^+$ (calcd. 1924.2161).
UV-vis: (CH_2Cl_2), 227 nm ($\varepsilon = 88 \times 10^3$ M^{-1} cm^{-1}), 264 nm ($\varepsilon = 59 \times 10^3$ M^{-1} cm^{-1}), 309 nm ($\varepsilon = 44 \times 10^3$ M^{-1} cm^{-1}).

[Gd{Au(L4-κS)}$_3$]

Yield: 86.0 mg (89 %).

Elemental analysis: Calcd. for $C_{51}H_{69}N_{15}O_6S_6Au_3Gd$: C, 31.8; H, 3.6; N, 10.9; S, 10.0 %. Found: C, 31.4; H, 3.8; N, 10.4; S, 10.0 %.

IR (KBr, cm^{-1}): 3066 (vw), 2970 (w), 2931 (w), 2870 (w), 1587 (m), 1560 (vs), 1512 (vs), 1450 (m), 1400 (m), 1357 (s), 1317 (m), 1246 (s), 1203 (m), 1124 (s), 1070 (m), 1018 (w), 912 (s), 858 (w), 839 (w), 750 (s), 663 (m), 632 (m), 484 (w), 432 (w), 410 (w).

ESI$^+$ MS (*m/z*): 1929.2168, 44 % $[M + H]^+$ (calcd. 1929.2190).

UV-vis (CH_2Cl_2): 227 nm ($\varepsilon = 98 \times 10^3$ M^{-1} cm^{-1}), 263 nm ($\varepsilon = 68 \times 10^3$ M^{-1} cm^{-1}), 309 nm ($\varepsilon = 50 \times 10^3$ M^{-1} cm^{-1}).

[Tb{Au(L4-κS)}$_3$]

Yield: 78.2 mg (81 %).

Elemental analysis: Calcd. for $C_{51}H_{69}N_{15}O_6S_6Au_3Tb$: C, 31.7; H, 3.6; N, 10.9; S, 10.0 %. Found: C, 31.9; H, 3.7; N, 10.8; S, 10.1 %.

IR (KBr, cm^{-1}): 3066 (vw), 2970 (w), 2931 (w), 2870 (w), 1587 (m), 1560 (vs), 1508 (vs), 1456 (m), 1357 (m), 1246 (s), 1124 (s), 1070 (m), 912 (m), 750 (m), 663 (m), 634 (m), 484 (w), 432 (w), 412 (w).

ESI$^+$ MS (*m/z*): 1952.2019, 100 % $[M + Na]^+$ (calcd. 1952.2022).

UV-vis (CH_2Cl_2): 265 nm ($\varepsilon = 79 \times 10^3$ M^{-1} cm^{-1}), 310 nm ($\varepsilon = 45 \times 10^3$ M^{-1} cm^{-1}).

[Dy{Au(L4-κS)}$_3$]

Yield: 93.0 mg (96 %).

Elemental analysis: Calcd. for $C_{51}H_{69}N_{15}O_6S_6Au_3Dy$: C, 31.7; H, 3.6; N, 10.9; S, 10.0 %. Found: C, 31.6; H, 3.6; N, 10.3; S, 10.0 %.

IR (KBr, cm^{-1}): 3066 (vw), 2970 (w), 2931 (w), 2870 (w), 1587 (m), 1560 (vs), 1512 (vs), 1458 (m), 1404 (m), 1357 (s), 1317 (m), 1246 (s), 1203 (m), 1124 (s), 1070 (m), 1020 (w), 912 (s), 858 (w), 839 (w), 750 (s), 663 (m), 634 (m), 484 (w), 432 (w), 410 (w).

ESI$^+$ MS (*m/z*): 1935.2172, 100 % $[M + H]^+$ (calcd. 1935.2241).

UV-vis (CH_2Cl_2): 227 nm ($\varepsilon = 334 \times 10^3$ M^{-1} cm^{-1}), 264nm ($\varepsilon = 250 \times 10^3$ M^{-1} cm^{-1}), 310 nm ($\varepsilon = 182 \times 10^3$ M^{-1} cm^{-1}).

[Ho{Au(L4-κS)}$_3$]

Yield: 83.0 mg (86 %).

Elemental analysis: Calcd. for $C_{51}H_{69}N_{15}O_6S_6Au_3Ho$: C, 31.6; H, 3.6; N, 10.9; S, 9.9 %. Found: C, 31.6; H, 3.6; N, 10.3; S, 10.0 %.

IR (KBr, cm^{-1}): 3066 (vw), 2970 (w), 2931 (w), 2870 (w), 1587 (m), 1560 (vs), 1512 (vs), 1458 (m), 1404 (m), 1357 (s), 1317 (m), 1246 (s), 1203 (m), 1124 (s), 1070 (m), 1020 (w), 912 (s), 858 (w), 839 (w), 750 (s), 663 (m), 634 (m), 484 (w), 432 (w), 410 (w).

ESI$^+$ MS (*m/z*): 1936.2224, 45 % $[M + H]^+$ (calcd. 1936.2252).

UV-vis (CH_2Cl_2): 265 nm ($\varepsilon = 53 \times 10^3$ M^{-1} cm^{-1}), 310 nm ($\varepsilon = 34 \times 10^3$ M^{-1} cm^{-1}).

[Er{Au(L4-κS)}$_3$]

Yield: 85.5 mg (88 %).

Elemental analysis: Calcd. for $C_{51}H_{69}N_{15}O_6S_6Au_3Er$: C, 31.6; H, 3.6; N, 10.8; S, 9.9 %. Found: C, 31.6; H, 3.7; N, 10.3; S, 9.9 %.

IR (KBr, cm^{-1}): 3066 (vw), 2970 (w), 2931 (w), 2870 (w), 1587 (m), 1560 (vs), 1512 (vs), 1458 (m), 1404 (m), 1357 (s), 1317 (m), 1246 (s), 1203 (m), 1124 (s), 1070 (m), 1020 (w), 912 (s), 858 (w), 839 (w), 750 (s), 663 (m), 634 (m), 484 (w), 432 (w), 410 (w).

ESI$^+$ MS (*m/z*): 1937.2222, 100 % $[M + H]^+$ (calcd. 1937.2252).

UV-vis (CH_2Cl_2): 227 nm ($\varepsilon = 58 \times 10^3$ M^{-1} cm^{-1}), 264 nm ($\varepsilon = 39 \times 10^3$ M^{-1} cm^{-1}), 309 nm ($\varepsilon = 27 \times 10^3$ M^{-1} cm^{-1}).

[Tm{Au(L4-κS)}$_3$]

Yield: 86.5 mg (89 %).

Elemental analysis: Calcd. for $C_{51}H_{69}N_{15}O_6S_6Au_3Tm$: C, 31.6; H, 3.6; N, 10.8; S, 9.9 %. Found: C, 31.2; H, 3.5; N, 10.5; S, 9.9 %.

IR (KBr, cm^{-1}): 3066 (vw), 2970 (w), 2931 (w), 2870 (w), 1587 (m), 1560 (vs), 1512 (vs), 1458 (m), 1404 (m), 1357 (s), 1317 (m), 1246 (s), 1203 (m), 1124 (s), 1070 (m), 1020 (w), 912 (s), 858 (w), 839 (w), 750 (s), 663 (m), 634 (m), 484 (w), 432 (w), 410 (w).

ESI$^+$ MS (*m/z*): 1940.2262, 50 % $[M + H]^+$ (calcd. 1940.2291).

UV-vis (CH_2Cl_2): 265 nm ($\varepsilon = 63 \times 10^3$ M^{-1} cm^{-1}), 310 nm ($\varepsilon = 46 \times 10^3$ M^{-1} cm^{-1}).

[Yb{Au(L4-κS)}$_3$]

Yield: 86.4 mg (89 %).

Elemental analysis Calcd. for $C_{51}H_{69}N_{15}O_6S_6Au_3Yb$: C, 31.5; H, 3.6; N, 10.8; S, 9.9 %. Found: C, 31.5; H, 3.6; N, 10.7; S, 9.9 %.

IR (KBr, cm^{-1}): 3066 (vw), 2970 (w), 2931 (w), 2870 (w), 1591 (m), 1564 (vs), 1514 (vs), 1458 (m), 1359 (m), 1246 (s), 1124 (s), 1070 (m), 914 (m), 856 (m), 750 (m), 661 (m), 634 (m), 486 (w), 430 (w).

ESI$^+$ MS (*m/z*): 1945.2332, 100 % $[M + H]^+$ (calcd. 1945.2337).

UV-vis (CH_2Cl_2): 227 nm ($\varepsilon = 128 \times 10^3$ M^{-1} cm^{-1}), 264 nm ($\varepsilon = 85 \times 10^3$ M^{-1} cm^{-1}), 309 nm ($\varepsilon = 60 \times 10^3$ M^{-1} cm^{-1}).

[Lu{Au(L4-κS)}$_3$]

Yield: 84.2 mg (87 %).

Elemental analysis: Calcd. for $C_{51}H_{69}N_{15}O_6S_6Au_3Lu$: C, 31.5; H, 3.6; N, 10.8; S, 9.9 %. Found: C, 31.5; H, 3.6; N, 10.8; S, 9.8 %.

IR (KBr, cm^{-1}): 2974 (w), 29313 (w), 28720 (w), 1589 (m), 1560 (vs), 1517 (vs), 1458 (m), 1436 (m), 1406 (m), 1382 (m), 1357 (m), 1315 (w), 1294 (w), 1246 (s), 1124 (s), 1068 (m), 914 (m), 756 (w), 659 (w), 632 (w), 484 (w), 437 (w).

ESI$^+$ MS (*m/z*): 1946.2431, 100 % $[M + H]^+$ (calcd. 1946.2356).

UV-vis (CH_2Cl_2): 274 nm ($\varepsilon = 14 \times 10^3$ M^{-1} cm^{-1}), 310 nm ($\varepsilon = 18 \times 10^3$ M^{-1} cm^{-1}).

4.4.2. Sc^{3+}, In^{3+} and Ga^{3+} Complexes with Gold(I) Coronands

H_2L4 (59.3 mg, 0.15 mmol) was added to a suspension of [AuCl(THT)] (48.0 mg, 0.15 mmol) and $M(NO_3)_3 \cdot nH_2O$ (M = Sc, In), (0.05 mmol) in 3 mL of MeOH. The mixture was stirred at room temperature for 30 minutes before the addition of 6 drops of triethylamine. The mixture was stirred for additional 1.5 h. During this time, a colourless precipitate was obtained, which was filtered off, washed with a small amount of MeOH and dried in the air. The solid was dissolved in CH_2Cl_2 (1mL) and overlayered with MeOH (1 mL), which was added carefully on the wall of the vial. Single crystals suitable for X-ray diffraction were obtained from slow diffusion of MeOH into the CH_2Cl_2 solution.

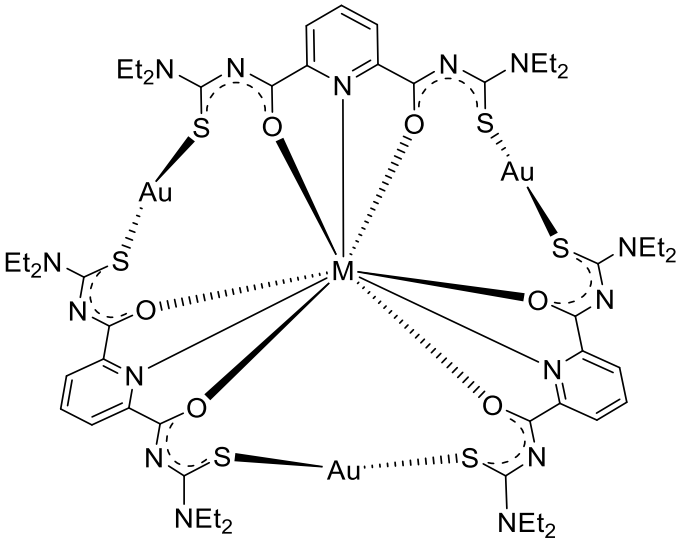

M = Sc, In

[Sc{Au(L4-κS)}$_3$]

Yield: 65.5 mg (72 %).

Elemental analysis: Calcd. for $C_{51}H_{69}N_{15}O_6S_6Au_3Sc$: C, 33.7; H, 3.9; N, 11.6; S, 10.6 %. Found: C, 33.7; H, 3.9; N, 11.4; S, 10.6 %.

IR (KBr, cm^{-1}): 3072 (vw), 2970 (w), 2931 (w), 2870 (w), 1591 (m), 1564 (vs), 1508 (vs), 1458 (m), 1357 (m), 1246 (s), 1124 (s), 1068 (m), 914 (m), 854 (m), 754 (m), 659 (m), 486 (w), 453 (w), 426 (w).

^{1}H NMR (400 MHz, $CDCl_3$, ppm): 7.89 (d, J = 8.0 Hz, 2H, Py); 7.80 (t, J = 8.0 Hz, 1H, Py); 3.72 (m, 2H, CH_2); 3.45 (m, 6H, CH_2); 1.08 (t, J = 8.0 Hz, 12H, CH_3).

^{13}C{^{1}H} NMR ($CDCl_3$, ppm): 184.4 (C=O); 166.2 (C=S); 150.1, 137.7, 124.2 (Py); 46.9, 46.1 (CH_2); 13.0, 12.6 (CH_3).

^{45}Sc NMR (CH_2Cl_2, ppm): 6.81.

ESI$^+$ MS (*m/z*): 1816.2544, 100 % $[M + H]^+$ (calcd. 1816.2508); 1838.2359, 44 % $[M + Na]^+$ (calcd. 1838.2327).

UV-vis (CH_2Cl_2): 226 nm ($\varepsilon = 60 \times 10^3$ M^{-1} cm^{-1}), 265 nm ($\varepsilon = 39 \times 10^3$ M^{-1} cm^{-1}), 311 nm ($\varepsilon = 26 \times 10^3$ M^{-1} cm^{-1}).

[In{Au(L4-κS)}$_3$]

Yield: 86.0 mg (91 %).

Elemental analysis Calcd. for $C_{51}H_{69}N_{15}O_6S_6Au_3In$: C, 32.5; H, 3.7; N, 11.1; S, 10.2 %. Found: C, 32.6; H, 3.9; N, 11.2; S, 10.4 %.

IR (KBr, cm^{-1}): 2974 (m), 2931 (m), 2870 (w), 1597 (m), 1560 (vs), 1516 (vs), 1458 (m), 1431 (m), 1408 (m), 1377 (w), 1357 (s), 1319 (m), 1246 (s), 1205 (m), 1124 (s), 1074 (m), 914 (m), 862 (w), 750 (m), 663 (m), 653 (m), 634 (m), 486 (w), 449 (w).

^{1}H NMR (400 MHz, $CDCl_3$, ppm): 8.15 (d, J = 8.0 Hz, 2H, Py); 7.89 (t, J = 8.0 Hz, 1H, Py); 3.73 (m, 2H, CH_2); 3.45 (m, 6H, CH_2); 1.09 (br, 12H, CH_3).

^{13}C{^{1}H} NMR ($CDCl_3$, ppm): 183.1 (C=O); 162.6 (C=S); 145.7, 138.5, 125.1 (Py); 46.7, 46.1 (CH_2); 12.9, 12.7 (CH_3).

ESI$^+$ MS (*m/z*): 1295.1030, 100 % $[M -Au -L4 + H]^+$ (calcd. 1295.1202), 1908.1793, 5 % $[M + Na]^+$ (calcd. 1908.1813).

UV-vis (CH_2Cl_2): 228 nm (ε = 69 x10^3 M^{-1} cm^{-1}), 262 nm (ε = 42 x10^3 M^{-1} cm^{-1}), 308 nm (ε = 30 x10^3 M^{-1} cm^{-1}).

[Ga{Au(L4-κS)}$_2$](NO$_3$)

H_2L4 (39.9 mg, 0.1 mmol) was added to a suspension of [AuCl(THT)] (32.5 mg, 0.1 mmol) and $Ga(NO_3)_3 \cdot nH_2O$ (12.8 mg, 0.05 mmol) in 3 mL of MeOH. The mixture was stirred at room temperature for 30 minutes before the addition of 6 drops of triethylamine. The mixture was stirred for additional 1.5 h. During this time, a colourless precipitate was obtained, which was filtered off, washed with a small amount of MeOH and dried in the air. The solid was dissolved in 0.5 mL of CH_2Cl_2 and 0.5 mL of $CHCl_3$. The solution was overlayered with 1 mL of MeOH, which was added carefully on the vial. Single crystals suitable for X-ray diffraction were obtained from slow diffusion of MeOH into the $CHCl_3/CH_2Cl_2$ solution.

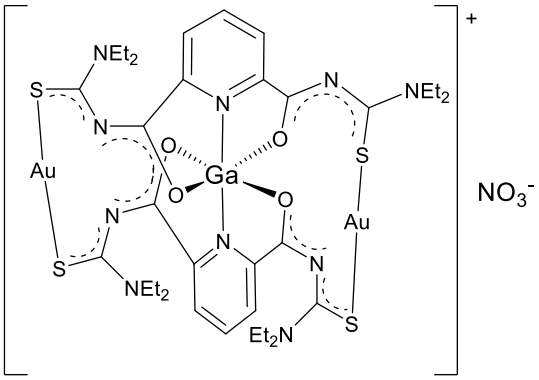

Yield: 44.0 mg (63 %).

Elemental analysis: Calcd. for $C_{36}H_{50.5}Au_2Cl_{3.5}N_{11}O_{7.5}S_4Ga$ ($[Ga\{Au(L4-\kappa S)\}_2](NO_3) \cdot 0.5CHCl_3 \cdot CH_2Cl_2 \cdot 0.5MeOH$): C, 30.1; H, 3.5; N, 10.7; S, 8.9 %. Found: C, 28.7; H, 3.5; N, 10.6; S, 9.6 %.

IR (KBr, cm^{-1}): 3066 (vw), 2970 (w), 2931 (w), 2870 (w), 1591 (m), 1564 (vs), 1514 (vs), 1458 (m), 1359 (m), 1246 (s), 1124 (s), 1070 (m), 914 (m), 845 (br), 833 (br), 750 (m), 661 (m), 634 (m), 558 (m), 486 (w), 430 (w).

^{1}H NMR (400 MHz, $CDCl_3$, ppm): 8.1 (d, J = 8.0 Hz, 2H, Py); 7.68 (t, J = 8.0 Hz, 1H, Py); 3.73 (m, 2H, CH_2); 3.45 (m, 6H, CH_2); 1.1 (br, 12H, CH_3).

^{13}C{^{1}H} NMR ($CDCl_3$, ppm): 182.8 (C=O); 162.2 (C=S); 145.5, 137.5, 125.7 (Py); 46.4, 46.6 (CH_2); 12.8, 12.9 (CH_3).

ESI^{+} MS (*m/z*): 1249.1341, 100 % $[M]^{+}$ (calcd. 1249.1168).

UV-vis (CH_2Cl_2): 227 nm (ε = 30 x10^3 M^{-1} cm^{-1}), 260 nm (ε = 35 x10^3 M^{-1} cm^{-1}), 307 nm (ε = 28 x10^3 M^{-1} cm^{-1}).

4.4.3. M^{2+} Complexes with a Binuclear Gold(I) Coronand (M = Mn, Fe, Co, Ni, Cu, Zn, Hg)

H_2L4 (39.9 mg, 0.1 mmol) was added to a suspension of [AuCl(THT)] (32.5 mg, 0.1 mmol) and $Cu(OAc)_2 \cdot H_2O$, $Zn(OAc)_2 \cdot 2H_2O$, $M(OAc)_2 \cdot 4H_2O$ (M = Mn, Co, or Ni), $Fe(SO_4)_2 \cdot 7H_2O$, [Fe(acac)$_3$] or $HgCl_2$ (0.05 mmol) in 3 mL of MeOH. For each reaction, a colour change could be observed. The mixture was stirred at room temperature for 30 minutes before the addition of 4 drops of triethylamine. During an additional stirring of 1.5 h. green (for Cu^{2+} or Ni^{2+}), colourless (for Zn^{2+}), yellow (for Mn^{2+}), caramel (for Co^{2+}) and dark blue (for Fe^{2+}) solids were formed. They were filtered off, washed with a small amount of MeOH, and dried in the air. The product with Hg^{2+} stayed in the solution after addition of Et_3N. The dried solids were dissolved in CH_2Cl_2 (1 mL) and overlayered with MeOH (1 mL), which was added carefully on the wall of the vial. Single crystals suitable for X-ray diffraction were obtained from slow diffusion of the MeOH into the CH_2Cl_2 solutions. In the case of Hg^{2+}, colourless single crystals were obtained by slow evaporation of the solvent. The elemental analysis were performed from finely powdered and carefully dried samples.

[Mn{Au(L4-κS)}$_2$]

Yield: 46.0 mg (75 %).

Elemental analysis: Calcd. for $C_{34}H_{46}N_{10}O_4S_4Au_2Mn$: C, 33.1; H, 3.8; N, 11.3; S, 10.4 %. Found: C, 33.1; H, 3.8; N, 11.3; S, 10.4 %.

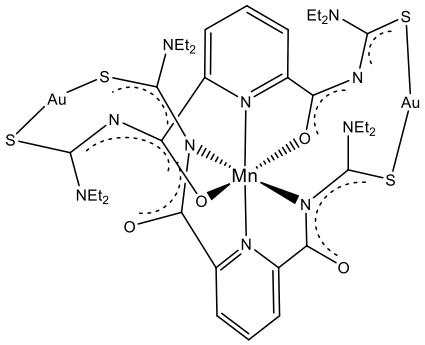

IR (KBr, cm^{-1}): 3431 (w), 2970 (w), 2931 (w), 2870 (w), 1624 (m), 1558 (vs), 1500 (vs), 1431 (s), 1406 (m), 1348 (m), 1311 (m), 1292 (m), 1238 (s), 1118 (m), 1066 (m), 852 (w), 758 (m), 682 (w), 669 (w).

ESI$^+$ MS (*m/z*): 1258.1215, 100 % $[M + Na]^+$ (calcd. 1258.1190).

UV-vis (CH_2Cl_2): 227 nm (ε = 35 x10^3 M^{-1} cm^{-1}), 258 nm (ε = 27 x10^3 M^{-1} cm^{-1}), 280 nm (ε = 28 x10^3 M^{-1} cm^{-1}), 300 nm (ε = 27 x10^3 M^{-1} cm^{-1}).

[Fe{Au(L4-κS)}$_2$]

Yield: 32.0 mg (52 %).

Elemental analysis: Calcd. for $C_{34}H_{46}N_{10}O_4S_4Au_2Fe$: C, 33.0; H, 3.8; N, 11.3; S, 10.4 %. Found: C, 33.1; H, 3.8; N, 11.2; S, 10.4 %.

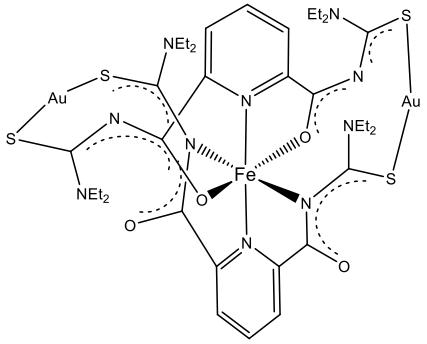

IR (KBr, cm^{-1}): 2974 (s), 2937 (s), 2738 (s), 1624 (m), 1558 (vs), 1500 (vs), 1431 (s), 1406 (m), 1348 (m), 1311 (m), 1292 (m), 1238 (s), 1118 (m), 1066 (m), 852 (w), 758 (m), 682 (w), 669 (w).

ESI$^+$ MS (*m/z*): 1259.1165, 100 % $[M + Na]^+$ (calcd. 1259.1159).

UV-vis (CH_2Cl_2): 227 nm (ε = 35 x10^3 M^{-1} cm^{-1}), 258 nm (ε = 27 x10^3 M^{-1} cm^{-1}), 280 nm (ε = 28 x10^3 M^{-1} cm^{-1}), 300 nm (ε = 27 x10^3 M^{-1} cm^{-1}).

[Co{Au(L4-κS)}$_2$]

Yield: 54.5 mg (88 %).

Elemental analysis: Calcd. for $C_{34}H_{46}N_{10}O_4S_4Au_2Co$: C, 33.0; H, 3.7; N, 11.3; S, 10.4 %. Found: C, 33.0; H, 3.7; N, 11.3; S, 10.4 %.

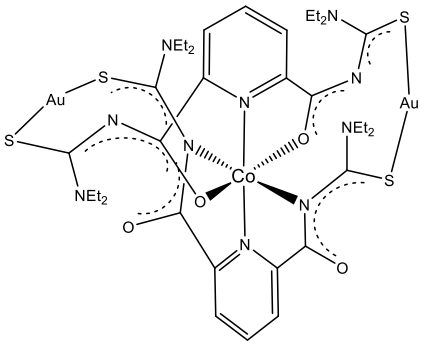

IR (KBr, cm^{-1}): 3446 (w), 2974 (w), 2931 (w), 2872 (w), 1627 (m), 1550 (vs), 1508 (vs), 1431 (s), 1400 (m), 1355 (m), 1313 (m), 1294 (w), 1244 (s), 1122 (m), 1068 (m), 914 (w), 846 (w), 759 (m), 669 (m), 484 (w).

ESI$^+$ MS (*m/z*): 1240.1515, 100 % $[M + H]^+$ (calcd. 1240.1322).

UV-vis (CH_2Cl_2): 227 nm (ε = 73 x10^3 M^{-1} cm^{-1}), 256 nm (ε = 60 x10^3 M^{-1} cm^{-1}), 284 nm (ε = 57 x10^3 M^{-1} cm^{-1}).

[Ni{Au(L4-κS)}$_2$]

Yield: 44.0 mg (71 %).

Elemental analysis: Calcd. for $C_{34}H_{46}N_{10}O_4S_4Au_2Ni$: C, 32.9; H, 3.7; N, 11.3; S, 10.3 %. Found: C, 33.0; H, 3.8; N, 11.3; S, 10.4 %.

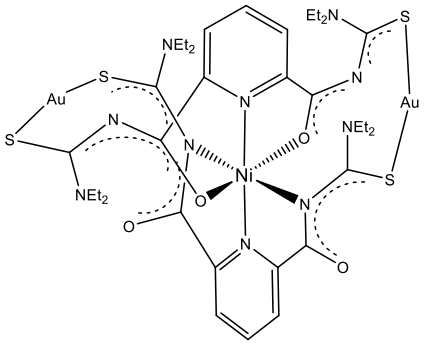

IR (KBr, cm^{-1}): 3446 (w), 2974 (w), 2933 (w), 2872 (w), 1627 (m), 1550 (vs), 1508 (vs), 1431 (s), 1406 (m), 1377 (m), 1355 (m), 1313 (m), 1242 (s), 1122 (m), 1072 (m), 842 (w), 758 (m), 653 (m), 480 (w).

ESI$^+$ MS (*m/z*): 1261.1253, 100 % $[M + Na]^+$ (calcd. 1261.1163).

UV-vis: (CH_2Cl_2), 227 nm (ε = 59 x10^3 M^{-1} cm^{-1}), 254 nm (ε = 49 x10^3 M^{-1} cm^{-1}), 295 nm (ε = 44 x10^3 M^{-1} cm^{-1}).

[Cu{Au(L4-κS)}$_2$]

Yield: 51.5 mg (83 %).

Elemental analysis: Calcd. for $C_{34}H_{46}N_{10}O_4S_4Au_2Cu$: C, 32.8; H, 3.7; N, 11.3; S, 10.3 %. Found: C, 32.8; H, 3.8; N, 11.3; S,10.4 %.

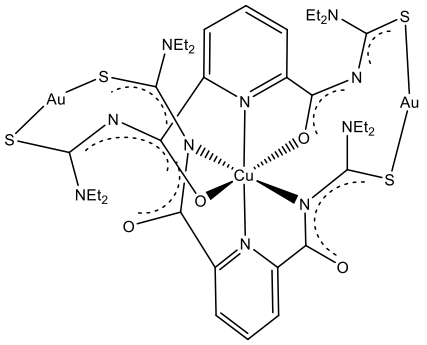

IR (KBr, cm^{-1}): 3431 (w), 2974 (w), 2931 (w), 2872 (w), 1629 (m), 1550 (vs), 1508 (vs), 1431 (s), 1400 (s), 1355 (s), 1313 (m), 1240 (s), 1122 (m), 1076 (m), 842 (w), 761 (m), 682 (m), 657 (w), 482 (w).

ESI$^+$ MS (*m/z*): 1244.1392, 27 % $[M + H]^+$ (calcd. 1244.1286); 1266.1208, 11 % $[M + Na]^+$ (calcd. 1266.1106); 1282.0948, 5 % $[M + K]^+$ (calcd. 1282.0845).

UV-vis (CH_2Cl_2): 228 nm (ε = 58 x10^3 M^{-1} cm^{-1}), 258 nm (ε = 45 x10^3 M^{-1} cm^{-1}), 300 nm (ε = 33 x10^3 M^{-1} cm^{-1}).

EPR ($CHCl_3$): $g_{\parallel}$ = 2.249, $g_{\perp}$ = 2.095, $A_{\parallel}$ = 129.0 · 10^{-4} cm^{-1}, $A_{\perp}$ = 35.0 · 10^{-4} cm^{-1}, g_0 = 2.135, a_0 = 70 · 10^{-4} cm^{-1}.

[Zn{Au(L4-κS)}$_2$]

Yield: 51.0 mg (82 %).

Elemental analysis: Calcd. for $C_{34}H_{46}N_{10}O_4S_4Au_2Zn$: C, 32.8; H, 3.7; N, 11.2; S, 10.3 %. Found: C, 32.8; H, 3.8; N, 10.3; S, 10.3 %.

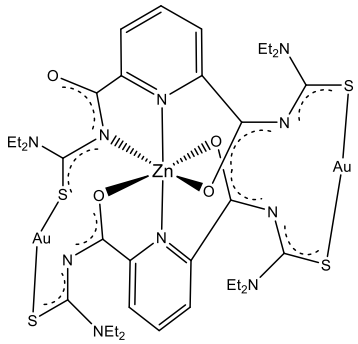

IR (KBr, cm^{-1}): 3433 (w), 2974 (w), 2931 (w), 2870 (w), 1589 (w), 1560 (vs), 1508 (vs), 1431 (s), 1404 (s), 1355 (s), 1313 (m), 1242 (s), 1122 (m), 1070 (m), 842 (w), 759 (s), 638 (m), 484 (w), 430 (w).

ESI$^+$ MS (*m/z*): 1245.1352, 100 % $[M + H]^+$ (calcd. 1245.1282).

UV-vis (CH_2Cl_2): 227 nm (ε = 67 x10^3 M^{-1} cm^{-1}), 256 nm (ε = 52 x10^3 M^{-1} cm^{-1}), 306 nm (ε = 49 x10^3 M^{-1} cm^{-1}).

[Hg{Au(L4-κS)}$_2$]

Yield: 102.0 mg (74 %).

Elemental analysis: Calcd. for $C_{35.5}H_{52}N_{10}O_{5.5}S_4Au_2Hg$ ([Hg{Au(L4-κS)}$_2$] ·1.5H_2O C, 29.8; H, 3.6; N, 9.8; S, 9.0 %. Found: C, 29.7; H, 3.3; N, 10.3; S, 9.3 %.

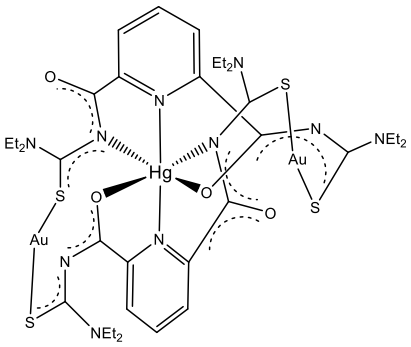

IR (KBr, cm^{-1}): 3421 (br), 2972 (w), 2931 (w), 2868 (w), 1685 (vw), 1624 (w), 1595 (w), 1577 (vs), 1554 (s), 1508 (vs), 1429 (s), 1384 (m), 1354 (m), 1309 (m), 1236 (m), 1072 (m), 919 (w), 852 (w), 758 (s), 680 (w), 663 (w), 474 (w).

^{1}H NMR (400 MHz, $CDCl_3$, ppm): 8.5 (d, J = 8.0 Hz, 2H, Py); 8.1 (t, J = 8.0 Hz, 1H, Py); 3.7 (m, 8H, CH_2); 1.1 (br, 12H, CH_3).

ESI$^+$ MS (*m/z*): 1383.1738, 28.6 % $[M + H]^+$ (calcd. 1383.1696).

UV-vis (CH_2Cl_2): 227 nm (ε = 35 x10^3 M^{-1} cm^{-1}), 258 nm (ε = 27 x10^3 M^{-1} cm^{-1}), 280 nm (ε = 28 x10^3 M^{-1} cm^{-1}), 300 nm (ε = 27 x10^3 M^{-1} cm^{-1}).

[Ni{Au(L4-κS)}$_2$] *via* metal exchange from [{Ca$_2$(MeOH)$_3$(H$_2$O)}{Au(L4-κS)}$_4$]

A solution of $Ni(OAc)_2·4H_2O$ (12.4 mg, 0.05 mmol) in 1mL of MeOH was added dropwise to a solution of [{$Ca_2(MeOH)_3(H_2O)$}{Au(L4-κS)}$_4$] (25.0 mg, 0.01 mmol) dissolved in 1 mL of CH_2Cl_2. The colour of the solution changed to green. After stirring for 1 hour, the green solution was filtered *via* celite. The resulting solution was allowed to stand overnight and green single crystals suitable for X-ray diffraction were obtained by slow evaporation of the solvents.

Yield: 8.5 mg (65 %).

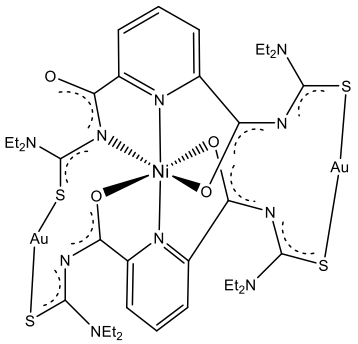

Elemental analysis: Calcd. for $C_{34}H_{46}N_{10}O_4S_4Au_2Ni$: C, 32.9; H, 3.7; N, 11.3; S, 10.3 %. Found: C, 32.9; H, 3.8; N, 11.3; S, 10.5 %.

IR (KBr, cm^{-1}): 3433 (w), 2974 (w), 2931 (w), 2872 (w), 1624 (w), 1552 (vs), 1508 (vs), 1431 (s), 1404 (m), 1355 (m), 1313 (m), 1242 (s), 1122 (m), 1072 (m), 842 (m), 761 (s), 669 (m), 482 (w).

ESI$^+$ MS (*m/z*): 1261.1214, 100 % $[M + Na]^+$ (calcd. 1261.1163).

UV/Vis (CH_2Cl_2): 228 nm (ε = 57 x10^3 M^{-1} cm^{-1}), 252 nm (ε = 47 x10^3 M^{-1} cm^{-1}), 292 nm (ε = 43 x10^3 M^{-1} cm^{-1}), 320 nm (ε = 32 x10^3 M^{-1} cm^{-1}).

5. References

[1] Gimeno, M.C. and Laguna, A. *Modern Supramolecular Gold Chemistry: Gold-Metal Interactions and Applications.* (2008) Ch. 1 pp. 1-63, Wiley-VCH, Germany.

[2] Schmidbaur, H. and Schier, A. *Chem. Soc. Rev.*, **37** (2008) 1931-1951.

[3] Schmidbaur, H. *Chem. Soc. Rev.*, **24** (1995) 391-401.

[4] Hutchings, G.J., Brust, M. and Schmidbaur, H. *Chem. Soc. Rev.*, **37** (2008) 1759-1765.

[5] Raubenheimer, H.G. and Schmidbaur, H. *J. Chem. Educ.*, **91** (2014) 2024-2036.

[6] Pyykkö, P. *Chem. Soc. Rev.*, **37** (2008) 1967-1997.

[7] Hashmi, A.S.K. and Rudolph, M. *Chem. Soc. Rev.*, **37** (2008) 1766-1775.

[8] Marion, N. and Nolan, S.P. *Chem. Soc. Rev.*, **37** (2008) 1776-1782.

[9] Shu, X.-Z., Nguyen, S.C., He, Y., Oba, F., Zhang, Q., Canlas, C., Somorjai, G.A., Alivisatos, A.P. and Toste, F.D. *J. Am. Chem. Soc.*, **137** (2015) 7083-7086.

[10] Häkkinen, H. *Chem. Soc. Rev.*, **37** (2008) 1847-1859.

[11] Gong, J. and Mullins, C.B. *Acc. Chem. Res.*, **42** (2009) 1063-1073.

[12] Grzelczak, M., Pérez-Juste, J., Mulvaney, P. and Liz-Marzán, L.M. *Chem. Soc. Rev.*, **37** (2008) 1783-1791.

[13] Myroshnychenko, V., Rodríguez-Fernández, J., Pastoriza-Santos, I., Funston, A.M., Novo, C., Mulvaney, P., Liz-Marzán, L.M. and de Abajo, F.J.G. *Chem. Soc. Rev.*, **37** (2008) 1792-1805.

[14] Sperling, R.A., Gil, P.R., Zhang, F., Zanella, M. and Parak, W.J. *Chem. Soc. Rev.*, **37** (2008) 1896-1908.

[15] Shaw, C.F. *Chem. Rev.*, **99** (1999) 2589-2600.

[16] Bau, R. *J. Am. Chem. Soc.*, **120** (1998) 9380-9381.

[17] Puddephatt, R.J., *Chem. Soc. Rev.*, **37** (2008) 2012-2027.

[18] Vittal, J.J. and Puddephatt, R.J. *Gold: Inorganic & Coordination Chemistry. Encyclopedia of Inorganic Chemistry*. (2006) pp, 1-15. John Wiley & Sons, Ltd.

[19] Puddephatt, R.J., Wilkinson, G., Gillard, R.D. and McCleverty, J.A. *Comprehensive Coordination Chemistry*, Vol. 5 (1987) pp. 861-923, Pergamon, Oxford.

[20] Puddephatt, R.J. *The Chemistry of Gold*, (1978) Elsevier, Amsterdam.

[21] Vicente, J., Chicote, M.T. and Bermúdez, M.D. *J. Chem. Soc. Dalton Trans.*, (1986) 2361-2366.

[22] Parish, R.V. *Gold Bull.*, **30** (1997) 3-12.

[23] Armer, B. and Schmidbaur, H. *Angew. Chem. Int. Ed.*, **9** (1970) 101-113.

[24] Bertrand, B. and Casini, A. *Dalton Trans.,* **43** (2014) 4209-4219.

[25] Albrecht, M. *Chem. Rev.*, **110** (2010) 576-623.

[26] Bourissou, D., Guerret, O., Gabbaï, F.P. and Bertrand, G. *Chem. Rev.*, **100** (2000) 39-91.

[27] Hopkinson, M.N., Richter, C., Schedler, M. and Glorius, F. *Nature*, **510** (2014) 485-496.

[28] Lehn, J.-M. *Science*, **260** (1993) 1762-1763.

[29] Sauvage, J.-P. and Dietrich-Buchecker, C. *Molecular Catenanes, Rotaxanes and Knots,* Wiley-VCH Verlag, Germany.

[30] Stang, P.J. and Olenyuk, B. *Acc. Chem. Res.*, **30** (1997) 502-518.

[31] Beissel, T., Powers, R.E. and Raymond, K.N. *Angew. Chem. Int. Ed. Engl.*, **35** (1996) 1084-1086.

[32] Fujita, M., Oguro, D., Miyazawa, M., Oka, H., Yamaguchi, K. and Ogura, K. *Nature*, **378** (1995) 469-471.

[33] Cotton, F.A., Lin, C. and Murillo, C.A. *Acc. Chem. Res.*, **34** (2001) 759-771.

[34] Yaghi, O.M, *Nature Mater.*, **6** (2007) 92-93.

[35] Chui, S.S., Chen, R. and Che, C.-M. *Angew. Chem. Int. Ed.*, **45** (2006) 1621-1624.

[36] Wiseman, M.R., Marsh, P.A., Bishop, P.T., Brisdon, B.J. and Mahon, M.F. *J. Am. Chem. Soc.*, **122** (2000) 12598-12599.

[37] Mingos, D.M.P., Yau, J., Menzer, S. and Williams, D.J., *Angew. Chem.*, **107** (1995) 2045-2047; *Angew. Chem. Int. Ed. Engl.*, **34** (1995) 1894-1895.

[38] Puddephatt, R.J., *Chem. Soc. Rev.*, **37** (2008) 2012-2027.

[39] Olmos, M.H. and Laguna, A. *Modern Supramolecular Gold Chemistry: Gold-Metal Interactions and Applications.* (2008) Ch. 5 pp. 295-345 Wiley-VCH, Germany.

[40] Ehlich, H., Schier, A. and Schmidbaur, H. *Inorg. Chem.*, **41** (2002) 3721-3727.

[41] Puddephatt, R.J. *Coord. Chem. Rev.*, **216-217** (2001) 313-332.

[42] a) Hunks, W.J., McDonald, M.A., Jennings, M.C. and Puddephatt, R.J. *Organometallics*, **19** (2000) 5063-5070. b) Irwin, M.J., Jia, G., Payne, N.C. and Puddephatt, R.J. *Organometallics*, **15** (1996) 51-57. c) Irwin, M.J., Vittal, J.J. and Puddephatt, R.J. *Organometallics*, **16** (1997) 3541-3547. d) McArdle, C.P., Jennings, M.C., Vittal, J.J. and Puddephatt, R.J. *Chem. Eur. J.*, **7** (2001) 3572- 3583.

[43] Mohr, F., Jennings, M.C. and Puddephatt, R.J. *Angew. Chem. Int. Ed.*, **43** (2004) 969-971.

[44] Berners-Price, S.J. and Filipovska, A. *Metallomics*, **3** (2011) 863-873.

[45] Fricker, S.P. *Gold Bull.*, **29** (1996) 53-60.

[46] Ruben, H., Zalkin, A., Faltens, M. and Templeton, D.H. *Inorg. Chem.*, **13** (1974) 1836-1839.

[47] Tiekink, E.R.T. *Inflammopharmacology*, **16** (2008) 138-142.

[48] Porter, L.C., Fackler Junior, J.P., Costamagna, J. and Schmidt, R. *Acta Crystallogr., Sect. C: Cryst. Struct. Commun.*, **48** (1992) 1751-1754.

[49] Mirabelli, C.K., Johnson, R.K., Hill, D.T., Faucette, L.F., Girard, G.R., Kuo, G.Y., Sung, C.M. and Crooke, S.T. *J. Med. Chem.*, **29** (1986) 218-223.

[50] Ronconi, L., Giovagnini, L., Marzano, C., Bettìo, F., Graziani, R., Pilloni, G. and Fregona, D. *Inorg. Chem.*, **44** (2005) 1867-1881.

[51] Casini, A., Hartinger, C., Gabbiani, C., Mini, E., Dyson, P.J., Keppler, B.K. and Messori, L. J. *Inorg. Biochem.*, **102** (2008) 564-575.

[52] Henderson, W., Nicholson, B.K., Faville, S.J., Fan, D. and Ranford, J.D. *J. Organomet. Chem.*, **631** (2001) 41-46.

[53] Milacic, V., Chen, D., Ronconi, L., Landis-Piwowar, K.R., Fregona, D., and Dou, Q.P. *Cancer Res.*, **66** (2006) 10478-10486.

[54] Bardají, M., Laguna, A. and Pérez, M.R. *Organometallics*, **21** (2002) 1877-1881.

[55] Tzeng, B.-C., Li, D., Peng, S.-M. and Che, C.-M. *J. Chem. Soc. Dalton Trans.*, (1993) 2365-2371.

[56] Serratrice, M., Cinellu, M.A., Maiore, L., Pilo, M., Zucca, A., Gabbiani, C., Guerri, A., Landini, I., Nobili, S., Mini, E. and Messori, L. *Inorg. Chem.*, **51** (2012) 3161-3171.

[57] Maia, P.I da S., Deflon, V.M. and Abram, U. *Future Med. Chem.*, **6** (2014) 1515-1536.

[58] Yang, T., Tu, C., Zhang, J., Lin, L., Zhang, X., Liu, Q., Ding, J., Xu, Q. and Guo, Z. *Dalton Trans.*, (2003) 3419-3424.

[59] Sun, R.W.-Y. and Che, C.-M. *Coord. Chem. Rev.*, **253** (2009) 1682–1691.

[60] Rubbiani, R., Kitanovic, I., Alborzinia, H., Can, S., Kitanovic, A., Onambele, L.A., Stefanopoulou, M., Geldmacher, Y., Sheldrick, W.S., Wolber, G., Prokop, A., Wölfl, S. and Ott, I. *J. Med. Chem.*, **53** (2010) 8608-8618.

[61] Hickey, J.L., Ruhayel, R.A., Barnard, P.J., Baker, M.V., Berners-Price, S.J. and Filipovska, A. *J. Am. Chem. Soc.*, **130** (2008) 12570-12571.

[62] Yan, J.J., Chow, A.L.-F., Leung, C.-H., Sun, R.W.-Y., Ma, D.-L. and Che, C.-M. *Chem. Commun.,* **46** (2010) 3893-3895.

[63] Parish, R.V., Howe, B.P., Wright, J.P., Mack, J., Pritchard, R.G., Buckley, R.G., Elsome, A.M. and Fricker, S.P. *Inorg. Chem.*, **35** (1996) 1659-1666.

[64] Lehn, J.-M. *Chem. Soc. Rev.*, **36** (2007) 151-160.

[65] Chakrabarty, R., Mukherjee, P.S. and Stang, P.J. *Chem. Rev.*, **111** (2011) 6810-6918.

[66] Sauvage, J.-P., *Transition Metals in Supramolecular Chemistry*, Vol. 5., (1999) Section 1, pp. 1, John Wiley & Sons Ltd. UK.

[67] Desiraju, G.R. *The crystal as Supramolecular Entity - Perspectives in Supramolecular Chemistry*, Vol 2 (1996) John Wiley & Sons Ltd. UK.

[68] Atkinson, I.M. and Lindoy, L.F. *Self-Assembly in Supramolecular Systems,* (2000) Section 1.2, pp. 3-5. Cambridge University Press. UK.

[69] Lehn, J.-M., *Supramolecular Chemistry - Concepts and Perspectives,* (1995) Section 9.3, pp. 144-145, Wiley-VCH, Germany.

[70] Lehn, J.-M., Rigault, A., Siegel, J., Harrowfield, J., Chevrier, B. and Moras, D. *Proc.Natl. Acad. Sci.*, **84** (1987) 2565-2569.

[71] Hasenknopf, B., Lehn, J.-M., Boumediene, N., Dupont-Gervais, A., Van Dorsselaer, A., Kneisel, B. and Fensk, D. *J. Am. Chem. Soc.*, **119** (1997) 10956-10962.

[72] Lee, C.F., Leigh, D.A., Pritchard, R.G., Schultz, D., Teat, S.J., Timco, G.A. and Winpenny, R.E.P. *Nature*, **458** (2009) 314-318.

[73] Hori, A., Sawada, T., Yamashita, K. and Fujita, M. *Angew. Chem. Int. Ed.*, **44** (2005) 4896-4899.

[74] Fujita, M. and Ogura, K. *Coord. Chem. Rev.*, **148** (1996) 249-264.

[75] Gil-Ramírez, G., Leigh, D.A. and Stephens, A.J. *Angew. Chem. Int. Ed.*, **54** (2015) 6110-6150.

[76] Fujita, M., Ibukuro, F., Hagihara, H. and Ogura. K. *Nature*, **367** (1994) 720-723.

[77] Burchell, T.J., Eisler, D.J. and Puddephatt, R.J. *Inorg. Chem.*, **43** (2004) 5550-5557.

[78] Holliday, B.J. and Mirkin, C.A. *Angew. Chem. Int. Ed.*, **40** (2001) 2022-2043.

[79] Buchecker, C.D., Colasson, B., Fujita, M., Hori, A., Geum, N., Sakamoto, S., Yamaguchi, K. and Sauvage, J.P. *J. Am. Chem. Soc.*, **125** (2003) 5717-5725.

[80] Sinha, N. and Hahn, F.E. *Acc. Chem. Res.*, **50** (2017) 2167-2184.

[81] Escartí, F., Miranda, C., Lamarque, L., Latorre, J., García-España, E., Kumar, M., Arán, V.J. and Navarro, P. *Chem. Commun.*, (2002) 936-937.

[82] Roche, S., Haslam, C., Adams, H., Heath, S.L. and Thomas, J.A. *Chem. Commun.*, (1998) 1681-1682.

[83] Atkinson, I.M. and Lindoy, L.F. *Self-Assembly in Supramolecular Systems,* (2000) Section 7.2, pp. 199; Cambridge University Press. UK.

[84] Iritani, K., Tahara, K., De Feyter, S. and Tobe, Y. *Langmuir*, **33** (2017) 4601-4618.

[85] Cram, D.J. and Cram, J.M. *Science*, **183** (1974) 803-809.

[86] Cram, D.J. *Angew. Chem. Int. Ed.*, **27** (1988) 1009-1020.

[87] Yang, H., Yuan, B. and Zhang, X. *Acc. Chem. Res.*, **47** (2014) 2106-2115.

[88] Padersen, C.J. *Angew. Chem. Int. Ed. Engl.*, **27** (1988) 1021-1027.

[89] Lehn, J.-M. *Angew. Chem. Int. Ed. Engl.*, **27** (1988) 89-112.

[90] Seanger, W. *Angew. Chem. Int. Ed. Engl.*, **19** (1980) 344-362.

[91] Amirnejat, S., Movahedi, F., Masrouri, H., Mohadesi, M. and Kassaee, M.Z. *J. Mol. Catal. A-Chem.,* **378** (2013) 135-141.

[92] Cauzzi, D., Lanfranchi, M., Marzolini, G., Predieri, G., Tiripicchio, A., Costa, M. and Zanoni, R. *J.Organomet. Chem.*, **488** (1995) 115-125.

[93] Nkabyo, H.A., Hannekom, D., McKenzie, J. and Koch, K.R. *J. Coord. Chem.*, **67** (2014) 4039-4060.

[94] Gunasekaran, N., Ramesh, P., Nanjappa, M., Ponnuswamy, G. and Karvembu, R. *Dalton Trans*., **40** (2011) 12519-12526.

[95] Abram, U., Abram, S., Alberto, R. and Schibli, R. *Inorg. Chim. Acta*, **248** (1996) 193-202.

[96] a) Nguyen, H.H. and Abram, U. *Inorg.Chem*., **46** (2007) 5310-5319. b) Barolli, J.P., Maia, P.I.S., Colina-Vegas, L., Moreira, J., Plutin, A.M., Mocelo, R., Deflon, V.M., Cominetti, M.R., Camargo-Mathias, M.I. and Batista, A.A. *Polyhedron*, **126** (2017) 33-41.

[97] Xie, J., Cheng, Z., Yang, W., Liu, H., Zhou, W., Li, M. and Xu, Y. *Appl Organometal. Chem.*, **29** (2015) 157-164.

[98] Yang, W., Liu, H., Li, M., Wang, F., Zhou, W. and Fan, J. *J. Inorg. Biochem.*, **116** (2012) 97-105.

[99] Gunasekaran, N., Remya, N., Radhakrishnan, S. and Karvembu, R. *J. Coord. Chem.*, **64** (2011) 491-501.

[100] a) Reinel, M., Richter, R. and Kirmse, R. *Z. Anorg. Allg. Chem.*, **628** (2002) 41-44. b) Gruschinski, S. and Rodenstein, A. *Z. Anorg. Allg. Chem.*, **638** (2012) 1179-1186. c) O'Reilly, B., Plutin, A.M., Perez, H., Calderon, O., Ramos, R., Martinez, R., Toscano, R.A., Duque, J., Rodriguez-Solla, H., Martinez-Alvarez, R., Suarez, M. and Martin, N. *Polyhedron*, **36** (2012) 133-140. d) Che, D.J., Li, G., Yao, X.L.; Yu, Z. and Zhou, D.P. *J. Chem. Soc. Dalton Trans.*, (1999) 2683-2687.

[101] a) Mandal, H. and Ray, D. *Inorg Chim Acta*, **414** (2014) 127-133. b) Bensch, W. and Schuster, M. *Z. Anorg. Allg. Chem.*, **615** (1992) 93-96.

[102] a) Zhao, X.Y., Zhu, C.B., Li, H.P., Yang, Y. and Roesky, H.W. *Z. Anorg. Allg. Chem.*, **640** (2014) 1614-1621. b) Okuniewski, A., Rosiak, D., Chojnacki, J. and Becker, B. *Polyhedron*, **90** (2015) 47-57. c) Schmitt, B., Gerber, T.I.A., Hosten, E. and Betz, R. *Inorg. Chem. Commun.*, **24** (2012) 136-139.

[103] Bensch, W. and Schuster, M. *Z. Anorg. Allg. Chem.*, **611** (1992) 99-102.

[104] Weber, G. Hartung, J. and Beyer, L. *Tetrahedron Lett.*, **29** (1988) 3475-3476.

[105] Nguyen, H.H., Jegathesh, J.J., Maia, P.I.S., Deflon, V.M., Gust, R., Bergemann, S. and Abram, U. *Inorg. Chem.*, **48** (2009) 9353-9364.

[106] Nguyen, H.H., Deflon, V.M. and Abram, U. *Eur. J. Inorg. Chem.*, **21** (2009) 3179-3187.

[107] Beyer, L. and Widera, R. *Tetrahedron Lett.*, **23** (1982) 1881-1882.

[108] Nguyen, H.H. and Abram, U. *Polyhedron*, **28** (2009) 3945-3952.

[109] Nguyen, H.H., Trieu, T.N. and Abram, U. *Z. Anorg. Allg. Chem.*, **637** (2011) 1330-1333.

[110] Hartung, J., Weber, G., Beyer, L. and Szargan, R. *Z. Anorg. Allg. Chem.*, **523** (1985) 153-160.

[111] Abram, U., Münze, R., Hartung, J., Beyer, L., Kirmse, R., Köhler, K., Stach, J., Behm, H. and Beurskens, P.T. *Inorg. Chem.*, **28** (1989) 834-839.

[112] Braun, U., Sieler, J., Richter, R., Hettich, B. and Simon, A. *Z. Anorg. Allg. Chem.*, **557** (1988) 134-142.

[113] Richter, R., Schröder, U., Kampf, M., Hartung, J. and Beyer, L. *Z. Anorg. Allg. Chem.*, **623** (1997) 1021-1026.

[114] Schröder, U., Richter, R., Hartung, J., Abram, U. and Beyer, L. *Z. Naturforsch.*, **52b** (1997) 620-628.

[115] Vijayan, P., Viswanathamurthi, P., Sugumar, P., Ponnuswamy, M.N., Malecki, J.G., Velmurugan, K., Nandhakumar, R., Balakumaran, M.D. and Kalaichelvan, P.T. *Appl. Organometal. Chem.*, (2016) 1-23.

[116] Nguyen, H.H., Le, C.D., Pham, C.T., Trieu, T.N., Hagenbach, A. and Abram, U. *Polyhedron*, **48** (2012) 181-188.

[117] Santos, I.G., Hagenbach A. and Abram, U. *Dalton Trans.*, (2004) 677-682.

[118] Schroer, J. and Abram, U. *Polyhedron*, **28** (2009) 2277-2283.

[119] Nguyen, H.H., Grewe, J., Schroer, J., Kuhn, B. and Abram, U. *Inorg. Chem*., **47** (2008) 5236-5144.

[120] Maia, P.I. da S., Nguyen, H.H., Ponader, D., Hagenbach, A., Bergemann, S., Gust, R., Deflon, V.M. and Abram, U. *Inorg. Chem.*, **51** (2012) 1604-1613.

[121] Maia, P.I., Carneiro, Z.A., Lopes, C.D., Oliveira, C.G., Silva, J.S., de Albuquerque, S., Hagenbach, A., Gust, R., Deflon, V.M. and Abram, U. *Dalton Trans.*, **46** (2017) 2559-2571.

[122] Maia, P.I. da S., Nguyen, H.H., Hagenbach, A., Bergemann, S., Gust, R., Deflon, V.M. and Abram, U. *Dalton Trans.*, **42** (2013) 5111-5121.

[123] Schroer, J. and Abram, U. *Polyhedron*, **33** (2012) 218-222.

[124] Nguyen, H.H., Castillo Gomez, J.D. and Abram, U. *Inorg. Chem. Commun.*, **26** (2012) 72-76.

[125] Nguyen, T.B.Y., Nguyen, M.H., Abram, U. and Nguyen, H.H. *Z. Anorg. Allg. Chem.*, **641** (2015) 1737-1743.

[126] Koch, K.R., Hallale, O., Bourne, S.A., Miller, J. and Bacsa, J. *J. Mol. Struct.*, **561** (2001) 185-196.

[127] Koch, K.R., Bourne, S.A., Coetzee, A. and Miller, J. *J. Chem. Soc., Dalton Trans.*, (1999) 3157-3161.

[128] Rodenstein, A., Griebel, J., Richter, R. and Kirmse, R. *Z. Anorg. Allg. Chem.*, **634** (2008) 867-874.

[129] Rodenstein, A., Richter, R. and Kirmse, R. *Z. Anorg. Allg. Chem.*, **633** (2007) 1713-1717.

[130] Westra, A.N., Bourne, S.A. and Koch, K.R. *Dalton Trans.*, (2005) 2816-2924.

[131] Schwade, V.D., Kirsten, L., Hagenbach, A., Lang, E.S. and Abram, U. *Polyhedron*, **55** (2013) 155-161.

[132] Pham, C.T. *Doctoral Thesis Freie Universität Berlin*, (2016).

[133] Wioppiold, T.A., Ackermann, J., Lang, E.S. and Abram, U. *Polyhedron*, **87** (2015) 202-207.

[134] Nguyen, H.H., Jegathesh, J.J., Takiden, A., Hauenstein, D., Pham, C.T., Lee, C.D. and Abram, U. *Dalton Trans.*, **45** (2016) 10771-10779.

[135] Mack, J., Ortner, K. and Abram, U. *Z. Anorg. Allg. Chem.*, **623** (1997) 873-879.

[136] Silverstain, R.M., Webster, F.X. and Kiemle, D.J. *Identification of Organic Compounds*, Sec. 2.6 (2005) pp. 82-126, John Wiley & Sons, US.

[137] Castiñeiras, A., Dehnen, S., Fuchs, A., García-Santos, I. and Sevillano, P. *Dalton Trans.*, (2009) 2731-2739.

[138] Ortner, K. and Abram, U. *Inorg. Chem. Commun.*, **7** (1998) 251-253.

[139] Casas, J.S., Castaño, M.V., Cifuentes, M.C., García-Monteagudo, J.C., Sánchez, A., Sordo, J. and Abram, U. *J. Inorg. Biochem.*, **98** (2004) 1009-1016.

[140] Abram, U., Mack, J., Ortner, K. and Müller, M. *J. Chem. Soc., Dalton Trans.*, (1998) 1011-1019.

[141] Ortner, K. and Abram, U. *Polyhedron*, **18** (1999) 749-754.

[142] Gomes, L.R., Santos, L.M.N.B.F., Coutinho, J.A.P., Schröder, B. and Low, J.N. *Acta Cryst.*, **E66** (2010) o870.

[143] Vijayan, P., Viswanathamurthi, P., Sugumar, P., Ponnuswamy, M.N., Malecki, J.G., Velmurugan, K., Nandhakumar, R., Balakumaran, M.D. and Kalaichelvan, P.T. *Appl. Organometal. Chem.*, **31** (2017) 3652-3675.

[144] Abram, U., Ortner, K., Gust, R. and Sommer, K. *J. Chem. Soc., Dalton Trans.*, (2000) 735-744.

[145] Köhler, R., Hoyer, E., Beyer, L. and Weber, G. Patent, DE, (1990), DD282910 A5 19900926.

[146] Castillo Gomez, J.D., Nguyen, H.H., Hagenbach, A. and Abram, U. *Polyhedron*, **43** (2012) 123-130.

[147] Eikens, W., Jones, P.G., Lautner, J. and Thöne, C. *Z. Naturforsch.*, **49b** (1994) 21-26.

[148] Henderson, W., Nicholson, B.K. and Tiekink, E.R.T. *Inorg. Chim. Acta*, **359** (2006) 204-214.

[149] Jegathesh, J.J. *Doctoral Thesis Freie Universität Berlin,* (2013).

[150] Luckay, R.C., Mebrahtu, F., Esterhuysen, C. and Koch, K.R. *Inorg. Chem. Commun.*, **13** (2010) 468-470.

[151] Pathaneni, S.S. and Desiraju, G.R. *J. Chem. Soc., Dalton Trans.*, (1993) 319-322.

[152] Janiak, C. J. *Chem Soc., Dalton Trans.*, (2000) 3885-3896.

[153] Gutíerrez, A., Bernal, J., Villacampa, M.D., Cativiela, C., Laguna, A. and Gimeno, M.C. *Inorg. Chem.*, **52** (2013) 6473-6480.

[154] Behrendt, S., Beyer, L., Dietze, F., Kleinpeter, E. and Hoyer, E. *Inorg. Chim. Acta*, **43** (1980) 141-144.

[155] Burdett, J.K., Hoffmann, R. and Fay, R.C. *Inorg. Chem.*, **17** (1978) 2553-2568.

[156] Fangna, D., Haiyan, H., Dongliang, G., Fei, Y., Xiaoliang, Q. and Daofeng, S. *Cryst. Eng. Commun.*, **11** (2009) 2516-2522.

[157] Binnemans, K., Herck, K.V. and Görller-Warland, C. *Chem. Phys. Lett.*, **266** (1997) 297-302.

[158] Demirer, T.I., *Master Thesis, Freie Universität Berlin* (2018).

[159] Le Borgne, T., Bénech, J.-M., Floquet, S., Bernardinelli, G., Aliprandini, C., Bettens, P. and Piguet, C. *Dalton Trans.*, (2003) 3856-3868.

[160] Ilmi, R. and Iftikhar, K., *J. Coord. Chem.*, **65** (2012) 403-419.

[161] Tanase, S., Gallego, P.M., de Gelder, R. and Fu, W.T. *Inorg. Chim. Acta*, **360** (2007) 102-108.

[162] Renaud, F., Piguet, C., Bernardinelli, G., Bünzli, J.-C.G. and Hopfgartner, G. *Chem. Eur. J.* **3** (1997) 1646-1659.

[163] Senegas, J.-M., Bernardinelli, G., Imbert, D., Bünzli, J.-C.G., Morgantini, P.-Y., Weber, J. and Piguet, C. *Inorg. Chem.*, **42** (2003) 4680-4695.

[164] Platas-Iglesias, C., Piguet, C., André, N. and Bünzli, J.-C.G. *J. Chem. Soc. Dalton Trans.*, (2001) 3084-3091.

[165] Abdulkader, A. *Master Thesis Freie Universität Berlin* (2011).

[166] Kumar, K.S., Schäfer, B., Lebedkin, S., Karmazin, L., Kappes, M.M. and Ruben, M. *Dalton Trans.*, **44** (2015) 15611-15619.

[167] Bailar, J.C., Emeléus, H.J., Nyholm, R.S. and Trotman-Dickenson, A.F. *Comprehensive Inorganic Chemistry*, vol. 4 (1973) Sec. 4 pp. 7; Pergamon Press Ltd. Oxford, UK.

[168] Görrler-Walrand, C. and Binnemans, K. *Handbook on the Physics and Chemistry of Rare Earths*, Vol. 25 (1998) pp. 101; Elsevier, Amsterdam.

[169] Bünzli, J.-C.G. and Choppin, G.R. *Lanthanide Probes in Life, Chemical and Earth Science, Theory and Practice*. Ch. **7** (1989) Elsevier, Amsterdam.

[170] Eliseeva, S.V. and Bünzli, J.-C.G. *Chem. Soc. Rev.*, **39** (2010) 189-227.

[171] Carnall, W.T., Fields, P.R. and Rajnak, K. *J. Chem. Phys.*, **49** (1968) 4412-4423.

[172] Carnall, W.T., Fields, P.R. and Wybourne, B.G. *J. Chem. Phys.*, **42** (1965) 3797-3806.

[173] Judd, B.R. *Phys. Rev.*, **127** (1962) 750-761.

[174] Ofelt, G.S. *J. Chem. Phys.*, **37** (1962) 511-520.

[175] Binnemans, K. *Coord. Chem. Rev.*, **295** (2015) 1-45.

[176] Werts, M.H.V., Jukes, R.T.F. and Verhoeven, J.W. *Phys. Chem. Chem. Phys.*, **4** (2002) 1542-1548.

[177] Binnemans, K. and Gschneidner Jr., K.A. *Handbook on the Physics and Chemistry of Rare Earths*, vol. 35 (2005) pp.107-272; Elsevier, Amsterdam.

[178] Wu, Y., Jinzhang, G. and Jingwan, K. *Spectrosc. Lett.*, **28** (1995) 921-936.

[179] Seminara, A. and Musumeci, A. *Inorg. Chim. Acta*, **95** (1984) 291-307.

[180] Shannon, R.D. *Acta Crystallogr. Sect A*, **32** (1976) 751-767.

[181] a) Aghabozorg, H., Ramezanipour, F., Kheirollahi, P.D., Saei, A.A., Shokrollahi, A., Shamsipur, M., Manteghi, F., Soleimannejad, J. and Sharif, M.A. *Z. Anorg. Allg. Chem.*, **632** (2006) 147-154. b) Soleimannejad, J., Sheshmani, S., Solimannejad, M., Nazarnia, E. and Hosseinabadi, F. *J. Struct. Chem.*, **55** (2014) 342-352. c) Aghabozorg, H., Ghadermazi, M., Sheshmani, S. and Nakhjavan, B. *Acta Crystallogr. Sect E*, **62** (2006) m2371-m2373.

[182] Craig, A.S., Helps, I.M. and Parker, D. *Polyhedron*, **8** (1989) 2481-2484.

[183] Anderson, T.J., Neuman, M.A. and Melson, G.A., *Inorg. Chem.*, **12** (1973) 927- 930.

[184] Arif, A.M., Hart, F.A., Hursthouse, M.B., Thornton-Pett, M. and Zhu, W. *J. Chem. Soc. Dalton Trans.*, (1984) 2449-2454.

[185] Meehan, P.R., Aris, D.R. and Willey, G.R. *Coord. Chem. Rev.*, **181** (1999) 121-145.

[186] McRitchie, D.D., Palenik, R.C. and Palenik, G.J. *Inorg. Chim. Acta*, **20** (1976) L27-L28.

[187] Melson, G.A. and Stotz, R.W. *Coord. Chem. Rev.*, **7** (1971) 133-160.

[188] Rossini, A.J. and Schurko, R.W. *J. Am. Chem Soc.*, **128** (2006) 10391-10402.

[189] McClevery, J.A and Meyer, T.J. *Comprehensive Coordination Chemistry II*, vol. 4 (2004) Sec. 4.1 pp. 1-24; Elsevier Ltd. Oxford, UK.

[190] Bandoli, G., Dolmella, A., Tisato, F., Porchia, M. and Refosco, F. *Coord. Chem. Rev.*, **253** (2009) 56-77.

[191] Soleimannejad, J. and Nazarnia, E. *J. Mol. Struct.*, **1116** (2016) 207-217.

[192] West, D.X., Carlson, C.S., Liberta, A.E., Albert, J.N. and Daniel, C.R. *Transit. Met. Chem.*, **15** (1990) 341-344.

[193] Siddiqi, K.S., Khan, S. and Nami, S.A.A. *J. Incl. Phenom. Macro.*, **55** (2006) 359-366.

[194] Lever, A.B.P. *Electronic Spectra of Inorganic and Coordination Compounds,* (1968); John Wiley, New York.

[195] Chandra, S. and Gupta, L.K. *Spectrochim. Acta Part A*, **60** (2004) 1563-1571.

[196] Silvestru, C. and Laguna, A. *Modern Supramolecular Gold Chemistry: Gold-Metal Interactions and Applications.* (2008) Ch. 4 pp. 181-293; Wiley-VCH, Germany.

[197] Gaussview 5.0, Gaussian Inc.: Wallingford, CT, (2000-2008).

[198] WinEPR SimFonia, Bruker Instruments, Inc.: Billerica, (1995) MA, USA,.

[199] SOROBAN, Freie Universität Berlin, https://www.zedat.fu-berlin.de/HPC.

[200] Gaussian 09, Revision A.02, Frisch, M.J., Trucks, G.W., Schlegel, H.B., Scuseria, G.E., Robb, M.A., Cheeseman, J.R., Scalmani, G., Barone, V., Petersson, G.A., Nakatsuji, H., Li, X., Caricato, M., Marenich, A., Bloino, J., Janesko, B.G., Gomperts, R., Mennucci, B., Hratchian, H.P., Ortiz, J.V., Izmaylov, A.F., Sonnenberg, J.L., Williams-Young, D.,

Ding, F., Lipparini, F., Egidi, F., Goings, J., Peng, B., Petrone, A., Henderson, T., Ranasinghe, D., Zakrzewski, V.G., Gao, J., Rega, N., Zheng, G., Liang, W., Hada, M., Ehara, M., Toyota, K., Fukuda, R., Hasegawa, J., Ishida, M., Nakajima, T., Honda, Y., Kitao, O., Nakai, H., Vreven, T., Throssell, K., Montgomery, J.A.Jr., Peralta, J.E., Ogliaro, F., Bearpark, M., Heyd, J.J., Brothers, E., Kudin, K.N., Staroverov, V.N., Keith, T., Kobayashi, R., Normand, J., Raghavachari, K., Rendell, A., Burant, J.C., Iyengar, S.S., Tomasi, J., Cossi, M., Millam, J.M., Klene, M., Adamo, C., Cammi, R., Ochterski, J.W., Martin, R.L., Morokuma, K., Farkas, O., Foresman, J.B. and Fox, D.J. Gaussian, Inc., Wallingford CT, (2016).

[201] Gaussian 16, Revision A.03, Frisch, M.J., Trucks, G.W., Schlegel, H.B., Scuseria, G.E., Robb, M.A., Cheeseman, J.R., Scalmani, G., Barone, V., Petersson, G.A., Nakatsuji, H., Li, X., Caricato, M., Marenich, A., Bloino, J., Janesko, B.G., Gomperts, R., Mennucci, B., Hratchian, H.P., Ortiz, J.V., Izmaylov, A.F., Sonnenberg, J.L., Williams-Young, D., Ding, F., Lipparini, F., Egidi, F., Goings, J., Peng, B., Petrone, A., Henderson, T., Ranasinghe, D., Zakrzewski, V.G., Gao, J., Rega, N., Zheng, G., Liang, W., Hada, M., Ehara, M., Toyota, K., Fukuda, R., Hasegawa, J., Ishida, M., Nakajima, T., Honda, Y., Kitao, O., Nakai, H., Vreven, T., Throssell, K., Montgomery, J.A.Jr., Peralta, J.E., Ogliaro, F., Bearpark, M., Heyd, J.J., Brothers, E., Kudin, K.N., Staroverov, V.N., Keith, T., Kobayashi, R., Normand, J., Raghavachari, K., Rendell, A., Burant, J.C., Iyengar, S.S., Tomasi, J., Cossi, M., Millam, J.M., Klene, M., Adamo, C., Cammi, R., Ochterski, J.W., Martin, R.L., Morokuma, K., Farkas, O., Foresman, J.B. and Fox, D.J. Gaussian, Inc., Wallingford CT, (2016).

[202] Vosko, S.H., Wilk, L. and Nusair, M. *Can. J. Phys.*, **58** (1980) 1200-1211.

[203] Becke, A.D. *J. Chem. Phys.*, **98** (1993) 5648-5652.

[204] Lee, C., Yang, W. and Parr, R.G. *Phys. Rev. B.*, **37** (1988) 785-789.

[205] Feller, D. *J. Comput. Chem.*, **17** (1996) 1571-1586.

[206] Schuchardt, K.L., Didier, B.T., Elsethagen, T., Sun, L., Gurumoorthi, V, Chase, J.L. and Windus, T.L., *J. Chem. Inf. Model.*, **47** (2007) 1045-1052.

[207] Kretschmar, M. CHECK-HKL, Universität Tübingen, Germany (1998).

[208] Sheldrick, G.M. SADABS, Universität Göttingen, Germany (2014).

[209] X-RED32, STOE & Cie GmbH: Darmstadt, Germany (2002).

[210] Sheldrick, G.M. *Acta Crystallogr. Sect. A*, **64** (2008) 112-122.

[211] Sheldrick, G.M *Acta Crystallogr. Sect. C*, **71** (2015) 3-8.

[212] Farrugia, L. *J. Appl. Crystallogr.*, **45** (2012) 849-854.

[213] Diamond Crystal and Molecular Structure Visualization; Crystal Impact - Dr. H. Putz and Dr. K. Brandenburg GbR, Bonn Germany.

[214] Persistence of Vision Raytracer (Version 3.6), http://www.povray.org/.

[215] Uson, R., Laguna, A. and Laguna, M. *Inorg. Synth.*, **26** (1989) 85-86.

[216] Kowala, C. and Swan, J.M. *Aust. J. Chem.*, **19** (1966) 547-554.

[217] Brauer, G. *Handbook of Preparative Inorganic Chemistry*, Vol. 1 (1963) pp. 1057-1059.

[218] Dixon, A.E. and Taylor, J. *J. Chem. Soc., Trans.*, **101** (1912) 558-561.

[219] Yokoyama, M., Ikuma, T., Obara, N. and Togo, H., *J. Chem. Soc., Perkin Trans.*, **1** (1990) 3243-3245.

Appendix

Crystallographic Data

[Au(damp-κC^1,N)(L1)](PF$_6$)

Table A1: Crystal data and structure refinement for [Au(damp-κC^1,N)(L1)](PF$_6$).

Empirical formula	$C_{21}H_{27}AuF_6N_3OPS$	
Formula weight	711.45	
Temperature	100(2) K	
Wavelength	0.71073 Å	
Crystal system	Monoclinic	
Space group	$P2_1/c$	
Unit cell dimensions	a = 12.0877(4) Å	α = 90°.
	b = 14.6537(5) Å	β = 105.473(1)°.
	c = 14.4133(4) Å	γ = 90°.
Volume	2460.5(1) Å^3	
Z	4	
Density (calculated)	1.921 g/cm^3	
Absorption coefficient	6.194 mm^{-1}	
F(000)	1384	
Crystal size	0.15 x 0.05 x 0.03 mm^3	
Theta range for data collection	2.402 to 24.998°.	
Index ranges	-13<=h<=14, -17<=k<=15, -17<=l<=17	
Reflections collected	24495	
Independent reflections	4333 [R(int) = 0.0318]	
Completeness to theta = 24.998°	99.9 %	
Absorption correction	Semi-empirical from equivalents	
Max. and min. transmission	0.7456 and 0.6833	
Refinement method	Full-matrix least-squares on F^2	
Data / restraints / parameters	4333 / 1 / 296	
Goodness-of-fit on F^2	1.177	
Final R indices [I>2sigma(I)]	R1 = 0.0250, wR2 = 0.0532	
R indices (all data)	R1 = 0.0318, wR2 = 0.0551	
Largest diff. peak and hole	2.709 and -0.591 e · Å^{-3}	
Diffractometer	Bruker D8 Venture	

Table A2: Atomic coordinates (x 10^4) and equivalent isotropic displacement parameters (Å^2 x 10^3) for [Au(damp-κC^1,N)(L1)](PF_6). U(eq) is defined as one third of the trace of the orthogonalized U^{ij} tensor.

x	y	z	U(eq)	
C(1)	6634(4)	9082(3)	8214(3)	17(1)
C(2)	7793(4)	9280(3)	8368(3)	22(1)
C(3)	8466(4)	9504(4)	9279(3)	26(1)
C(4)	7976(5)	9537(4)	10047(3)	28(1)
C(5)	6819(4)	9352(4)	9895(3)	25(1)
C(6)	6148(4)	9116(3)	8988(3)	21(1)
C(12)	4000(4)	8538(3)	6314(3)	16(1)
C(13)	2806(4)	8196(3)	7392(3)	21(1)
C(14)	2444(5)	9091(4)	7745(4)	35(1)
C(15)	1975(4)	8125(3)	5608(3)	21(1)
C(16)	1860(4)	7142(4)	5277(4)	28(1)
C(21)	5541(4)	8611(3)	3696(3)	16(1)
C(22)	4480(4)	8839(3)	3065(3)	17(1)
C(23)	4365(4)	8792(3)	2085(3)	21(1)
C(24)	5269(4)	8547(3)	1735(3)	22(1)
C(25)	6329(4)	8341(3)	2357(3)	21(1)
C(26)	6468(4)	8363(3)	3350(3)	17(1)
C(27)	7558(4)	8093(3)	4073(3)	18(1)
C(28)	8421(4)	8066(4)	5815(3)	22(1)
C(29)	8071(4)	9522(3)	4966(4)	22(1)
Au(1)	5936(1)	8654(1)	5140(1)	13(1)
F(1)	9620(3)	11316(3)	8301(2)	48(1)
F(2)	8379(2)	11186(2)	6823(2)	36(1)
F(3)	9885(2)	11070(2)	6177(2)	37(1)
F(4)	11120(2)	11198(2)	7649(2)	31(1)
F(5)	9736(3)	10117(2)	7357(3)	47(1)
F(6)	9769(3)	12266(2)	7121(3)	49(1)
N(21)	7638(3)	8575(3)	5013(2)	13(1)
N(11)	4818(3)	8727(2)	7124(2)	13(1)
N(12)	2991(3)	8296(3)	6419(3)	17(1)
P(1)	9750(1)	11195(1)	7243(1)	20(1)
S(1)	4052(1)	8663(1)	5110(1)	20(1)
C(11)	5962(4)	8820(3)	7217(3)	13(1)

O(11)	6507(2)	8729(2)	6655(2)	13(1)

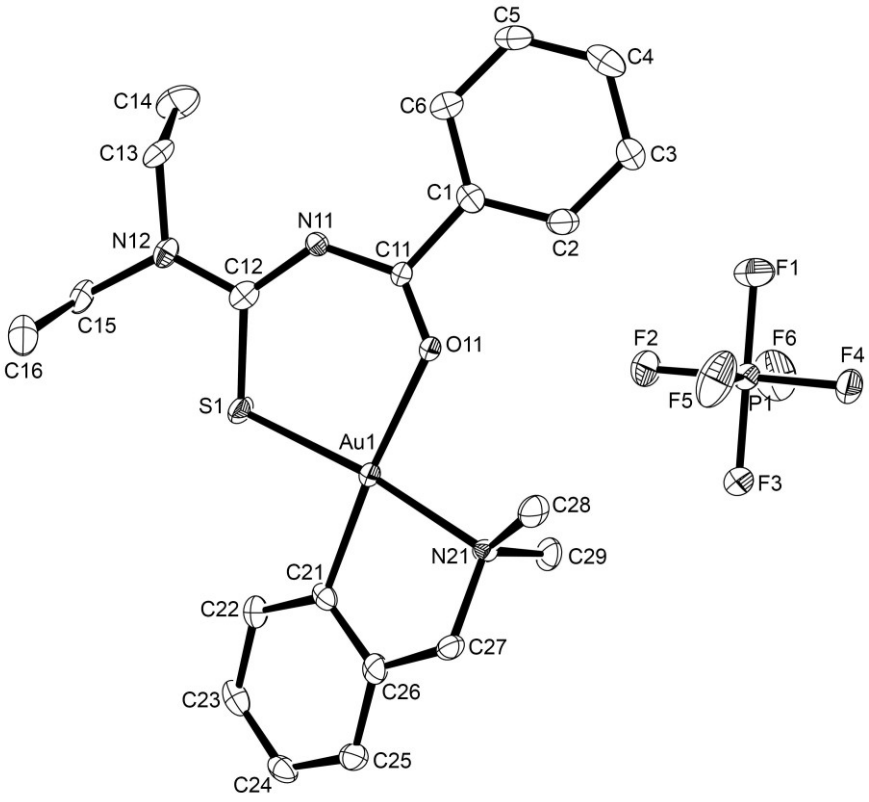

Figure A1: Ellipsoid plot of [Au(damp-κC^1,N)(L1)](PF_6). Thermal ellipsoids are at 50 % of probability. The hydrogen atoms have been omitted for clarity.

[Au(Hdamp-κC^1)(L2)](PF$_6$)

Table A3: Crystal data and structure refinement for [Au(Hdamp-κC^1)(L2)](PF$_6$).

Empirical formula	$C_{27}H_{32}AuF_6N_4OPS$	
Formula weight	802.56	
Temperature	100(2) K	
Wavelength	0.71073 Å	
Crystal system	Monoclinic	
Space group	$P2_1/n$	
Unit cell dimensions	a = 8.126(2) Å	α = 90°.
	b = 25.700(5) Å	β = 103.084(4)°.
	c = 14.855(3) Å	γ = 90°.
Volume	3022(1) Å^3	
Z	4	
Density (calculated)	1.764 g/cm^3	
Absorption coefficient	5.055 mm^{-1}	
F(000)	1576	
Crystal size	0.12 x 0.09 x 0.06 mm^3	
Theta range for data collection	2.639 to 24.998°.	
Index ranges	-9<=h<=9, -30<=k<=30, -17<=l<=17	
Reflections collected	105553	
Independent reflections	5316 [R(int) = 0.2204]	
Completeness to theta = 24.998°	99.9 %	
Absorption correction	Semi-empirical from equivalents	
Max. and min. transmission	0.7456 and 0.5678	
Refinement method	Full-matrix least-squares on F^2	
Data / restraints / parameters	5316 / 0 / 370	
Goodness-of-fit on F^2	1.153	
Final R indices [I>2sigma(I)]	R1 = 0.0368, wR2 = 0.0779	
R indices (all data)	R1 = 0.0464, wR2 = 0.0797	
Largest diff. peak and hole	1.545 and -2.683 e · Å^{-3}	
Diffractometer	Bruker D8 Venture	

Table A4: Atomic coordinates (x 10^4) and equivalent isotropic displacement parameters ($Å^2$ x 10^3) for [Au(Hdamp-κC^1)(L2)](PF_6). U(eq) is defined as one third of the trace of the orthogonalized U^{ij} tensor.

	x	y	z	U(eq)
Au(1)	8957(1)	7977(1)	6175(1)	13(1)
P(1)	6438(2)	9749(1)	2800(1)	21(1)
S(1)	7428(2)	7255(1)	6285(1)	17(1)
O(1)	10316(5)	8630(2)	6086(3)	14(1)
F(3)	4730(4)	9936(1)	2102(3)	27(1)
N(1)	9509(6)	7819(2)	4920(3)	14(1)
F(1)	8140(5)	9571(2)	3508(3)	33(1)
F(4)	7172(5)	9559(2)	1947(3)	33(1)
C(35)	12246(8)	8981(2)	5248(4)	18(1)
C(22)	9010(8)	7897(2)	8189(4)	18(1)
F(2)	5676(4)	9942(2)	3659(3)	28(1)
F(5)	5636(5)	9186(1)	2882(3)	31(1)
N(11)	7971(6)	7035(2)	4546(3)	17(1)
F(6)	7231(5)	10317(2)	2738(3)	32(1)
N(12)	7461(6)	6358(2)	5434(3)	16(1)
C(21)	8450(7)	8205(2)	7399(4)	13(1)
C(23)	8722(7)	8049(2)	9034(4)	19(1)
C(11)	8637(7)	7479(2)	4324(4)	15(1)
C(2)	7642(7)	8049(2)	2950(4)	17(1)
C(36)	11065(7)	8606(2)	5353(4)	14(1)
C(1)	8316(7)	7575(2)	3306(4)	14(1)
C(3)	7276(8)	8132(3)	2007(4)	21(2)
C(13)	7367(8)	6000(2)	4651(5)	24(2)
C(31)	10677(7)	8197(2)	4716(4)	15(1)
C(32)	11579(8)	8142(2)	4023(4)	17(1)
C(25)	7253(8)	8809(2)	8327(4)	19(1)
C(34)	13109(8)	8933(3)	4545(4)	21(1)
C(33)	12782(7)	8516(2)	3943(4)	19(1)
C(12)	7731(7)	6872(2)	5374(4)	14(1)
C(26)	7562(7)	8668(2)	7475(4)	14(1)
C(15)	7304(8)	6110(2)	6308(4)	19(1)
C(6)	8627(7)	7183(2)	2711(4)	17(1)

C(24)	7831(7)	8501(3)	9101(4)	20(1)
N(21)	8342(6)	9387(2)	6515(4)	21(1)
C(4)	7619(8)	7749(3)	1414(4)	21(1)
C(5)	8313(8)	7279(3)	1768(4)	21(2)
C(27)	6960(8)	9022(2)	6655(4)	18(1)
C(16)	5502(9)	6066(3)	6415(5)	30(2)
C(28)	7812(10)	9652(3)	5588(5)	35(2)
C(29)	8818(8)	9777(3)	7259(5)	30(2)
C(14)	9071(9)	5763(3)	4646(5)	38(2)

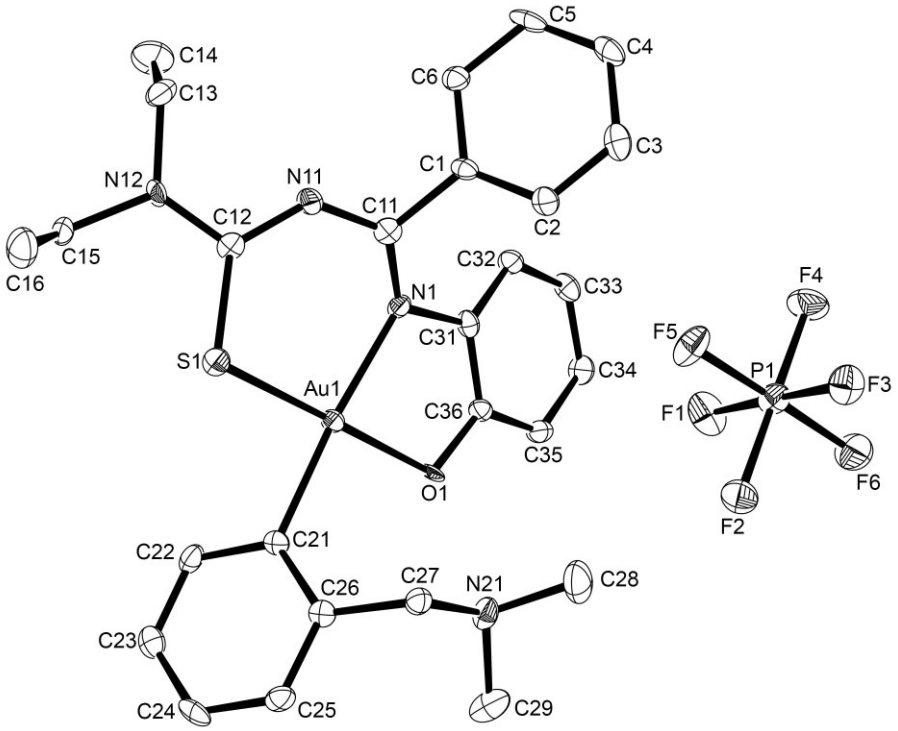

Figure A2: Ellipsoid plot of [Au(Hdamp-κC^1)(L2)](PF_6). Thermal ellipsoids are at 50 % of probability. The hydrogen atoms have been omitted for clarity.

$H_2L3 \cdot 2EtOH$

Table A5: Crystal data and structure refinement for $H_2L3 \cdot 2EtOH$.

Empirical formula	$C_{30}H_{48}N_6O_2S_2$	
Formula weight	588.86	
Temperature	200(2) K	
Wavelength	0.71073 Å	
Crystal system	Tetragonal	
Space group	$P4_32_12$	
Unit cell dimensions	a = 9.1374(3) Å	α = 90°.
	b = 9.1374(3) Å	β = 90°.
	c = 42.468(3) Å	γ = 90°.
Volume	3545.7(3) $Å^3$	
Z	4	
Density (calculated)	1.103 g/cm^3	
Absorption coefficient	0.183 mm^{-1}	
F(000)	1272	
Crystal size	0.25 x 0.18 x 0.11 mm^3	
Theta range for data collection	3.189 to 26.785°.	
Index ranges	-11<=h<=10, -11<=k<=11, -53<=l<=53	
Reflections collected	30899	
Independent reflections	3773 [R(int) = 0.0713]	
Completeness to theta = 25.242°	99.4 %	
Absorption correction	None	
Refinement method	Full-matrix least-squares on F^2	
Data / restraints / parameters	3773 / 0 / 184	
Goodness-of-fit on F^2	0.878	
Final R indices [I>2sigma(I)]	R1 = 0.0415, wR2 = 0.0973	
R indices (all data)	R1 = 0.0760, wR2 = 0.1084	
Absolute structure parameter	0.11(4)	
Largest diff. peak and hole	0.251 and -0.264 e · $Å^{-3}$	
Diffractometer	IPDS STOE	

Table A6: Atomic coordinates (x 10^4) and equivalent isotropic displacement parameters ($Å^2$ x 10^3) for $H_2L3 \cdot 2EtOH$. U(eq) is defined as one third of the trace of the orthogonalized U^{ij} tensor.

	x	y	z	U(eq)
C(1)	4692(3)	1823(3)	537(1)	60(1)
C(2)	5388(3)	1109(3)	783(1)	67(1)
C(3)	5131(4)	-338(4)	840(1)	78(1)
C(4)	4160(5)	-1110(4)	656(1)	85(1)
C(5)	3437(5)	-417(4)	419(1)	88(1)
C(6)	3701(4)	1046(4)	354(1)	78(1)
C(11)	5102(3)	3348(3)	458(1)	59(1)
C(12)	4562(3)	4419(3)	943(1)	60(1)
C(13)	4858(4)	4981(4)	1505(1)	78(1)
C(14)	4779(5)	3608(4)	1702(1)	93(1)
C(15)	7018(3)	4851(3)	1150(1)	70(1)
C(16)	7486(4)	6413(4)	1086(1)	85(1)
C(31)	6039(3)	4892(3)	23(1)	72(1)
C(41)	7093(7)	-299(6)	-196(2)	170(3)
C(42)	6002(9)	195(5)	-405(1)	155(2)
N(11)	5234(3)	4422(3)	654(1)	63(1)
N(12)	5429(3)	4719(3)	1188(1)	65(1)
N(31)	5508(3)	3545(3)	157(1)	65(1)
O(1)	5621(7)	1646(4)	-355(1)	169(2)
S(1)	2728(1)	4217(1)	986(1)	77(1)

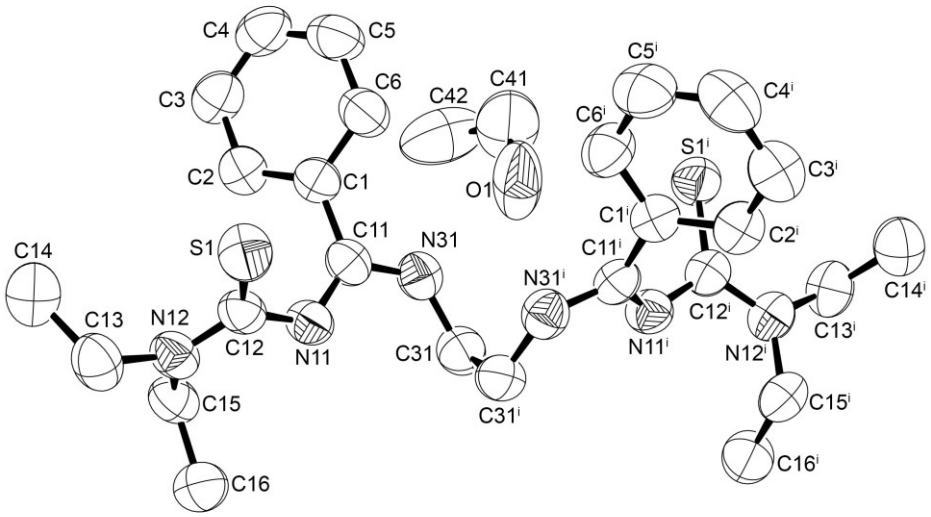

Figure A3: Ellipsoid plot of $H_2L3 \cdot 2EtOH$. Thermal ellipsoids are at 50 % of probability. The hydrogen atoms have been omitted for clarity.

$[\{AuCl\}_2(H_2L3\text{-}\kappa S)] \cdot 2CH_2Cl_2$

Table A7: Crystal data and structure refinement for $[\{AuCl\}_2(H_2L3\text{-}\kappa S)] \cdot 2CH_2Cl_2$.

Empirical formula	$C_{28}H_{40}Au_2Cl_6N_6S_2$	
Formula weight	1131.41	
Temperature	100(2) K	
Wavelength	0.71073 Å	
Crystal system	Monoclinic	
Space group	C2/c	
Unit cell dimensions	a = 23.730(1) Å	α = 90°.
	b = 11.2514(6) Å	β = 124.344(2)°.
	c = 17.3632(9) Å	γ = 90°.
Volume	3827.7(3) $Å^3$	
Z	4	
Density (calculated)	1.963 g/cm^3	
Absorption coefficient	8.213 mm^{-1}	
F(000)	2168	
Crystal size	0.20 x 0.05 x 0.05 mm^3	
Theta range for data collection	2.394 to 27.958°.	
Index ranges	-31<=h<=31, -13<=k<=14, -22<=l<=22	
Reflections collected	21698	
Independent reflections	4582 [R(int) = 0.0634]	
Completeness to theta = 25.242°	99.5 %	
Absorption correction	Semi-empirical from equivalents	
Max. and min. transmission	0.7456 and 0.4031	
Refinement method	Full-matrix least-squares on F^2	
Data / restraints / parameters	4582 / 0 / 199	
Goodness-of-fit on F^2	1.027	
Final R indices [I>2sigma(I)]	R1 = 0.0324, wR2 = 0.0642	
R indices (all data)	R1 = 0.0490, wR2 = 0.0704	
Largest diff. peak and hole	1.850 and -1.912 e · $Å^{-3}$	
Diffractometer	Bruker D8 Venture	

Table A8: Atomic coordinates (x 10^4) and equivalent isotropic displacement parameters ($Å^2$ x 10^3) for $[\{AuCl\}_2(H_2L3\text{-}\kappa S)] \cdot 2CH_2Cl_2$. U(eq) is defined as one third of the trace of the orthogonalized U^{ij} tensor.

	x	y	z	U(eq)
Au(1)	6717(1)	4766(1)	8709(1)	17(1)
S(1)	7233(1)	5968(1)	8243(1)	19(1)
Cl(1)	6223(1)	3499(1)	9190(1)	24(1)
Cl(2)	5634(1)	43(2)	8786(2)	67(1)
C(1)	5700(2)	4499(4)	6298(3)	14(1)
N(31)	4989(2)	5584(4)	6637(3)	14(1)
Cl(3)	6770(1)	-1188(2)	8917(2)	65(1)
C(31)	4804(2)	6603(4)	6969(3)	15(1)
C(6)	5493(2)	3374(4)	6401(3)	18(1)
C(5)	5602(2)	2386(5)	6031(4)	22(1)
N(11)	5917(2)	6561(4)	6904(3)	15(1)
N(12)	6746(2)	7457(4)	6826(3)	15(1)
C(2)	6023(2)	4596(4)	5832(3)	15(1)
C(11)	5558(2)	5585(4)	6647(3)	14(1)
C(12)	6578(2)	6670(4)	7231(3)	13(1)
C(3)	6135(3)	3588(5)	5479(3)	20(1)
C(13)	7456(2)	7751(5)	7178(4)	21(1)
C(4)	5927(3)	2491(5)	5567(4)	24(1)
C(14)	7730(2)	6947(5)	6766(4)	26(1)
C(15)	6219(2)	8078(5)	5977(3)	17(1)
C(16)	5993(3)	9211(5)	6199(4)	26(1)
C(10)	6432(7)	135(9)	9012(12)	131(6)

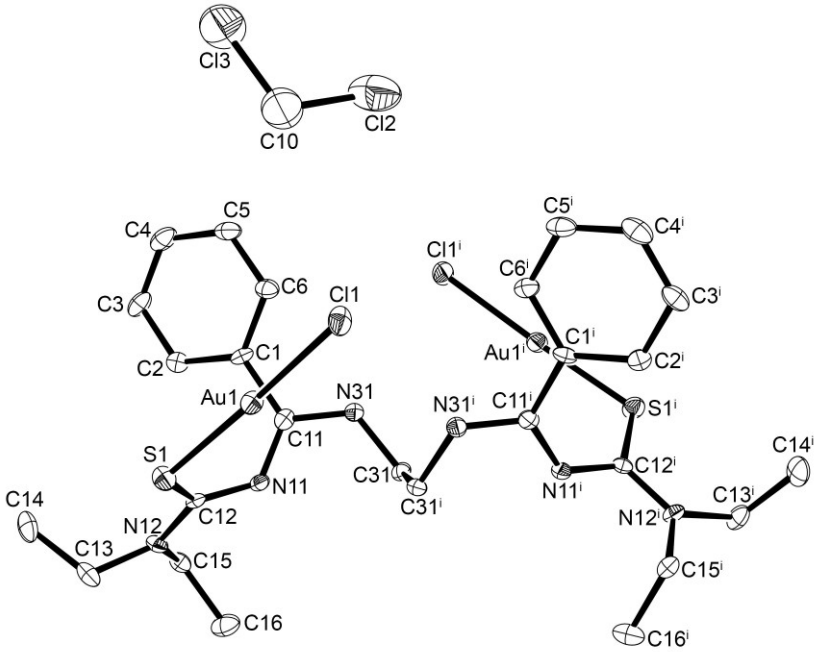

Figure A4: Ellipsoid plot of $[\{AuCl\}_2(H_2L3\text{-}\kappa S)] \cdot 2CH_2Cl_2$. Thermal ellipsoids are at 50 % of probability. The hydrogen atoms have been omitted for clarity.

[{Au(SCN)}$_2$(H$_2$L3-κS)] · 2MeOH

Table A9: Crystal data and structure refinement for [{Au(SCN)}$_2$(H$_2$L3-κS)] · 2MeOH.

Empirical formula	$C_{30}H_{44}Au_2N_8O_2S_4$	
Formula weight	1070.90	
Temperature	200(2) K	
Wavelength	0.71073 Å	
Crystal system	Triclinic	
Space group	$P\bar{1}$	
Unit cell dimensions	a = 9.620(1) Å	α = 100.60(1)°.
	b = 9.731(1) Å	β = 113.46(1)°.
	c = 11.521(1) Å	γ = 90.14(1)°.
Volume	969.0(2) Å^3	
Z	1	
Density (calculated)	1.835 g/cm^3	
Absorption coefficient	7.814 mm^{-1}	
F(000)	518	
Crystal size	0.17 x 0.09 x 0.05 mm^3	
Theta range for data collection	3.281 to 26.997°.	
Index ranges	-10<=h<=12, -12<=k<=12, -14<=l<=14	
Reflections collected	9783	
Independent reflections	4231 [R(int) = 0.0322]	
Completeness to theta = 25.242°	99.5 %	
Absorption correction	Integration	
Max. and min. transmission	0.4454 and 0.1553	
Refinement method	Full-matrix least-squares on F^2	
Data / restraints / parameters	4231 / 0 / 214	
Goodness-of-fit on F^2	0.990	
Final R indices [I>2sigma(I)]	R1 = 0.0243, wR2 = 0.0555	
R indices (all data)	R1 = 0.0292, wR2 = 0.0567	
Largest diff. peak and hole	0.573 and -1.105 e · Å^{-3}	
Diffractometer	IPDS STOE	

Table A10: Atomic coordinates (x 10^4) and equivalent isotropic displacement parameters ($Å^2$ x 10^3) for [{Au(SCN)}$_2$(H_2L3-κS)] · 2MeOH. U(eq) is defined as one third of the trace of the orthogonalized U^{ij} tensor.

	x	y	z	U(eq)
Au(1)	621(1)	3810(1)	3999(1)	36(1)
S(2)	-1691(1)	3221(2)	2282(1)	57(1)
N(21)	-752(5)	2300(6)	263(4)	80(1)
C(21)	-1090(5)	2673(5)	1108(4)	51(1)
S(1)	2955(1)	4486(1)	5621(1)	37(1)
C(12)	3579(4)	3050(3)	6327(3)	29(1)
N(12)	4789(3)	3252(3)	7444(3)	32(1)
C(13)	5425(5)	2058(4)	8049(4)	39(1)
C(14)	4799(6)	1840(5)	9022(4)	58(1)
C(15)	5627(5)	4633(4)	8112(4)	45(1)
C(16)	6880(6)	4896(5)	7685(6)	65(1)
N(11)	2844(3)	1752(3)	5878(3)	30(1)
C(11)	2476(4)	1010(3)	4721(3)	27(1)
C(1)	3206(4)	1235(3)	3832(3)	29(1)
C(2)	2358(4)	1030(4)	2507(3)	35(1)
C(3)	3056(5)	1239(4)	1706(4)	44(1)
C(4)	4589(5)	1645(4)	2212(4)	44(1)
C(5)	5435(5)	1847(4)	3522(4)	40(1)
C(6)	4756(4)	1651(3)	4342(4)	32(1)
N(31)	1473(3)	-106(3)	4319(3)	33(1)
C(31)	667(4)	-436(3)	5077(4)	33(1)
O(10)	-111(6)	2004(4)	8073(4)	86(1)
C(10)	699(7)	3224(6)	8137(7)	82(2)

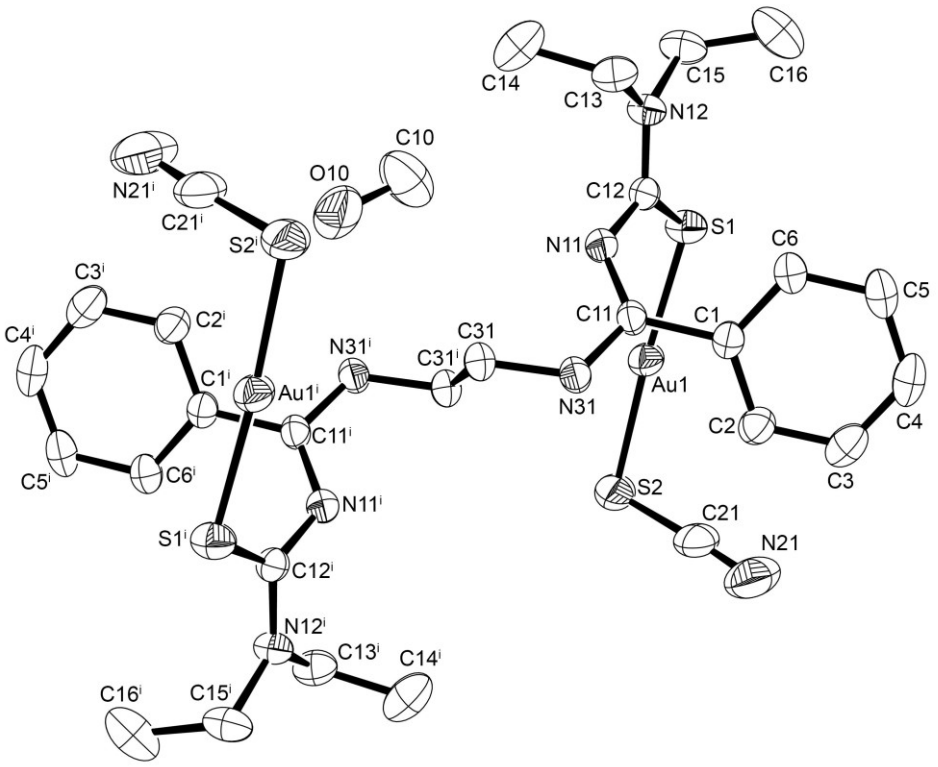

Figure A5: Ellipsoid plot of [{Au(SCN)}$_2$(H_2L3-κS)] · 2MeOH. Thermal ellipsoids are at 50 % of probability. The hydrogen atoms have been omitted for clarity.

$[\{Au(PPh_3)\}_2(H_2L3\text{-}\kappa S)](PF_6)_2$

Table A11: Crystal data and structure refinement for $[\{Au(PPh_3)\}_2(H_2L3\text{-}\kappa S)](PF_6)_2$

Empirical formula	$C_{62}H_{62}Au_2F_{12}N_6P_4S_2$	
Formula weight	1701.11	
Temperature	100(2) K	
Wavelength	0.71073 Å	
Crystal system	Monoclinic	
Space group	C2/c	
Unit cell dimensions	a = 26.198(2) Å	α = 90°.
	b = 10.5982(6) Å	β = 117.213(1)°.
	c = 25.776(1) Å	γ = 90°.
Volume	6364.5(6) $Å^3$	
Z	4	
Density (calculated)	1.775 g/cm^3	
Absorption coefficient	4.851 mm^{-1}	
F(000)	3336	
Crystal size	0.23 x 0.08 x 0.06 mm^3	
Theta range for data collection	2.489 to 27.147°.	
Index ranges	-33<=h<=32, -13<=k<=13, -29<=l<=33	
Reflections collected	43707	
Independent reflections	7036 [R(int) = 0.0290]	
Completeness to theta = 25.242°	99.6 %	
Absorption correction	Semi-empirical from equivalents	
Max. and min. transmission	0.7455 and 0.4024	
Refinement method	Full-matrix least-squares on F^2	
Data / restraints / parameters	7036 / 0 / 392	
Goodness-of-fit on F^2	1.093	
Final R indices [I>2sigma(I)]	R1 = 0.0218, wR2 = 0.0522	
R indices (all data)	R1 = 0.0233, wR2 = 0.0528	
Largest diff. peak and hole	1.195 and -1.027 e · $Å^{-3}$	
Diffractometer	Bruker D8 Venture	

Table A12: Atomic coordinates (x 10^4) and equivalent isotropic displacement parameters ($Å^2$ x 10^3) for [{Au(PPh_3)}$_2$(H_2L3-κS)](PF_6)$_2$. U(eq) is defined as one third of the trace of the orthogonalized U^{ij} tensor.

	x	y	z	U(eq)
C(1)	5364(1)	2824(2)	8870(1)	11(1)
C(2)	5941(1)	2983(3)	9005(1)	13(1)
C(3)	6194(1)	2190(3)	8761(1)	15(1)
C(4)	5881(1)	1213(3)	8395(1)	17(1)
C(5)	5313(1)	1027(3)	8275(1)	17(1)
C(6)	5053(1)	1834(3)	8505(1)	14(1)
C(11)	5076(1)	3732(2)	9093(1)	10(1)
C(12)	4190(1)	3925(2)	8236(1)	11(1)
C(13)	3221(1)	3448(3)	7462(1)	20(1)
C(14)	2894(1)	4689(3)	7322(1)	24(1)
C(15)	3499(1)	3002(3)	8516(1)	17(1)
C(16)	3708(2)	1680(3)	8745(2)	31(1)
C(31)	5174(1)	5255(3)	9852(1)	13(1)
C(41)	5796(1)	8086(3)	9125(1)	12(1)
C(42)	6214(1)	8927(3)	9499(1)	16(1)
C(43)	6069(1)	9863(3)	9783(1)	18(1)
C(44)	5504(1)	9975(3)	9691(1)	19(1)
C(45)	5088(1)	9130(3)	9328(1)	18(1)
C(46)	5234(1)	8185(3)	9047(1)	14(1)
C(51)	6230(1)	7834(2)	8283(1)	10(1)
C(52)	6783(1)	8343(3)	8546(1)	14(1)
C(53)	6973(1)	9094(3)	8227(1)	17(1)
C(54)	6617(1)	9328(3)	7641(1)	19(1)
C(56)	5874(1)	8077(3)	7693(1)	13(1)
C(61)	6571(1)	6038(3)	9217(1)	12(1)
C(62)	6685(1)	5885(3)	9797(1)	16(1)
C(63)	7117(1)	5063(3)	10155(1)	23(1)
C(64)	7436(1)	4409(3)	9940(2)	26(1)
C(65)	7329(1)	4565(3)	9366(2)	23(1)
C(66)	6896(1)	5370(3)	9003(1)	17(1)
Au(1)	5186(1)	5681(1)	8190(1)	9(1)
F(1)	6592(1)	4292(2)	11071(1)	53(1)

F(2)	6413(1)	2720(2)	10439(1)	45(1)
F(3)	5968(1)	2795(3)	11017(2)	62(1)
F(4)	6836(1)	2842(3)	11811(1)	52(1)
F(5)	7263(1)	2808(2)	11230(1)	39(1)
F(6)	6628(1)	1298(2)	11162(1)	39(1)
N(11)	4532(1)	4036(2)	8812(1)	10(1)
N(12)	3673(1)	3428(2)	8073(1)	14(1)
N(31)	5390(1)	4249(2)	9620(1)	11(1)
P(1)	5959(1)	6931(1)	8703(1)	9(1)
P(2)	6608(1)	2797(1)	11122(1)	17(1)
S(1)	4360(1)	4485(1)	7697(1)	14(1)
C(55)	6069(1)	8812(3)	7374(1)	17(1)

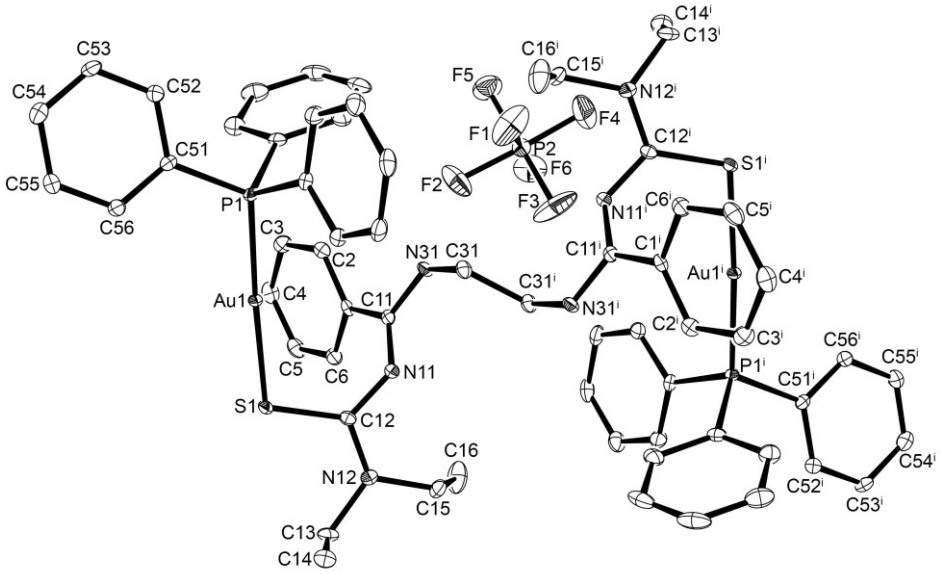

Figure A6: Ellipsoid plot of $[\{Au(PPh_3)\}_2(H_2L3\text{-}\kappa S)](PF_6)_2$. Thermal ellipsoids are at 50 % of probability. The hydrogen atoms have been omitted for clarity.

[{AuCl}$_2$(H$_2$L4-κS)]

Table A13: Crystal data and structure refinement for [{AuCl}$_2$(H$_2$L4-κS)].

Empirical formula	$C_{17}H_{25}Au_2Cl_2N_5O_2S_2$	
Formula weight	860.37	
Temperature	99(2) K	
Wavelength	0.71073 Å	
Crystal system	Monoclinic	
Space group	$P2_1/c$	
Unit cell dimensions	a = 7.840(1) Å	α = 90°.
	b = 21.273(3) Å	β = 99.02(1)°.
	c = 15.049(3) Å	γ = 90°.
Volume	2478.8(7) Å^3	
Z	4	
Density (calculated)	2.305 g/cm^3	
Absorption coefficient	12.231 mm^{-1}	
F(000)	1608	
Crystal size	0.18 x 0.06 x 0.05 mm^3	
Theta range for data collection	2.355 to 28.657°.	
Index ranges	-10<=h<=9, -28<=k<=28, -20<=l<=20	
Reflections collected	85691	
Independent reflections	6281 [R(int) = 0.0886]	
Completeness to theta = 25.242°	100.0 %	
Absorption correction	Semi-empirical from equivalents	
Max. and min. transmission	0.7457 and 0.5613	
Refinement method	Full-matrix least-squares on F^2	
Data / restraints / parameters	6281 / 0 / 274	
Goodness-of-fit on F^2	1.043	
Final R indices [I>2sigma(I)]	R1 = 0.0318, wR2 = 0.0348	
R indices (all data)	R1 = 0.0603, wR2 = 0.0381	
Largest diff. peak and hole	0.837 and -1.201 e · Å^{-3}	
Diffractometer	Bruker D8 Venture	

Table A14: Atomic coordinates (x 10^4) and equivalent isotropic displacement parameters ($Å^2$x 10^3) for [{AuCl}$_2$(H_2L4-κS)]. U(eq) is defined as one third of the trace of the orthogonalized U^{ij} tensor.

	x	y	z	U(eq)
C(101)	6245(5)	382(2)	4263(3)	11(1)
C(102)	6354(5)	858(2)	4902(3)	14(1)
C(103)	7412(5)	767(2)	5718(3)	13(1)
C(104)	8290(5)	201(2)	5875(3)	12(1)
C(105)	8055(5)	-252(2)	5203(3)	10(1)
C(11)	5161(5)	493(2)	3364(3)	12(1)
C(12)	4646(5)	84(2)	1819(3)	14(1)
C(13)	5311(6)	1192(2)	1544(3)	19(1)
C(14)	6980(6)	1204(2)	1169(4)	36(1)
C(15)	3127(5)	585(2)	480(3)	20(1)
C(16)	1315(6)	701(2)	681(3)	26(1)
C(21)	8946(5)	-874(2)	5393(3)	11(1)
C(22)	9032(5)	-1935(2)	4782(3)	13(1)
C(25)	10436(5)	-2841(2)	5565(3)	19(1)
C(26)	12314(6)	-2653(2)	5791(3)	29(1)
Au(1)	4509(1)	-1346(1)	2564(1)	14(1)
Au(2)	9084(1)	-1382(1)	2807(1)	14(1)
Cl(1)	4840(1)	-2124(1)	3625(1)	19(1)
Cl(2)	8778(1)	-575(1)	1800(1)	20(1)
N(1)	7073(4)	-170(2)	4399(2)	10(1)
N(11)	5632(4)	134(2)	2682(2)	12(1)
N(12)	4384(4)	592(2)	1330(2)	15(1)
N(21)	8239(4)	-1350(2)	4828(2)	11(1)
N(22)	9314(4)	-2278(2)	5516(2)	12(1)
O(11)	3990(3)	875(1)	3255(2)	17(1)
O(21)	10142(3)	-946(1)	6000(2)	15(1)
S(1)	3842(1)	-633(1)	1445(1)	18(1)
S(2)	9626(1)	-2192(1)	3793(1)	18(1)
C(23)	8460(5)	-2164(2)	6313(3)	18(1)
C(24)	6770(6)	-2523(2)	6227(3)	28(1)

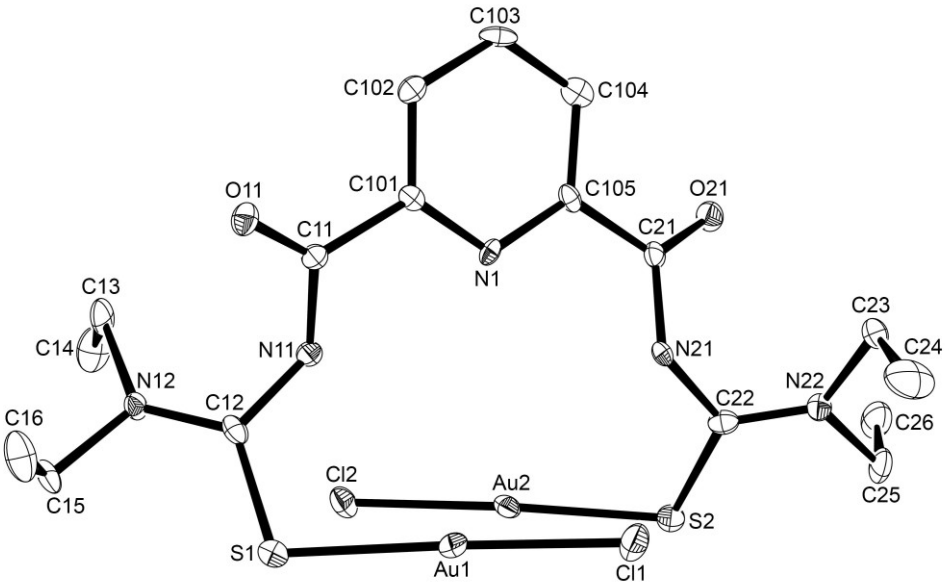

Figure A7: Ellipsoid plot of [{AuCl}$_2$(H_2L4-κS)]. Thermal ellipsoids are at 50 % of probability. The hydrogen atoms have been omitted for clarity.

[{Au(PPh$_3$)}$_2$(L4-κS)]

Table A15: Crystal data and structure refinement for [{Au(PPh$_3$)}$_2$(L4-κS)].

Empirical formula	$C_{53}H_{53}Au_2N_5O_2P_2S_2$	
Formula weight	1311.99	
Temperature	200(2) K	
Wavelength	0.71073 Å	
Crystal system	Monoclinic	
Space group	$P2_1/n$	
Unit cell dimensions	a = 9.0940(6) Å	α = 90°.
	b = 21.766(1) Å	β = 104.760(5)°.
	c = 13.1519(9) Å	γ = 90°.
Volume	2517.4(3) Å^3	
Z	2	
Density (calculated)	1.731 g/cm^3	
Absorption coefficient	6.013 mm^{-1}	
F(000)	1284	
Crystal size	0.26 x 0.18 x 0.18 mm^3	
Theta range for data collection	3.338 to 25.999°.	
Index ranges	-11<=h<=11, -26<=k<=26, -16<=l<=12	
Reflections collected	14876	
Independent reflections	4927 [R(int) = 0.0338]	
Completeness to theta = 25.242°	99.7 %	
Absorption correction	Integration	
Max. and min. transmission	0.3653 and 0.1827	
Refinement method	Full-matrix least-squares on F^2	
Data / restraints / parameters	4927 / 340 / 344	
Goodness-of-fit on F^2	1.321	
Final R indices [I>2sigma(I)]	R1 = 0.0679, wR2 = 0.1473	
R indices (all data)	R1 = 0.0751, wR2 = 0.1497	
Largest diff. peak and hole	2.524 and -1.874 e · Å^{-3}	
Diffractometer	IPDS STOE	

Table A16: Atomic coordinates (x 10^4) and equivalent isotropic displacement parameters ($Å^2$ x 10^3) for [{Au(PPh_3)}$_2$(L4-κS)]. U(eq) is defined as one third of the trace of the orthogonalized U^{ij} tensor.

	x	y	z	U(eq)
N(11)	4310(30)	10119(11)	2184(16)	46(3)
N(21)	6630(30)	9928(11)	7702(16)	46(3)
C(21)	5960(30)	10055(19)	6858(15)	40(3)
C(11)	4420(30)	9928(19)	3072(15)	40(3)
O(2)	4223(19)	10249(9)	6853(13)	50(3)
O(1)	2655(19)	9838(9)	3122(13)	50(3)
N(1)	4947(13)	10003(10)	4967(11)	35(3)
C(1)	5318(14)	9947(8)	4009(9)	34(4)
C(2)	6829(16)	9882(6)	3984(8)	34(4)
C(3)	7969(13)	9874(6)	4917(10)	26(3)
C(4)	7599(15)	9930(7)	5874(8)	43(5)
C(5)	6088(16)	9995(9)	5900(9)	36(4)
C(51)	8395(14)	8112(6)	3606(9)	39(2)
C(52)	9451(14)	7829(6)	4439(10)	47(3)
C(53)	10992(16)	7986(7)	4635(12)	60(3)
C(54)	11433(18)	8423(7)	4037(13)	64(4)
C(55)	10436(17)	8732(7)	3237(13)	62(3)
C(56)	8894(16)	8560(7)	3026(11)	52(3)
C(31)	6000(13)	7820(5)	4565(9)	38(2)
C(32)	5674(15)	8330(6)	5101(10)	47(3)
C(33)	5431(17)	8274(7)	6094(11)	55(3)
C(34)	5462(16)	7712(7)	6539(11)	51(3)
C(35)	5745(18)	7199(7)	6030(11)	58(4)
C(36)	6039(14)	7250(6)	5049(10)	43(3)
C(42)	6255(13)	7157(5)	2725(9)	36(2)
C(43)	4783(15)	6956(6)	2172(11)	47(3)
C(44)	4604(16)	6376(7)	1735(12)	57(3)
C(45)	5845(15)	6001(6)	1778(11)	47(3)
C(46)	7276(15)	6194(6)	2302(10)	45(3)
C(47)	7463(14)	6771(5)	2776(10)	41(3)
Au(1)	4856(1)	8581(1)	2215(1)	42(1)
P(1)	6416(3)	7914(1)	3305(2)	34(1)

S(1)	3209(4)	9139(2)	933(3)	51(1)
C(12A)	3469(19)	9908(6)	1262(10)	58(3)
N(12A)	3390(20)	10304(7)	447(11)	47(4)
C(13A)	2860(30)	10134(17)	-678(15)	54(5)
C(14A)	1180(30)	10156(14)	-1110(20)	64(7)
C(15A)	3660(20)	10966(8)	666(15)	50(4)
C(16A)	2390(30)	11270(13)	990(30)	89(8)
C(12B)	3469(19)	9908(6)	1262(10)	58(3)
N(12B)	2590(40)	10287(12)	530(20)	50(6)
C(13B)	2390(50)	10160(30)	-600(20)	54(5)
C(14B)	800(60)	9940(30)	-1040(50)	64(7)
C(15B)	2160(40)	10912(13)	800(30)	50(4)
C(16B)	3350(60)	11390(20)	830(50)	89(8)

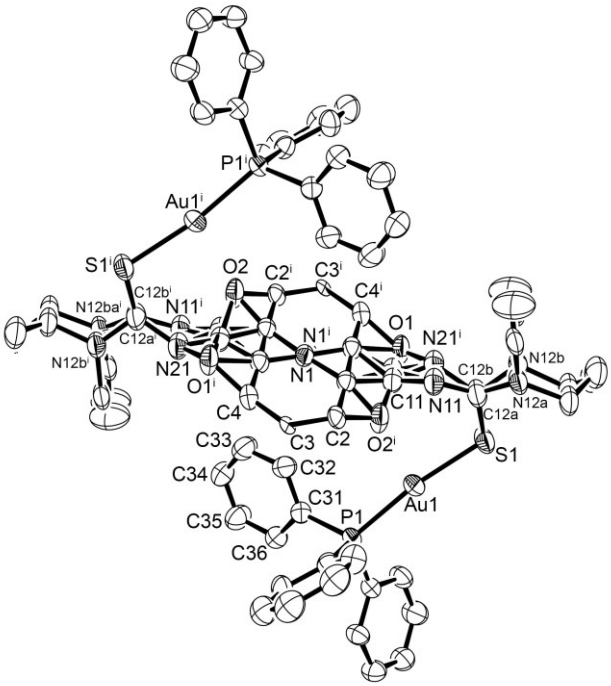

Figure A8: Ellipsoid plot of [{Au(PPh_3)}$_2$(L4-κS)]. Thermal ellipsoids are at 50 % of probability. The hydrogen atoms have been omitted for clarity.

[{$Ca_2(MeOH)_3(H_2O)$}{Au(L4-κS)}$_4$] · 0.5CH_2Cl_2 · 2MeOH

Table A17: Crystal data and structure refinement for [{$Ca_2(MeOH)_3(H_2O)$}{Au(L4-κS)}$_4$] · 0.5CH_2Cl_2 · 2MeOH.

Empirical formula	$C_{73.5}H_{115}Au_4Ca_2ClN_{20}O_{14}S_8$	
Formula weight	2662.80	
Temperature	99(2) K	
Wavelength	0.71073 Å	
Crystal system	Monoclinic	
Space group	Cc	
Unit cell dimensions	a = 34.634(5) Å	α = 90°.
	b = 14.663(2) Å	β = 128.923(3)°.
	c = 26.174(6) Å	γ = 90°.
Volume	10341(3) Å^3	
Z	4	
Density (calculated)	1.710 g/cm^3	
Absorption coefficient	6.006 mm^{-1}	
F(000)	5236	
Crystal size	0.32 x 0.07 x 0.07 mm^3	
Theta range for data collection	2.285 to 27.967°.	
Index ranges	-45<=h<=45, -19<=k<=19, -34<=l<=33	
Reflections collected	116409	
Independent reflections	23397 [R(int) = 0.0279]	
Completeness to theta = 25.242°	99.9 %	
Absorption correction	Semi-empirical from equivalents	
Max. and min. transmission	0.7456 and 0.5142	
Refinement method	Full-matrix least-squares on F^2	
Data / restraints / parameters	23397 / 55 / 1102	
Goodness-of-fit on F^2	1.037	
Final R indices [I>2sigma(I)]	R1 = 0.0251, wR2 = 0.0608	
R indices (all data)	R1 = 0.0272, wR2 = 0.0619	
Absolute structure parameter	0.189(4)	
Largest diff. peak and hole	1.841 and -1.451 e · Å^{-3}	
Diffractometer	Bruker D8 Venture	

Table A18: Atomic coordinates (x 10^4) and equivalent isotropic displacement parameters ($Å^2$ x 10^3) for $[\{Ca_2(MeOH)_3(H_2O)\}\{Au(L4\text{-}\kappa S)\}_4] \cdot 0.5CH_2Cl_2 \cdot 2MeOH$. U(eq) is defined as one third of the trace of the orthogonalized U^{ij} tensor.

	x	y	z	U(eq)
C(105)	1639(2)	6470(4)	4952(3)	17(1)
C(201)	-284(2)	6388(4)	2504(3)	17(1)
C(405)	3225(2)	6326(5)	3630(3)	26(1)
C(305)	1753(2)	7194(4)	1256(3)	21(1)
C(104)	1762(2)	6280(5)	5568(3)	24(1)
C(202)	-781(2)	6230(5)	1986(3)	25(1)
C(404)	3737(3)	6334(6)	4124(4)	35(2)
C(304)	1608(3)	7016(5)	639(4)	30(2)
C(103)	1551(3)	6814(5)	5767(4)	30(2)
C(203)	-1002(3)	6694(5)	1408(4)	28(2)
C(403)	3946(3)	6977(7)	4618(4)	40(2)
C(303)	1298(3)	6285(6)	289(4)	32(2)
C(102)	1230(3)	7509(5)	5368(4)	26(1)
C(204)	-723(2)	7313(5)	1355(3)	24(1)
C(402)	3648(3)	7585(6)	4622(4)	33(2)
C(302)	1126(2)	5773(5)	554(3)	25(1)
C(101)	1122(2)	7648(4)	4760(3)	20(1)
C(205)	-223(2)	7415(4)	1888(3)	17(1)
C(401)	3139(3)	7527(5)	4124(3)	27(1)
C(301)	1276(2)	6019(4)	1164(3)	20(1)
C(10)	2165(5)	4920(7)	3485(5)	59(3)
C(11)	743(2)	8328(4)	4262(3)	20(1)
C(12)	184(2)	9394(4)	4150(3)	21(1)
C(13A)	687(4)	10793(7)	4664(7)	28(3)
C(14A)	876(5)	10971(8)	4288(7)	38(2)
C(13B)	626(8)	10769(14)	4300(13)	24(4)
C(14B)	940(11)	11018(16)	5020(15)	38(2)
C(15)	-255(3)	10855(5)	3952(5)	39(2)
C(16)	-531(4)	11146(6)	3260(5)	48(2)
C(21)	1860(2)	5959(4)	4699(3)	19(1)
C(22)	2578(2)	5022(5)	5164(4)	23(1)
C(23)	2284(3)	3543(5)	5163(4)	33(2)

C(24)	1845(3)	3378(5)	4452(4)	37(2)
C(25)	3132(4)	3707(6)	5472(6)	58(3)
C(30)	824(4)	4920(5)	2826(4)	39(2)
C(71)	124(2)	7994(4)	1864(3)	16(1)
C(72)	106(2)	8860(4)	1094(3)	19(1)
C(73)	189(4)	10141(5)	560(4)	41(2)
C(74)	722(4)	10473(6)	980(6)	59(3)
C(75)	-165(4)	10367(5)	1137(5)	40(2)
C(76)	-718(4)	10449(7)	616(6)	58(3)
C(40)	1393(4)	9156(7)	3547(6)	63(3)
C(51)	-1(2)	5957(4)	3171(3)	18(1)
C(52)	-176(2)	5196(4)	3802(3)	20(1)
C(53)	-221(3)	3974(5)	4410(4)	37(2)
C(54)	-732(3)	4013(8)	4213(4)	60(3)
C(55)	-322(3)	3654(5)	3384(4)	35(2)
C(56)	159(4)	3355(6)	3533(5)	52(2)
C(61)	2783(3)	8113(5)	4110(3)	29(2)
C(62)	2799(3)	9196(5)	4807(4)	47(2)
C(63)	2779(4)	10624(6)	5315(6)	62(1)
C(64)	2249(5)	10950(8)	4932(8)	81(2)
C(65)	3020(4)	10611(6)	4577(6)	62(1)
C(66)	3564(5)	10648(8)	5051(8)	81(2)
C(81)	2965(3)	5703(5)	3049(4)	28(1)
C(82)	3117(3)	4725(5)	2492(4)	36(2)
C(83)	3317(4)	3340(6)	3107(6)	57(2)
C(84)	2903(5)	3094(8)	3116(7)	70(2)
C(85)	3044(4)	3244(6)	1979(6)	57(2)
C(86)	3501(5)	3029(8)	2056(7)	70(2)
C(31)	1088(2)	5552(4)	1484(3)	20(1)
C(32)	407(3)	4597(5)	1137(3)	22(1)
C(33)	-60(5)	3243(6)	1038(6)	62(1)
C(34)	-460(5)	2951(9)	326(8)	81(2)
C(35)	710(5)	3085(6)	1162(7)	62(1)
C(36)	1183(5)	2978(8)	1864(8)	81(2)
C(41)	2141(2)	7902(5)	1710(4)	23(1)
C(42)	2707(3)	8884(5)	1781(4)	28(2)
C(43)	3169(3)	10283(6)	1966(5)	45(2)

C(44)	3421(4)	10644(7)	2634(5)	58(3)
Au(1)	-198(1)	7379(1)	4017(1)	23(1)
Au(3)	175(1)	6718(1)	967(1)	18(1)
Au(2)	2773(1)	7162(1)	5164(1)	27(1)
Au(4)	3080(1)	6788(1)	2033(1)	29(1)
Ca(1)	903(1)	7061(1)	3363(1)	16(1)
Ca(2)	2025(1)	6859(1)	2722(1)	21(1)
N(1)	1321(2)	7135(3)	4557(3)	17(1)
N(2)	-6(2)	6965(3)	2446(2)	15(1)
N(4)	2936(2)	6909(4)	3636(3)	22(1)
N(3)	1588(2)	6715(3)	1517(3)	20(1)
N(11)	616(2)	8949(4)	4510(3)	25(1)
N(12)	198(2)	10312(4)	4213(4)	38(2)
N(21)	2198(2)	5358(4)	5110(3)	24(1)
N(22)	2662(2)	4129(4)	5252(3)	30(1)
N(71)	-98(2)	8542(4)	1346(3)	19(1)
N(72)	48(2)	9749(4)	935(3)	29(1)
N(51)	-291(2)	5462(4)	3236(3)	22(1)
N(52)	-218(2)	4314(4)	3886(3)	26(1)
N(61)	2983(3)	8790(4)	4553(3)	41(2)
N(62)	2859(4)	10111(5)	4887(5)	65(2)
N(81)	3257(2)	5165(4)	3027(3)	36(1)
N(82)	3150(3)	3807(5)	2513(4)	48(2)
N(31)	764(2)	4898(4)	1129(3)	23(1)
N(32)	355(2)	3682(4)	1139(4)	32(1)
N(41)	2271(2)	8448(4)	1440(3)	30(1)
N(42)	2710(2)	9768(5)	1699(4)	36(2)
O(21)	1693(2)	6135(3)	4118(2)	21(1)
O(71)	577(2)	7928(3)	2330(2)	21(1)
O(51)	455(2)	6053(3)	3574(2)	20(1)
O(61)	2327(2)	7957(3)	3680(2)	31(1)
O(81)	2496(2)	5741(3)	2640(3)	29(1)
O(31)	1254(2)	5810(3)	2046(2)	23(1)
O(41)	2292(2)	7926(3)	2286(2)	26(1)
O(10)	2063(2)	5857(3)	3473(2)	27(1)
O(11)	597(2)	8279(3)	3688(2)	22(1)
O(20)	1403(2)	7989(4)	2371(2)	28(1)
O(30)	889(2)	5852(3)	2730(2)	23(1)

O(40)	1498(2)	8188(3)	3592(2)	27(1)
S(1)	-387(1)	8864(1)	3692(1)	30(1)
S(2)	3019(1)	5705(1)	5218(1)	31(1)
S(7)	368(1)	8154(1)	840(1)	20(1)
S(5)	-23(1)	5936(1)	4427(1)	27(1)
S(6)	2557(1)	8645(1)	5131(1)	42(1)
S(8)	2933(1)	5271(1)	1778(1)	40(1)
S(3)	-31(1)	5284(1)	1068(1)	23(1)
S(4)	3272(1)	8303(1)	2257(1)	34(1)
O(60)	61(2)	9640(4)	2726(3)	49(2)
C(60)	-472(4)	9483(7)	2234(5)	50(2)
O(70)	248(4)	1422(7)	2664(5)	33(2)
C(70)	711(6)	1595(14)	2828(9)	44(3)
O(80)	-646(4)	12192(7)	1540(5)	33(2)
C(80)	-826(6)	12840(13)	1694(9)	44(3)
Cl(1)	2779(4)	9856(8)	3137(5)	117(3)
Cl(2)	1905(4)	10830(6)	2820(5)	132(4)
C(1)	2173(10)	9772(16)	2879(15)	78(7)
C(26)	3122(5)	3282(8)	4975(8)	82(4)
C(45A)	2267(15)	10320(40)	1450(20)	49(11)
C(46A)	1937(8)	10381(19)	712(14)	72(5)
C(45B)	2239(12)	10270(30)	1254(19)	49(11)
C(46B)	2065(7)	10549(15)	1638(12)	72(5)

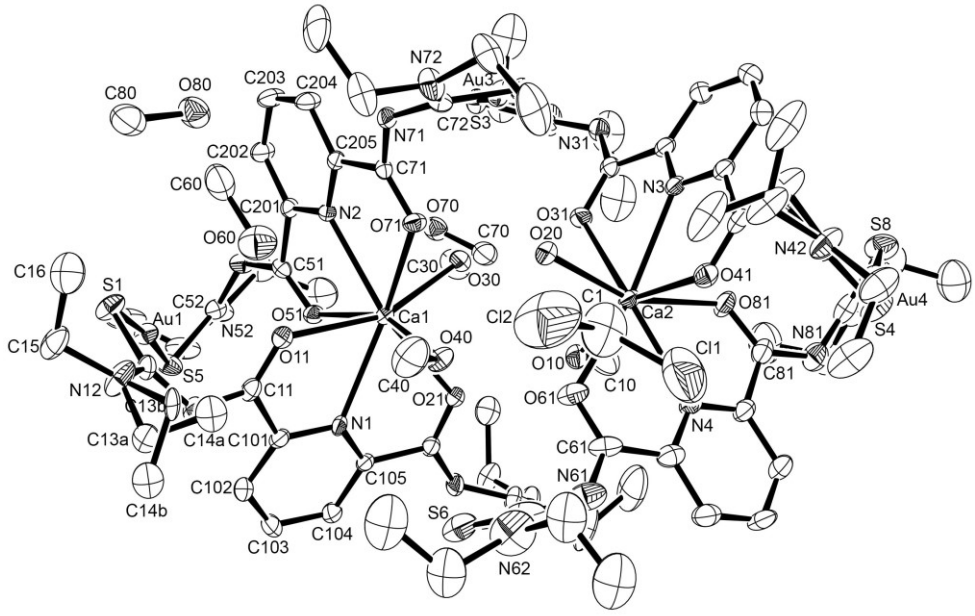

Figure A9: Ellipsoid plot of $[\{Ca_2(MeOH)_3(H_2O)\}\{Au(L4\text{-}\kappa S)\}_4] \cdot 0.5CH_2Cl_2 \cdot 2MeOH$. Thermal ellipsoids are at 50 % of probability. The hydrogen atoms have been omitted for clarity.

[{$Sr_2(MeOH)_2(H_2O)_2$}{Au(L4-κS)}$_4$] · MeOH · 1.5H_2O

Table A19: Crystal data and structure refinement for [{$Sr_2(MeOH)_2(H_2O)_2$}{Au(L4-κS)}$_4$] · MeOH · 1.5H_2O.

Empirical formula	$C_{71}H_{109}Au_4N_{20}O_{14.5}S_8Sr_2$	
Formula weight	2694.36	
Temperature	111(2) K	
Wavelength	0.71073 Å	
Crystal system	Monoclinic	
Space group	Cc	
Unit cell dimensions	a = 35.077(3) Å	α = 90°.
	b = 14.640(1) Å	β = 128.863(2)°.
	c = 26.354(2) Å	γ = 90°.
Volume	10538 (1) $Å^3$	
Z	4	
Density (calculated)	1.698 g/cm^3	
Absorption coefficient	6.772 mm^{-1}	
F(000)	5244	
Crystal size	0.29 x 0.21 x 0.12 mm^3	
Theta range for data collection	2.267 to 27.935°.	
Index ranges	-46<=h<=46, -19<=k<=19, -34<=l<=34	
Reflections collected	277277	
Independent reflections	25243 [R(int) = 0.0831]	
Completeness to theta = 25.242°	99.9 %	
Absorption correction	Semi-empirical from equivalents	
Max. and min. transmission	0.7456 and 0.4101	
Refinement method	Full-matrix least-squares on F^2	
Data / restraints / parameters	25243 / 177 / 926	
Goodness-of-fit on F^2	1.113	
Final R indices [I>2sigma(I)]	R1 = 0.0418, wR2 = 0.0988	
R indices (all data)	R1 = 0.0467, wR2 = 0.1013	
Absolute structure parameter	0.629(8)*	
Largest diff. peak and hole	1.661 and -2.244 e · $Å^{-3}$	
Diffractometer	Bruker D8 Venture	

* There was no centrosymmetric space group found.

Table A20: Atomic coordinates (x 10^4) and equivalent isotropic displacement parameters ($Å^2$ x 10^3) for $[\{Sr_2(MeOH)_2(H_2O)_2\}\{Au(L4\text{-}\kappa S)\}_4] \cdot MeOH \cdot 1.5H_2O$. U(eq) is defined as one third of the trace of the orthogonalized U^{ij} tensor.

	x	y	z	U(eq)
S(1)	9459(1)	9115(2)	4962(2)	34(1)
O(21)	10071(3)	7018(6)	2883(4)	21(2)
N(1)	9493(3)	7994(7)	3008(5)	18(2)
N(2)	10873(4)	7905(6)	5209(5)	19(2)
O(11)	9931(3)	8966(5)	4109(4)	23(2)
O(31)	11234(3)	8921(6)	4757(4)	22(2)
O(51)	10164(4)	6701(6)	4372(4)	30(2)
N(31)	11748(4)	9676(7)	5749(5)	23(2)
C(11)	9477(4)	9015(7)	3709(5)	20(2)
N(51)	10178(4)	6112(7)	5196(5)	27(2)
C(201)	11187(4)	8585(8)	5598(5)	19(2)
C(31)	11400(4)	9081(8)	5335(5)	18(2)
N(11)	9185(4)	9500(7)	3763(4)	23(2)
N(32)	12185(4)	10906(8)	5842(5)	32(2)
C(205)	10677(4)	7395(8)	5420(5)	22(2)
C(32)	12118(4)	10011(8)	5784(6)	22(2)
C(101)	9212(4)	8544(8)	3065(5)	19(2)
C(105)	9272(4)	7515(8)	2452(5)	21(2)
C(51)	10307(5)	6698(8)	4949(6)	27(3)
C(12)	9305(4)	9801(8)	4324(5)	21(2)
C(102)	8712(4)	8661(10)	2560(6)	34(3)
C(202)	11304(4)	8797(9)	6199(5)	28(3)
C(104)	8781(4)	7569(10)	1937(6)	31(3)
C(204)	10787(4)	7571(9)	6023(6)	24(2)
N(12)	9268(4)	10693(7)	4378(5)	35(2)
C(13)	9297(7)	11101(12)	4913(9)	53(1)
S(6)	9463(1)	9608(2)	1585(2)	26(1)
S(2)	9885(1)	6715(2)	1445(1)	24(1)
S(4)	12774(1)	6670(3)	2822(2)	39(1)
S(8)	12498(2)	9730(3)	2427(2)	53(1)
N(3)	12481(3)	8070(7)	4261(4)	21(2)
N(21)	9400(3)	6377(7)	1922(5)	25(2)

C(21)	9623(4)	6948(7)	2425(5)	17(2)
N(4)	11081(4)	8246(7)	2034(5)	20(2)
O(61)	10741(3)	9165(6)	2555(4)	23(2)
N(72)	12378(6)	4884(9)	5507(8)	53(3)
O(81)	12062(3)	9247(6)	3267(4)	32(2)
C(71)	12321(5)	6863(8)	4735(6)	29(3)
O(41)	11786(3)	7023(7)	2798(4)	31(2)
C(63)	10169(7)	11834(12)	1633(9)	53(1)
O(71)	11865(3)	7002(7)	4295(4)	35(2)
C(53)	9285(7)	4165(11)	4636(10)	53(1)
N(61)	10233(4)	10006(7)	1607(5)	26(2)
C(72)	12331(6)	5805(10)	5434(9)	43(2)
N(62)	9834(4)	11206(8)	1632(6)	35(3)
C(22)	9613(4)	6047(9)	1689(5)	26(2)
C(42)	12210(4)	6123(9)	2311(6)	30(3)
C(61)	10562(4)	9375(8)	1982(5)	18(2)
C(305)	12768(4)	8644(8)	4256(5)	23(2)
C(52)	9743(5)	5631(9)	4819(7)	33(3)
C(62)	9888(4)	10303(8)	1634(5)	22(2)
C(405)	10767(4)	8933(8)	1688(5)	20(2)
C(81)	12523(4)	9273(9)	3682(6)	30(3)
C(25)	9317(7)	4556(11)	1712(9)	53(1)
N(71)	12521(4)	6218(8)	5190(5)	36(2)
N(52)	9767(5)	4725(8)	4897(7)	49(3)
C(401)	11260(4)	7776(8)	1782(5)	21(2)
N(42)	12207(4)	5228(10)	2210(6)	42(3)
C(304)	13265(4)	8652(9)	4752(6)	30(3)
N(81)	12822(4)	9793(8)	3678(6)	41(3)
N(22)	9552(4)	5136(7)	1533(6)	33(2)
C(41)	11642(4)	7076(9)	2233(6)	27(3)
C(203)	11106(5)	8298(11)	6416(6)	34(3)
C(74)	11747(8)	4042(15)	5497(11)	70(1)
C(43)	12670(7)	4699(12)	2507(9)	53(1)
C(403)	10799(5)	8694(8)	822(6)	29(3)
C(404)	10613(4)	9175(9)	1074(6)	26(2)
N(41)	11783(4)	6556(9)	1962(6)	39(3)
C(402)	11103(5)	7949(8)	1159(6)	26(2)

C(303)	13472(5)	8028(9)	5245(7)	32(3)
C(73)	12288(7)	4385(11)	5907(9)	53(1)
C(64)	10629(8)	12010(15)	2327(11)	70(1)
C(301)	12677(4)	7475(8)	4752(5)	22(2)
C(24)	10197(8)	4401(15)	1572(11)	70(1)
C(15)	9165(7)	11322(11)	3865(9)	53(1)
C(23)	9695(7)	4731(12)	1163(9)	53(1)
C(33)	11818(7)	11482(12)	5757(9)	53(1)
C(302)	13174(5)	7417(10)	5252(5)	32(3)
C(65)	9434(7)	11640(11)	1549(9)	53(1)
C(82)	12690(5)	10242(10)	3139(8)	43(2)
C(55)	10259(7)	4245(11)	5332(9)	53(1)
C(34)	11378(8)	11651(15)	5048(11)	70(1)
C(45)	11746(7)	4706(11)	1811(9)	53(1)
C(35)	12644(7)	11313(11)	6037(9)	53(1)
N(82)	12759(7)	11151(10)	3204(9)	68(4)
C(26)	8771(8)	4491(15)	1171(11)	70(1)
C(44)	12890(8)	4385(15)	3150(11)	70(1)
C(46)	11551(8)	4487(15)	2148(11)	70(1)
C(66)	9016(8)	11936(15)	859(11)	70(1)
C(54)	9075(8)	3885(15)	4001(11)	70(1)
C(36)	12611(8)	11706(15)	5542(11)	70(1)
C(83)	12579(7)	11738(11)	2571(10)	53(1)
C(16)	9641(8)	11608(15)	4008(11)	70(1)
C(85)	12932(7)	11615(11)	3798(9)	53(1)
C(84)	13018(8)	11910(15)	2654(11)	70(1)
C(56)	10435(8)	4077(15)	4962(11)	70(1)
C(14)	8803(8)	11156(15)	4750(11)	70(1)
C(86)	12509(8)	11873(15)	3778(11)	70(1)
O(40)	10415(3)	9223(6)	3278(4)	25(2)
O(10)	11573(3)	9217(6)	4075(4)	30(2)
O(20)	10909(3)	6846(7)	2976(5)	40(2)
O(30)	11042(4)	6680(8)	4186(5)	45(3)
C(40)	10329(7)	10119(11)	3350(8)	47(4)
C(10)	11658(10)	10129(14)	4054(11)	79(7)
C(75)	12522(6)	4386(11)	5169(9)	53(1)
C(76)	13037(8)	4349(15)	5620(11)	70(1)
O(50)	9590(6)	5406(10)	3384(8)	24(3)

C(50)	9079(9)	5560(20)	2910(13)	37(6)
O(60)	12304(8)	5320(20)	3717(11)	61(7)
O(70)	9779(8)	3614(16)	3299(13)	60(6)
C(70)	10189(12)	3300(30)	3380(19)	72(11)
O(80)	11471(9)	4111(18)	3448(16)	76(9)
O(90)	8958(14)	2843(16)	2242(17)	89(10)
Au(2)	9687(1)	8175(1)	1530(1)	21(1)
Au(1)	9335(1)	7651(1)	4607(1)	28(1)
Au(3)	12286(1)	7855(1)	5755(1)	27(1)
Au(4)	12612(1)	8194(1)	2641(1)	36(1)
Sr(2)	11526(1)	8106(1)	3297(1)	22(1)
Sr(1)	10442(1)	7941(1)	3954(1)	16(1)
S(7)	12075(1)	6373(2)	5727(2)	40(1)
S(5)	9182(1)	6153(2)	4326(2)	43(1)
C(103)	8499(5)	8201(9)	1983(7)	33(3)
S(3)	12534(1)	9318(2)	5806(2)	29(1)

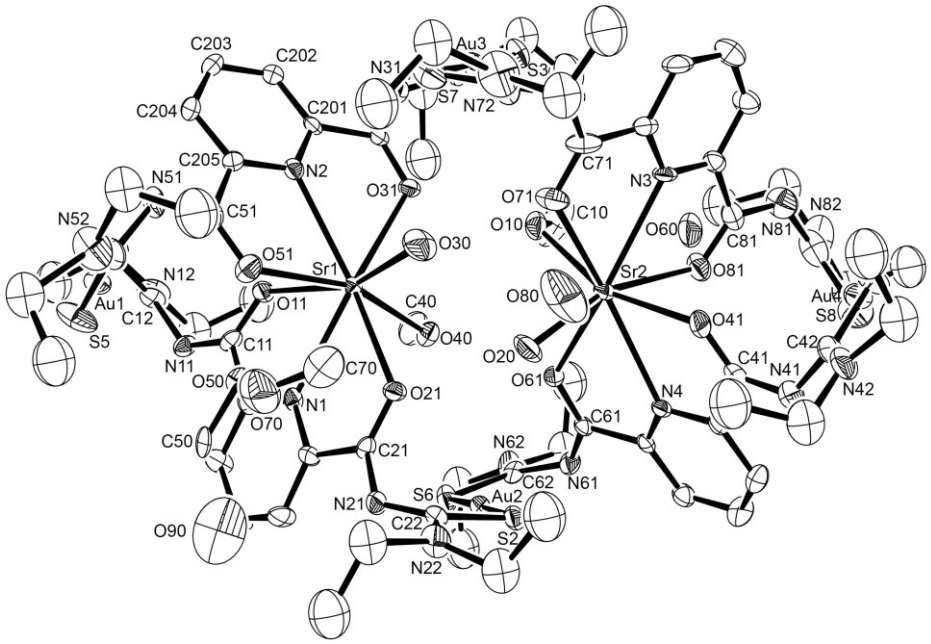

Figure A10: Ellipsoid plot of $[\{Sr_2(MeOH)_2(H_2O)_2\}\{Au(L4\text{-}\kappa S)\}_4] \cdot MeOH \cdot 1.5H_2O$. Thermal ellipsoids are at 50 % of probability. The hydrogen atoms have been omitted for clarity.

[{Ba$_2$(μ-OH$_2$)}{Au(L4-κS)}$_4$] · CH$_2$Cl$_2$ · 6MeOH

Table A21: Crystal data and structure refinement for [{Ba$_2$(μ-OH$_2$)}{Au(L4-κS)}$_4$] · CH$_2$Cl$_2$ · 6MeOH.

Empirical formula	$C_{75}H_{120}Au_4Ba_2Cl_2N_{20}O_{15}S_8$	
Formula weight	2931.83	
Temperature	200(2) K	
Wavelength	0.71073 Å	
Crystal system	Monoclinic	
Space group	P2/n	
Unit cell dimensions	a = 14.5416(6) Å	α = 90°.
	b = 14.3408(6) Å	β = 102.291(4)°.
	c = 27.309(1) Å	γ = 90°.
Volume	5564.4(4) Å^3	
Z	2	
Density (calculated)	1.750 g/cm^3	
Absorption coefficient	6.208 mm^{-1}	
F(000)	2840	
Crystal size	0.25 x 0.06 x 0.05 mm^3	
Theta range for data collection	2.018 to 24.999°.	
Index ranges	-17<=h<=17, -17<=k<=17, -32<=l<=32	
Reflections collected	43038	
Independent reflections	9801 [R(int) = 0.0849]	
Completeness to theta = 24.999°	99.9 %	
Absorption correction	Integration	
Max. and min. transmission	0.5093 and 0.2024	
Refinement method	Full-matrix least-squares on F^2	
Data / restraints / parameters	9801 / 27 / 619	
Goodness-of-fit on F^2	1.057	
Final R indices [I>2sigma(I)]	R1 = 0.0542, wR2 = 0.1380	
R indices (all data)	R1 = 0.0755, wR2 = 0.1472	
Largest diff. peak and hole	1.816 and -1.286 e · Å^{-3}	
Diffractometer	IPDS STOE	

Table A22: Atomic coordinates (x 10^4) and equivalent isotropic displacement parameters ($Å^2$ x 10^3) for $[\{Ba_2(\mu\text{-}OH_2)\}\{Au(L4\text{-}\kappa S)\}_4] \cdot CH_2Cl_2 \cdot 6MeOH$. U(eq) is defined as one third of the trace of the orthogonalized U^{ij} tensor.

	x	y	z	U(eq)
C(105)	6204(7)	2638(7)	5289(4)	49(2)
C(201)	5238(7)	3077(7)	7899(3)	47(2)
C(104)	5743(8)	2400(8)	4804(4)	59(3)
C(202)	4311(8)	3191(8)	7894(4)	64(3)
C(103)	5076(9)	1697(8)	4745(4)	67(3)
C(203)	3910(9)	2705(9)	8218(5)	72(3)
C(102)	4857(8)	1285(8)	5162(4)	59(3)
C(204)	4474(9)	2093(8)	8551(4)	64(3)
C(101)	5367(7)	1590(7)	5628(3)	47(2)
C(205)	5404(7)	2009(7)	8529(4)	50(2)
C(11)	5148(7)	1196(7)	6109(3)	48(2)
C(12)	3749(8)	776(8)	6336(4)	60(3)
C(13)	3506(9)	-872(8)	6148(5)	71(3)
C(14)	4287(12)	-1374(11)	6483(6)	101(5)
C(21)	6948(7)	3376(7)	5377(4)	54(2)
C(22)	7820(8)	4363(7)	4969(4)	55(3)
C(23)	6690(10)	5651(10)	4759(5)	82(4)
C(24)	6379(15)	5908(15)	5198(8)	144(8)
C(25)	8434(9)	5943(8)	4852(5)	71(3)
C(26)	8543(11)	6132(12)	4323(5)	107(5)
C(31)	5712(7)	3587(7)	7532(3)	46(2)
C(32)	5480(8)	4761(7)	6927(4)	56(3)
C(33)	5802(14)	6256(11)	6524(6)	105(5)
C(34)	6792(16)	6410(15)	6489(7)	141(8)
C(35)	5955(15)	6107(11)	7469(5)	115(6)
C(36)	5140(20)	6588(18)	7572(7)	178(10)
C(41)	6048(8)	1331(7)	8856(3)	50(2)
C(42)	6020(8)	269(7)	9512(4)	59(3)
C(43)	6155(9)	-1173(8)	10016(5)	71(3)
C(44)	7145(11)	-1476(9)	10129(6)	101(5)
C(45)	5309(11)	-1157(9)	9108(5)	82(4)
C(46)	5799(18)	-1947(18)	8932(9)	180(11)

Au(1)	4370(1)	2961(1)	6466(1)	64(1)
Au(4)	6320(1)	2353(1)	9961(1)	62(1)
Ba(1)	7216(1)	2622(1)	6671(1)	47(1)
N(1)	6021(5)	2233(5)	5691(3)	45(2)
N(2)	5787(6)	2491(5)	8202(3)	48(2)
N(11)	4358(6)	737(7)	6054(3)	60(2)
N(21)	7068(6)	3825(6)	4957(3)	56(2)
N(22)	7676(7)	5256(6)	4857(3)	63(2)
N(31)	5256(6)	4330(6)	7332(3)	55(2)
N(32)	5743(9)	5639(7)	6964(3)	83(3)
N(41)	5612(6)	722(6)	9101(3)	56(2)
N(42)	5860(7)	-646(6)	9549(3)	60(2)
O(10)	7500	1321(7)	7500	60(3)
O(11)	5744(5)	1343(5)	6510(2)	54(2)
O(21)	7372(5)	3538(5)	5813(2)	58(2)
O(31)	6488(5)	3286(5)	7464(2)	49(2)
O(41)	6904(5)	1353(5)	8854(3)	59(2)
S(1)	3433(3)	1771(3)	6618(2)	94(1)
S(2)	8946(2)	3924(2)	5045(1)	69(1)
S(3)	5312(2)	4197(2)	6350(1)	63(1)
S(4)	6654(3)	806(2)	10046(1)	73(1)
N(12A)	3115(14)	35(12)	6274(11)	43(5)
C(15A)	2213(16)	53(17)	6418(8)	60(8)
C(16A)	2250(30)	-330(50)	6922(13)	180(30)
N(12B)	3380(20)	-48(15)	6465(9)	57(7)
C(15B)	2770(20)	-100(30)	6824(13)	97(12)
C(16B)	1760(20)	-150(40)	6607(16)	128(16)
O(20)	5866(7)	267(8)	7334(3)	90(3)
O(30)	8156(9)	-212(11)	9187(6)	143(5)
C(20)	5172(12)	208(11)	7619(5)	99(5)
C(30)	7950(20)	-598(19)	8704(10)	187(11)
O(40)	8486(9)	4727(9)	6405(4)	116(4)
C(40)	9330(15)	5043(15)	6294(6)	125(6)
Cl(1)	3085(9)	-4264(13)	6461(5)	201(7)
C(1E)	2360(30)	-3540(30)	6365(18)	171(15)
Cl(2)	1997(14)	-2854(11)	6686(6)	193(6)

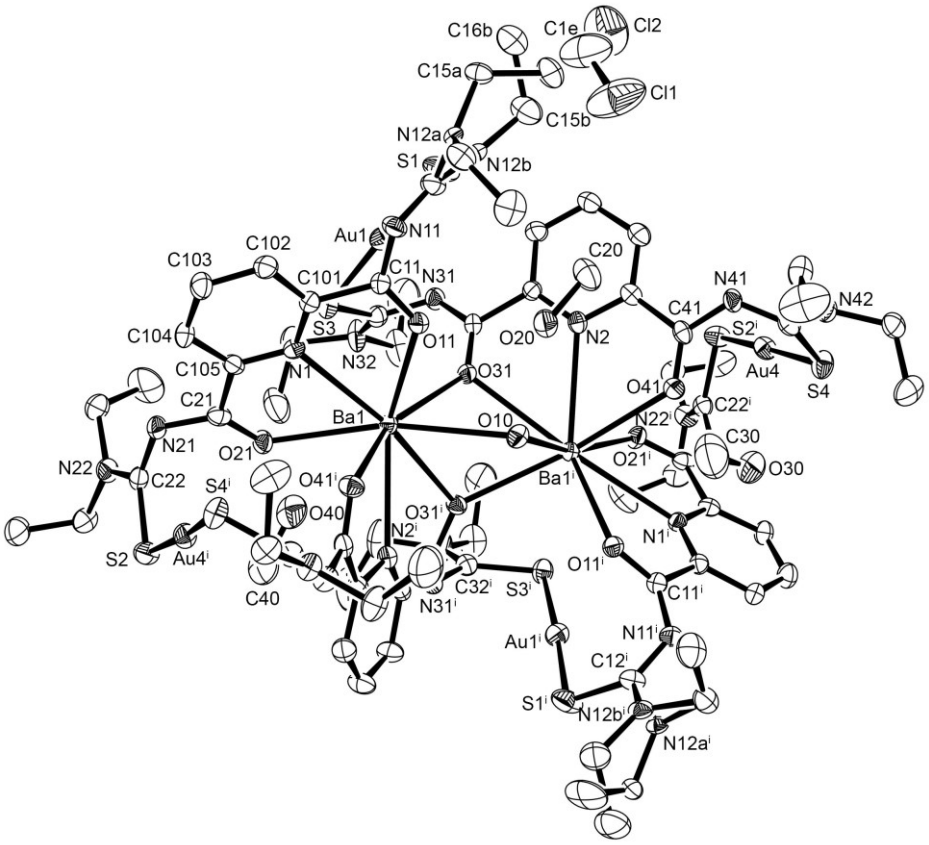

Figure A11: Ellipsoid plot of $[\{Ba_2(\mu\text{-}OH_2)\}\{Au(L4\text{-}\kappa S)\}_4] \cdot CH_2Cl_2 \cdot 6MeOH$. Thermal ellipsoids are at 30 % of probability. The hydrogen atoms have been omitted for clarity.

[La{Au(L4-κS)}$_3$]

Table A23: Crystal data and structure refinement for [La{Au(L4-κS)}$_3$].

Empirical formula	$C_{51}H_{69}Au_3LaN_{15}O_6S_6$	
Formula weight	1910.38	
Temperature	100(2) K	
Wavelength	0.71073 Å	
Crystal system	Trigonal	
Space group	$P\bar{3}$	
Unit cell dimensions	a = 16.412(1) Å	α = 90°.
	b = 16.412(1) Å	β = 90°.
	c = 14.592(8) Å	γ = 120°.
Volume	3404(2) Å^3	
Z	2	
Density (calculated)	1.864 g/cm^3	
Absorption coefficient	7.298 mm^{-1}	
F(000)	1836	
Crystal size	0.45 x 0.17 x 0.08 mm^3	
Theta range for data collection	2.482 to 26.376°.	
Index ranges	-20<=h<=18, -20<=k<=20, -15<=l<=18	
Reflections collected	21952	
Independent reflections	4642 [R(int) = 0.0580]	
Completeness to theta = 25.242°	99.9 %	
Absorption correction	Semi-empirical from equivalents	
Max. and min. transmission	0.1115 and 0.0563	
Refinement method	Full-matrix least-squares on F^2	
Data / restraints / parameters	4642 / 4 / 252	
Goodness-of-fit on F^2	1.057	
Final R indices [I>2sigma(I)]	R1 = 0.0473, wR2 = 0.1224	
R indices (all data)	R1 = 0.0602, wR2 = 0.1331	
Largest diff. peak and hole	2.953 and -3.661 e · Å^{-3}	
Diffractometer	Bruker D8 Venture	

Table A24: Atomic coordinates (x 10^4) and equivalent isotropic displacement parameters ($Å^2$ x 10^3) for [La{Au(L4-κS)}$_2$]. U(eq) is defined as one third of the trace of the orthogonalized U^{ij} tensor.

	x	y	z	U(eq)
C(101)	4269(5)	9082(5)	7576(5)	25(2)
C(102)	4688(5)	10040(6)	7763(6)	28(2)
C(103)	5312(5)	10419(6)	8488(6)	31(2)
C(104)	5536(5)	9836(5)	8997(6)	26(2)
C(105)	5083(5)	8882(5)	8765(5)	23(1)
C(21)	3514(5)	8583(6)	6881(5)	29(2)
C(22)	2554(7)	8776(9)	5854(7)	54(3)
C(25)	3484(10)	9107(12)	4474(7)	80(5)
C(26)	3737(13)	8368(16)	4351(10)	114(7)
C(11)	5267(5)	8178(5)	9257(5)	23(1)
C(12)	6496(5)	8167(5)	10097(5)	22(1)
C(15)	7374(5)	7977(5)	11378(5)	27(2)
C(16)	8320(6)	8853(6)	11459(8)	47(2)
C(13)	6184(6)	8489(6)	11635(6)	30(2)
C(14)	5236(7)	7676(6)	11913(7)	40(2)
N(1)	4462(4)	8517(4)	8084(4)	24(1)
N(21)	3353(5)	9120(5)	6332(5)	35(2)
N(11)	5991(5)	8558(4)	9812(5)	28(1)
N(12)	6666(5)	8186(4)	10990(5)	27(1)
O(11)	3092(4)	7692(4)	6867(4)	34(1)
O(21)	4712(4)	7319(3)	9107(4)	26(1)
S(1)	7043(2)	7759(1)	9357(1)	31(1)
La(1)	3333	6667	7985(1)	24(1)
Au(1)	6881(1)	8139(1)	7901(1)	33(1)
N(22A)	2639(9)	9012(10)	4962(8)	27(1)
C(23A)	1672(16)	8155(16)	4414(15)	60(5)
C(24A)	1289(18)	8754(18)	4053(16)	64(5)
N(22B)	2521(8)	8567(10)	4948(8)	27(1)
C(23B)	1844(16)	8857(16)	4385(15)	60(5)
C(24B)	1247(19)	7826(17)	4133(18)	64(5)
S(2)	1476(2)	8368(3)	6400(2)	64(1)

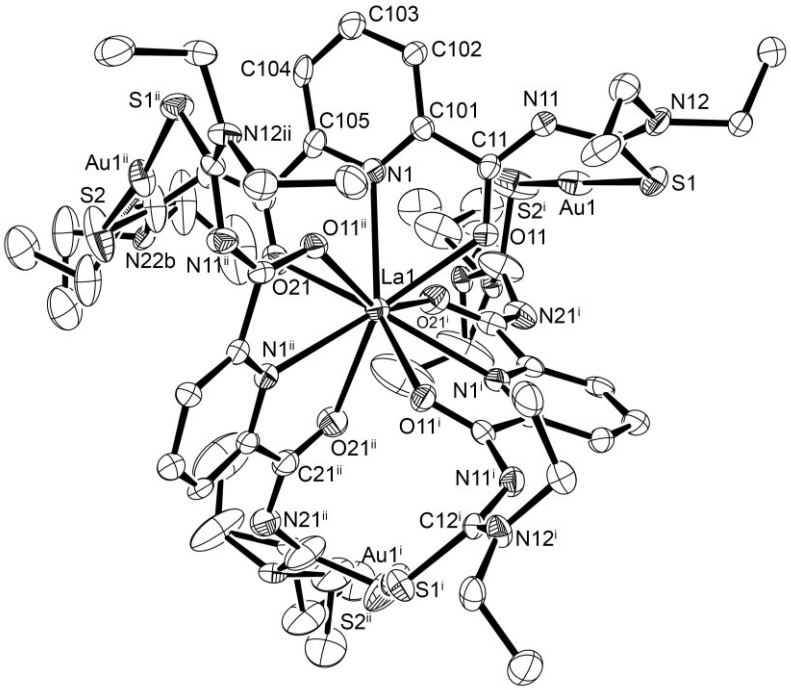

Figure A12: Ellipsoid plot of [La{Au(L4-κS)}$_3$]. Thermal ellipsoids are at 30 % of probability. The hydrogen atoms have been omitted for clarity.

[La{Au(L4-κS)}$_3$] (SQUEEZE)

Table A25: Crystal data and structure refinement for [La{Au(L4-κS)}$_3$]. **(SQUEEZE)**

Empirical formula	$C_{51}H_{69}Au_3LaN_{15}O_6S_6$	
Formula weight	1910.38	
Temperature	100(2) K	
Wavelength	0.71073 Å	
Crystal system	Trigonal	
Space group	$P\bar{3}$	
Unit cell dimensions	a = 16.412(1) Å	α = 90°.
	b = 16.412(1) Å	β = 90°.
	c = 14.592(8) Å	γ = 120°.
Volume	3404(2) Å^3	
Z	2	
Density (calculated)	1.864 g/cm^3	
Absorption coefficient	7.298 mm^{-1}	
F(000)	1836	
Crystal size	0.45 x 0.17 x 0.08 mm^3	
Theta range for data collection	2.482 to 26.375°.	
Index ranges	-20<=h<=18, -20<=k<=20, -15<=l<=18	
Reflections collected	21952	
Independent reflections	4642 [R(int) = 0.0563]	
Completeness to theta = 25.242°	99.9 %	
Absorption correction	Semi-empirical from equivalents	
Max. and min. transmission	0.115 and 0.0563	
Refinement method	Full-matrix least-squares on F^2	
Data / restraints / parameters	4642 / 4 / 252	
Goodness-of-fit on F^2	1.055	
Final R indices [I>2sigma(I)]	R1 = 0.0428, wR2 = 0.1034	
R indices (all data)	R1 = 0.0513, wR2 = 0.1079	
Largest diff. peak and hole	2.369 and -3.540 e · Å^{-3}	
Diffractometer	Bruker D8 Venture	

Table A26: Atomic coordinates (x 10^4) and equivalent isotropic displacement parameters ($Å^2$ x 10^3) for [La{Au(L4-κS)}$_3$]. U(eq) is defined as one third of the trace of the orthogonalized U^{ij} tensor. **(SQUEEZE)**

	x	y	z	U(eq)
C(105)	4268(4)	9082(4)	7576(4)	24(1)
C(104)	4689(4)	10042(5)	7763(5)	29(1)
C(103)	5311(4)	10418(5)	8488(5)	32(1)
C(102)	5535(4)	9834(4)	8994(5)	26(1)
C(101)	5084(4)	8883(4)	8767(4)	23(1)
C(21)	3515(4)	8584(5)	6883(4)	29(1)
C(22)	2554(6)	8776(7)	5854(5)	53(2)
C(25)	3486(8)	9111(10)	4475(6)	83(4)
C(26)	3750(11)	8368(13)	4364(8)	115(6)
C(11)	5267(4)	8177(4)	9256(4)	23(1)
C(12)	6497(4)	8167(4)	10099(4)	23(1)
C(15)	7372(5)	7978(4)	11375(4)	27(1)
C(16)	8324(5)	8853(5)	11460(7)	48(2)
C(13)	6182(5)	8488(5)	11634(5)	30(1)
C(14)	5235(5)	7676(5)	11913(5)	40(2)
N(1)	4461(3)	8518(4)	8084(4)	24(1)
N(21)	3354(4)	9123(4)	6332(4)	36(1)
N(11)	5990(4)	8557(4)	9812(4)	28(1)
N(12)	6665(4)	8185(4)	10988(4)	27(1)
O(21)	3091(3)	7690(3)	6869(3)	34(1)
O(11)	4713(3)	7318(3)	9106(3)	27(1)
S(1)	7042(1)	7760(1)	9357(1)	30(1)
La(1)	3333	6667	7985(1)	25(1)
Au(1)	6881(1)	8139(1)	7901(1)	34(1)
N(22A)	2643(7)	9012(9)	4960(6)	27(1)
C(23A)	1652(13)	8131(14)	4406(13)	62(4)
C(24A)	1292(15)	8758(15)	4061(13)	64(4)
N(22B)	2517(7)	8562(9)	4947(7)	27(1)
C(23B)	1841(13)	8861(14)	4383(12)	62(4)
C(24B)	1225(16)	7823(14)	4128(15)	64(4)
S(2)	1475(2)	8368(2)	6401(1)	64(1)

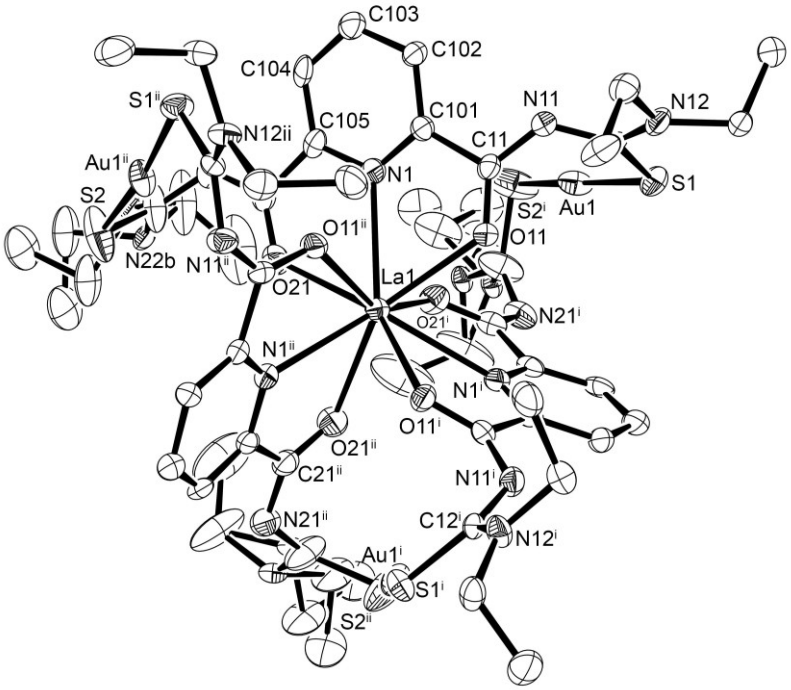

Figure A13: Ellipsoid plot of [La{Au(L4-κS)}$_3$]. Thermal ellipsoids are at 50 % of probability. The hydrogen atoms have been omitted for clarity. **(SQUEEZE)**

[Ce{Au(L4-κS)}$_3$]

Table A27: Crystal data and structure refinement for [Ce{Au(L4-κS)}$_3$].

Empirical formula	$C_{51}H_{69}Au_3CeN_{15}O_6S_6$	
Formula weight	1911.59	
Temperature	150(2) K	
Wavelength	0.71073 Å	
Crystal system	Trigonal	
Space group	$P\bar{3}$	
Unit cell dimensions	a = 16.3263(5) Å	α = 90°.
	b = 16.3263(5) Å	β = 90°.
	c = 14.6155(5) Å	γ = 120°.
Volume	3373.8(2) Å^3	
Z	2	
Density (calculated)	1.882 g/cm^3	
Absorption coefficient	7.405 mm^{-1}	
F(000)	1838	
Crystal size	0.15 x 0.12 x 0.10 mm^3	
Theta range for data collection	2.495 to 24.993°.	
Index ranges	-19<=h<=19, -19<=k<=19, -17<=l<=17	
Reflections collected	21486	
Independent reflections	3809 [R(int) = 0.0531]	
Completeness to theta = 24.993°	95.9 %	
Absorption correction	Semi-empirical from equivalents	
Max. and min. transmission	0.7456 and 0.5650	
Refinement method	Full-matrix least-squares on F^2	
Data / restraints / parameters	3809 / 5 / 257	
Goodness-of-fit on F^2	1.057	
Final R indices [I>2sigma(I)]	R1 = 0.0343, wR2 = 0.0795	
R indices (all data)	R1 = 0.0461, wR2 = 0.0849	
Largest diff. peak and hole	1.777 and -1.715 e · Å^{-3}	
Diffractometer	Bruker D8 Venture	

Table A28: Atomic coordinates (x 10^4) and equivalent isotropic displacement parameters (Å^2 x 10^3) for [Ce{Au(L4-κS)}$_3$]. U(eq) is defined as one third of the trace of the orthogonalized U^{ij} tensor.

	x	y	z	U(eq)
C(101)	5071(4)	6187(4)	8750(4)	20(1)
C(102)	5524(5)	5688(4)	8967(5)	24(1)
C(103)	5318(5)	4892(5)	8454(5)	29(2)
C(104)	4678(5)	4647(5)	7726(5)	24(2)
C(105)	4248(5)	5176(4)	7556(4)	21(1)
C(11)	5245(4)	7066(4)	9251(4)	20(1)
C(12)	6471(4)	8304(5)	10105(4)	19(1)
C(13)	6185(5)	7690(5)	11638(5)	28(2)
C(14)	5253(6)	7564(5)	11948(6)	38(2)
C(15)	7378(5)	9389(5)	11360(5)	28(2)
C(16)	8329(6)	9455(6)	11425(7)	49(2)
C(21)	3484(5)	4926(5)	6865(5)	23(2)
C(22)	2486(6)	3777(6)	5860(5)	45(2)
C(23)	3408(8)	4371(7)	4471(6)	65(3)
C(24)	3684(9)	5406(8)	4379(8)	76(4)
Au(1)	6863(1)	8701(1)	7907(1)	30(1)
Ce(1)	3333	6667	7968(1)	20(1)
N(1)	4445(4)	5936(4)	8075(4)	19(1)
N(11)	5959(4)	7409(4)	9821(4)	24(1)
N(12)	6655(4)	8467(4)	10984(4)	22(1)
N(21)	3309(4)	4220(4)	6318(4)	30(1)
O(11)	4693(3)	7384(3)	9086(3)	24(1)
O(21)	3074(3)	5407(3)	6864(3)	28(1)
S(1)	7008(1)	9264(1)	9356(1)	28(1)
S(2)	1411(2)	3132(2)	6417(2)	55(1)
N(22A)	2462(9)	3970(14)	4955(8)	44(5)
C(25A)	1812(13)	2991(13)	4392(12)	38(3)
C(26A)	1192(18)	3463(17)	4206(17)	54(4)
N(22B)	2540(9)	3677(10)	4958(7)	44(5)
C(25B)	1585(10)	3504(11)	4402(10)	38(3)
C(26B)	1242(12)	2471(12)	4059(11)	54(4)

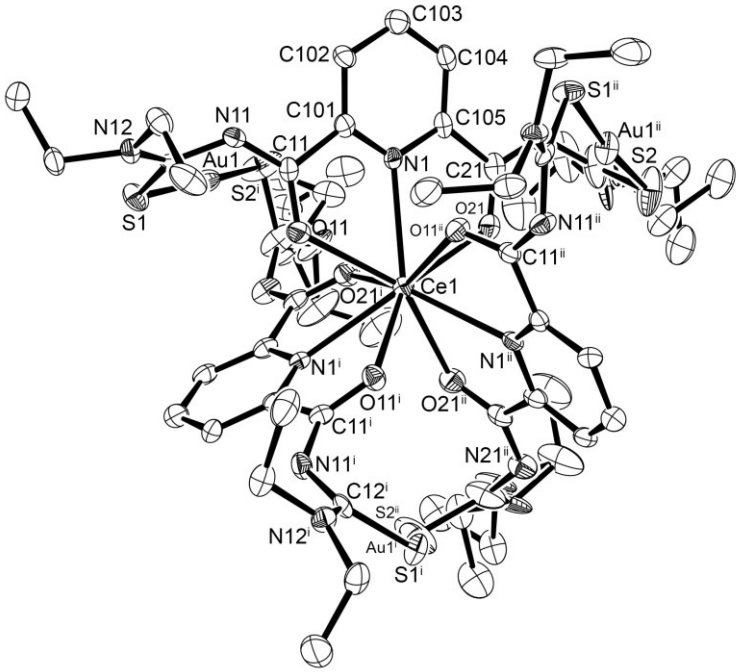

Figure A14: Ellipsoid plot of [Ce{Au(L4-κS)}$_3$]. Thermal ellipsoids are at 50 % of probability. The hydrogen atoms have been omitted for clarity.

$[Nd\{Au(L4\text{-}\kappa S)\}_3]\cdot 0.5CH_2Cl_2$

Table A29: Crystal data and structure refinement for $[Nd\{Au(L4\text{-}\kappa S)\}_3]\cdot 0.5CH_2Cl_2$.

Empirical formula	$C_{51.5}H_{70}Au_3ClN_{15}NdO_6S_6$	
Formula weight	1958.17	
Temperature	100(2) K	
Wavelength	0.71073 Å	
Crystal system	Triclinic	
Space group	$P\bar{1}$	
Unit cell dimensions	a = 16.3186(7) Å	α = 90°. *
	b = 16.3186(7) Å	β = 90°.
	c = 14.5915(5) Å	γ = 120°.
Volume	3365.1(2) $Å^3$	
Z	2	
Density (calculated)	1.933 g/cm^3	
Absorption coefficient	7.560 mm^{-1}	
F(000)	1884	
Crystal size	0.35 x 0.06 x 0.05 mm^3	
Theta range for data collection	2.496 to 27.125°.	
Index ranges	-20<=h<=20, -20<=k<=20, -15<=l<=18	
Reflections collected	24574	
Independent reflections	14294 [R(int) = 0.0417]	
Completeness to theta = 25.242°	96.5 %	
Absorption correction	Semi-empirical from equivalents	
Max. and min. transmission	0.7455 and 0.5305	
Refinement method	Full-matrix least-squares on F^2	
Data / restraints / parameters	14294 / 43 / 746	
Goodness-of-fit on F^2	1.033	
Final R indices [I>2sigma(I)]	R1 = 0.0490, wR2 = 0.0835	
R indices (all data)	R1 = 0.0840, wR2 = 0.0954	
Largest diff. peak and hole	2.778 and -2.384 e · $Å^{-3}$	
Diffractometer	Bruker D8 Venture	

* The unit cell parameters of the trigonal cell were kept for comparison with the squeezed structure.

Table A30: Atomic coordinates (x 10^4) and equivalent isotropic displacement parameters ($Å^2$ x 10^3) for $[Nd\{Au(L4\text{-}\kappa S)\}_3] \cdot 0.5CH_2Cl_2$. U(eq) is defined as one third of the trace of the orthogonalized U^{ij} tensor.

	x	y	z	U(eq)
Au(2)	8166(1)	1312(1)	2089(1)	29(1)
Nd(1)	6668(1)	3335(1)	1991(1)	20(1)
Au(3)	8693(1)	6859(1)	2089(1)	29(1)
Au(1)	3145(1)	1837(1)	2087(1)	29(1)
C(203)	4894(6)	5302(6)	1549(6)	27(2)
S(5)	7744(2)	732(2)	641(1)	25(1)
S(3)	9271(2)	7014(2)	642(1)	25(1)
S(1)	2989(2)	2258(2)	640(1)	25(1)
S(2)	8598(2)	1745(3)	3575(2)	57(1)
S(6)	8259(3)	6861(2)	3578(2)	57(1)
N(1)	5574(4)	1514(5)	1903(4)	18(1)
N(2)	5942(5)	4431(4)	1910(4)	16(1)
O(51)	7291(4)	2618(4)	877(4)	21(1)
S(4)	3143(2)	1405(2)	3576(2)	57(1)
O(11)	5321(4)	2706(4)	875(4)	22(1)
N(31)	7412(5)	5956(5)	164(4)	19(2)
N(51)	8538(5)	2577(5)	167(4)	20(2)
O(31)	7382(4)	4672(4)	880(4)	22(1)
O(61)	7628(4)	4585(4)	3096(4)	26(1)
N(11)	4042(5)	1460(5)	164(4)	22(2)
N(32)	8484(5)	6667(5)	-993(4)	19(2)
O(41)	5424(4)	3045(4)	3096(4)	27(1)
O(21)	6958(4)	2379(4)	3100(4)	27(1)
N(3)	8485(5)	4060(5)	1903(4)	19(2)
C(104)	5340(5)	1(6)	2272(5)	20(1)
N(52)	8175(5)	1513(5)	-997(4)	19(2)
N(12)	3336(5)	1819(5)	-997(4)	18(1)
C(304)	10005(6)	5344(6)	2276(6)	22(2)
C(101)	4943(6)	1132(6)	1236(5)	17(2)
C(202)	5695(6)	5521(6)	1019(5)	21(2)
C(201)	6193(5)	5057(5)	1233(5)	18(2)
C(32)	8313(6)	6475(6)	-117(5)	17(2)
C(21)	6541(6)	1493(7)	3114(5)	23(2)

N(21)	6703(5)	956(5)	3681(5)	28(2)
N(41)	4257(5)	3302(5)	3677(5)	29(2)
C(301)	8868(6)	3810(6)	1233(5)	19(2)
C(204)	4656(6)	4662(6)	2273(6)	24(2)
C(11)	4768(6)	1836(6)	737(5)	20(2)
C(302)	9819(6)	4304(5)	1020(5)	18(2)
C(41)	4958(6)	3469(6)	3106(5)	21(2)
C(61)	8519(6)	5044(6)	3114(5)	21(2)
N(61)	9053(6)	5749(5)	3685(5)	28(2)
C(31)	7064(6)	5232(6)	727(5)	16(2)
C(102)	4484(6)	174(6)	1019(6)	19(2)
C(51)	8160(6)	2927(6)	727(5)	19(2)
C(305)	9044(6)	4816(6)	2434(5)	20(2)
C(205)	5199(6)	4238(6)	2433(5)	20(2)
C(105)	5777(5)	969(6)	2437(5)	20(1)
C(52)	8165(6)	1680(6)	-107(5)	20(2)
C(12)	3527(6)	1839(5)	-112(5)	16(2)
C(14)	1654(7)	1112(7)	-1439(8)	40(3)
C(33)	9402(6)	7384(6)	-1369(6)	23(2)
C(53)	7983(6)	599(6)	-1366(6)	24(2)
C(13)	2609(6)	2012(6)	-1372(6)	26(2)
C(103)	4690(6)	-404(6)	1551(6)	24(2)
C(54)	8881(7)	536(7)	-1435(7)	37(2)
C(303)	10397(6)	5102(6)	1559(6)	28(2)
C(34)	9457(7)	8349(7)	-1432(8)	42(3)
C(62)	8672(9)	6191(7)	4141(6)	44(3)
C(22)	7528(8)	1333(9)	4146(6)	44(3)
C(23)	6601(9)	1005(10)	5523(6)	58(4)
C(42)	3810(7)	2482(8)	4137(6)	46(3)
C(63)	8992(10)	5598(8)	5535(7)	58(4)
C(24)	6335(10)	1759(11)	5620(8)	72(4)
C(15)	3815(6)	1512(6)	-1655(5)	21(2)
C(55)	8495(6)	2301(6)	-1648(5)	22(2)
C(16)	4769(6)	2322(6)	-1951(6)	29(2)
C(56)	7682(6)	2444(6)	-1948(6)	28(2)
C(43)	4391(8)	3394(9)	5530(7)	62(4)
C(44)	5418(10)	3665(10)	5620(8)	71(4)

C(64)	8242(11)	4577(9)	5623(8)	73(4)
N(62A)	8888(13)	6338(11)	5044(10)	28(2)
C(65A)	8121(15)	6489(15)	5550(14)	42(2)
C(66A)	8696(16)	7488(14)	5940(13)	42(2)
N(62B)	8485(12)	6053(11)	5052(10)	28(2)
C(65B)	8781(13)	6976(13)	5594(12)	42(2)
C(66B)	7717(13)	6532(15)	5774(13)	42(2)
C(35)	7694(6)	6193(6)	-1660(5)	22(2)
C(36)	7552(6)	5238(6)	-1948(6)	27(2)
N(42A)	3653(11)	2542(10)	5040(10)	28(2)
C(45A)	3524(14)	1629(14)	5549(13)	42(2)
C(46A)	2511(14)	1223(16)	5946(13)	42(2)
N(42B)	3957(11)	2432(9)	5052(9)	28(2)
C(45B)	3034(13)	1812(13)	5596(12)	42(2)
C(46B)	3467(15)	1166(16)	5766(14)	42(2)
N(22A)	7456(10)	1125(13)	5044(10)	28(2)
C(25A)	8378(14)	1888(15)	5562(13)	42(2)
C(26A)	8772(16)	1279(15)	5946(13)	42(2)
N(22B)	7573(9)	1535(12)	5059(10)	28(2)
C(25B)	8185(14)	1217(13)	5603(13)	42(2)
C(26B)	8817(16)	2276(13)	5777(14)	42(2)
Cl(2A)	9060(14)	9343(18)	6334(12)	139(4)
Cl(1A)	10214(15)	10820(16)	6326(12)	139(4)
C(20A)	10267(15)	9786(16)	6270(20)	20(1)
Cl(2B)	9920(20)	9990(30)	5219(11)	139(4)
Cl(1B)	10800(17)	9800(20)	6382(14)	139(4)
C(20B)	9656(19)	9590(30)	6328(17)	20(1)

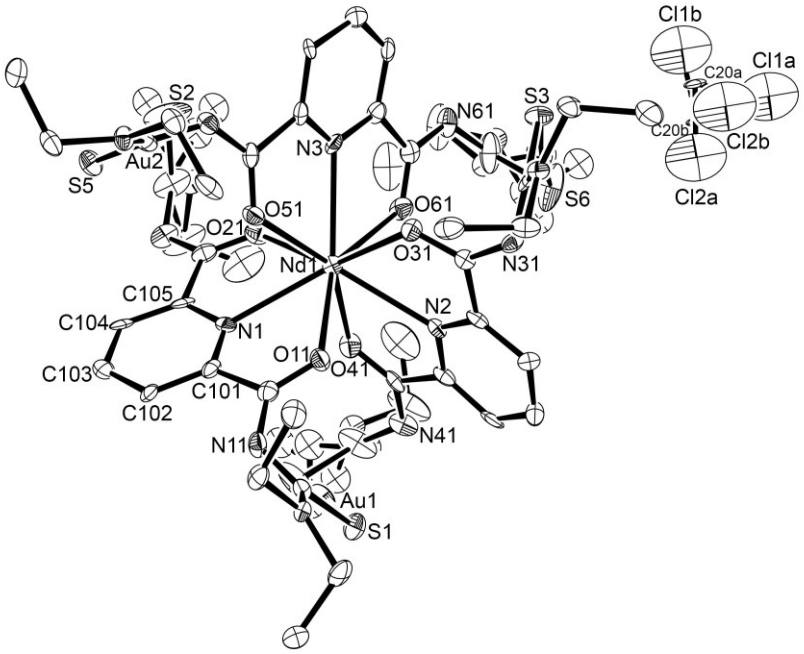

Figure A15: Ellipsoid plot of $[Nd\{Au(L4\text{-}\kappa S)\}_3] \cdot 0.5CH_2Cl_2$. Thermal ellipsoids are at 50 % of probability. The hydrogen atoms have been omitted for clarity.

[Nd{Au(L4-κS)}$_3$] (SQUEEZE)

Table A31: Crystal data and structure refinement for [Nd{Au(L4-κS)}$_3$]. **(SQUEEZE)**

Empirical formula	$C_{51}H_{69}Au_3N_{15}NdO_6S_6$	
Formula weight	1915.71	
Temperature	100(2) K	
Wavelength	0.71073 Å	
Crystal system	Trigonal	
Space group	$P\bar{3}$	
Unit cell dimensions	a = 16.354(2) Å	α = 90°.
	b = 16.354(2) Å	β = 90°.
	c = 14.621(1) Å	γ = 120°.
Volume	3386.5(9) Å^3	
Z	2	
Density (calculated)	1.879 g/cm^3	
Absorption coefficient	7.471 mm^{-1}	
F(000)	1842	
Crystal size	0.35 x 0.06 x 0.05 mm^3	
Theta range for data collection	2.491 to 27.035°.	
Index ranges	-20<=h<=20, -20<=k<=20, -18<=l<=15	
Reflections collected	24209	
Independent reflections	4954 [R(int) = 0.0553]	
Completeness to theta = 25.242°	99.9 %	
Absorption correction	Semi-empirical from equivalents	
Max. and min. transmission	0.1506 and 0.1022	
Refinement method	Full-matrix least-squares on F^2	
Data / restraints / parameters	4954 / 3 / 258	
Goodness-of-fit on F^2	1.098	
Final R indices [I>2sigma(I)]	R1 = 0.0470, wR2 = 0.0792	
R indices (all data)	R1 = 0.0633, wR2 = 0.0835	
Largest diff. peak and hole	2.695 and -2.596 e · Å^{-3}	
Diffractometer	Bruker D8 Venture	

Table A32: Atomic coordinates (x 10^4) and equivalent isotropic displacement parameters ($Å^2$ x 10^3) for [Nd{Au(L4-κS)}$_3$]. U(eq) is defined as one third of the trace of the orthogonalized U^{ij} tensor. **(SQUEEZE)**

	x	y	z	U(eq)
C(101)	1135(5)	4942(5)	1235(4)	21(1)
C(102)	179(5)	4487(5)	1023(5)	23(1)
C(103)	-402(5)	4696(5)	1557(5)	28(2)
C(104)	-10(5)	5330(5)	2272(5)	26(2)
C(105)	961(5)	5767(5)	2426(4)	22(1)
C(11)	1838(5)	4768(5)	726(4)	22(1)
C(12)	1838(4)	3525(5)	-109(4)	19(1)
C(13)	2013(5)	2609(5)	-1369(5)	26(2)
C(14)	1120(6)	1657(5)	-1435(6)	42(2)
C(15)	1502(5)	3807(5)	-1650(4)	26(2)
C(16)	2319(5)	4767(5)	-1949(5)	30(2)
C(21)	1483(5)	6531(5)	3111(4)	25(2)
C(22)	1329(7)	7523(6)	4141(5)	46(2)
C(23)	1000(9)	6599(7)	5530(6)	65(3)
N(1)	1517(4)	5572(4)	1906(4)	21(1)
N(11)	1461(4)	4043(4)	164(4)	24(1)
N(12)	1819(4)	3337(4)	-1001(4)	21(1)
N(21)	949(5)	6700(5)	3683(4)	32(1)
O(11)	2708(3)	5324(3)	879(3)	25(1)
O(21)	2376(4)	6956(3)	3102(3)	30(1)
S(1)	2257(1)	2987(1)	641(1)	28(1)
S(2)	1742(2)	8599(2)	3578(1)	61(1)
Nd(1)	3333	6667	1991(1)	23(1)
Au(1)	1835(1)	3144(1)	2088(1)	32(1)
N(22A)	1535(11)	7614(10)	5041(7)	31(3)
C(25A)	2009(12)	8478(12)	5601(10)	36(3)
C(26A)	1284(14)	8768(13)	5944(11)	54(4)
N(22B)	1073(12)	7379(12)	5039(8)	31(3)
C(25B)	1232(12)	8199(11)	5597(10)	36(3)
C(26B)	2295(14)	8890(15)	5821(14)	54(4)
C(24)	1756(9)	6331(8)	5625(7)	72(3)

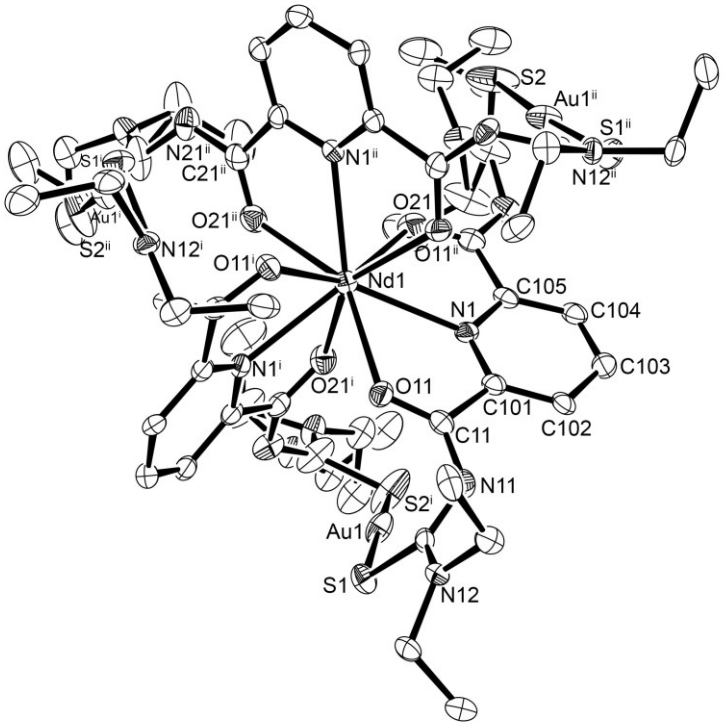

Figure A16: Ellipsoid plot of [Nd{Au(L4-κS)}$_3$]. Thermal ellipsoids are at 50 % of probability. The hydrogen atoms have been omitted for clarity. **(SQUEEZE)**

[Sm{Au(L4-κS)}$_3$]

Table A33: Crystal data and structure refinement for [Sm{Au(L4-κS)}$_3$].

Empirical formula	$C_{51}H_{69}Au_3N_{15}O_6S_6Sm$	
Formula weight	1921.82	
Temperature	100(2) K	
Wavelength	0.71073 Å	
Crystal system	Trigonal	
Space group	$P\bar{3}$	
Unit cell dimensions	a = 16.2775(8) Å	α = 90°.
	b = 16.2775(8) Å	β = 90°.
	c = 14.5918(6) Å	γ = 120°.
Volume	3348.2(4) Å^3	
Z	2	
Density (calculated)	1.906 g/cm^3	
Absorption coefficient	7.658 mm^{-1}	
F(000)	1846	
Crystal size	0.22 x 0.15 x 0.06 mm^3	
Theta range for data collection	2.503 to 27.908°.	
Index ranges	-21<=h<=21, -21<=k<=21, -19<=l<=19	
Reflections collected	40610	
Independent reflections	5346 [R(int) = 0.0814]	
Completeness to theta = 25.242°	99.9 %	
Absorption correction	Semi-empirical from equivalents	
Max. and min. transmission	0.7456 and 0.4274	
Refinement method	Full-matrix least-squares on F^2	
Data / restraints / parameters	5346 / 8 / 251	
Goodness-of-fit on F^2	1.153	
Final R indices [I>2sigma(I)]	R1 = 0.0661, wR2 = 0.1380	
R indices (all data)	R1 = 0.0847, wR2 = 0.1457	
Largest diff. peak and hole	4.356 and -3.997 e · Å^{-3}	
Diffractometer	Bruker D8 Venture	

Table A34: Atomic coordinates (x 10^4) and equivalent isotropic displacement parameters (Å^2 x 10^3) for [Sm{Au(L4-κS)}$_3$]. U(eq) is defined as one third of the trace of the orthogonalized U^{ij} tensor.

	x	y	z	U(eq)
C(101)	9019(8)	4217(7)	7428(7)	18(2)
C(102)	10004(8)	4656(7)	7294(8)	22(2)
C(103)	10398(8)	5307(8)	6580(8)	25(2)
C(104)	9819(8)	5508(7)	6028(7)	19(2)
C(105)	8856(7)	5049(7)	6230(7)	18(2)
C(11)	8148(7)	5212(7)	5725(7)	19(2)
C(12)	8151(7)	6465(7)	4880(7)	17(2)
C(13)	7993(8)	7399(7)	3638(7)	21(2)
C(14)	8885(9)	8349(8)	3582(10)	36(3)
C(15)	8500(8)	6201(8)	3344(7)	22(2)
C(16)	7688(8)	5243(9)	3035(8)	29(3)
C(21)	8492(8)	3446(7)	8111(7)	20(2)
C(22)	8627(12)	2444(10)	9138(8)	42(4)
C(23)	8942(13)	3347(10)	10539(9)	49(3)
C(24)	8222(14)	3648(12)	10627(11)	57(4)
Au(1)	8175(1)	6846(1)	7083(1)	27(1)
N(1)	8460(6)	4411(6)	6902(6)	17(2)
N(11)	8529(6)	5940(6)	5152(6)	20(2)
N(12)	8180(6)	6660(6)	3999(6)	18(2)
N(21)	9012(7)	3270(7)	8688(6)	26(2)
O(11)	7280(5)	4660(5)	5874(5)	20(2)
O(21)	7595(6)	3021(5)	8085(5)	25(2)
S(1)	7734(2)	6997(2)	5642(2)	24(1)
S(2)	8215(4)	1372(3)	8566(2)	55(1)
Sm(1)	6667	3333	6983(1)	18(1)
N(22A)	8451(15)	2411(10)	10053(9)	28(5)
C(25A)	7970(20)	1514(17)	10593(15)	49(3)
C(26A)	8700(20)	1209(19)	10918(17)	45(5)
N(22B)	8890(20)	2548(15)	10023(11)	28(5)
C(25B)	8730(20)	1736(19)	10592(18)	49(3)
C(26B)	7650(20)	1060(20)	10820(20)	45(5)

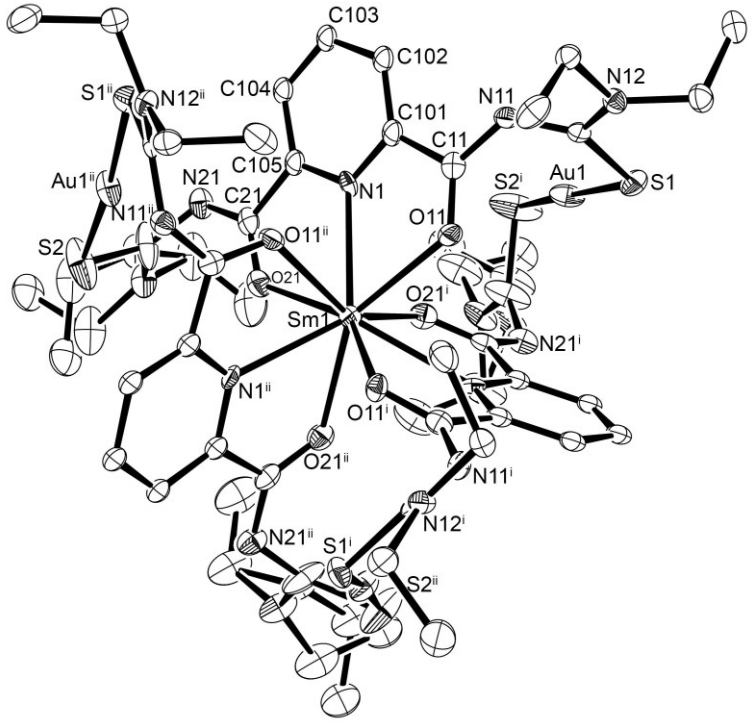

Figure A17: Ellipsoid plot of [Sm{Au(L4-κS)}$_3$]. Thermal ellipsoids are at 50 % of probability. The hydrogen atoms have been omitted for clarity.

[Sm{Au(L4-κS)}$_3$] (SQUEEZE)

Table A35: Crystal data and structure refinement for [Sm{Au(L4-κS)}$_3$]. **(SQUEEZE)**

Empirical formula	$C_{51}H_{69}Au_3N_{15}O_6S_6Sm$	
Formula weight	1921.82	
Temperature	100(2) K	
Wavelength	0.71073 Å	
Crystal system	Trigonal	
Space group	$P\bar{3}$	
Unit cell dimensions	a = 16.2775(8) Å	α = 90°.
	b = 16.2775(8) Å	β = 90°.
	c = 14.5918(6) Å	γ = 120°.
Volume	3348.2(4) Å^3	
Z	2	
Density (calculated)	1.906 g/cm^3	
Absorption coefficient	7.658 mm^{-1}	
F(000)	1846	
Crystal size	0.22 x 0.15 x 0.06 mm^3	
Theta range for data collection	2.503 to 24.985°.	
Index ranges	-19<=h<=19, -19<=k<=19, -17<=l<=17	
Reflections collected	30669	
Independent reflections	3864 [R(int) = 0.0604]	
Completeness to theta = 24.985°	98.3 %	
Absorption correction	Semi-empirical from equivalents	
Max. and min. transmission	0.7456 and 0.4274	
Refinement method	Full-matrix least-squares on F^2	
Data / restraints / parameters	3864 / 8 / 227	
Goodness-of-fit on F^2	1.032	
Final R indices [I>2sigma(I)]	R1 = 0.0469, wR2 = 0.0944	
R indices (all data)	R1 = 0.0542, wR2 = 0.0972	
Largest diff. peak and hole	2.643 and -2.540 e · Å^{-3}	
Diffractometer	Bruker D8 Venture	

Table A36: Atomic coordinates (x 10^4) and equivalent isotropic displacement parameters ($Å^2$ x 10^3) for [Sm{Au(L4-κS)}$_3$]. U(eq) is defined as one third of the trace of the orthogonalized U^{ij} tensor. **(SQUEEZE)**

	x	y	z	U(eq)
C(11)	8151(6)	5211(6)	5723(6)	20(2)
C(12)	8157(6)	6459(6)	4881(6)	16(2)
C(13)	7997(6)	7403(6)	3636(6)	23(2)
C(14)	8890(8)	8348(7)	3580(8)	38(3)
C(15)	8500(6)	6199(6)	3344(6)	20(2)
C(16)	7691(7)	5239(7)	3037(7)	29(2)
C(21)	8493(7)	3443(6)	8114(6)	21(2)
C(22)	8623(10)	2441(8)	9135(7)	44(3)
C(23)	8949(10)	3347(9)	10538(7)	51(3)
C(24)	8218(11)	3641(10)	10625(9)	62(4)
Au(1)	8176(1)	6846(1)	7083(1)	28(1)
N(1)	8462(5)	4411(5)	6902(5)	17(2)
N(11)	8526(5)	5937(5)	5151(5)	19(2)
N(12)	8178(5)	6660(5)	3997(5)	18(2)
N(21)	9015(6)	3273(6)	8689(5)	26(2)
O(11)	7281(4)	4656(4)	5875(4)	20(1)
O(21)	7597(5)	3021(4)	8083(4)	25(1)
S(1)	7735(2)	6998(2)	5643(2)	24(1)
S(2)	8216(3)	1374(2)	8565(2)	54(1)
Sm(1)	6667	3333	6982(1)	18(1)
N(22A)	8462(13)	2402(9)	10060(8)	32(5)
C(25A)	7974(16)	1506(14)	10601(12)	51(3)
C(26A)	8715(15)	1213(16)	10922(14)	47(4)
N(22B)	8890(20)	2548(14)	10019(11)	32(5)
C(25B)	8750(20)	1744(17)	10586(15)	51(3)
C(26B)	7676(18)	1050(20)	10800(20)	47(4)
C(105)	9017(6)	4211(6)	7427(6)	20(1)
C(102)	9806(6)	5500(6)	6036(6)	20(1)
C(101)	8860(6)	5052(6)	6230(6)	20(1)
C(104)	9998(6)	4657(6)	7294(6)	20(1)
C(103)	10395(6)	5303(6)	6583(6)	20(1)

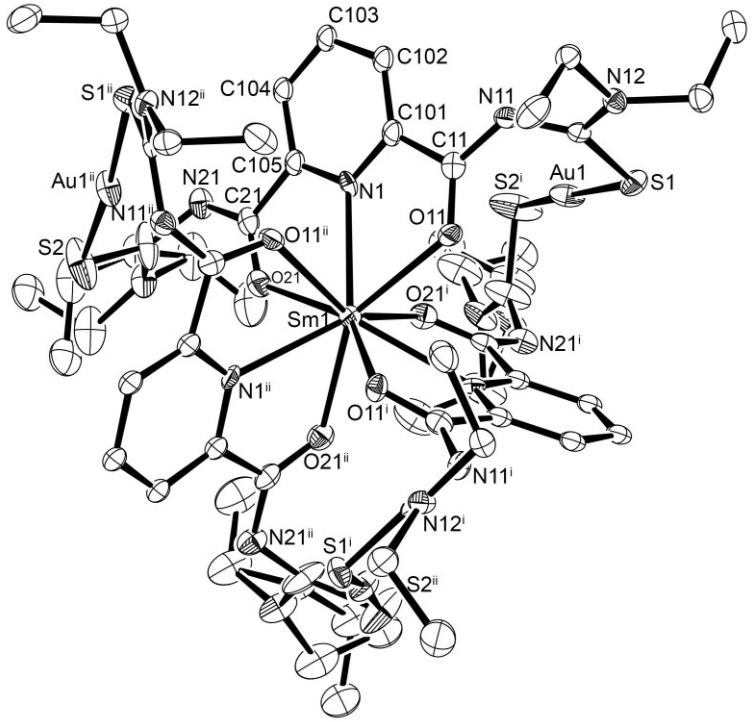

Figure A18: Ellipsoid plot of [Sm{Au(L4-κS)}$_3$]. Thermal ellipsoids are at 50 % of probability. The hydrogen atoms have been omitted for clarity. **(SQUEEZE)**

[Eu{Au(L4-κS)}$_3$]

Table A37: Crystal data and structure refinement for [Eu{Au(L4-κS)}$_3$].

Empirical formula	$C_{51}H_{69}Au_3EuN_{15}O_6S_6$	
Formula weight	1923.43	
Temperature	100(2) K	
Wavelength	0.71073 Å	
Crystal system	Trigonal	
Space group	$P\bar{3}$	
Unit cell dimensions	a = 16.251(2) Å	α = 90°.
	b = 16.251(2) Å	β = 90°.
	c = 14.599(1) Å	γ = 120°.
Volume	3338.9(7) Å^3	
Z	2	
Density (calculated)	1.913 g/cm^3	
Absorption coefficient	7.740 mm^{-1}	
F(000)	1848	
Crystal size	0.25 x 0.08 x 0.05 mm^3	
Theta range for data collection	2.791 to 24.990°.	
Index ranges	-19<=h<=17, -19<=k<=19, -17<=l<=14	
Reflections collected	16616	
Independent reflections	3835 [R(int) = 0.0415]	
Completeness to theta = 24.990°	97.9 %	
Absorption correction	Semi-empirical from equivalents	
Max. and min. transmission	0.7455 and 0.6077	
Refinement method	Full-matrix least-squares on F^2	
Data / restraints / parameters	3835 / 2 / 231	
Goodness-of-fit on F^2	1.006	
Final R indices [I>2sigma(I)]	R1 = 0.0600, wR2 = 0.1337	
R indices (all data)	R1 = 0.0708, wR2 = 0.1437	
Largest diff. peak and hole	3.243 and -3.044 e · Å^{-3}	
Diffractometer	Bruker D8 Venture	

Table A38: Atomic coordinates (x 10^4) and equivalent isotropic displacement parameters ($Å^2$ x 10^3) for [Eu{Au(L4-κS)}$_3$]. U(eq) is defined as one third of the trace of the orthogonalized U^{ij} tensor.

	x	y	z	U(eq)
C(11)	8470(9)	3432(9)	1883(8)	22(3)
C(12)	8604(14)	2421(12)	862(10)	44(4)
C(15)	8935(13)	3323(12)	-545(10)	43(3)
C(16)	8211(15)	3625(14)	-623(12)	56(5)
C(21)	8141(9)	5199(8)	4273(8)	19(2)
C(22)	8147(8)	6456(8)	5121(8)	17(2)
C(101)	9007(9)	4203(8)	2551(9)	19(1)
C(102)	9989(9)	4650(8)	2691(9)	19(1)
C(103)	10379(10)	5289(9)	3392(10)	27(3)
C(104)	9811(9)	5501(8)	3954(8)	19(1)
C(105)	8853(9)	5050(8)	3765(8)	19(1)
N(1)	8458(7)	4399(7)	3093(7)	20(2)
N(11)	8991(8)	3251(8)	1312(7)	29(3)
N(12)	8590(16)	2420(11)	-44(9)	72(6)
N(21)	8523(7)	5925(7)	4852(7)	22(2)
O(11)	7583(6)	3016(6)	1915(6)	26(2)
S(1)	8187(4)	1352(3)	1443(3)	52(1)
Au(1)	8657(1)	1818(1)	2921(1)	28(1)
Eu(1)	6667	3333	3018(1)	19(1)
O(21)	7271(6)	4645(6)	4122(6)	23(2)
N(22)	8179(7)	6649(7)	6003(8)	23(2)
C(23)	8500(9)	6201(9)	6657(8)	20(3)
C(24)	7691(8)	5236(10)	6963(9)	27(3)
C(25)	7990(10)	7389(9)	6378(9)	25(3)
C(26)	8881(11)	8344(10)	6422(13)	43(4)
S(2)	7728(2)	6987(2)	4361(2)	25(1)
C(13A)	7940(20)	1430(20)	-593(16)	43(3)
C(14A)	8701(19)	1190(20)	-910(20)	54(7)
C(13B)	8660(30)	1750(30)	-550(20)	43(3)
C(14B)	7610(30)	1060(40)	-840(30)	54(7)

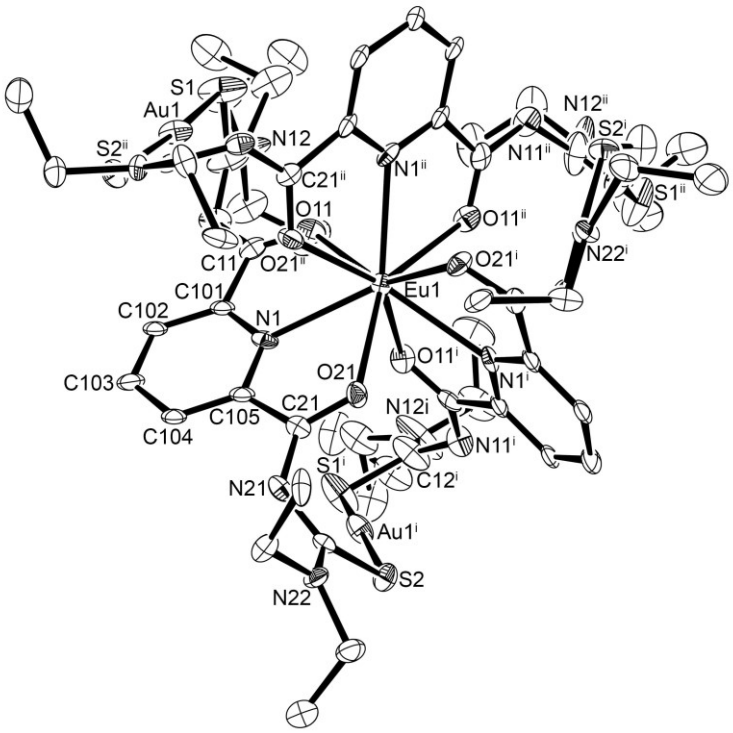

Figure A19: Ellipsoid plot of [Eu{Au(L4-κS)}$_3$]. Thermal ellipsoids are at 50 % of probability. The hydrogen atoms have been omitted for clarity.

[Eu{Au(L4-κS)}$_3$] (SQUEEZE)

Table A39: Crystal data and structure refinement for [Eu{Au(L4-κS)}$_3$]. **(SQUEEZE)**

Empirical formula	$C_{51}H_{69}Au_3EuN_{15}O_6S_6$	
Formula weight	1923.43	
Temperature	100(2) K	
Wavelength	0.71073 Å	
Crystal system	Trigonal	
Space group	$P\bar{3}$	
Unit cell dimensions	a = 16.251(2) Å	α = 90°.
	b = 16.251(2) Å	β = 90°.
	c = 14.599(1) Å	γ = 120°.
Volume	3338.9(7) Å^3	
Z	2	
Density (calculated)	1.913 g/cm^3	
Absorption coefficient	7.740 mm^{-1}	
F(000)	1848	
Crystal size	0.25 x 0.08 x 0.05 mm^3	
Theta range for data collection	2.507 to 24.990°.	
Index ranges	-19<=h<=17, -19<=k<=19, -17<=l<=14	
Reflections collected	16466	
Independent reflections	3804 [R(int) = 0.0402]	
Completeness to theta = 24.990°	97.1 %	
Absorption correction	Semi-empirical from equivalents	
Max. and min. transmission	0.7455 and 0.6077	
Refinement method	Full-matrix least-squares on F^2	
Data / restraints / parameters	3804 / 2 / 231	
Goodness-of-fit on F^2	0.847	
Final R indices [I>2sigma(I)]	R1 = 0.0535, wR2 = 0.1168	
R indices (all data)	R1 = 0.0609, wR2 = 0.1208	
Largest diff. peak and hole	2.724 and -2.809 e · Å^{-3}	
Diffractometer	Bruker D8 Venture	

Table A40: Atomic coordinates (x 10^4) and equivalent isotropic displacement parameters (Å^2 x 10^3) for [Eu{Au(L4-κS)}$_3$]. U(eq) is defined as one third of the trace of the orthogonalized U ij tensor. **(SQUEEZE)**

	x	y	z	U(eq)
C(11)	8473(8)	3431(7)	1881(7)	23(2)
C(12)	8608(12)	2425(10)	865(9)	44(4)
C(15)	8936(12)	3326(11)	-541(8)	47(3)
C(16)	8206(13)	3625(12)	-619(10)	58(4)
C(21)	8145(7)	5206(7)	4274(7)	18(2)
C(22)	8151(7)	6456(7)	5120(7)	17(2)
C(101)	9012(7)	4204(7)	2550(7)	19(1)
C(102)	9988(7)	4653(6)	2692(7)	19(1)
C(103)	10380(8)	5289(7)	3389(8)	27(3)
C(104)	9808(7)	5495(7)	3953(7)	19(1)
C(105)	8855(7)	5052(7)	3763(7)	19(1)
N(1)	8460(6)	4403(6)	3094(6)	19(2)
N(11)	8991(7)	3254(7)	1309(6)	29(2)
N(12)	8588(13)	2421(9)	-46(7)	68(5)
N(21)	8523(6)	5924(6)	4852(6)	21(2)
O(11)	7582(6)	3015(5)	1915(5)	26(2)
S(1)	8187(3)	1351(2)	1443(2)	51(1)
Au(1)	8657(1)	1818(1)	2921(1)	28(1)
Eu(1)	6667	3333	3018(1)	19(1)
O(21)	7271(5)	4645(5)	4124(5)	22(2)
N(22)	8179(6)	6649(6)	6005(6)	21(2)
C(23)	8493(8)	6194(8)	6658(7)	21(2)
C(24)	7688(7)	5230(8)	6960(8)	26(2)
C(25)	7994(8)	7396(8)	6376(8)	26(2)
C(26)	8876(9)	8345(9)	6426(10)	42(3)
S(2)	7728(2)	6987(2)	4360(2)	25(1)
C(13A)	7930(20)	1422(18)	-592(13)	47(3)
C(14A)	8710(17)	1192(18)	-906(16)	57(6)
C(13B)	8670(30)	1740(20)	-550(19)	47(3)
C(14B)	7630(30)	1040(30)	-830(30)	57(6)

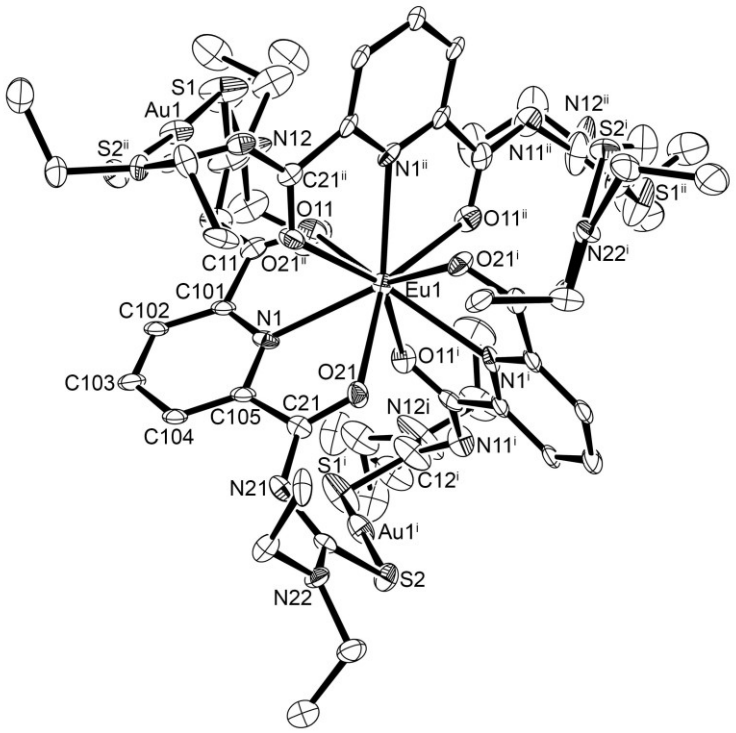

Figure A20: Ellipsoid plot of [Eu{Au(L4-κS)}$_3$]. Thermal ellipsoids are at 50 % of probability. The hydrogen atoms have been omitted for clarity. **(SQUEEZE)**

[Gd{Au(L4-κS)}$_3$]

Table A41: Crystal data and structure refinement for [Gd{Au(L4-κS)}$_3$].

Empirical formula	$C_{51}H_{69}Au_3GdN_{15}O_6S_6$	
Formula weight	1928.72	
Temperature	100(2) K	
Wavelength	0.71073 Å	
Crystal system	Trigonal	
Space group	$P\bar{3}$	
Unit cell dimensions	a = 16.250(1) Å	α = 90°.
	b = 16.250(1) Å	β = 90°.
	c = 14.596(1) Å	γ = 120°.
Volume	3337.9(5) Å^3	
Z	2	
Density (calculated)	1.919 g/cm^3	
Absorption coefficient	7.796 mm^{-1}	
F(000)	1850	
Crystal size	0.26 x 0.11 x 0.05 mm^3	
Theta range for data collection	2.507 to 27.134°.	
Index ranges	-20<=h<=20, -20<=k<=20, -18<=l<=18	
Reflections collected	73896	
Independent reflections	4930 [R(int) = 0.0584]	
Completeness to theta = 25.242°	99.9 %	
Absorption correction	Semi-empirical from equivalents	
Max. and min. transmission	0.1506 and 0.0757	
Refinement method	Full-matrix least-squares on F^2	
Data / restraints / parameters	4930 / 4 / 251	
Goodness-of-fit on F^2	1.089	
Final R indices [I>2sigma(I)]	R1 = 0.0524, wR2 = 0.1269	
R indices (all data)	R1 = 0.0590, wR2 = 0.1309	
Largest diff. peak and hole	4.390 and -3.582 e · Å^{-3}	
Diffractometer	Bruker D8 Venture	

Table A42: Atomic coordinates (x 10^4) and equivalent isotropic displacement parameters (Å^2 x 10^3)

for [Gd{Au(L4-κS)}$_3$]. U(eq) is defined as one third of the trace of the orthogonalized U^{ij} tensor.

	x	y	z	U(eq)
C(101)	3804(6)	4962(6)	3774(6)	22(2)
C(102)	4306(6)	4505(6)	3965(6)	24(2)
C(103)	5089(6)	4708(6)	3417(7)	28(2)
C(104)	5328(6)	5346(6)	2698(6)	27(2)
C(105)	4785(6)	5785(6)	2573(6)	23(2)
C(11)	2937(6)	4801(6)	4287(5)	20(2)
C(12)	1691(6)	3550(6)	5118(5)	20(2)
C(13)	588(6)	2607(6)	6366(6)	26(2)
C(14)	530(7)	1655(7)	6413(8)	41(2)
C(15)	2292(6)	3804(6)	6662(6)	27(2)
C(16)	2459(7)	4776(7)	6957(7)	33(2)
C(21)	5019(6)	6559(6)	1890(6)	25(2)
C(22)	6172(8)	7562(8)	861(7)	45(3)
C(23)	5594(8)	6654(9)	-544(7)	55(3)
C(24)	4569(9)	6366(10)	-630(8)	57(3)
N(1)	4048(5)	5597(5)	3104(5)	20(1)
N(11)	2594(5)	4077(5)	4856(5)	24(2)
N(12)	1513(5)	3346(5)	6008(5)	23(1)
N(21)	5717(5)	6735(6)	1304(5)	30(2)
O(11)	2626(4)	5357(4)	4133(4)	24(1)
O(21)	4563(5)	6988(5)	1926(4)	30(1)
S(1)	737(2)	3016(2)	4355(2)	28(1)
S(2)	6821(3)	8635(2)	1436(2)	58(1)
Gd(1)	3333	6667	3029(1)	22(1)
Au(1)	1343(1)	3170(1)	2918(1)	32(1)
N(22A)	6317(9)	7505(9)	-45(7)	23(1)
C(25A)	6478(13)	8499(13)	-593(12)	33(3)
C(26A)	7481(15)	8804(16)	-933(14)	46(4)
N(22B)	5992(11)	7610(9)	-48(8)	23(1)
C(25B)	7002(14)	8299(13)	-590(12)	33(3)
C(26B)	6554(18)	8913(18)	-818(16)	46(4)

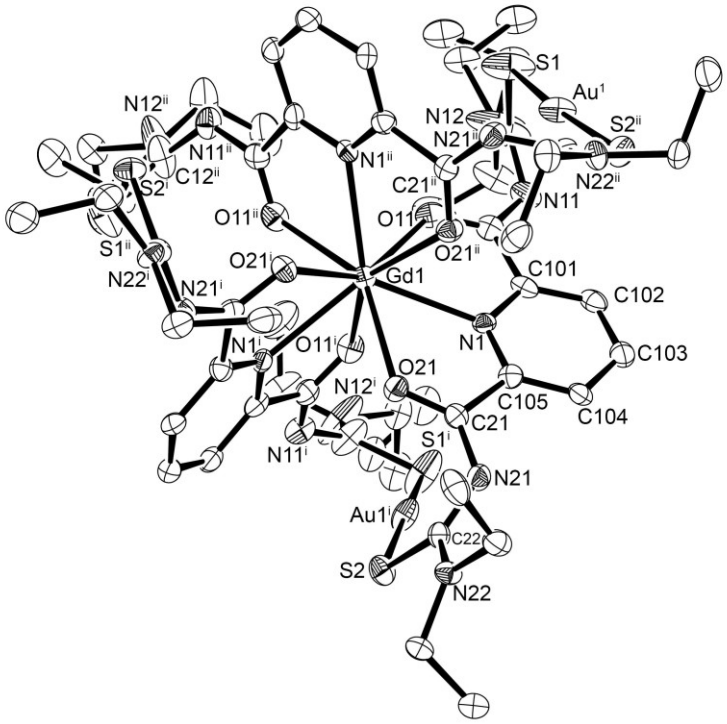

Figure A21: Ellipsoid plot of [Gd{Au(L4-κS)}$_3$]. Thermal ellipsoids are at 50 % of probability. The hydrogen atoms have been omitted for clarity.

[Gd{Au(L4-κS)}$_3$] (SQUEEZE)

Table A43: Crystal data and structure refinement for [Gd{Au(L4-κS)}$_3$]. **(SQUEEZE)**

Empirical formula	$C_{51}H_{69}Au_3GdN_{15}O_6S_6$	
Formula weight	1928.72	
Temperature	100(2) K	
Wavelength	0.71073 Å	
Crystal system	Trigonal	
Space group	$P\bar{3}$	
Unit cell dimensions	a = 16.250(1) Å	α = 90°.
	b = 16.250(1) Å	β = 90°.
	c = 14.596(1) Å	γ = 120°.
Volume	3337.9(5) Å^3	
Z	2	
Density (calculated)	1.919 g/cm^3	
Absorption coefficient	7.796 mm^{-1}	
F(000)	1850	
Crystal size	0.26 x 0.11 x 0.05 mm^3	
Theta range for data collection	2.507 to 27.134°.	
Index ranges	-20<=h<=20, -20<=k<=20, -18<=l<=18	
Reflections collected	73896	
Independent reflections	4930 [R(int) = 0.0564]	
Completeness to theta = 25.242°	99.9 %	
Absorption correction	Semi-empirical from equivalents	
Max. and min. transmission	0.1506 and 0.0757	
Refinement method	Full-matrix least-squares on F^2	
Data / restraints / parameters	4930 / 2 / 254	
Goodness-of-fit on F^2	1.249	
Final R indices [I>2sigma(I)]	R1 = 0.0490, wR2 = 0.0921	
R indices (all data)	R1 = 0.0528, wR2 = 0.0935	
Largest diff. peak and hole	3.112 and -3.246 e · Å^{-3}	
Diffractometer	Bruker D8 Venture	

Table A44: Atomic coordinates (x 10^4) and equivalent isotropic displacement parameters ($Å^2$ x 10^3) for [Gd{Au(L4-κS)}$_3$]. U(eq) is defined as one third of the trace of the orthogonalized U^{ij} tensor. **(SQUEEZE)**

	x	y	z	U(eq)
C(101)	4788(5)	5783(5)	2573(5)	23(1)
C(102)	5328(5)	5344(5)	2698(5)	26(2)
C(103)	5089(5)	4708(5)	3418(5)	28(2)
C(104)	4307(5)	4506(5)	3967(5)	24(1)
C(105)	3806(5)	4963(5)	3774(5)	22(1)
C(11)	5024(5)	6560(5)	1890(5)	25(1)
C(12)	6172(6)	7563(7)	859(5)	45(2)
C(21)	2935(5)	4802(5)	4287(4)	21(1)
C(22)	1693(5)	3552(5)	5118(4)	20(1)
C(23)	587(5)	2604(5)	6365(5)	26(2)
C(24)	530(6)	1653(6)	6417(7)	41(2)
C(25)	2294(5)	3805(5)	6663(5)	26(2)
C(26)	2459(5)	4777(6)	6958(5)	32(2)
N(1)	4049(4)	5596(4)	3103(4)	20(1)
N(11)	5718(4)	6733(5)	1304(4)	31(1)
N(12)	6164(7)	7558(6)	-45(5)	74(3)
N(21)	2594(4)	4078(4)	4857(4)	25(1)
N(22)	1513(4)	3346(4)	6007(4)	21(1)
O(11)	4561(4)	6987(4)	1928(3)	29(1)
O(21)	2626(3)	5359(3)	4134(3)	24(1)
S(1)	6821(2)	8636(2)	1437(1)	58(1)
S(2)	738(1)	3017(1)	4355(1)	28(1)
Gd(1)	3333	6667	3029(1)	22(1)
Au(1)	6830(1)	8173(1)	2918(1)	32(1)
C(15A)	7000(11)	8300(11)	-592(10)	34(3)
C(16A)	6558(15)	8921(15)	-819(14)	49(4)
C(15B)	6475(11)	8507(11)	-593(9)	34(3)
C(16B)	7484(12)	8812(13)	-928(11)	49(4)
C(13)	5602(7)	6652(8)	-542(6)	56(3)
C(14)	4571(7)	6366(8)	-629(7)	59(3)

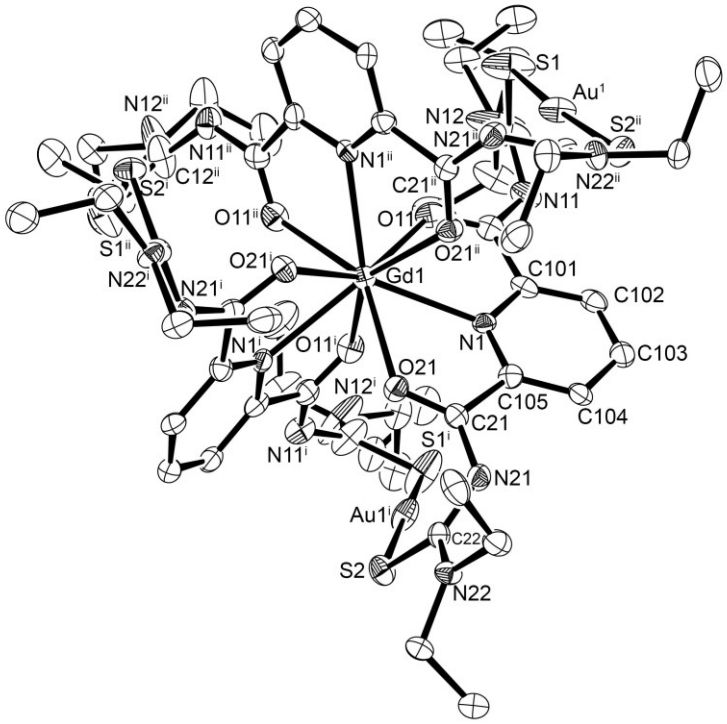

Figure A22: Ellipsoid plot of [Gd{Au(L4-κS)}$_3$]. Thermal ellipsoids are at 50 % of probability. The hydrogen atoms have been omitted for clarity. **(SQUEEZE)**

[Tb{Au(L4-κS)}$_3$] · 0.5CHCl$_3$

Table A45: Crystal data and structure refinement for [Tb{Au(L4-κS)}$_3$] · 0.5CHCl$_3$.

Empirical formula	$C_{51.5}H_{69}Au_3Cl_{1.5}N_{15}O_6S_6Tb$	
Formula weight	1989.57	
Temperature	104(2) K	
Wavelength	0.71073 Å	
Crystal system	Triclinic	
Space group	$P\bar{1}$	
Unit cell dimensions	a = 16.236(1) Å	α = 90°. *
	b = 16.236(1) Å	β = 90°.
	c = 14.588(1) Å	γ = 120°.
Volume	3330.1(4) Å^3	
Z	2	
Density (calculated)	1.984 g/cm^3	
Absorption coefficient	7.880 mm^{-1}	
F(000)	1909	
Crystal size	0.26 x 0.12 x 0.08 mm^3	
Theta range for data collection	2.509 to 27.148°.	
Index ranges	-20<=h<=20, -20<=k<=20, -18<=l<=18	
Reflections collected	74613	
Independent reflections	14671 [R(int) = 0.0412]	
Completeness to theta = 25.242°	99.8 %	
Absorption correction	Semi-empirical from equivalents	
Max. and min. transmission	0.7455 and 0.4724	
Refinement method	Full-matrix least-squares on F^2	
Data / restraints / parameters	14671 / 21 / 824	
Goodness-of-fit on F^2	1.041	
Final R indices [I>2sigma(I)]	R1 = 0.0309, wR2 = 0.0631	
R indices (all data)	R1 = 0.0371, wR2 = 0.0659	
Largest diff. peak and hole	2.027 and -2.514 e · Å^{-3}	
Diffractometer	Bruker D8 Venture	

* The unit cell parameters of the trigonal cell were kept for comparison with the squeezed structure.

Table A46: Atomic coordinates (x 10^4) and equivalent isotropic displacement parameters ($Å^2$ x 10^3) for [Tb{Au(L4-κS)}$_3$] · 0.5$CHCl_3$. U(eq) is defined as one third of the trace of the orthogonalized U^{ij} tensor.

	x	y	z	U(eq)
Au(1)	3180(1)	6821(1)	2921(1)	27(1)
Tb(1)	6667(1)	8334(1)	3033(1)	17(1)
Au(2)	8179(1)	6360(1)	2921(1)	27(1)
Au(3)	8641(1)	11820(1)	2921(1)	27(1)
S(2)	9256(1)	11976(1)	4354(1)	23(1)
S(6)	7719(1)	5742(1)	4355(1)	24(1)
S(4)	3024(1)	7281(1)	4356(1)	24(1)
S(3)	8651(1)	6841(2)	1444(1)	57(1)
S(1)	3188(1)	6350(1)	1445(1)	57(1)
O(21)	7374(2)	9634(2)	4135(2)	19(1)
N(1)	5951(3)	9394(3)	3102(2)	16(1)
S(5)	8161(2)	11812(1)	1444(1)	57(1)
O(61)	7262(2)	7628(2)	4136(2)	19(1)
O(41)	5367(2)	7738(2)	4137(2)	19(1)
O(31)	7000(2)	7444(3)	1937(2)	24(1)
N(41)	4087(3)	6490(3)	4859(3)	20(1)
N(61)	8508(3)	7595(3)	4862(3)	20(1)
N(42)	3349(3)	6835(3)	6007(3)	18(1)
N(62)	8164(3)	6513(3)	6006(3)	18(1)
N(2)	5607(3)	6558(3)	3103(2)	16(1)
N(21)	7403(3)	10914(3)	4861(3)	19(1)
N(22)	8486(3)	11650(3)	6005(3)	19(1)
N(3)	8439(3)	9050(3)	3103(2)	16(1)
C(105)	6191(3)	10028(3)	3776(3)	17(1)
C(202)	5351(3)	5030(3)	2688(3)	21(1)
C(305)	8839(3)	8809(3)	3775(3)	18(1)
C(205)	4970(3)	6164(3)	3776(3)	18(1)
C(41)	4805(3)	6870(3)	4287(3)	17(1)
N(31)	6744(3)	6038(3)	1304(3)	28(1)
C(62)	8138(3)	6692(3)	5115(3)	16(1)
C(102)	4679(3)	9650(3)	2691(3)	21(1)
C(302)	9969(3)	10319(3)	2692(3)	21(1)
C(101)	5216(3)	9208(3)	2561(3)	19(1)

C(201)	5791(3)	6007(3)	2562(3)	18(1)
C(22)	8308(3)	11444(3)	5118(3)	16(1)
C(21)	7064(3)	10193(3)	4286(3)	16(1)
C(104)	5690(3)	10490(3)	3961(3)	20(1)
C(61)	8128(3)	7938(3)	4283(3)	17(1)
C(301)	8993(3)	9784(3)	2564(3)	19(1)
C(23)	9411(3)	12394(4)	6365(3)	23(1)
C(42)	3557(3)	6862(3)	5120(3)	17(1)
C(31)	6572(3)	6554(4)	1887(3)	23(1)
C(43)	2606(3)	7018(3)	6367(3)	22(1)
C(63)	7984(3)	5592(3)	6368(3)	23(1)
C(64)	8886(4)	5535(4)	6416(5)	39(1)
C(203)	4712(3)	4630(4)	3409(4)	26(1)
C(44)	1649(4)	6111(4)	6415(5)	39(1)
C(103)	4913(3)	10289(3)	3406(4)	25(1)
C(24)	9467(4)	13353(4)	6417(5)	39(1)
C(303)	10372(4)	10083(4)	3406(3)	25(1)
O(51)	7556(2)	9556(2)	1936(2)	24(1)
O(11)	5445(2)	8001(2)	1936(2)	24(1)
C(204)	4510(3)	5201(3)	3963(3)	19(1)
N(11)	4293(3)	8256(3)	1301(3)	28(1)
C(304)	9802(3)	9311(3)	3958(3)	20(1)
N(51)	8966(3)	10708(3)	1303(3)	28(1)
C(11)	4981(3)	8428(3)	1889(3)	22(1)
C(65)	8487(3)	7294(3)	6664(3)	20(1)
C(45)	3805(3)	6509(3)	6668(3)	22(1)
C(25)	7705(3)	11193(4)	6666(3)	22(1)
C(51)	8448(4)	10023(3)	1888(3)	23(1)
C(46)	4772(4)	7314(4)	6961(3)	29(1)
C(26)	7542(4)	10223(4)	6962(4)	29(1)
C(66)	7680(4)	7453(4)	6963(4)	29(1)
C(12)	3842(4)	7426(5)	860(4)	44(2)
C(52)	8587(6)	11167(4)	862(4)	45(2)
C(34)	6377(5)	6806(6)	-628(4)	50(2)
C(33)	6664(5)	6051(6)	-542(4)	50(2)
N(52A)	8603(6)	11175(5)	-47(3)	73(2)
C(53A)	7959(11)	11497(9)	-590(8)	28(4)

C(54A)	8630(9)	12507(8)	-900(8)	34(4)
N(52B)	8603(6)	11175(5)	-47(3)	73(2)
C(53B)	8681(9)	11992(9)	-597(7)	37(3)
C(54B)	7635(10)	11531(13)	-817(11)	51(4)
C(56)	8202(5)	9580(5)	-627(4)	48(2)
C(55)	8944(6)	10611(4)	-542(4)	51(2)
N(12A)	3682(7)	7525(9)	-16(8)	28(3)
C(13A)	3044(9)	6712(8)	-586(7)	33(4)
C(14A)	3459(14)	6082(12)	-827(11)	48(5)
N(12B)	3947(9)	7348(7)	-73(7)	25(3)
C(13B)	3506(8)	6444(9)	-599(8)	29(3)
C(14B)	2498(9)	6131(10)	-891(8)	42(4)
C(16)	5427(5)	8624(5)	-626(4)	47(2)
C(15)	4388(4)	8329(5)	-543(4)	51(2)
C(32A)	7489(17)	6250(10)	868(8)	18(4)
N(32A)	7570(4)	6399(6)	-48(3)	73(2)
C(35A)	8297(8)	6319(8)	-594(7)	30(2)
C(36A)	8907(10)	7375(9)	-818(9)	41(2)
C(32B)	7674(14)	6591(11)	853(8)	20(3)
N(32B)	7570(4)	6399(6)	-48(3)	73(2)
C(35B)	8536(8)	7044(9)	-586(7)	30(2)
C(36B)	8867(9)	6360(9)	-900(8)	41(2)
Cl(2)	328(9)	6088(8)	8621(5)	158(2)
Cl(1)	713(10)	4655(9)	8625(5)	158(2)
Cl(3)	-1057(9)	4260(9)	8628(5)	158(2)
Cl(4)	0(11)	5001(13)	10200(4)	158(2)
C(100)	9(11)	5026(11)	9061(8)	158(2)

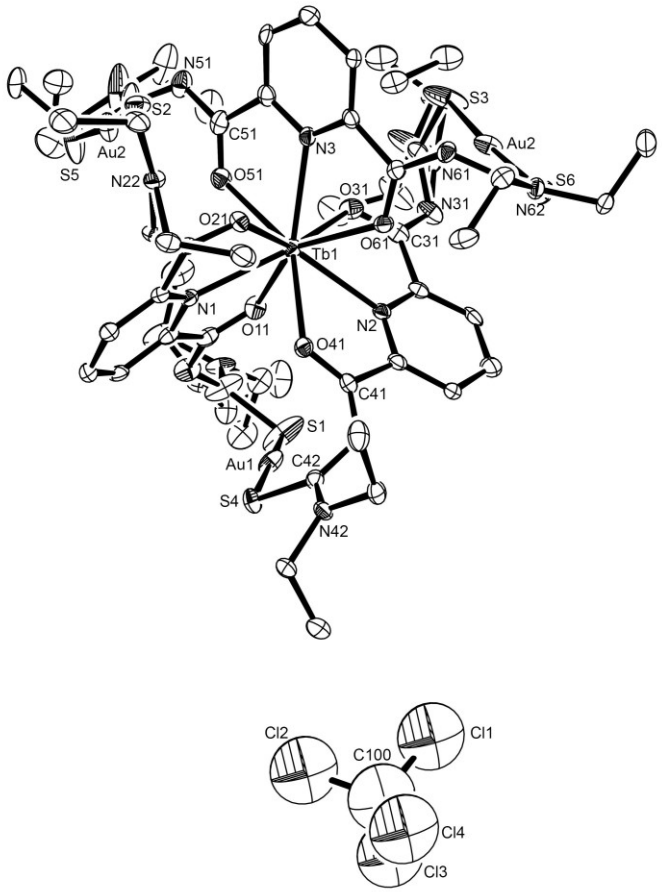

Figure A23: Ellipsoid plot of [Tb{Au(L4-κS)}$_3$] · 0.5$CHCl_3$. Thermal ellipsoids are at 50 % of probability. The hydrogen atoms have been omitted for clarity.

[Tb{Au(L4-κS)}$_3$] (SQUEEZE)

Table A47: Crystal data and structure refinement for [Tb[Au(L4-κS)}$_3$]. **(SQUEEZE)**

Empirical formula	$C_{51}H_{69}Au_3N_{15}O_6S_6Tb$	
Formula weight	1930.39	
Temperature	104(2) K	
Wavelength	0.71073 Å	
Crystal system	Trigonal	
Space group	$P\bar{3}$	
Unit cell dimensions	a = 16.236(1) Å	α = 90°.
	b = 16.236(1) Å	β = 90°.
	c = 14.588(1) Å	γ = 120°.
Volume	3330.1(5) Å^3	
Z	2	
Density (calculated)	1.925 g/cm^3	
Absorption coefficient	7.880 mm^{-1}	
F(000)	1852	
Crystal size	0.26 x 0.12 x 0.08 mm^3	
Theta range for data collection	2.509 to 27.148°.	
Index ranges	-20<=h<=20, -20<=k<=20, -18<=l<=18	
Reflections collected	74613	
Independent reflections	4911 [R(int) = 0.0434]	
Completeness to theta = 25.242°	99.9 %	
Absorption correction	Semi-empirical from equivalents	
Max. and min. transmission	0.7455 and 0.4724	
Refinement method	Full-matrix least-squares on F^2	
Data / restraints / parameters	4911 / 21 / 254	
Goodness-of-fit on F^2	1.101	
Final R indices [I>2sigma(I)]	R1 = 0.0265, wR2 = 0.0543	
R indices (all data)	R1 = 0.0283, wR2 = 0.0550	
Largest diff. peak and hole	1.688 and -2.863 e · Å^{-3}	
Diffractometer	Bruker D8 Venture	

Table A48: Atomic coordinates (x 10^4) and equivalent isotropic displacement parameters ($Å^2$ x 10^3) for [Tb{Au(L4-κS)}$_3$]. U(eq) is defined as one third of the trace of the orthogonalized U^{ij} tensor. **(SQUEEZE)**

	x	y	z	U(eq)
Tb(1)	3333	6667	1967(1)	16(1)
Au(2)	6820(1)	8179(1)	2079(1)	26(1)
S(1)	6976(1)	7720(1)	645(1)	23(1)
O(11)	4633(2)	7260(2)	865(2)	18(1)
S(2)	6812(1)	8650(1)	3556(1)	56(1)
O(21)	4555(2)	6999(2)	3064(2)	23(1)
N(11)	5913(2)	8511(2)	138(2)	19(1)
N(1)	4049(2)	5607(2)	1897(2)	16(1)
N(12)	6651(2)	8166(2)	-1006(2)	18(1)
C(101)	3809(2)	4971(2)	1224(2)	17(1)
N(21)	5707(2)	6743(3)	3698(2)	27(1)
C(11)	5191(3)	8129(3)	716(2)	16(1)
C(102)	4310(3)	4509(3)	1040(3)	19(1)
C(12)	6444(2)	8136(2)	-119(2)	15(1)
C(21)	5020(3)	6574(3)	3111(3)	22(1)
C(13)	7392(3)	7983(3)	-1366(3)	22(1)
C(14)	8351(3)	8886(3)	-1413(4)	38(1)
C(22)	6162(3)	7578(4)	4140(3)	43(1)
C(105)	4784(3)	5790(2)	2435(2)	18(1)
C(104)	5322(2)	5353(3)	2310(3)	20(1)
C(103)	5087(3)	4711(3)	1589(3)	24(1)
C(15)	6194(3)	8491(3)	-1667(2)	20(1)
C(16)	5225(3)	7681(3)	-1963(3)	28(1)
C(26)	4574(4)	6378(4)	5628(4)	48(1)
N(22A)	6170(4)	7570(4)	5048(3)	69(2)
C(23A)	6485(6)	8545(7)	5588(6)	33(1)
C(24A)	7502(7)	8867(8)	5899(6)	44(2)
N(22B)	6170(4)	7570(4)	5048(3)	69(2)
C(23B)	6973(7)	8296(7)	5598(6)	33(1)
C(24B)	6542(9)	8918(9)	5833(8)	44(2)
C(25)	5612(4)	6663(4)	5542(3)	50(2)

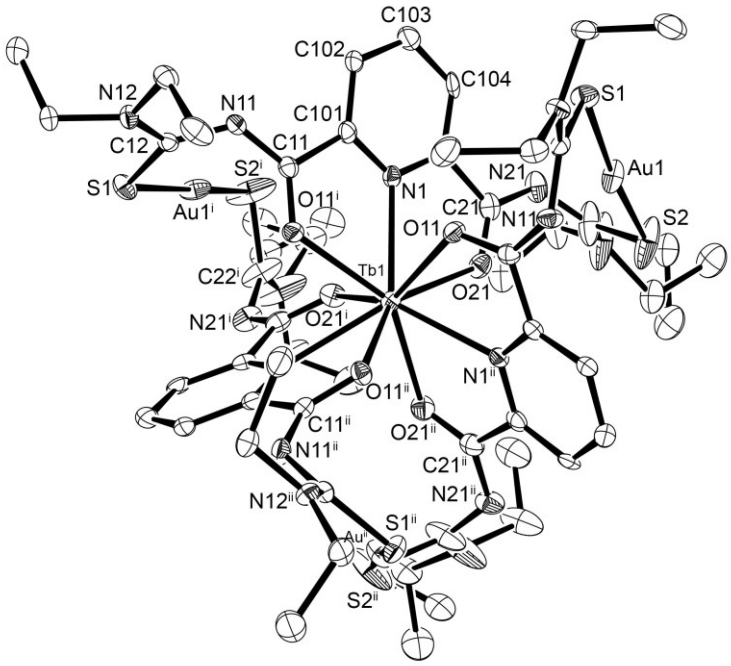

Figure A24: Ellipsoid plot of [Tb{Au(L4-κS)}$_3$]. Thermal ellipsoids are at 50 % of probability. The hydrogen atoms have been omitted for clarity. **(SQUEEZE)**

[Dy{Au(L4-κS)}$_3$]

Table A49: Crystal data and structure refinement for [Dy{Au(L4-κS)}$_3$].

Empirical formula	$C_{51}H_{69}Au_3DyN_{15}O_6S_6$	
Formula weight	1933.97	
Temperature	133(2) K	
Wavelength	0.71073 Å	
Crystal system	Trigonal	
Space group	$P\bar{3}$	
Unit cell dimensions	a = 16.212(1) Å	α = 90°.
	b = 16.212(1) Å	β = 90°.
	c = 14.601(1) Å	γ = 120°.
Volume	3323.4(5) Å^3	
Z	2	
Density (calculated)	1.933 g/cm^3	
Absorption coefficient	7.956 mm^{-1}	
F(000)	1854	
Crystal size	0.29 x 0.13 x 0.08 mm^3	
Theta range for data collection	2.513 to 27.150°.	
Index ranges	-20<=h<=20, -20<=k<=20, -18<=l<=18	
Reflections collected	32962	
Independent reflections	4891 [R(int) = 0.0823]	
Completeness to theta = 25.242°	99.9 %	
Absorption correction	Semi-empirical from equivalents	
Max. and min. transmission	0.1506 and 0.0785	
Refinement method	Full-matrix least-squares on F^2	
Data / restraints / parameters	4891 / 4 / 215	
Goodness-of-fit on F^2	1.200	
Final R indices [I>2sigma(I)]	R1 = 0.0730, wR2 = 0.1583	
R indices (all data)	R1 = 0.0933, wR2 = 0.1658	
Largest diff. peak and hole	4.134 and -3.919 e · Å^{-3}	
Diffractometer	Bruker D8 Venture	

Table A50: Atomic coordinates (x 10^4) and equivalent isotropic displacement parameters ($Å^2$x 10^3) for [Dy{Au(L4-κS)}$_3$]. U(eq) is defined as one third of the trace of the orthogonalized U^{ij} tensor.

	x	y	z	U(eq)
C(101)	4965(9)	3806(9)	6226(9)	23(1)
C(102)	4515(9)	4306(9)	6049(9)	23(1)
C(103)	4720(9)	5078(9)	6615(9)	23(1)
C(104)	5346(9)	5324(9)	7320(9)	23(1)
C(105)	5801(9)	4790(9)	7439(9)	23(1)
C(11)	4822(9)	2943(9)	5710(8)	21(3)
C(12)	3565(9)	1699(9)	4881(8)	20(3)
C(13)	2604(9)	596(9)	3638(10)	26(3)
C(14)	1659(11)	550(11)	3584(13)	47(4)
C(15)	3799(10)	2293(10)	3330(9)	29(3)
C(16)	4765(11)	2447(11)	3016(10)	36(4)
C(21)	6587(9)	5016(10)	8114(8)	23(3)
C(22)	7592(12)	6158(12)	9122(10)	44(4)
C(23)	6702(13)	5634(13)	10540(10)	49(4)
C(24)	6404(15)	4583(14)	10621(12)	61(5)
N(1)	5612(7)	4044(8)	6898(7)	21(2)
N(11)	4111(8)	2618(8)	5131(7)	23(2)
N(12)	3359(8)	1524(8)	3989(7)	26(2)
N(21)	6765(8)	5715(9)	8695(8)	30(3)
O(11)	5382(6)	2635(6)	5863(6)	21(2)
O(21)	7004(6)	4555(7)	8061(6)	26(2)
S(1)	3040(3)	750(3)	5639(2)	30(1)
S(2)	8668(3)	6811(4)	8545(3)	51(1)
Dy(1)	6667	3333	6967(1)	20(1)
Au(1)	3183(1)	1368(1)	7070(1)	30(1)
N(22A)	7588(13)	6296(15)	10036(10)	26(2)
C(25A)	8550(20)	6480(20)	10580(19)	49(4)
C(26A)	8780(30)	7470(20)	10920(20)	61(5)
N(22B)	7626(14)	5990(20)	10034(12)	26(2)
C(25B)	8330(30)	6980(30)	10560(20)	49(4)
C(26B)	8950(40)	6550(30)	10820(30)	61(5)

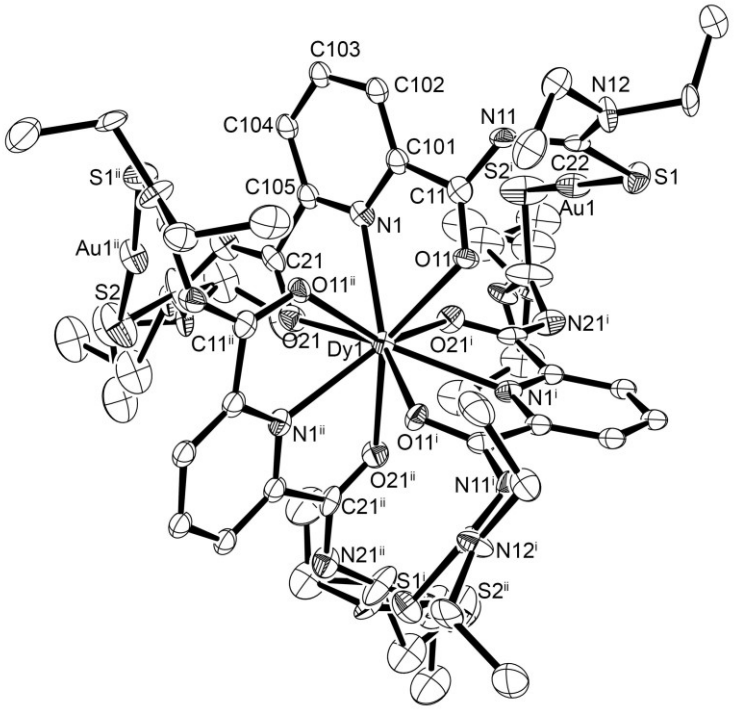

Figure A25: Ellipsoid plot of [Dy{Au(L4-κS)}$_3$]. Thermal ellipsoids are at 50 % of probability. The hydrogen atoms have been omitted for clarity.

[Dy{Au(L4-κS)}$_3$] (SQUEEZE)

Table A51: Crystal data and structure refinement for [Dy{Au(L4-κS)}$_3$]. **(SQUEEZE)**

Empirical formula	$C_{51}H_{69}Au_3DyN_{15}O_6S_6$	
Formula weight	1933.97	
Temperature	133(2) K	
Wavelength	0.71073 Å	
Crystal system	Trigonal	
Space group	$P\bar{3}$	
Unit cell dimensions	a = 16.212(1) Å	α = 90°.
	b = 16.212(1) Å	β = 90°.
	c = 14.601(1) Å	γ = 120°.
Volume	3323.4(5) Å^3	
Z	2	
Density (calculated)	1.933 g/cm^3	
Absorption coefficient	7.956 mm^{-1}	
F(000)	1854	
Crystal size	0.29 x 0.13 x 0.08 mm^3	
Theta range for data collection	2.790 to 24.973°.	
Index ranges	-19<=h<=19, -19<=k<=19, -17<=l<=17	
Reflections collected	26824	
Independent reflections	3869 [R(int) = 0.0697]	
Completeness to theta = 24.973°	99.1 %	
Absorption correction	Semi-empirical from equivalents	
Max. and min. transmission	0.1506 and 0.0785	
Refinement method	Full-matrix least-squares on F^2	
Data / restraints / parameters	3869 / 4 / 210	
Goodness-of-fit on F^2	1.124	
Final R indices [I>2sigma(I)]	R1 = 0.0634, wR2 = 0.1362	
R indices (all data)	R1 = 0.0762, wR2 = 0.1420	
Largest diff. peak and hole	3.208 and -3.146 e · Å^{-3}	
Diffractometer	Bruker D8 Venture	

Table A52: Atomic coordinates (x 10^4) and equivalent isotropic displacement parameters ($Å^2$ x 10^3) for [Dy{Au(L4-κS)}$_3$]. U(eq) is defined as one third of the trace of the orthogonalized U^{ij} tensor. **(SQUEEZE)**

	x	y	z	U(eq)
C(101)	4963(8)	3802(8)	6226(8)	22(1)
C(102)	4523(8)	4312(8)	6048(8)	22(1)
C(103)	4717(8)	5080(8)	6616(8)	22(1)
C(104)	5343(8)	5322(8)	7321(8)	22(1)
C(105)	5799(8)	4795(8)	7437(8)	22(1)
C(11)	4828(8)	2947(8)	5711(7)	22(2)
C(12)	3566(7)	1704(8)	4879(7)	18(2)
C(13)	2602(8)	601(8)	3638(8)	26(3)
C(14)	1649(10)	550(10)	3581(11)	47(4)
C(15)	3799(9)	2298(9)	3327(8)	28(3)
C(16)	4766(10)	2453(9)	3020(9)	36(3)
C(21)	6586(8)	5017(8)	8113(7)	24(3)
C(22)	7594(10)	6159(10)	9124(9)	44(4)
C(23)	6706(11)	5632(11)	10539(9)	50(4)
C(24)	6404(12)	4583(12)	10622(10)	60(4)
N(1)	5615(6)	4047(7)	6899(6)	21(2)
N(11)	4110(7)	2616(7)	5132(6)	23(2)
N(12)	3359(7)	1521(7)	3989(6)	26(2)
N(21)	6766(7)	5715(8)	8695(7)	31(2)
O(11)	5385(5)	2637(5)	5864(5)	21(2)
O(21)	7008(6)	4553(6)	8059(5)	27(2)
S(1)	3039(2)	750(2)	5639(2)	30(1)
S(2)	8668(3)	6811(3)	8544(2)	51(1)
Dy(1)	6667	3333	6967(1)	20(1)
Au(1)	3183(1)	1368(1)	7070(1)	30(1)
N(22A)	7589(11)	6290(12)	10037(9)	26(2)
C(25A)	8563(19)	6494(18)	10587(16)	50(4)
C(26A)	8800(20)	7494(19)	10903(18)	60(4)
N(22B)	7629(13)	5984(19)	10035(11)	26(2)
C(25B)	8320(20)	7000(20)	10550(20)	50(4)
C(26B)	8960(30)	6580(30)	10800(30)	60(4)

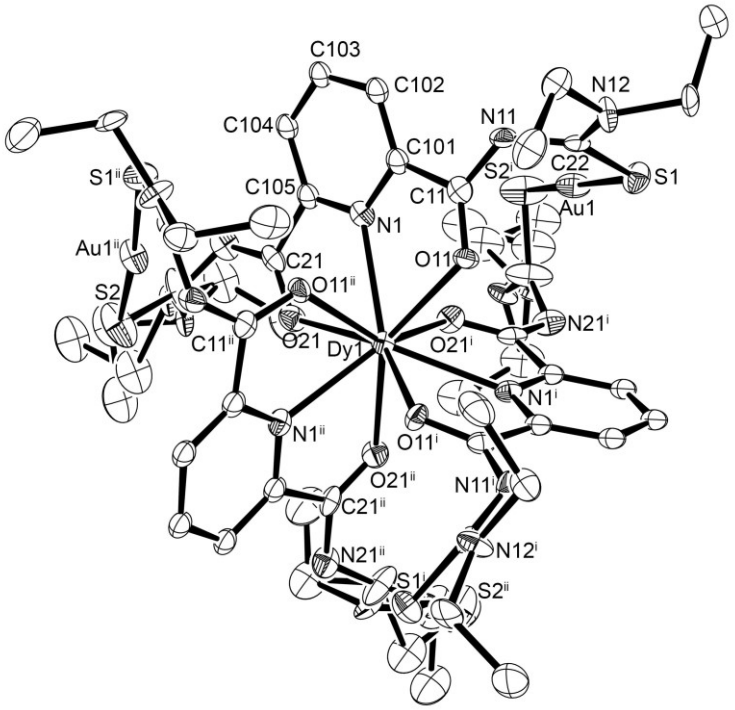

Figure A26: Ellipsoid plot of [Dy{Au(L4-κS)}$_3$]. Thermal ellipsoids are at 50 % of probability. The hydrogen atoms have been omitted for clarity. **(SQUEEZE)**

[Ho{Au(L4-κS)}$_3$]

Table A53: Crystal data and structure refinement for [Ho{Au(L4-κS)}$_3$].

Empirical formula	$C_{51}H_{69}Au_3HoN_{15}O_6S_6$	
Formula weight	1936.40	
Temperature	105(2) K	
Wavelength	0.71073 Å	
Crystal system	Trigonal	
Space group	$P\bar{3}$	
Unit cell dimensions	a = 16.2209(9) Å	α = 90°.
	b = 16.2209(9) Å	β = 90°.
	c = 14.6230(9) Å	γ = 120°.
Volume	3332.1(4) Å^3	
Z	2	
Density (calculated)	1.930 g/cm^3	
Absorption coefficient	8.002 mm^{-1}	
F(000)	1856	
Crystal size	0.19 x 0.17 x 0.09 mm^3	
Theta range for data collection	2.511 to 27.178°.	
Index ranges	-20<=h<=20, -20<=k<=20, -18<=l<=18	
Reflections collected	79051	
Independent reflections	4926 [R(int) = 0.0630]	
Completeness to theta = 25.242°	99.9 %	
Absorption correction	Semi-empirical from equivalents	
Max. and min. transmission	0.7454 and 0.3292	
Refinement method	Full-matrix least-squares on F^2	
Data / restraints / parameters	4926 / 4 / 252	
Goodness-of-fit on F^2	1.122	
Final R indices [I>2sigma(I)]	R1 = 0.0437, wR2 = 0.1096	
R indices (all data)	R1 = 0.0498, wR2 = 0.1128	
Largest diff. peak and hole	6.153 and -2.454 e · Å^{-3}	
Diffractometer	Bruker D8 Venture	

Table A54: Atomic coordinates (x 10^4) and equivalent isotropic displacement parameters ($Å^2$ x 10^3) for [Ho{Au(L4-κS)}$_3$]. U(eq) is defined as one third of the trace of the orthogonalized U^{ij} tensor.

	x	y	z	U(eq)
C(101)	1177(5)	4985(5)	6224(5)	17(1)
C(102)	208(5)	4517(5)	6051(5)	20(1)
C(103)	-366(5)	4713(5)	6613(6)	25(2)
C(104)	37(5)	5351(5)	7327(5)	21(2)
C(105)	1022(5)	5801(5)	7441(5)	19(1)
C(11)	1878(5)	4823(5)	5711(5)	17(1)
C(12)	1872(5)	3569(5)	4879(5)	16(1)
C(13)	1516(5)	3802(6)	3327(5)	23(2)
C(14)	2309(6)	4766(6)	3020(6)	31(2)
C(15)	2015(5)	2605(5)	3639(5)	23(2)
C(16)	1107(6)	1638(6)	3604(8)	40(2)
C(21)	1580(6)	6589(5)	8110(5)	22(2)
C(22)	1447(9)	7595(7)	9137(6)	42(2)
C(23)	1087(9)	6698(8)	10540(6)	48(3)
C(24)	1827(9)	6408(8)	10625(7)	48(3)
Au(1)	1817(1)	3193(1)	7073(1)	27(1)
Ho(1)	3333	6667	6960(1)	17(1)
N(1)	1576(4)	5622(4)	6895(4)	16(1)
N(11)	1497(4)	4108(4)	5130(4)	20(1)
N(12)	1835(4)	3354(5)	3991(4)	21(1)
N(21)	1068(5)	6759(5)	8698(4)	29(2)
O(11)	2747(3)	5384(3)	5857(3)	19(1)
O(21)	2467(4)	7010(4)	8053(4)	25(1)
S(1)	2291(1)	3042(1)	5645(1)	24(1)
S(2)	1874(3)	8671(2)	8544(2)	55(1)
N(22A)	1650(10)	7655(8)	10050(7)	21(1)
C(25A)	1334(12)	8345(11)	10581(11)	30(3)
C(26A)	2390(14)	8922(16)	10821(15)	43(3)
N(22B)	1226(10)	7538(8)	10035(7)	21(1)
C(25B)	2057(13)	8543(11)	10575(11)	30(3)
C(26B)	1375(14)	8879(14)	10895(13)	43(3)

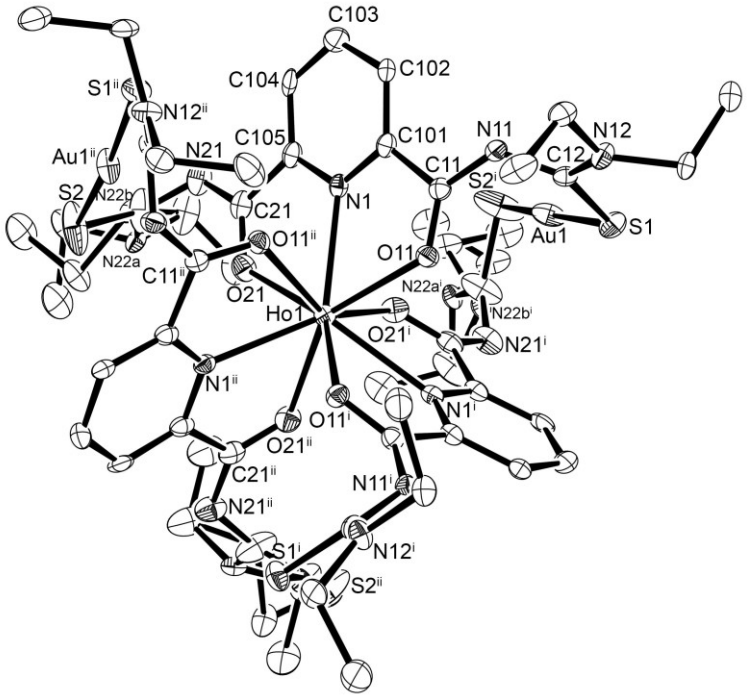

Figure A27: Ellipsoid plot of [Ho{Au(L4-κS)}$_3$]. Thermal ellipsoids are at 35 % of probability. The hydrogen atoms have been omitted for clarity.

[Ho{Au(L4-κS)}$_3$] (SQUEEZE)

Table A55: Crystal data and structure refinement for [Ho{Au(L4-κS)}$_3$]. **(SQUEEZE)**

Empirical formula	$C_{51}H_{69}Au_3HoN_{15}O_6S_6$	
Formula weight	1936.40	
Temperature	105(2) K	
Wavelength	0.71073 Å	
Crystal system	Trigonal	
Space group	$P\bar{3}$	
Unit cell dimensions	a = 16.2209(9) Å	α = 90°.
	b = 16.2209(9) Å	β = 90°.
	c = 14.6230(9) Å	γ = 120°.
Volume	3332.1(4) Å^3	
Z	2	
Density (calculated)	1.930 g/cm^3	
Absorption coefficient	8.002 mm^{-1}	
F(000)	1856	
Crystal size	0.19 x 0.17 x 0.09 mm^3	
Theta range for data collection	2.511 to 27.178°.	
Index ranges	-20<=h<=20, -20<=k<=20, -18<=l<=18	
Reflections collected	79051	
Independent reflections	4926 [R(int) = 0.0617]	
Completeness to theta = 25.242°	99.9 %	
Absorption correction	Semi-empirical from equivalents	
Max. and min. transmission	0.7454 and 0.3292	
Refinement method	Full-matrix least-squares on F^2	
Data / restraints / parameters	4926 / 4 / 252	
Goodness-of-fit on F^2	1.226	
Final R indices [I>2sigma(I)]	R1 = 0.0345, wR2 = 0.0691	
R indices (all data)	R1 = 0.0391, wR2 = 0.0705	
Largest diff. peak and hole	1.605 and -2.400 e · Å^{-3}	
Diffractometer	Bruker D8 Venture	

Table A56: Atomic coordinates (x 10^4) and equivalent isotropic displacement parameters ($Å^2$ x 10^3) for [Ho{Au(L4-κS)}$_3$]. U(eq) is defined as one third of the trace of the orthogonalized U^{ij} tensor. **(SQUEEZE)**

	x	y	z	U(eq)
C(101)	1176(4)	4984(4)	6225(3)	17(1)
C(102)	206(4)	4519(4)	6049(4)	20(1)
C(103)	-366(4)	4713(4)	6610(4)	25(1)
C(104)	38(4)	5353(4)	7327(4)	21(1)
C(105)	1018(4)	5800(4)	7441(3)	19(1)
C(11)	1880(4)	4825(4)	5709(3)	17(1)
C(12)	1872(3)	3570(4)	4879(3)	16(1)
C(13)	1512(4)	3802(4)	3327(4)	22(1)
C(14)	2311(4)	4768(4)	3021(4)	31(1)
C(15)	2015(4)	2603(4)	3639(4)	23(1)
C(16)	1107(5)	1639(4)	3601(5)	39(2)
C(21)	1576(4)	6587(4)	8110(3)	22(1)
C(22)	1445(6)	7596(5)	9134(4)	41(2)
C(23)	1084(6)	6698(6)	10542(4)	48(2)
C(24)	1825(6)	6404(6)	10629(5)	47(2)
Au(1)	1817(1)	3194(1)	7073(1)	27(1)
Ho(1)	3333	6667	6960(1)	17(1)
N(1)	1574(3)	5621(3)	6895(3)	16(1)
N(11)	1498(3)	4108(3)	5130(3)	20(1)
N(12)	1836(3)	3353(3)	3990(3)	20(1)
N(21)	1065(4)	6759(4)	8700(3)	29(1)
O(11)	2748(2)	5386(2)	5857(2)	18(1)
O(21)	2468(3)	7011(3)	8052(2)	24(1)
S(1)	2291(1)	3043(1)	5645(1)	24(1)
S(2)	1873(2)	8671(1)	8544(1)	54(1)
N(22A)	1659(8)	7670(6)	10046(6)	20(1)
C(25A)	1332(9)	8342(8)	10579(8)	30(2)
C(26A)	2393(10)	8937(12)	10823(10)	44(3)
N(22B)	1226(7)	7535(6)	10036(5)	20(1)
C(25B)	2070(9)	8560(8)	10578(8)	30(2)
C(26B)	1370(10)	8880(10)	10894(9)	44(3)

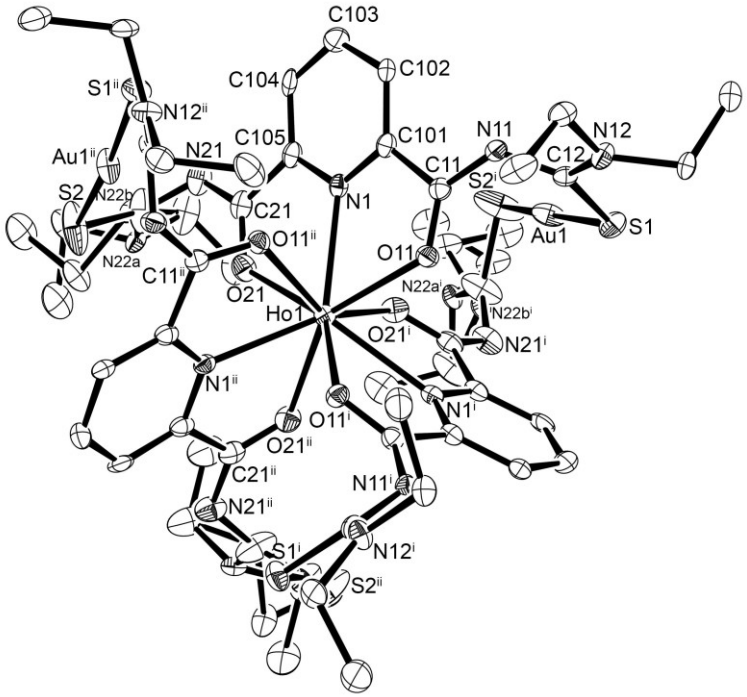

Figure A28: Ellipsoid plot of [Ho{Au(L4-κS)}$_3$]. Thermal ellipsoids are at 35 % of probability. The hydrogen atoms have been omitted for clarity. **(SQUEEZE)**

[Tm{Au(L4-κS)}$_3$]

Table A57: Crystal data and structure refinement for [Tm{Au(L4-κS)}$_3$].

Empirical formula	$C_{51}H_{69}Au_3N_{15}O_6S_6Tm$	
Formula weight	1940.40	
Temperature	105(2) K	
Wavelength	0.71073 Å	
Crystal system	Monoclinic	
Space group	C2/c	
Unit cell dimensions	a = 22.780(2) Å	α = 90°.
	b = 13.556(1) Å	β = 96.340(3)°.
	c = 20.961(2) Å	γ = 90°.
Volume	6433.2(9) Å^3	
Z	4	
Density (calculated)	2.003 g/cm^3	
Absorption coefficient	8.438 mm^{-1}	
F(000)	3720	
Crystal size	0.23 x 0.23 x 0.15 mm^3	
Theta range for data collection	2.507 to 27.153°.	
Index ranges	-29<=h<=29, -17<=k<=17, -26<=l<=26	
Reflections collected	124203	
Independent reflections	7112 [R(int) = 0.0812]	
Completeness to theta = 25.242°	99.9 %	
Absorption correction	Semi-empirical from equivalents	
Max. and min. transmission	0.7455 and 0.4768	
Refinement method	Full-matrix least-squares on F^2	
Data / restraints / parameters	7112 / 49 / 362	
Goodness-of-fit on F^2	1.035	
Final R indices [I>2sigma(I)]	R1 = 0.0308, wR2 = 0.0693	
R indices (all data)	R1 = 0.0335, wR2 = 0.0711	
Largest diff. peak and hole	2.654 and -3.073 e · Å^{-3}	
Diffractometer	Bruker D8 Venture	

Table A58: Atomic coordinates (x 10^4) and equivalent isotropic displacement parameters ($Å^2$ x 10^3) for [Tm{Au(L4-κS)}$_3$]. U(eq) is defined as one third of the trace of the orthogonalized U^{ij} tensor.

	x	y	z	U(eq)
C(101)	1006(2)	4198(3)	1527(2)	16(1)
C(201)	-175(3)	1317(4)	1960(4)	47(2)
C(102)	1253(3)	4582(5)	1005(3)	44(1)
C(103)	933(3)	5253(5)	622(4)	44(1)
C(104)	376(2)	5535(5)	754(3)	35(1)
C(105)	163(2)	5130(4)	1291(2)	19(1)
C(11)	1263(2)	3382(3)	1948(2)	16(1)
C(12)	1976(2)	2168(4)	2055(3)	26(1)
C(13)	2667(2)	3030(5)	2836(3)	41(2)
C(14)	2311(3)	3343(7)	3371(3)	55(2)
C(21)	-419(2)	5382(3)	1519(2)	19(1)
C(22)	-1096(2)	6701(4)	1395(2)	22(1)
C(23)	-1706(2)	6410(5)	391(2)	31(1)
C(24)	-2020(3)	5446(5)	486(3)	40(1)
C(25)	-1959(2)	7794(5)	1093(3)	37(1)
C(26)	-1761(3)	8696(5)	758(3)	47(2)
C(31)	-303(2)	1955(4)	1386(3)	39(2)
Au(1)	996(1)	1644(1)	899(1)	34(1)
Au(2)	0	7139(1)	2500	18(1)
N(1)	472(2)	4477(3)	1664(2)	13(1)
N(2)	0	1807(4)	2500	33(2)
N(11)	1789(2)	3071(3)	1840(2)	21(1)
N(12)	2428(2)	2110(4)	2505(2)	37(1)
N(21)	-723(2)	6068(3)	1176(2)	23(1)
N(22)	-1581(2)	6946(4)	997(2)	26(1)
O(11)	951(1)	3053(2)	2362(2)	20(1)
O(31)	-266(2)	2872(3)	1467(2)	27(1)
S(1)	1680(1)	1099(1)	1703(1)	41(1)
S(2)	-978(1)	7302(1)	2136(1)	26(1)
S(3)	340(1)	2132(1)	60(1)	43(1)
Tm(1)	0	3610(1)	2500	14(1)
N(31A)	-499(4)	1625(6)	771(4)	21(1)
C(32A)	-394(4)	1931(9)	197(5)	28(2)

N(32A)	-826(3)	1970(7)	-293(4)	31(1)
C(33A)	-1443(4)	1725(9)	-108(5)	36(1)
C(35A)	-775(5)	2030(9)	-908(5)	36(1)
C(34A)	-1724(6)	2572(12)	117(7)	60(2)
C(36A)	-981(7)	1613(13)	-1262(7)	60(2)
N(31B)	-402(4)	1314(6)	927(4)	21(1)
C(32B)	-299(5)	1557(9)	342(6)	28(2)
N(32B)	-711(4)	1327(7)	-167(4)	31(1)
C(33B)	-1305(5)	906(9)	35(6)	36(1)
C(35B)	-593(6)	1120(9)	-785(5)	38(3)
C(34B)	-1695(7)	1694(13)	176(8)	60(2)
C(36B)	-777(7)	1114(15)	-1283(7)	60(2)
C(15A)	2645(8)	1031(11)	2624(9)	36(1)
C(16A)	2431(11)	740(20)	3289(9)	60(2)
C(15B)	2750(6)	1217(11)	2793(9)	36(1)
C(16B)	2332(9)	580(20)	3171(11)	60(2)
O(21)	-575(1)	4904(2)	1982(2)	18(1)
C(202)	-191(3)	290(5)	1963(4)	44(1)
C(203)	0	-207(7)	2500	44(1)

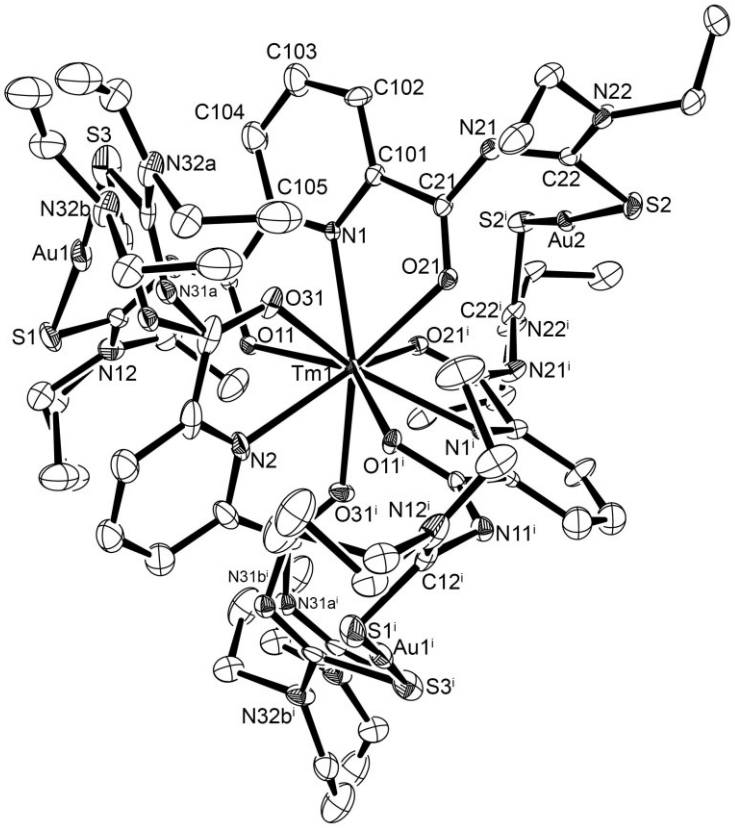

Figure A29: Ellipsoid plot of [Tm{Au(L4-κS)}$_3$]. Thermal ellipsoids are at 50 % of probability. The hydrogen atoms have been omitted for clarity.

[Yb{Au(L4-κS)}$_3$]

Table A59: Crystal data and structure refinement for [Yb{Au(L4-κS)}$_3$].

Empirical formula	$C_{51}H_{69}Au_3N_{15}O_6S_6Yb$	
Formula weight	1944.51	
Temperature	100(2) K	
Wavelength	0.71073 Å	
Crystal system	Trigonal	
Space group	$P\bar{3}$	
Unit cell dimensions	a = 16.116(1) Å	α = 90°.
	b = 16.116(1) Å	β = 90°.
	c = 14.557(1) Å	γ = 120°.
Volume	3274.2(6) Å^3	
Z	2	
Density (calculated)	1.972 g/cm^3	
Absorption coefficient	8.363 mm^{-1}	
F(000)	1862	
Crystal size	0.18 x 0.06 x 0.05 mm^3	
Theta range for data collection	2.528 to 24.998°.	
Index ranges	-19<=h<=19, -15<=k<=19, -17<=l<=17	
Reflections collected	16039	
Independent reflections	3837 [R(int) = 0.0630]	
Completeness to theta = 24.998°	99.4 %	
Absorption correction	Semi-empirical from equivalents	
Max. and min. transmission	0.1495 and 0.0654	
Refinement method	Full-matrix least-squares on F^2	
Data / restraints / parameters	3837 / 35 / 213	
Goodness-of-fit on F^2	1.083	
Final R indices [I>2sigma(I)]	R1 = 0.0718, wR2 = 0.1568	
R indices (all data)	R1 = 0.0836, wR2 = 0.1634	
Largest diff. peak and hole	4.734 and -4.055 e · Å^{-3}	
Diffractometer	Bruker D8 Venture	

Table A60: Atomic coordinates (x 10^4) and equivalent isotropic displacement parameters ($Å^2$ x 10^3) for [Yb{Au(L4-κS)}$_3$]. U(eq) is defined as one third of the trace of the orthogonalized U^{ij} tensor.

	x	y	z	U(eq)
Yb(1)	3333	6667	8038(1)	14(1)
Au(1)	1807(1)	8610(1)	7935(1)	23(1)
S(1)	6946(3)	7699(3)	9359(3)	20(1)
S(2)	1300(3)	8097(4)	6465(3)	39(1)
O(11)	4589(7)	7230(7)	9135(6)	14(2)
N(11)	5862(9)	8490(9)	9882(8)	15(3)
N(12)	6638(8)	8159(9)	11022(7)	12(2)
C(11)	5163(11)	8101(11)	9293(10)	17(3)
C(12)	6403(10)	8118(10)	10131(9)	12(3)
C(13)	7406(12)	7994(15)	11371(11)	31(2)
C(14)	8359(13)	8892(14)	11391(14)	36(5)
N(1)	4368(9)	8412(9)	8103(8)	14(1)
C(103)	5277(10)	10352(11)	8371(10)	14(1)
C(102)	5470(10)	9777(11)	8944(10)	14(1)
C(15)	6174(12)	8467(13)	11683(10)	23(4)
N(21)	3216(10)	8914(11)	6294(8)	24(3)
C(101)	5016(10)	8821(11)	8769(10)	14(1)
N(22)	2339(12)	8509(14)	4951(10)	44(4)
C(16)	5220(13)	7693(12)	11997(11)	28(4)
C(22)	2365(14)	8518(16)	5876(11)	35(5)
C(24)	3565(14)	8150(16)	4360(12)	40(3)
C(23)	3252(13)	8883(15)	4443(11)	31(2)
C(104)	4646(10)	9967(11)	7659(10)	14(1)
C(5)	4188(10)	8969(11)	7552(10)	15(3)
C(21)	3398(11)	8404(12)	6888(9)	17(3)
C(25A)	1426(19)	7940(20)	4426(18)	31(2)
C(26A)	1120(20)	8630(30)	4100(20)	40(3)
C(25B)	1620(30)	8650(30)	4440(30)	31(2)
C(26B)	1040(40)	7600(30)	4230(30)	40(3)
O(21)	2971(8)	7516(8)	6954(7)	21(2)

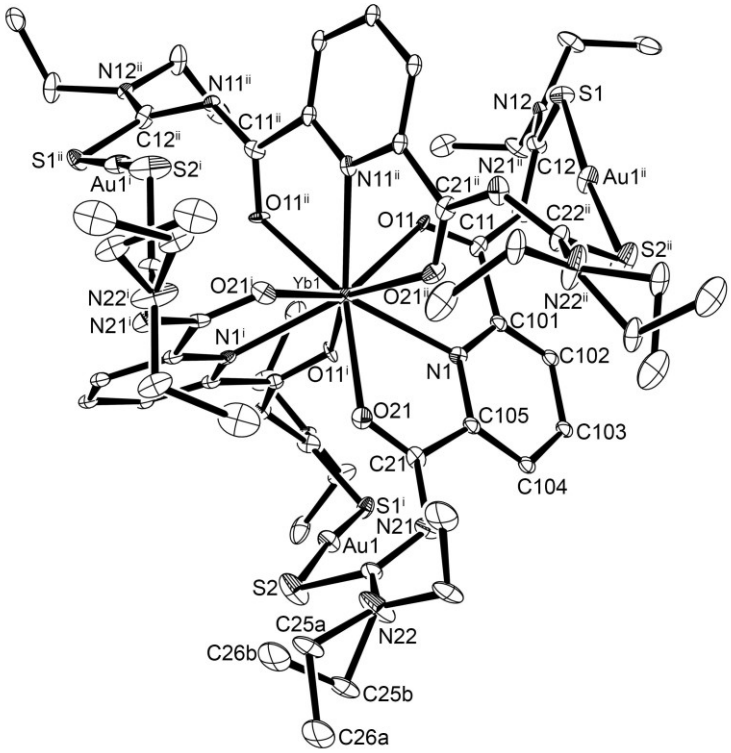

Figure A30: Ellipsoid plot of [Yb{Au(L4-κS)}$_3$]. Thermal ellipsoids are at 35 % of probability. The hydrogen atoms have been omitted for clarity.

[Yb{Au(L4-κS)}$_3$] (SQUEEZE)

Table A61: Crystal data and structure refinement for [Yb{Au(L4-κS)}$_3$]. **(SQUEEZE)**

Empirical formula	$C_{51}H_{69}Au_3N_{15}O_6S_6Yb$	
Formula weight	1944.51	
Temperature	100(2) K	
Wavelength	0.71073 Å	
Crystal system	Trigonal	
Space group	$P\bar{3}$	
Unit cell dimensions	a = 16.116(1) Å	α = 90°.
	b = 16.116(1) Å	β = 90°.
	c = 14.557(1) Å	γ = 120°.
Volume	3274.2(6) Å^3	
Z	2	
Density (calculated)	1.972 g/cm^3	
Absorption coefficient	8.363 mm^{-1}	
F(000)	1862	
Crystal size	0.18 x 0.06 x 0.05 mm^3	
Theta range for data collection	2.528 to 24.998°.	
Index ranges	-19<=h<=19, -15<=k<=19, -17<=l<=17	
Reflections collected	15961	
Independent reflections	3813 [R(int) = 0.0613]	
Completeness to theta = 24.998°	98.7 %	
Absorption correction	Semi-empirical from equivalents	
Max. and min. transmission	0.1495 and 0.0654	
Refinement method	Full-matrix least-squares on F^2	
Data / restraints / parameters	3813 / 53 / 201	
Goodness-of-fit on F^2	1.073	
Final R indices [I>2sigma(I)]	R1 = 0.0653, wR2 = 0.1402	
R indices (all data)	R1 = 0.0759, wR2 = 0.1450	
Largest diff. peak and hole	4.251 and -3.782 e · Å^{-3}	
Diffractometer	Bruker D8 Venture	

Table A62: Atomic coordinates (x 10^4) and equivalent isotropic displacement parameters (Å^2 x 10^3) for [Yb{Au(L4-κS)}$_3$]. U(eq) is defined as one third of the trace of the orthogonalized U^{ij} tensor. **(SQUEEZE)**

	x	y	z	U(eq)
Yb(1)	3333	6667	8038(1)	14(1)
Au(1)	1807(1)	8610(1)	7935(1)	23(1)
S(1)	6947(3)	7698(3)	9359(2)	21(1)
S(2)	1301(3)	8098(4)	6465(2)	38(1)
O(11)	4587(6)	7229(6)	9136(6)	14(2)
N(11)	5860(8)	8487(8)	9883(7)	14(2)
N(12)	6641(7)	8163(8)	11023(6)	12(2)
C(11)	5158(10)	8099(10)	9297(8)	16(3)
C(12)	6406(10)	8120(11)	10133(9)	21(2)
C(13)	7405(11)	7992(12)	11371(9)	28(2)
C(14)	8362(12)	8893(12)	11397(13)	37(4)
N(1)	4371(8)	8415(8)	8104(7)	13(2)
C(103)	5277(9)	10351(10)	8371(9)	16(1)
C(102)	5468(9)	9774(10)	8943(9)	16(1)
C(15)	6177(11)	8472(12)	11687(9)	28(2)
N(21)	3217(9)	8911(9)	6293(7)	23(3)
C(101)	5014(9)	8818(10)	8769(9)	16(1)
N(22)	2341(10)	8513(13)	4951(8)	44(3)
C(16)	5213(12)	7689(11)	11995(10)	30(4)
C(22)	2369(10)	8528(11)	5875(9)	21(2)
C(24)	3568(13)	8158(15)	4361(11)	45(4)
C(23)	3255(11)	8890(13)	4446(9)	28(2)
C(104)	4648(9)	9967(10)	7659(9)	16(1)
C(105)	4194(9)	8971(10)	7551(9)	16(1)
C(21)	3398(10)	8405(10)	6890(8)	17(3)
C(25A)	1424(17)	7939(19)	4426(15)	28(2)
C(26A)	1130(20)	8630(20)	4096(18)	45(4)
C(25B)	1610(30)	8650(30)	4460(20)	28(2)
C(26B)	1030(40)	7600(30)	4220(30)	45(4)
O(21)	2970(7)	7514(7)	6956(6)	21(2)

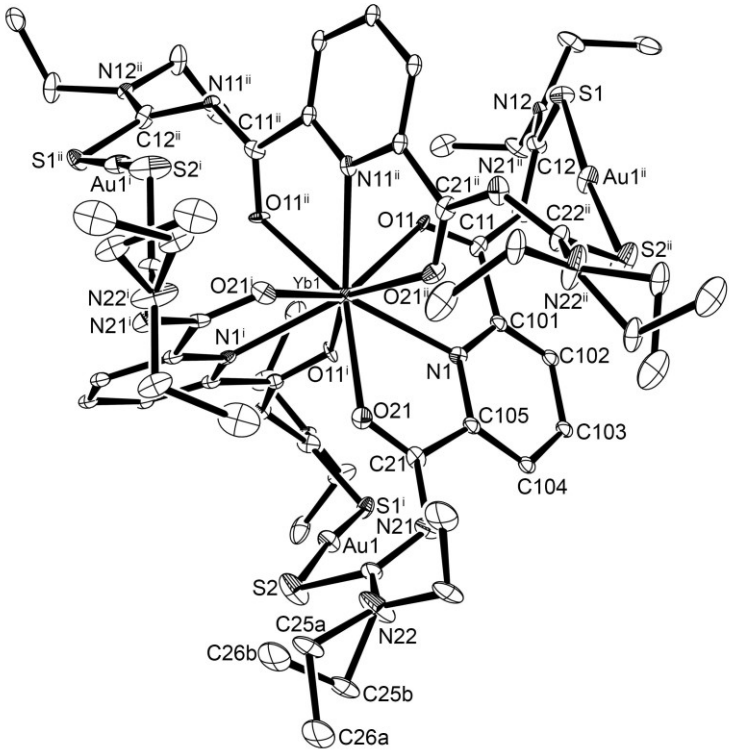

Figure A31: Ellipsoid plot of [Yb{Au(L4-κS)}$_3$]. Thermal ellipsoids are at 35 % of probability. The hydrogen atoms have been omitted for clarity. **(SQUEEZE)**

[Lu{Au(L4-κS)}$_3$]

Table A63: Crystal data and structure refinement for [Lu{Au(L4-κS)}$_3$].

Empirical formula	$C_{51}H_{69}Au_3LuN_{15}O_6S_6$	
Formula weight	1946.44	
Temperature	200(2) K	
Wavelength	0.71073 Å	
Crystal system	Triclinic	
Space group	$P\bar{1}$	
Unit cell dimensions	a = 13.652(1) Å	α = 89.14(1)°.
	b = 14.813(1) Å	β = 79.67(1)°.
	c = 16.537(1) Å	γ = 79.83(1)°.
Volume	3237.9(4) Å^3	
Z	2	
Density (calculated)	1.996 g/cm^3	
Absorption coefficient	8.537 mm^{-1}	
F(000)	1864	
Crystal size	0.30 x 0.30 x 0.20 mm^3	
Theta range for data collection	3.287 to 24.998°.	
Index ranges	-16<=h<=16, -17<=k<=17, -18<=l<=19	
Reflections collected	23211	
Independent reflections	11309 [R(int) = 0.0913]	
Completeness to theta = 24.998°	99.1 %	
Absorption correction	Integration	
Max. and min. transmission	0.2669 and 0.1284	
Refinement method	Full-matrix least-squares on F^2	
Data / restraints / parameters	11309 / 27 / 740	
Goodness-of-fit on F^2	0.942	
Final R indices [I>2sigma(I)]	R1 = 0.0447, wR2 = 0.1125	
R indices (all data)	R1 = 0.0553, wR2 = 0.1185	
Largest diff. peak and hole	1.772 and -2.581 e · Å^{-3}	
Diffractometer	IPDS STOE	

Table A64: Atomic coordinates (x 10^4) and equivalent isotropic displacement parameters ($Å^2$ x 10^3) for [Lu{Au(L4-κS)}$_3$]. U(eq) is defined as one third of the trace of the orthogonalized U^{ij} tensor.

	x	y	z	U(eq)
O(31)	7545(4)	6315(3)	1845(3)	29(1)
O(21)	9663(4)	7994(4)	2586(3)	31(1)
O(61)	7911(4)	8348(3)	1682(3)	28(1)
O(11)	7516(4)	6325(4)	3718(4)	32(1)
O(51)	9503(4)	5870(3)	2553(3)	31(1)
O(41)	7562(4)	8461(3)	3520(3)	29(1)
N(21)	10899(5)	8472(5)	3179(4)	31(1)
N(2)	9327(4)	6927(4)	1300(4)	24(1)
N(3)	6443(4)	7627(4)	2795(4)	24(1)
N(41)	6175(5)	9384(4)	4296(4)	31(1)
N(1)	9086(4)	7047(4)	3863(4)	23(1)
N(32)	6569(6)	4606(5)	634(5)	42(2)
N(31)	6160(5)	5958(4)	1380(4)	31(1)
N(11)	7535(5)	5577(5)	4952(4)	35(2)
C(31)	6614(6)	6433(5)	1825(5)	27(2)
C(21)	10144(5)	8010(5)	3164(4)	24(2)
N(22)	11554(6)	9587(5)	2391(5)	42(2)
C(41)	6621(6)	8756(5)	3733(5)	29(2)
N(42)	6866(6)	10554(5)	4753(5)	39(2)
N(61)	8175(5)	8917(5)	371(4)	36(2)
N(51)	10846(5)	4887(4)	1802(4)	36(2)
N(52)	11533(6)	3611(5)	2434(5)	41(2)
C(301)	5933(6)	7174(5)	2374(4)	24(2)
C(305)	5946(6)	8310(5)	3301(5)	26(2)
N(12)	6350(6)	4745(5)	5499(6)	54(2)
C(61)	8354(5)	8322(5)	945(5)	27(2)
C(51)	10114(6)	5607(5)	1904(5)	28(2)
C(12)	6616(7)	5550(6)	5281(6)	41(2)
C(103)	10153(6)	6649(6)	5136(5)	35(2)
C(201)	9993(5)	6147(5)	1151(5)	25(2)
C(104)	10428(6)	7268(6)	4524(5)	38(2)
C(203)	10386(6)	6475(6)	-268(5)	36(2)
C(105)	9874(6)	7455(5)	3900(5)	26(2)

N(62)	7295(6)	10384(5)	433(6)	48(2)
C(22)	11475(6)	8709(5)	2503(5)	29(2)
C(42)	6750(6)	9677(5)	4773(5)	36(2)
C(204)	9711(6)	7321(5)	-109(5)	31(2)
C(62)	7291(6)	9491(5)	432(5)	32(2)
C(52)	11362(6)	4510(5)	2366(5)	33(2)
C(205)	9186(5)	7504(5)	684(5)	25(2)
C(11)	7863(6)	6123(5)	4353(5)	29(2)
C(101)	8806(5)	6471(5)	4444(5)	26(2)
C(32)	6599(6)	5491(5)	683(5)	30(2)
C(302)	4906(6)	7393(6)	2423(5)	35(2)
C(102)	9330(6)	6251(6)	5100(5)	33(2)
C(303)	4376(6)	8119(6)	2960(6)	42(2)
C(202)	10532(6)	5890(5)	360(5)	33(2)
C(304)	4915(6)	8580(6)	3383(6)	37(2)
C(53)	11037(8)	3067(6)	1961(6)	50(2)
C(35)	6862(7)	4073(6)	-139(7)	51(3)
C(45)	7505(8)	10915(6)	5238(6)	45(2)
C(55)	12314(7)	3103(6)	2865(6)	46(2)
C(23)	12251(9)	9936(6)	1721(7)	54(3)
C(43)	6286(9)	11197(7)	4216(8)	63(3)
C(25)	10814(10)	10300(7)	2910(7)	65(3)
C(65)	6384(8)	11080(7)	336(7)	57(3)
C(14)	7217(9)	3597(7)	4451(9)	67(3)
C(13)	7114(8)	3911(6)	5324(7)	53(3)
C(33)	6179(8)	4125(7)	1371(7)	57(3)
C(15)	5363(10)	4636(8)	5978(9)	72(3)
C(56)	13331(8)	2864(9)	2313(7)	73(4)
C(46)	8629(9)	10685(9)	4846(8)	67(3)
C(66)	5757(10)	11407(9)	1144(8)	80(4)
C(54)	9986(10)	3012(9)	2417(8)	82(4)
C(34)	6948(14)	3811(11)	1890(10)	111(6)
C(24)	13134(10)	10245(10)	2011(9)	80(4)
C(36)	5956(8)	4021(10)	-534(9)	85(5)
C(63)	8173(10)	10740(8)	627(12)	99(5)
C(26)	9866(12)	10513(10)	2556(11)	102(6)
C(16)	5446(12)	4743(10)	6794(11)	90(5)

C(44)	6882(14)	11258(12)	3377(9)	101(5)
C(64)	8962(14)	10828(15)	-78(13)	142(7)
Lu(1)	8273(1)	7227(1)	2652(1)	24(1)
Au(3)	6645(1)	7576(1)	131(1)	38(1)
Au(2)	11990(1)	6521(1)	2384(1)	36(1)
Au(1)	6507(1)	7737(1)	5482(1)	39(1)
S(2)	12226(2)	7895(2)	1799(1)	40(1)
S(3)	7089(2)	6045(2)	-192(2)	45(1)
S(4)	7264(2)	8990(2)	5507(2)	49(1)
S(6)	6167(2)	9117(2)	402(2)	48(1)
S(5)	11904(2)	5142(2)	2997(2)	45(1)
S(1)	5670(2)	6538(2)	5538(2)	51(1)

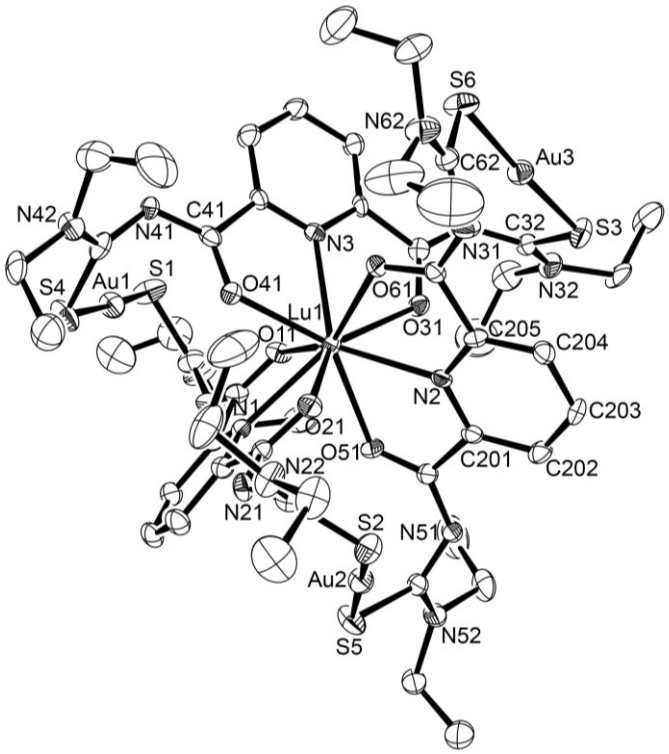

Figure A32: Ellipsoid plot of [Lu{Au(L4-κS)}$_3$]. Thermal ellipsoids are at 35 % of probability. The hydrogen atoms have been omitted for clarity.

[Sc{Au(L4-κS)}$_3$]

Table A65: Crystal data and structure refinement for [Sc{Au(L4-κS)}$_3$].

Empirical formula	$C_{51}H_{69}Au_3N_{15}O_6S_6Sc$	
Formula weight	1816.43	
Temperature	108(2) K	
Wavelength	0.71073 Å	
Crystal system	Triclinic	
Space group	$P\bar{1}$	
Unit cell dimensions	a = 13.5162(9) Å	α = 89.303(2)°.
	b = 14.7445(9) Å	β = 79.801(2)°.
	c = 16.353(1) Å	γ = 79.260(2)°.
Volume	3150.6(3) Å^3	
Z	2	
Density (calculated)	1.915 g/cm^3	
Absorption coefficient	7.324 mm^{-1}	
F(000)	1764	
Crystal size	0.20 x 0.17 x 0.10 mm^3	
Theta range for data collection	2.286 to 30.581°.	
Index ranges	-19<=h<=19, -21<=k<=21, -23<=l<=23	
Reflections collected	182795	
Independent reflections	19346 [R(int) = 0.0560]	
Completeness to theta = 25.242°	99.9 %	
Absorption correction	Semi-empirical from equivalents	
Max. and min. transmission	0.7461 and 0.5115	
Refinement method	Full-matrix least-squares on F^2	
Data / restraints / parameters	19346 / 0 / 740	
Goodness-of-fit on F^2	1.036	
Final R indices [I>2sigma(I)]	R1 = 0.0201, wR2 = 0.0414	
R indices (all data)	R1 = 0.0257, wR2 = 0.0429	
Largest diff. peak and hole	1.258 and -1.310 e · Å^{-3}	
Diffractometer	Bruker D8 Venture	

Table A66: Atomic coordinates (x 10^4) and equivalent isotropic displacement parameters ($Å^2$ x 10^3) for [Sc{Au(L4-κS)}$_3$]. U(eq) is defined as one third of the trace of the orthogonalized U^{ij} tensor.

	x	y	z	U(eq)
C(101)	9160(2)	7514(1)	715(1)	10(1)
C(201)	5964(2)	8316(1)	3292(1)	10(1)
C(301)	9836(2)	7465(1)	3889(1)	10(1)
C(102)	9663(2)	7310(2)	-99(1)	13(1)
C(202)	4905(2)	8570(2)	3404(1)	14(1)
C(302)	10397(2)	7288(2)	4525(1)	13(1)
C(103)	10335(2)	6472(2)	-270(1)	14(1)
C(203)	4378(2)	8082(2)	2966(1)	17(1)
C(303)	10134(2)	6648(2)	5122(1)	15(1)
C(104)	10500(2)	5871(2)	375(1)	12(1)
C(204)	4919(2)	7362(2)	2432(1)	14(1)
C(304)	9313(2)	6219(2)	5067(1)	12(1)
C(105)	9974(2)	6137(1)	1168(1)	10(1)
C(205)	5975(2)	7143(1)	2368(1)	9(1)
C(305)	8794(2)	6450(1)	4408(1)	10(1)
C(11)	8335(2)	8330(1)	991(1)	10(1)
C(12)	7262(2)	9551(2)	485(1)	12(1)
C(13)	8179(2)	10776(2)	684(2)	28(1)
C(14)	8927(2)	10887(2)	-83(2)	39(1)
C(15)	6380(2)	11159(2)	387(2)	21(1)
C(16)	5684(2)	11516(2)	1194(2)	29(1)
C(21)	10067(2)	5595(1)	1939(1)	10(1)
C(22)	11303(2)	4487(2)	2433(1)	12(1)
C(23)	11006(2)	3016(2)	2006(1)	18(1)
C(24)	9922(2)	2980(2)	2432(2)	27(1)
C(25)	12281(2)	3060(2)	2937(1)	17(1)
C(26)	13313(2)	2814(2)	2363(2)	26(1)
C(31)	6658(2)	8749(1)	3715(1)	10(1)
C(32)	6797(2)	9688(2)	4779(1)	12(1)
C(33)	6300(2)	11231(2)	4277(2)	20(1)
C(34)	6859(2)	11302(2)	3399(2)	32(1)
C(35)	7555(2)	10903(2)	5278(1)	16(1)
C(36)	8678(2)	10671(2)	4852(2)	22(1)

C(41)	6679(2)	6411(1)	1810(1)	10(1)
C(42)	6680(2)	5496(2)	635(1)	12(1)
C(43)	6923(2)	4116(2)	-273(1)	17(1)
C(44)	5972(2)	4105(2)	-644(2)	31(1)
C(45)	6267(2)	4081(2)	1254(2)	21(1)
C(46)	7047(2)	3767(2)	1816(2)	37(1)
C(51)	10101(2)	8034(1)	3146(1)	10(1)
C(52)	11449(2)	8728(2)	2491(1)	12(1)
C(53)	12284(2)	9913(2)	1697(1)	19(1)
C(54)	13149(2)	10239(2)	2014(2)	30(1)
C(55)	10769(2)	10333(2)	2834(2)	23(1)
C(56)	9801(2)	10507(2)	2455(2)	34(1)
C(61)	7861(2)	6099(1)	4285(1)	10(1)
C(62)	6570(2)	5541(1)	5213(1)	11(1)
C(63)	7085(2)	3885(2)	5284(1)	16(1)
C(64)	7254(2)	3549(2)	4386(2)	20(1)
C(65)	5340(2)	4665(2)	6015(1)	15(1)
C(66)	5417(2)	4795(2)	6918(2)	24(1)
Au(1)	6634(1)	7629(1)	138(1)	14(1)
Au(2)	11955(1)	6501(1)	2442(1)	12(1)
Au(3)	6528(1)	7723(1)	5431(1)	12(1)
N(1)	9314(1)	6936(1)	1330(1)	9(1)
N(2)	6480(1)	7618(1)	2788(1)	9(1)
N(3)	9058(1)	7050(1)	3833(1)	9(1)
N(11)	8164(1)	8961(1)	427(1)	13(1)
N(12)	7262(2)	10453(1)	507(1)	17(1)
N(21)	10788(1)	4844(1)	1848(1)	13(1)
N(22)	11501(2)	3567(1)	2495(1)	13(1)
N(31)	6224(1)	9411(1)	4266(1)	12(1)
N(32)	6874(1)	10573(1)	4788(1)	13(1)
N(41)	6242(1)	5915(1)	1364(1)	12(1)
N(42)	6674(1)	4602(1)	538(1)	14(1)
N(51)	10826(1)	8523(1)	3171(1)	12(1)
N(52)	11546(2)	9602(1)	2359(1)	15(1)
N(61)	7526(1)	5536(1)	4864(1)	13(1)
N(62)	6305(1)	4735(1)	5457(1)	12(1)
O(11)	7879(1)	8339(1)	1733(1)	12(1)

O(21)	9447(1)	5889(1)	2586(1)	12(1)
O(31)	7605(1)	8437(1)	3500(1)	11(1)
O(41)	7620(1)	6323(1)	1829(1)	11(1)
O(51)	9618(1)	7993(1)	2561(1)	11(1)
O(61)	7504(1)	6336(1)	3645(1)	12(1)
S(1)	6129(1)	9178(1)	434(1)	18(1)
S(2)	11835(1)	5129(1)	3074(1)	15(1)
S(3)	7339(1)	8948(1)	5485(1)	16(1)
S(4)	7126(1)	6103(1)	-237(1)	16(1)
S(5)	12243(1)	7857(1)	1830(1)	14(1)
S(6)	5638(1)	6551(1)	5458(1)	15(1)
Sc(1)	8270(1)	7234(1)	2644(1)	8(1)

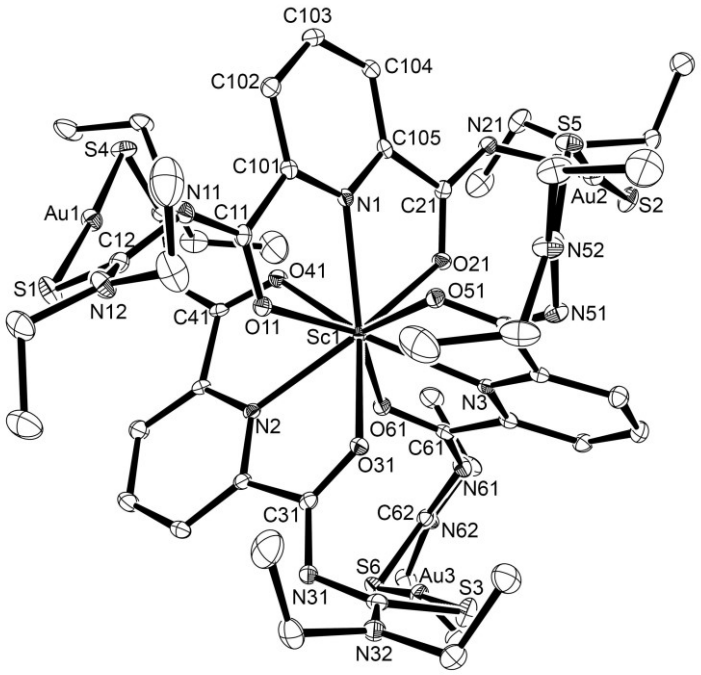

Figure A33: Ellipsoid plot of [Sc{Au(L4-κS)}$_3$]. Thermal ellipsoids are at 50 % of probability. The hydrogen atoms have been omitted for clarity.

[In{Au(L4-κS)}$_3$]

Table A67: Crystal data and structure refinement for [In{Au(L4-κS)}$_3$].

Empirical formula	$C_{51}H_{69}Au_3InN_{15}O_6S_6$	
Formula weight	1886.29	
Temperature	100(2) K	
Wavelength	0.71073 Å	
Crystal system	Monoclinic	
Space group	C2/c	
Unit cell dimensions	a = 22.773(2) Å	α = 90°.
	b = 13.501(1) Å	β = 95.340(2)°.
	c = 20.836(2) Å	γ = 90°.
Volume	6378(1) Å^3	
Z	4	
Density (calculated)	1.964 g/cm^3	
Absorption coefficient	7.490 mm^{-1}	
F(000)	3640	
Crystal size	0.28 x 0.16 x 0.16 mm^3	
Theta range for data collection	2.535 to 27.933°.	
Index ranges	-30<=h<=29, -17<=k<=17, -27<=l<=27	
Reflections collected	87745	
Independent reflections	7637 [R(int) = 0.0529]	
Completeness to theta = 25.242°	99.9 %	
Absorption correction	Semi-empirical from equivalents	
Max. and min. transmission	0.7456 and 0.4251	
Refinement method	Full-matrix least-squares on F^2	
Data / restraints / parameters	7637 / 23 / 368	
Goodness-of-fit on F^2	1.036	
Final R indices [I>2sigma(I)]	R1 = 0.0268, wR2 = 0.0610	
R indices (all data)	R1 = 0.0303, wR2 = 0.0629	
Largest diff. peak and hole	1.816 and -3.433 e · Å^{-3}	
Diffractometer	Bruker D8 Venture	

Table A68: Atomic coordinates (x 10^4) and equivalent isotropic displacement parameters ($Å^2$ x 10^3) for [In{Au(L4-κS)}$_3$]. U(eq) is defined as one third of the trace of the orthogonalized U^{ij} tensor.

	x	y	z	U(eq)
C(105)	152(2)	4885(3)	1320(2)	20(1)
C(201)	-192(2)	8581(3)	1965(3)	34(1)
C(104)	374(2)	4466(4)	785(2)	44(1)
C(202)	-207(2)	9614(4)	1955(4)	67(2)
C(103)	936(2)	4746(4)	650(2)	45(1)
C(203)	0	10119(5)	2500	68(2)
C(102)	1252(2)	5419(3)	1038(2)	24(1)
C(101)	994(1)	5808(3)	1562(2)	14(1)
C(11)	1252(2)	6622(2)	1983(2)	13(1)
C(12)	1959(2)	7859(3)	2060(2)	22(1)
C(13)	2652(2)	7067(4)	2850(2)	37(1)
C(14)	2288(2)	6749(5)	3389(2)	45(1)
C(15)	2683(2)	8920(4)	2677(3)	51(2)
C(16)	2372(3)	9437(5)	3200(3)	63(2)
C(21)	-438(2)	4635(3)	1540(2)	19(1)
C(22)	-1101(2)	3295(3)	1400(2)	24(1)
C(23)	-1702(2)	3588(4)	399(2)	35(1)
C(24)	-2021(2)	4554(5)	500(2)	44(1)
C(25)	-1948(2)	2181(4)	1097(2)	41(1)
C(26)	-1747(3)	1290(4)	736(2)	48(1)
C(31)	-333(2)	7942(4)	1389(2)	32(1)
N(1)	455(1)	5537(2)	1694(1)	13(1)
N(2)	0	8081(3)	2500	23(1)
N(11)	1779(1)	6938(2)	1865(2)	17(1)
N(12)	2418(2)	7944(3)	2498(2)	32(1)
N(21)	-735(1)	3953(3)	1189(2)	24(1)
N(22)	-1573(2)	3041(3)	1004(2)	30(1)
O(21)	-601(1)	5096(2)	2015(1)	17(1)
O(11)	944(1)	6956(2)	2405(1)	18(1)
O(31)	-295(1)	7022(2)	1457(1)	24(1)
In(1)	0	6357(1)	2500	12(1)
Au(1)	967(1)	8333(1)	908(1)	27(1)
Au(2)	0	2836(1)	2500	18(1)

S(1)	1644(1)	8913(1)	1699(1)	35(1)
S(2)	-975(1)	2665(1)	2139(1)	26(1)
S(3A)	326(3)	7741(6)	3(3)	21(1)
C(32A)	-398(4)	7943(7)	185(4)	31(1)
N(32A)	-720(3)	8743(5)	-146(3)	21(1)
N(31A)	-536(3)	8278(5)	770(3)	21(1)
C(35A)	-567(4)	8929(7)	-807(4)	31(1)
C(33A)	-1299(3)	9077(7)	11(4)	31(1)
C(36A)	-973(4)	8410(7)	-1300(4)	31(1)
C(34A)	-1718(4)	8214(7)	109(4)	31(1)
S(3B)	321(4)	7915(6)	146(4)	21(1)
C(32B)	-353(4)	8403(8)	327(4)	31(1)
N(32B)	-837(3)	7959(5)	-284(3)	21(1)
N(31B)	-470(4)	8597(6)	934(3)	21(1)
C(35B)	-753(4)	7890(7)	-979(4)	31(1)
C(33B)	-1459(4)	7991(7)	-149(4)	31(1)
C(36B)	-784(4)	8886(7)	-1304(4)	31(1)
C(34B)	-1677(4)	8952(7)	-26(4)	31(1)

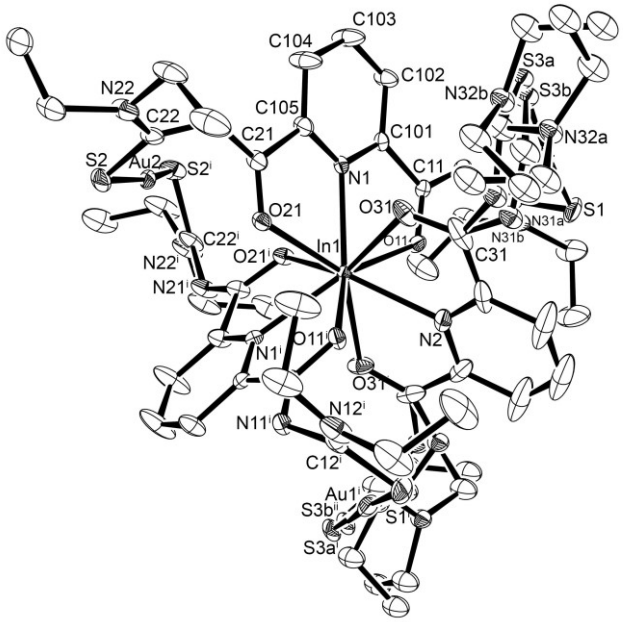

Figure A34: Ellipsoid plot of [In{Au(L4-κS)}$_3$]. Thermal ellipsoids are at 50 % of probability. The hydrogen atoms have been omitted for clarity.

$[Ga\{Au(L4\text{-}\kappa S)\}_2](NO_3) \cdot 0.5CHCl_3 \cdot CH_2Cl_2 \cdot 0.5MeOH$

Table A69: Crystal data and structure refinement for $[Ga\{Au(L4\text{-}\kappa S)\}_2](NO_3) \cdot 0.5CHCl_3 \cdot CH_2Cl_2 \cdot 0.5MeOH$.

Empirical formula	$C_{36}H_{50.5}Au_2Cl_{3.5}Ga_1N_{11}O_{7.5}S_4$	
Formula weight	1437.34	
Temperature	193(2) K	
Wavelength	0.71073 Å	
Crystal system	Monoclinic	
Space group	$P2_1/c$	
Unit cell dimensions	a = 10.020(7) Å	α = 90°.
	b = 19.210(1) Å	β = 96.068(2)°.
	c = 30.944(2) Å	γ = 90°.
Volume	5923.0(8) $Å^3$	
Z	4	
Density (calculated)	1.652 g/cm^3	
Absorption coefficient	5.741 mm^{-1}	
F(000)	2864	
Crystal size	0.42 x 0.33 x 0.04 mm^3	
Theta range for data collection	2.251 to 27.189°.	
Index ranges	-12<=h<=12, -24<=k<=23, -39<=l<=38	
Reflections collected	73946	
Independent reflections	13122 [R(int) = 0.0448]	
Completeness to theta = 25.242°	99.8 %	
Absorption correction	Semi-empirical from equivalents	
Max. and min. transmission	0.7455 and 0.3339	
Refinement method	Full-matrix least-squares on F^2	
Data / restraints / parameters	13122 / 15 / 669	
Goodness-of-fit on F^2	1.037	
Final R indices [I>2sigma(I)]	R1 = 0.0405, wR2 = 0.1045	
R indices (all data)	R1 = 0.0465, wR2 = 0.1077	
Largest diff. peak and hole	2.671 and -1.615 e · $Å^{-3}$	
Diffractometer	Bruker D8 Venture	

Table A70: Atomic coordinates (x 10^4) and equivalent isotropic displacement parameters ($Å^2$ x 10^3) for $[Ga\{Au(L4\text{-}\kappa S)\}_2](NO_3) \cdot 0.5CHCl_3 \cdot CH_2Cl_2 \cdot 0.5MeOH$. U(eq) is defined as one third of the trace of the orthogonalized U^{ij} tensor.

	x	y	z	U(eq)
C(10A)	8341(16)	5724(16)	2973(10)	71(4)
Cl(1A)	7068(6)	5373(3)	3219(3)	66(2)
Cl(2A)	9786(7)	5218(3)	3002(2)	64(2)
C(10B)	9080(30)	5070(50)	3110(30)	71(4)
Cl(1B)	7659(17)	5488(8)	2991(5)	44(4)
Cl(2B)	10450(14)	5461(7)	3301(5)	44(4)
O(40)	3490(20)	768(11)	160(5)	106(6)
C(40)	2790(20)	1114(10)	458(7)	73(6)
Cl(3)	8853(16)	723(9)	389(5)	258(9)
Cl(5)	6100(20)	1045(13)	54(5)	359(16)
Cl(4)	8239(16)	1148(8)	-498(7)	318(13)
C(20)	7668(16)	899(12)	-23(5)	71(4)
C(30A)	7450(30)	2014(11)	4024(10)	71(4)
Cl(6A)	7927(9)	2699(5)	3710(2)	86(3)
Cl(7A)	8679(11)	1400(4)	4152(5)	120(5)
C(30B)	8950(50)	1640(40)	4332(9)	71(4)
Cl(7B)	8151(17)	1233(8)	4721(4)	59(5)
Cl(6B)	7750(20)	1502(13)	3909(5)	97(8)
C(11)	3844(5)	4026(3)	2882(2)	22(1)
C(12)	2660(6)	3584(3)	3419(2)	26(1)
C(13)	4210(9)	3906(5)	4040(2)	53(2)
C(14)	4483(11)	4663(5)	4019(3)	73(3)
C(15)	1782(8)	3723(4)	4121(2)	47(2)
C(16)	1674(10)	3027(5)	4333(3)	62(2)
C(21)	5552(5)	5172(3)	1758(2)	17(1)
C(22)	6133(5)	5887(3)	1203(2)	20(1)
C(23)	5850(7)	6222(3)	438(2)	33(1)
C(24)	7207(8)	6327(4)	280(2)	47(2)
C(25)	5696(6)	4979(3)	661(2)	26(1)
C(26)	4218(6)	4798(3)	635(2)	29(1)
C(31)	963(5)	4664(3)	1791(2)	19(1)

C(32)	43(5)	3685(3)	1428(2)	22(1)
C(33)	-510(7)	2921(4)	795(2)	37(2)
C(34)	549(9)	2788(5)	492(3)	57(2)
C(35)	-736(7)	4219(4)	738(2)	37(2)
C(36)	491(8)	4609(4)	609(3)	48(2)
C(41)	3249(5)	6421(3)	2576(2)	21(1)
C(42)	4668(5)	7179(3)	2977(2)	22(1)
C(43)	3326(6)	7311(3)	3586(2)	33(1)
C(44)	3101(8)	6593(4)	3767(3)	51(2)
C(45)	5788(6)	7569(3)	3681(2)	30(1)
C(46)	5957(6)	8356(3)	3656(2)	32(1)
C(101)	5083(5)	3997(3)	2644(2)	20(1)
C(102)	6188(5)	3581(3)	2708(2)	26(1)
C(103)	7224(6)	3689(3)	2441(2)	28(1)
C(104)	7121(5)	4211(3)	2127(2)	22(1)
C(105)	5970(5)	4603(3)	2076(2)	18(1)
C(201)	720(5)	5397(3)	1944(2)	21(1)
C(202)	-419(5)	5806(3)	1869(2)	30(1)
C(203)	-344(6)	6489(3)	2022(3)	39(2)
C(204)	816(6)	6739(3)	2255(2)	32(1)
C(205)	1904(5)	6299(3)	2327(2)	23(1)
Au(1)	983(1)	3261(1)	2454(1)	22(1)
Au(2)	6054(1)	6903(1)	2065(1)	21(1)
Ga(1)	3400(1)	5068(1)	2258(1)	18(1)
N(1)	5005(4)	4485(2)	2335(1)	16(1)
N(2)	1809(4)	5657(2)	2166(2)	19(1)
N(10)	5987(8)	2832(5)	255(3)	61(2)
N(11)	3769(5)	3578(2)	3192(2)	23(1)
N(12)	2867(6)	3720(3)	3834(2)	35(1)
N(21)	6412(4)	5359(2)	1497(1)	19(1)
N(22)	5920(4)	5713(2)	791(1)	22(1)
N(31)	-49(4)	4345(2)	1588(2)	21(1)
N(32)	-371(5)	3609(3)	1011(2)	28(1)
N(41)	3468(4)	7035(2)	2735(2)	24(1)
N(42)	4604(5)	7344(2)	3387(2)	23(1)
O(1)	6751(8)	2573(4)	3(3)	90(2)
O(2)	6166(7)	3344(4)	445(2)	73(2)
O(3)	4926(10)	2492(7)	274(3)	124(4)

O(11)	3016(4)	4517(2)	2772(1)	22(1)
O(21)	4353(3)	5412(2)	1768(1)	20(1)
O(31)	2175(3)	4454(2)	1865(1)	20(1)
O(41)	4032(3)	5888(2)	2615(1)	22(1)
S(1)	1063(2)	3359(1)	3191(1)	29(1)
S(2)	6235(2)	6759(1)	1343(1)	25(1)
S(3)	556(2)	2965(1)	1739(1)	29(1)
S(4)	6189(1)	7245(1)	2769(1)	26(1)

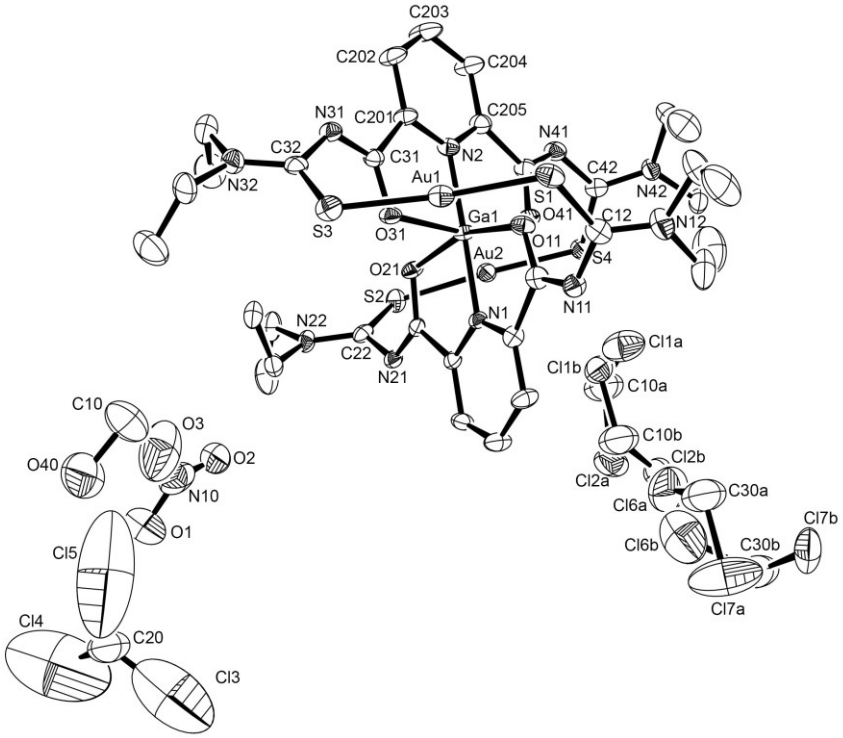

Figure A35: Ellipsoid plot of $[Ga\{Au(L4\text{-}\kappa S)\}_2](NO_3) \cdot 0.5CHCl_3 \cdot CH_2Cl_2 \cdot 0.5MeOH$. Thermal ellipsoids are at 50 % of probability. The hydrogen atoms have been omitted for clarity.

[Ga{Au(L4-κS)}$_2$](NO$_3$) (SQUEEZE)

Table A71: Crystal data and structure refinement for [Ga{Au(L4-κS)}$_2$](NO$_3$). **(SQUEEZE)**

Empirical formula	$C_{34}H_{46}Au_2GaN_{11}O_7S_4$	
Formula weight	1312.71	
Temperature	193(2) K	
Wavelength	0.71073 Å	
Crystal system	Monoclinic	
Space group	$P2_1/c$	
Unit cell dimensions	a = 10.020(7) Å	α = 90°.
	b = 19.210(1) Å	β = 96.068(2)°.
	c = 30.944(2) Å	γ = 90°.
Volume	5923.0(8) Å^3	
Z	4	
Density (calculated)	1.472 g/cm^3	
Absorption coefficient	5.578 mm^{-1}	
F(000)	2544	
Crystal size	0.42 x 0.33 x 0.04 mm^3	
Theta range for data collection	2.221 to 27.189°.	
Index ranges	-12<=h<=12, -24<=k<=23, -39<=l<=38	
Reflections collected	73994	
Independent reflections	13129 [R(int) = 0.0442]	
Completeness to theta = 25.242°	99.9 %	
Absorption correction	Semi-empirical from equivalents	
Max. and min. transmission	0.1859 and 0.0752	
Refinement method	Full-matrix least-squares on F^2	
Data / restraints / parameters	13129 / 0 / 541	
Goodness-of-fit on F^2	1.057	
Final R indices [I>2sigma(I)]	R1 = 0.0334, wR2 = 0.0847	
R indices (all data)	R1 = 0.0383, wR2 = 0.0865	
Largest diff. peak and hole	2.576 and -1.774 e · Å^{-3}	
Diffractometer	Bruker D8 Venture	

Table A72: Atomic coordinates (x 10^4) and equivalent isotropic displacement parameters ($Å^2$ x 10^3) for $[Ga\{Au(L4\text{-}\kappa S)\}_2](NO_3)$. U(eq) is defined as one third of the trace of the orthogonalized U^{ij} tensor. **(SQUEEZE)**

	x	y	z	U(eq)
Au(2)	983(1)	3261(1)	2454(1)	22(1)
Au(1)	6054(1)	6903(1)	2065(1)	21(1)
Ga(1)	3399(1)	5068(1)	2258(1)	17(1)
S(4)	555(1)	2965(1)	1739(1)	29(1)
S(1)	6235(1)	6759(1)	1343(1)	25(1)
S(3)	6189(1)	7246(1)	2769(1)	26(1)
S(2)	1062(1)	3358(1)	3190(1)	29(1)
O(11)	4351(3)	5413(2)	1768(1)	20(1)
O(41)	2174(3)	4455(2)	1865(1)	20(1)
O(21)	3014(3)	4517(2)	2771(1)	21(1)
O(31)	4031(3)	5888(2)	2614(1)	21(1)
N(2)	1807(3)	5657(2)	2165(1)	19(1)
N(31)	3466(3)	7036(2)	2735(1)	23(1)
N(41)	-50(3)	4348(2)	1588(1)	20(1)
N(42)	-368(4)	3606(2)	1012(1)	28(1)
C(32)	4667(4)	7179(2)	2978(1)	21(1)
C(205)	723(4)	5396(2)	1945(2)	21(1)
N(32)	4607(4)	7345(2)	3387(1)	24(1)
C(41)	958(4)	4666(2)	1790(1)	19(1)
C(31)	3249(4)	6421(2)	2576(1)	20(1)
C(201)	1905(4)	6297(2)	2327(1)	23(1)
C(42)	45(4)	3685(2)	1428(2)	22(1)
N(11)	6409(3)	5359(2)	1497(1)	19(1)
N(1)	5006(3)	4485(2)	2335(1)	16(1)
N(21)	3772(4)	3577(2)	3192(1)	23(1)
C(101)	5972(4)	4604(2)	2076(1)	18(1)
C(105)	5081(4)	3999(2)	2645(1)	20(1)
N(12)	5920(3)	5713(2)	791(1)	22(1)
C(11)	5555(4)	5171(2)	1758(1)	16(1)
C(21)	3848(4)	4026(2)	2882(2)	23(1)
C(16)	4219(5)	4801(3)	632(2)	29(1)
N(22)	2866(4)	3721(2)	3835(1)	35(1)

C(35)	5785(5)	7569(3)	3681(2)	30(1)
C(22)	2657(5)	3585(2)	3418(2)	26(1)
C(202)	811(4)	6738(2)	2255(2)	32(1)
C(204)	-418(4)	5804(2)	1869(2)	30(1)
C(12)	6133(4)	5887(2)	1203(1)	20(1)
C(15)	5698(5)	4979(2)	660(1)	26(1)
C(36)	5956(5)	8355(2)	3658(2)	32(1)
C(43)	-733(5)	4222(3)	737(2)	37(1)
C(203)	-347(5)	6486(3)	2023(2)	39(1)
C(13)	5845(5)	6225(3)	440(2)	32(1)
C(33)	3327(5)	7313(3)	3586(2)	31(1)
C(45)	-507(5)	2918(3)	796(2)	37(1)
C(44)	489(6)	4607(3)	609(2)	47(1)
C(34)	3098(7)	6588(3)	3766(2)	51(2)
C(25)	1780(6)	3724(3)	4122(2)	46(1)
C(46)	562(7)	2784(4)	496(2)	58(2)
C(14)	7207(6)	6327(3)	283(2)	47(2)
C(23)	4217(7)	3901(3)	4039(2)	52(2)
C(26)	1653(8)	3029(4)	4330(2)	63(2)
C(24)	4488(9)	4663(4)	4018(3)	75(2)
C(102)	7122(4)	4212(2)	2128(1)	23(1)
C(104)	6184(4)	3580(2)	2708(2)	26(1)
C(103)	7225(4)	3691(2)	2442(2)	29(1)
O(30)	6179(6)	3347(3)	444(2)	73(2)
N(10)	5990(6)	2839(4)	255(2)	61(2)
O(10)	6754(6)	2579(3)	0(2)	92(2)
O(20)	4916(8)	2499(5)	273(2)	126(3)

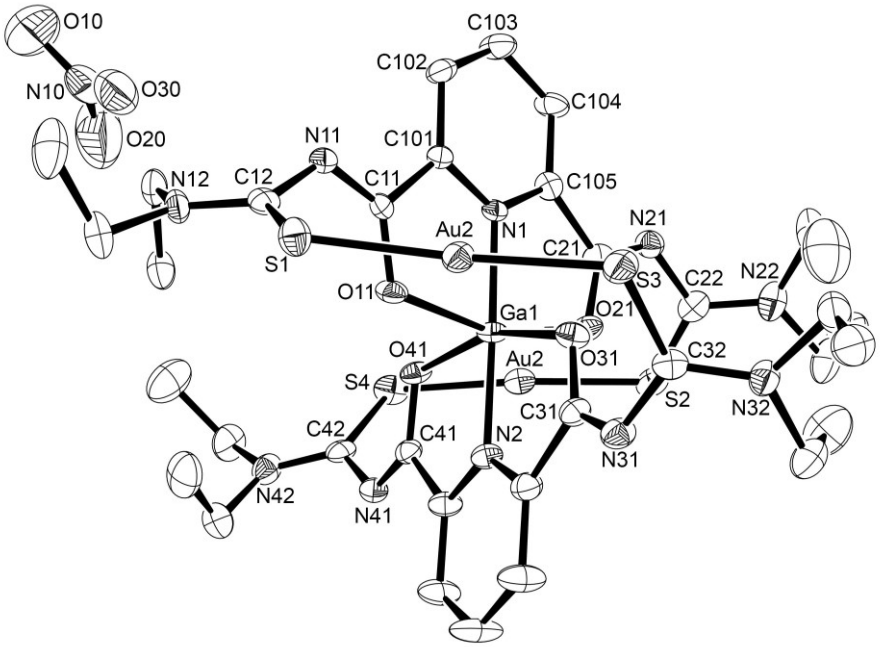

Figure A36: Ellipsoid plot of $[Ga\{Au(L4\text{-}\kappa S)\}_2](NO_3)$. Thermal ellipsoids are at 50 % of probability. The hydrogen atoms have been omitted for clarity. **(SQUEEZE)**

[Mn{Au(L4-κS)}$_2$] · 2MeOH · CH_2Cl_2

Table A73: Crystal data and structure refinement for [Mn{Au(L4-κS)}$_2$] · 2MeOH · CH_2Cl_2.

Empirical formula	$C_{37}H_{56}Au_2Cl_2MnN_{10}O_6S_4$	
Formula weight	1384.93	
Temperature	200(2) K	
Wavelength	0.71073 Å	
Crystal system	Monoclinic	
Space group	C2/c	
Unit cell dimensions	a = 12.080(6) Å	α = 90°.
	b = 17.515(1) Å	β = 93.383(4)°.
	c = 25.357(1) Å	γ = 90°.
Volume	5355.5(5) Å^3	
Z	4	
Density (calculated)	1.718 g/cm^3	
Absorption coefficient	6.002 mm^{-1}	
F(000)	2708	
Crystal size	0.22 x 0.16 x 0.05 mm^3	
Theta range for data collection	3.219 to 24.999°.	
Index ranges	-14<=h<=14, -20<=k<=20, -28<=l<=30	
Reflections collected	14411	
Independent reflections	4715 [R(int) = 0.0739]	
Completeness to theta = 24.999°	99.6 %	
Absorption correction	Integration	
Max. and min. transmission	0.1649 and 0.0914	
Refinement method	Full-matrix least-squares on F^2	
Data / restraints / parameters	4715 / 2 / 297	
Goodness-of-fit on F^2	1.064	
Final R indices [I>2sigma(I)]	R1 = 0.0488, wR2 = 0.1352	
R indices (all data)	R1 = 0.0522, wR2 = 0.1383	
Largest diff. peak and hole	3.399 and -1.778 e · Å^{-3}	
Diffractometer	IPDS STOE	

Table A74: Atomic coordinates (x 10^4) and equivalent isotropic displacement parameters ($Å^2$ x 10^3) for $[Mn\{Au(L4\text{-}\kappa S)\}_2] \cdot 2MeOH \cdot CH_2Cl_2$. U(eq) is defined as one third of the trace of the orthogonalized U ij tensor.

	x	y	z	U(eq)
C(101)	9259(6)	1218(4)	7192(3)	35(1)
C(201)	9312(5)	4440(4)	7800(3)	32(1)
C(202)	9270(7)	5234(4)	7806(3)	48(2)
C(203)	10000	5628(5)	7500	54(3)
C(11)	8474(6)	1680(4)	6845(3)	33(1)
C(12)	8072(5)	2878(3)	6508(3)	29(1)
C(21)	8614(5)	3926(3)	8115(3)	29(1)
C(22)	7067(5)	3948(4)	8645(2)	29(1)
C(23)	7572(6)	4850(4)	9344(3)	41(2)
C(24)	8615(7)	4544(6)	9612(4)	60(2)
C(25)	5875(6)	4031(5)	9402(3)	47(2)
C(26)	4944(7)	4582(7)	9297(4)	68(3)
Au(1)	6548(1)	3169(1)	7506(1)	33(1)
N(1)	10000	1593(4)	7500	30(2)
N(2)	10000	4071(4)	7500	29(2)
N(11)	8691(4)	2433(3)	6865(2)	27(1)
N(21)	7886(4)	4276(3)	8394(2)	31(1)
N(22)	6856(4)	4239(3)	9116(2)	34(1)
O(11)	7768(4)	1358(3)	6554(2)	47(1)
O(21)	8838(4)	3221(2)	8104(2)	31(1)
S(1)	6796(2)	3249(1)	6631(1)	40(1)
S(2)	6154(2)	3259(1)	8373(1)	40(1)
Mn(1)	10000	2832(1)	7500	27(1)
O(10)	6403(5)	1655(4)	5642(3)	57(2)
C(10)	5348(9)	1632(7)	5805(6)	80(3)
C(1E)	7280(30)	6788(18)	6274(13)	80(3)
Cl(1E)	6485(7)	5995(6)	6368(4)	73(2)
Cl(2E)	7329(8)	7102(6)	5624(5)	73(2)
C(1F)	6830(40)	6660(30)	6449(10)	80(3)
Cl(1F)	7835(8)	6101(7)	6838(5)	73(2)
Cl(2F)	7231(9)	6590(8)	5764(6)	73(2)
N(12)	8495(5)	3051(3)	6051(2)	37(1)

C(13)	9501(6)	2687(4)	5870(3)	41(2)
C(15)	7962(7)	3621(5)	5679(3)	54(2)
C(14)	9239(9)	2054(6)	5473(4)	62(2)
C(16)	8243(9)	4403(6)	5845(5)	72(3)
C(102)	9213(7)	414(4)	7191(3)	46(2)
C(103)	10000	32(6)	7500	57(3)

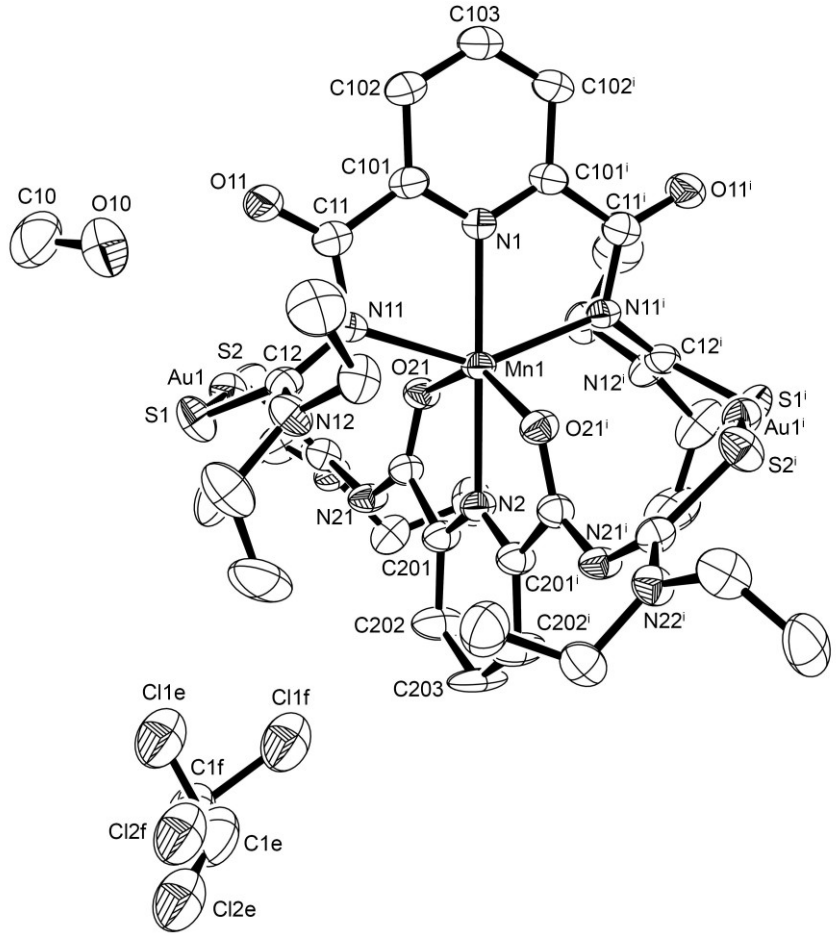

Figure A37: Ellipsoid plot of [Mn{Au(L4-κS)}$_2$] · 2MeOH · CH_2Cl_2. Thermal ellipsoids are at 50 % of probability. The hydrogen atoms have been omitted for clarity.

$[Co\{Au(L4\text{-}\kappa S)\}_2] \cdot MeOH \cdot H_2O \cdot 0.5CH_2Cl_2$

Table A75: Crystal data and structure refinement for $[Co\{Au(L4\text{-}\kappa S)\}_2] \cdot MeOH \cdot H_2O \cdot 0.5CH_2Cl_2$.

Empirical formula	$C_{35.5}H_{53}Au_2ClCoN_{10}O_6S_4$	
Formula weight	1332.43	
Temperature	100(2) K	
Wavelength	0.71073 Å	
Crystal system	Monoclinic	
Space group	$P2_1/n$	
Unit cell dimensions	a = 18.102(1) Å	α = 90°.
	b = 13.953(1) Å	β = 101.59°.
	c = 19.814(1) Å	γ = 90°.
Volume	4902.5(5) $Å^3$	
Z	4	
Density (calculated)	1.805 g/cm^3	
Absorption coefficient	6.580 mm^{-1}	
F(000)	2600	
Crystal size	0.28 x 0.16 x 0.05 mm^3	
Theta range for data collection	2.244 to 24.999°.	
Index ranges	-21<=h<=21, -16<=k<=16, -23<=l<=23	
Reflections collected	49727	
Independent reflections	8617 [R(int) = 0.0503]	
Completeness to theta = 24.999°	99.7 %	
Absorption correction	Semi-empirical from equivalents	
Max. and min. transmission	0.7454 and 0.4921	
Refinement method	Full-matrix least-squares on F^2	
Data / restraints / parameters	8617 / 30 / 549	
Goodness-of-fit on F^2	1.090	
Final R indices [I>2sigma(I)]	R1 = 0.0367, wR2 = 0.0827	
R indices (all data)	R1 = 0.0483, wR2 = 0.0896	
Largest diff. peak and hole	3.000 and -1.559 e · $Å^{-3}$	
Diffractometer	Bruker D8 Venture	

Table A76: Atomic coordinates (x 10^4) and equivalent isotropic displacement parameters (Å^2 x 10^3) for $[Co\{Au(L4\text{-}\kappa S)\}_2] \cdot MeOH \cdot H_2O \cdot 0.5CH_2Cl_2$. U(eq) is defined as one third of the trace of the orthogonalized U^{ij} tensor.

	x	y	z	U(eq)
Au(1)	4766(1)	8783(1)	9682(1)	18(1)
Au(2)	4082(1)	6540(1)	13223(1)	25(1)
Co(1)	4511(1)	7082(1)	11326(1)	14(1)
S(4)	5960(1)	8483(1)	9503(1)	19(1)
S(2)	3566(1)	9081(1)	9828(1)	24(1)
S(3)	2798(1)	6718(1)	13016(1)	25(1)
S(1)	5363(1)	6565(2)	13483(1)	37(1)
N(1)	4399(3)	5750(4)	10894(3)	15(1)
O(31)	3607(3)	7423(3)	11833(2)	20(1)
O(41)	5473(3)	7511(3)	10922(2)	16(1)
N(2)	4775(3)	8418(4)	11739(3)	17(1)
N(11)	5191(3)	6135(4)	12115(3)	18(1)
N(41)	6283(3)	8792(4)	10880(3)	18(1)
N(22)	2562(3)	8016(4)	10275(3)	20(1)
N(12)	6372(3)	6611(4)	12697(3)	23(1)
O(21)	3304(3)	6497(4)	9313(2)	30(1)
N(32)	2036(3)	8342(4)	12767(3)	23(1)
O(11)	5418(3)	4527(4)	12352(3)	37(1)
N(42)	7259(3)	8300(4)	10393(3)	20(1)
C(41)	5725(4)	8344(4)	11091(3)	14(1)
N(21)	3716(3)	7269(4)	10352(3)	16(1)
N(31)	3264(4)	8476(4)	12624(3)	24(1)
C(103)	4371(4)	3994(5)	10262(4)	22(2)
C(205)	5349(4)	8892(4)	11578(3)	15(1)
C(21)	3657(4)	6532(5)	9913(3)	18(1)
C(42)	6533(4)	8498(4)	10325(3)	17(1)
C(201)	4328(4)	8817(5)	12124(3)	22(2)
C(101)	4732(4)	4994(4)	11246(3)	16(1)
C(45)	7769(4)	8328(5)	11075(3)	25(2)
C(105)	4047(4)	5647(4)	10245(3)	14(1)
C(12)	5662(4)	6413(5)	12718(3)	22(2)

C(32)	2693(4)	7918(5)	12765(3)	22(2)
C(22)	3255(4)	8054(4)	10164(3)	17(1)
C(104)	4020(4)	4776(5)	9903(3)	19(1)
C(11)	5144(4)	5201(5)	11968(3)	20(1)
C(23)	2053(4)	8851(5)	10162(4)	25(2)
C(25)	2254(4)	7181(5)	10586(4)	24(2)
C(43)	7617(4)	8054(5)	9807(4)	24(2)
C(13)	6695(4)	6416(5)	12084(4)	27(2)
C(102)	4726(4)	4091(5)	10937(3)	19(1)
C(31)	3690(4)	8176(5)	12199(3)	20(2)
C(44)	7614(5)	6984(6)	9685(4)	34(2)
C(15)	6881(4)	7109(5)	13259(4)	29(2)
C(202)	4463(5)	9738(5)	12366(4)	35(2)
C(33)	1369(5)	7818(6)	12882(5)	37(2)
C(16)	6795(5)	8193(6)	13143(4)	38(2)
C(24)	2143(5)	9474(6)	10795(4)	36(2)
C(14)	7125(5)	5477(6)	12142(4)	36(2)
C(34)	961(7)	7385(8)	12210(6)	77(4)
C(35)	1940(5)	9393(5)	12648(4)	26(2)
C(204)	5519(4)	9819(5)	11813(3)	23(2)
C(36)	2117(5)	9931(5)	13319(4)	27(2)
C(46)	8162(5)	9291(5)	11217(4)	32(2)
C(26)	1759(5)	6557(6)	10055(4)	35(2)
C(203)	5068(5)	10233(5)	12208(4)	35(2)
O(30)	4170(14)	9227(17)	4027(10)	140(11)
C(1E)	4890(20)	8350(80)	5730(30)	287(12)
Cl(1E)	4653(12)	7740(30)	4978(10)	287(12)
Cl(2E)	4188(12)	8510(30)	6176(10)	287(12)
C(1F)	4860(80)	8390(50)	5420(30)	287(12)
Cl(1F)	4560(20)	7310(40)	5660(20)	287(12)
Cl(2F)	4900(20)	9220(40)	6056(19)	287(12)
O(20)	4980(30)	5800(40)	5460(20)	270(20)
C(10)	6238(6)	2536(7)	2090(5)	51(3)
O(10)	5673(6)	2617(7)	2471(6)	110(3)

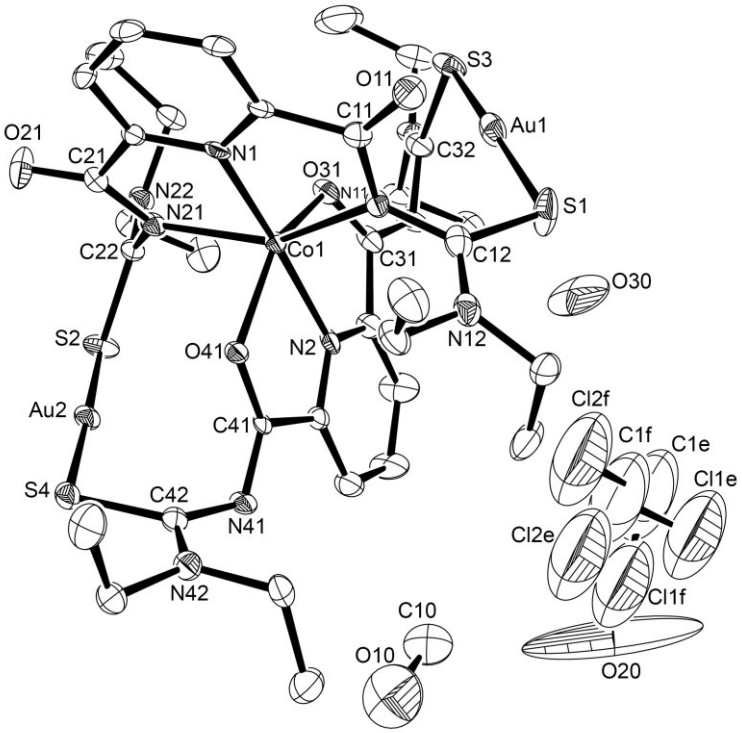

Figure A38: Ellipsoid plot of $[Co\{Au(L4\text{-}\kappa S)\}_2\}] \cdot MeOH \cdot H_2O \cdot 0.5CH_2Cl_2$. Thermal ellipsoids are at 50 % of probability. The hydrogen atoms have been omitted for clarity.

[Ni{Au(L4-κS)}$_2$] · MeOH

Table A77: Crystal data and structure refinement for [Ni{Au(L4-κS)}$_2$] · 2MeOH.

Empirical formula	$C_{36}H_{54}Au_2N_{10}NiO_6S_4$	
Formula weight	1303.77	
Temperature	200(2) K	
Wavelength	0.71073 Å	
Crystal system	Monoclinic	
Space group	C2/c	
Unit cell dimensions	a = 20.4250(9) Å	α = 90°.
	b = 16.2684(7) Å	β = 102.803(1)°.
	c = 13.7060(5) Å	γ = 90°.
Volume	4441.0(3) Å^3	
Z	4	
Density (calculated)	1.950 g/cm^3	
Absorption coefficient	7.254 mm^{-1}	
F(000)	2552	
Crystal size	0.22 x 0.08 x 0.05 mm^3	
Theta range for data collection	2.5 to 27.12°.	
Index ranges	-26<=h<=26, -20<=k<=19, -17<=l<=17	
Reflections collected	26869	
Independent reflections	4923 [R(int) = 0.0328]	
Completeness to theta = 25.242°	99.9 %	
Absorption correction	Semi-empirical from equivalents	
Max. and min. transmission	0.7455 and 0.5365	
Refinement method	Full-matrix least-squares on F^2	
Data / restraints / parameters	4923 / 3 / 272	
Goodness-of-fit on F^2	1.018	
Final R indices [I>2sigma(I)]	R1 = 0.0158, wR2 = 0.0326	
R indices (all data)	R1 = 0.0187, wR2 = 0.0335	
Largest diff. peak and hole	0.565 and -0.418 e · Å^{-3}	
Diffractometer	IPDS STOE	

Table A78: Atomic coordinates (x 10^4) and equivalent isotropic displacement parameters ($Å^2$ x 10^3) for [Ni{Au(L4-κS)}$_2$] · 2MeOH. U(eq) is defined as one third of the trace of the orthogonalized U^{ij} tensor.

	x	y	z	U(eq)
C(105)	5137(1)	6036(1)	1715(2)	8(1)
C(201)	5554(1)	9280(1)	2959(2)	8(1)
C(104)	5113(1)	5183(1)	1672(2)	12(1)
C(202)	5574(1)	10132(1)	2969(2)	10(1)
C(103)	5000	4759(2)	2500	14(1)
C(203)	5000	10562(2)	2500	12(1)
C(10)	3992(2)	7268(2)	6904(2)	30(1)
C(11)	4625(1)	6574(1)	4035(2)	10(1)
C(12)	4255(1)	7915(1)	4249(2)	10(1)
C(13)	3182(1)	7443(1)	3191(2)	12(1)
C(14)	2772(1)	6832(2)	3641(2)	21(1)
C(15)	3220(1)	8634(2)	4352(2)	18(1)
C(16)	3277(1)	9453(2)	3844(2)	24(1)
C(31)	6105(1)	8708(1)	3467(2)	8(1)
C(32)	7112(1)	8751(1)	4722(2)	10(1)
C(33)	8280(1)	8757(1)	5705(2)	13(1)
C(34)	8321(1)	9381(2)	6536(2)	17(1)
C(35)	7973(1)	9502(1)	4087(2)	15(1)
C(36)	8315(1)	9007(2)	3410(2)	21(1)
N(1)	5000	6441(2)	2500	8(1)
N(2)	5000	8876(2)	2500	7(1)
N(11)	4592(1)	7365(1)	3767(1)	8(1)
N(12)	3595(1)	7978(1)	3961(1)	10(1)
N(31)	6657(1)	9080(1)	3963(1)	10(1)
N(32)	7750(1)	8977(1)	4828(1)	10(1)
O(10)	3665(1)	6733(2)	6145(2)	41(1)
O(11)	4452(1)	6250(1)	4761(1)	17(1)
O(31)	5991(1)	7947(1)	3351(1)	9(1)
S(1)	4671(1)	8572(1)	5166(1)	16(1)
S(3)	6918(1)	8135(1)	5673(1)	11(1)
Ni(1)	5000	7662(1)	2500	6(1)
Au(1)	5781(1)	8275(1)	5426(1)	11(1)

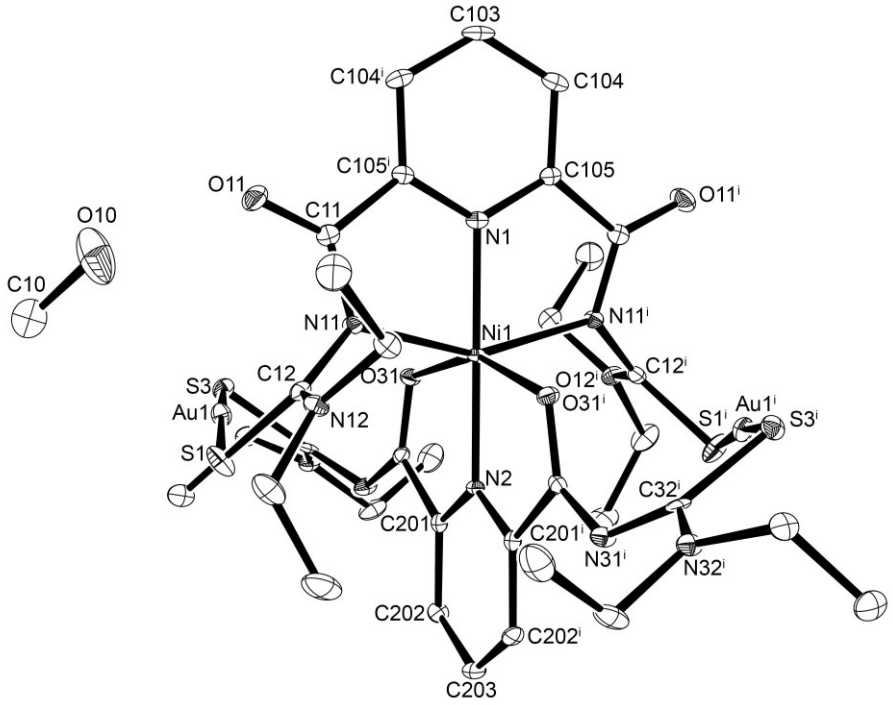

Figure A39: Ellipsoid plot of [Ni{Au(L4-κS)}$_2$] · 2MeOH. Thermal ellipsoids are at 50 % of probability. The hydrogen atoms have been omitted for clarity.

$[Cu\{Au(L4\text{-}\kappa S)\}_2] \cdot 0.5CH_2Cl_2 \cdot 0.5H_2O$

Table A79: Crystal data and structure refinement for $[Cu\{Au(L4\text{-}\kappa S)\}_2] \cdot 0.5CH_2Cl_2 \cdot 0.5H_2O$.

Empirical formula	$C_{34.5}H_{48}Au_2ClCuN_{10}O_{4.5}S_4$	
Formula weight	1295.99	
Temperature	200(2) K	
Wavelength	0.71073 Å	
Crystal system	Monoclinic	
Space group	$P2_1/n$	
Unit cell dimensions	a = 16.1249(8) Å	α = 90°.
	b = 15.9140(7) Å	β = 93.543(4)°.
	c = 18.7319(1) Å	γ = 90°.
Volume	4797.6(4) $Å^3$	
Z	4	
Density (calculated)	1.794 g/cm^3	
Absorption coefficient	6.816 mm^{-1}	
F(000)	2516	
Crystal size	0.23 x 0.18 x 0.11 mm^3	
Theta range for data collection	3.362 to 25.999°.	
Index ranges	-19<=h<=19, -19<=k<=17, -20<=l<=23	
Reflections collected	23582	
Independent reflections	9308 [R(int) = 0.0510]	
Completeness to theta = 25.242°	98.8 %	
Absorption correction	Integration	
Max. and min. transmission	0.2761 and 0.1478	
Refinement method	Full-matrix least-squares on F^2	
Data / restraints / parameters	9308 / 4 / 527	
Goodness-of-fit on F^2	0.971	
Final R indices [I>2sigma(I)]	R1 = 0.0411, wR2 = 0.0933	
R indices (all data)	R1 = 0.0593, wR2 = 0.0991	
Largest diff. peak and hole	1.826 and -1.542 e · $Å^{-3}$	
Diffractometer	IPDS STOE	

Table A80: Atomic coordinates (x 10^4) and equivalent isotropic displacement parameters ($Å^2$ x 10^3) for $[Cu\{Au(L4\text{-}\kappa S)\}_2] \cdot 0.5CH_2Cl_2 \cdot 0.5H_2O$. U(eq) is defined as one third of the trace of the orthogonalized U^{ij} tensor.

	x	y	z	U(eq)
C(101)	-560(4)	9390(4)	744(4)	36(1)
C(201)	-224(3)	11550(4)	3018(4)	35(1)
C(1E)	-424(10)	7025(9)	1993(9)	61(5)
C(102)	-487(5)	8948(5)	118(4)	51(2)
C(202)	-415(4)	11954(5)	3643(4)	40(2)
C(103)	298(5)	8681(5)	-52(4)	52(2)
C(203)	-635(4)	11475(5)	4218(4)	46(2)
C(104)	975(5)	8836(4)	412(4)	49(2)
C(205)	-442(3)	10247(4)	3537(3)	34(1)
C(105)	865(4)	9287(4)	1036(4)	37(1)
C(204)	-638(4)	10609(5)	4168(4)	41(2)
C(11)	-1384(4)	9687(4)	996(4)	42(2)
C(12)	-2012(4)	10222(4)	1987(4)	40(2)
C(13)	-2157(5)	8705(5)	2231(5)	57(2)
C(14)	-2760(6)	8209(6)	1741(5)	71(3)
C(15)	-3099(5)	9739(6)	2757(5)	66(2)
C(16)	-2776(6)	9958(7)	3495(6)	81(3)
C(21)	1550(4)	9571(4)	1551(3)	33(1)
C(22)	1859(3)	10516(4)	2478(4)	36(1)
C(23)	2973(4)	11560(5)	2588(4)	47(2)
C(24)	2678(6)	12319(5)	3002(6)	67(2)
C(25)	2204(5)	11311(5)	1415(5)	55(2)
C(26)	1997(5)	12216(5)	1261(5)	61(2)
C(31)	-8(3)	11992(4)	2345(4)	33(1)
C(32)	-46(4)	13303(4)	1795(4)	39(2)
C(33)	1072(4)	14123(5)	2392(5)	51(2)
C(34)	714(5)	14679(6)	2937(5)	66(2)
C(35)	437(5)	14592(6)	1204(5)	65(2)
C(36)	979(6)	14357(8)	620(6)	88(3)
C(41)	-388(3)	9308(4)	3414(4)	35(1)
C(42)	-151(4)	8072(4)	4082(3)	36(1)

C(43)	-1485(4)	7615(5)	4477(5)	54(2)
C(44)	-1645(6)	7978(7)	5191(5)	77(3)
C(45)	-244(5)	6680(5)	4636(5)	59(2)
C(46)	-328(7)	6001(6)	4071(6)	84(3)
N(1)	102(3)	9560(3)	1179(3)	33(1)
N(2)	-246(3)	10704(3)	2973(3)	33(1)
N(11)	-1304(3)	10061(3)	1629(3)	36(1)
N(12)	-2397(3)	9594(4)	2295(4)	50(2)
N(21)	1280(3)	10058(3)	2072(3)	37(1)
N(22)	2303(3)	11102(4)	2176(3)	40(1)
N(31)	-13(3)	12825(3)	2386(3)	40(1)
N(32)	464(3)	13970(4)	1782(3)	43(1)
N(41)	-472(3)	8840(4)	3997(3)	42(1)
N(42)	-600(3)	7482(4)	4373(3)	43(1)
O(10)	3182(5)	9404(6)	198(4)	41(2)
O(11)	-2019(3)	9558(4)	619(3)	55(1)
O(21)	2274(3)	9371(3)	1468(3)	48(1)
O(31)	171(2)	11548(3)	1825(2)	35(1)
O(41)	-268(3)	9052(3)	2801(2)	38(1)
S(1)	-2411(1)	11215(1)	2069(1)	60(1)
S(2)	2004(1)	10374(1)	3393(1)	45(1)
S(3)	-783(1)	13176(1)	1077(1)	45(1)
S(4)	876(1)	7831(1)	3902(1)	45(1)
Au(1)	-1605(1)	12141(1)	1511(1)	43(1)
Au(2)	1442(1)	9097(1)	3616(1)	39(1)
Cu(1)	-37(1)	10159(1)	2056(1)	32(1)
Cl(1)	266(9)	7758(9)	1989(8)	238(5)
Cl(2)	-748(10)	6760(10)	1176(7)	238(5)

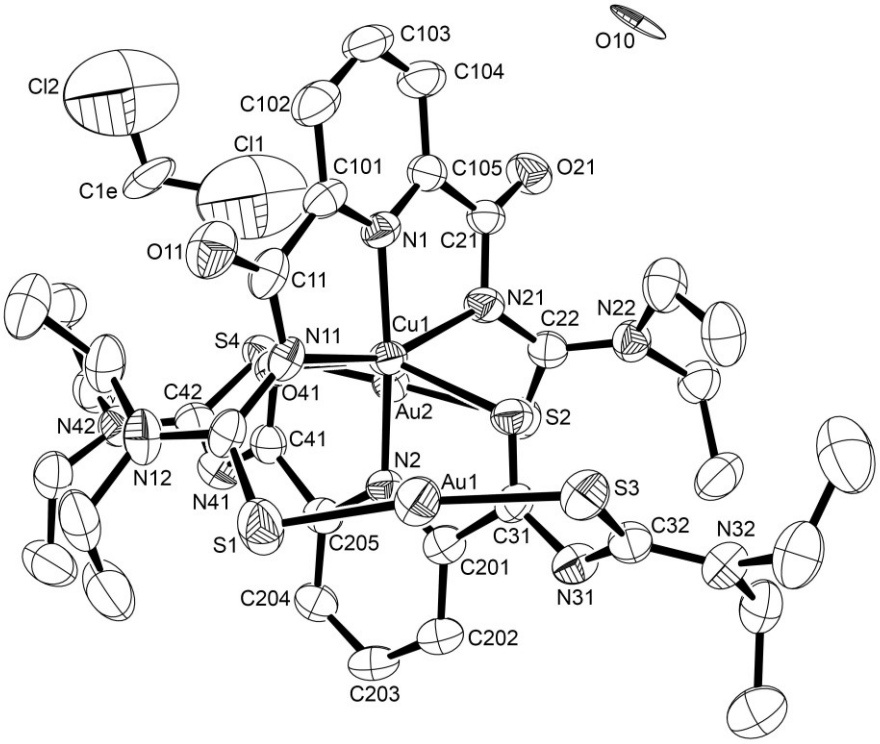

Figure A40: Ellipsoid plot of $[Cu\{Au(L4\text{-}\kappa S)\}_2] \cdot 0.5CH_2Cl_2 \cdot 0.5H_2O$. Thermal ellipsoids are at 50 % of probability. The hydrogen atoms have been omitted for clarity.

$[Zn\{Au(L4\text{-}\kappa S)\}_2] \cdot 0.5CH_2Cl_2 \cdot H_2O$

Table A81: Crystal data and structure refinement for $[Zn\{Au(L4\text{-}\kappa S)\}_2] \cdot 0.5CH_2Cl_2 \cdot H_2O$

Empirical formula	$C_{34.5}H_{47}Au_2ClN_{10}O_5S_4Zn$	
Formula weight	1304.81	
Temperature	100(2) K	
Wavelength	0.71073 Å	
Crystal system	Monoclinic	
Space group	$P2_1/c$	
Unit cell dimensions	a = 15.2417(4) Å	α = 90°.
	b = 22.4929(6) Å	β = 101.096(1)°.
	c = 14.3165(4) Å	γ = 90°.
Volume	4816.4(2) $Å^3$	
Z	4	
Density (calculated)	1.799 g/cm^3	
Absorption coefficient	6.848 mm^{-1}	
F(000)	2532	
Crystal size	0.22 x 0.07 x 0.05 mm^3	
Theta range for data collection	2.320 to 26.429°.	
Index ranges	-18<=h<=19, -28<=k<=28, -17<=l<=17	
Reflections collected	51442	
Independent reflections	9860 [R(int) = 0.0422]	
Completeness to theta = 25.242°	99.9 %	
Absorption correction	Semi-empirical from equivalents	
Max. and min. transmission	0.7454 and 0.6132	
Refinement method	Full-matrix least-squares on F^2	
Data / restraints / parameters	9860 / 3 / 534	
Goodness-of-fit on F^2	1.047	
Final R indices [I>2sigma(I)]	R1 = 0.0308, wR2 = 0.0699	
R indices (all data)	R1 = 0.0416, wR2 = 0.0743	
Largest diff. peak and hole	1.759 and -1.538 e · $Å^{-3}$	
Diffractometer	Bruker D8 Venture	

Table A82: Atomic coordinates (x 10^4) and equivalent isotropic displacement parameters ($Å^2$ x 10^3) for $[Zn\{Au(L4\text{-}\kappa S)\}_2] \cdot 0.5CH_2Cl_2 \cdot H_2O$. U(eq) is defined as one third of the trace of the orthogonalized U^{ij} tensor.

	x	y	z	U(eq)
C(101)	9199(3)	5535(2)	8650(4)	16(1)
C(205)	5530(3)	5468(2)	8839(3)	14(1)
C(102)	10090(3)	5704(2)	8794(4)	20(1)
C(204)	4625(3)	5335(2)	8730(4)	20(1)
C(103)	10510(3)	5890(2)	9697(4)	24(1)
C(203)	4374(3)	4744(2)	8788(4)	21(1)
C(104)	10032(3)	5907(2)	10431(4)	21(1)
C(202)	5022(3)	4302(2)	8942(3)	18(1)
C(105)	9139(3)	5722(2)	10237(3)	15(1)
C(201)	5915(3)	4468(2)	9036(3)	15(1)
C(11)	8653(3)	5384(2)	7695(4)	16(1)
C(12)	7205(3)	5192(2)	6895(3)	17(1)
C(13)	6071(4)	5672(3)	5676(4)	30(1)
C(14)	5193(4)	5592(3)	6018(5)	38(2)
C(15)	7115(4)	6287(2)	6846(4)	24(1)
C(16)	7705(4)	6585(2)	6234(5)	32(1)
C(21)	8526(3)	5699(2)	10940(4)	17(1)
C(42)	5654(3)	7092(2)	8761(4)	20(1)
C(45)	4521(4)	7270(2)	7308(4)	29(1)
C(46)	4828(4)	7271(3)	6353(4)	35(1)
C(31)	6720(3)	4066(2)	9240(3)	15(1)
C(32)	7247(3)	3096(2)	9316(4)	22(1)
C(33)	7998(5)	2219(3)	10138(5)	45(2)
C(34)	7533(6)	1662(3)	9675(6)	62(2)
C(35)	6906(4)	2827(3)	10858(4)	37(2)
C(36)	7417(5)	3277(4)	11551(5)	53(2)
C(41)	5947(3)	6079(2)	8832(4)	18(1)
C(22)	8387(3)	5988(2)	12475(4)	19(1)
C(23)	8418(4)	5883(3)	14192(4)	34(1)
C(24)	7935(5)	5319(4)	14389(5)	57(2)
C(25)	9688(4)	5539(3)	13475(4)	37(2)

C(26)	10422(4)	6000(4)	13682(6)	60(2)
N(1)	8758(3)	5539(2)	9369(3)	15(1)
N(2)	6142(3)	5037(2)	8981(3)	14(1)
N(11)	7813(3)	5233(2)	7734(3)	17(1)
N(12)	6834(3)	5684(2)	6493(3)	20(1)
N(41)	5366(3)	6522(2)	8702(3)	19(1)
N(42)	5236(3)	7464(2)	8087(3)	26(1)
N(31)	6566(3)	3493(2)	9255(3)	17(1)
N(32)	7371(3)	2723(2)	10054(3)	30(1)
N(21)	8859(3)	5939(2)	11771(3)	19(1)
N(22)	8794(3)	5820(2)	13329(3)	24(1)
O(11)	8982(2)	5422(2)	6968(3)	23(1)
O(21)	7785(2)	5439(2)	10677(2)	21(1)
O(31)	7481(2)	4320(2)	9398(2)	18(1)
O(41)	6780(2)	6102(2)	8908(3)	20(1)
S(1)	6864(1)	4516(1)	6381(1)	23(1)
S(4)	6444(1)	7400(1)	9670(1)	27(1)
S(3)	7885(1)	3010(1)	8444(1)	24(1)
S(2)	7329(1)	6309(1)	12362(1)	23(1)
Zn(1)	7470(1)	5251(1)	9173(1)	17(1)
Au(1)	7453(1)	3793(1)	7435(1)	18(1)
Au(2)	6913(1)	6764(1)	10914(1)	20(1)
Cl(1A)	9091(9)	7565(6)	5045(10)	138(3)
C(10A)	8640(30)	7691(15)	3887(15)	74(3)
Cl(2A)	9364(9)	7696(6)	3125(10)	138(3)
Cl(1B)	10218(12)	7682(9)	4062(15)	138(3)
C(10B)	9316(15)	7689(19)	4210(30)	74(3)
Cl(2B)	8449(13)	7978(10)	3879(16)	138(3)
C(43)	5429(4)	8113(2)	8112(4)	33(1)
C(44)	4865(4)	8433(3)	8714(5)	42(2)
O(20A)	281(7)	6010(4)	6244(7)	74(3)
O(20B)	606(15)	6340(10)	6551(15)	74(3)

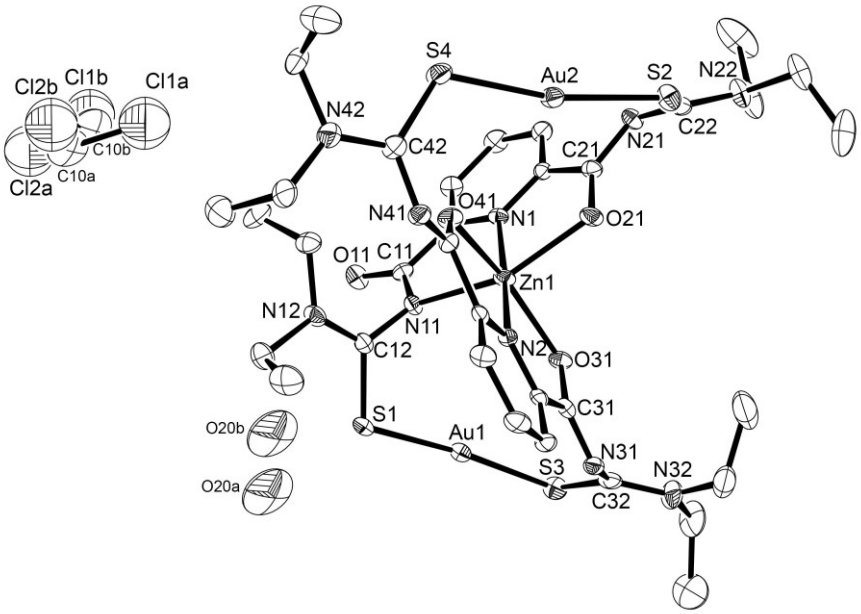

Figure A41: Ellipsoid plot of $[Zn\{Au(L4\text{-}\kappa S)\}_2] \cdot 0.5CH_2Cl_2 \cdot H_2O$. Thermal ellipsoids are at 50 % of probability. The hydrogen atoms have been omitted for clarity.

[Hg{Au(L4-κS)}$_2$] · 1.5MeOH

Table A83: Crystal data and structure refinement for [Hg{Au(L4-κS)}$_2$] · 1.5MeOH.

Empirical formula	$C_{35.5}H_{52}Au_2HgN_{10}O_{5.5}S_4$	
Formula weight	1429.63	
Temperature	100(2) K	
Wavelength	0.71073 Å	
Crystal system	Monoclinic	
Space group	P21/n	
Unit cell dimensions	a = 19.1355(9) Å	α = 90°.
	b = 16.8844(8) Å	β = 107.565(2)°.
	c = 29.818(1) Å	γ = 90°.
Volume	9184.8(7) Å^3	
Z	8	
Density (calculated)	2.068 g/cm^3	
Absorption coefficient	9.942 mm^{-1}	
F(000)	5448	
Crystal size	0.21 x 0.07 x 0.05 mm^3	
Theta range for data collection	2.233 to 27.182°	
Index ranges	-24<=h<=24, -21<=k<=21, -34<=l<=38	
Reflections collected	350476	
Independent reflections	20388 [R(int) = 0.1401]	
Completeness to theta = 25.242°	99.9 %	
Absorption correction	Semi-empirical from equivalents	
Max. and min. transmission	0.7455 and 0.4778	
Refinement method	Full-matrix least-squares on F^2	
Data / restraints / parameters	20388 / 31 / 1062	
Goodness-of-fit on F^2	1.028	
Final R indices [I>2sigma(I)]	R1 = 0.0320, wR2 = 0.0741	
R indices (all data)	R1 = 0.0419, wR2 = 0.0776	
Largest diff. peak and hole	4.071 and -3.584 e · Å^{-3}	
Diffractometer	Bruker D8 Venture	

Table A84: Atomic coordinates (x 10^4) and equivalent isotropic displacement parameters ($Å^2$ x 10^3) for [Hg{Au(L4-κS)}$_2$] · 1.5MeOH. U(eq) is defined as one third of the trace of the orthogonalized U^{ij} tensor.

	x	y	z	U(eq)
C(55A)	7403(4)	4704(4)	9107(3)	43(2)
C(56A)	7754(11)	4265(9)	8795(6)	65(6)
C(55B)	7403(4)	4704(4)	9107(3)	43(2)
C(56B)	7204(7)	4622(8)	9596(4)	38(4)
S(8)	10425(1)	3578(1)	8591(1)	29(1)
S(1)	17888(1)	8640(1)	11336(1)	45(1)
S(7)	8694(1)	8766(1)	8944(1)	47(1)
S(5)	7043(1)	6767(1)	8392(1)	44(1)
S(4)	14768(1)	6153(1)	10738(1)	48(1)
O(61)	10480(2)	6596(2)	8915(1)	31(1)
O(21)	14488(2)	8607(2)	11063(1)	24(1)
O(31)	15938(2)	9823(2)	11454(1)	24(1)
O(81)	9232(2)	5111(2)	8503(1)	27(1)
O(11)	16641(2)	9233(2)	9980(1)	25(1)
N(2)	15905(2)	8417(2)	11888(2)	20(1)
N(1)	15118(2)	8815(2)	10380(1)	17(1)
N(12)	17557(2)	7881(3)	10529(2)	22(1)
O(71)	8851(2)	8498(2)	7702(2)	35(1)
O(51)	7989(2)	6102(2)	9783(1)	35(1)
N(41)	15755(2)	7102(3)	11346(2)	24(1)
N(11)	16588(2)	8593(3)	10653(1)	21(1)
N(4)	9094(2)	6443(3)	7957(2)	24(1)
N(31)	16423(3)	10408(3)	12179(2)	26(1)
O(41)	15494(2)	6378(2)	11933(2)	36(1)
N(32)	16406(3)	11756(3)	12126(2)	27(1)
N(42)	16208(3)	6086(3)	10998(2)	26(1)
N(3)	9635(3)	6253(3)	9480(1)	24(1)
N(81)	9403(3)	4362(3)	7900(2)	26(1)
N(21)	13343(2)	8731(3)	10521(2)	21(1)
N(71)	9276(3)	7853(3)	8411(2)	29(1)
C(12)	17307(3)	8372(3)	10790(2)	22(1)
C(102)	15094(3)	9169(3)	9604(2)	22(1)

N(22)	12462(3)	9046(3)	10862(2)	28(1)
C(101)	15473(3)	8982(3)	10065(2)	20(1)
N(62)	12473(3)	6878(3)	9370(2)	32(1)
C(21)	14067(3)	8708(3)	10656(2)	18(1)
N(72)	9890(3)	9029(3)	8700(2)	31(1)
C(31)	16134(3)	9816(3)	11897(2)	21(1)
C(32)	16662(3)	11076(3)	12024(2)	23(1)
N(61)	11507(3)	6234(3)	9510(2)	34(1)
C(22)	12940(3)	8516(3)	10797(2)	24(1)
N(51)	8179(3)	6119(3)	9049(2)	26(1)
C(105)	14393(3)	8855(3)	10261(2)	16(1)
C(41)	15662(3)	7005(3)	11768(2)	26(1)
C(81)	9282(3)	5027(3)	8097(2)	21(1)
N(52)	7071(3)	5402(3)	8840(2)	35(1)
N(82)	9206(3)	3046(3)	8005(2)	37(1)
C(11)	16298(3)	8949(3)	10230(2)	20(1)
C(205)	15779(3)	7727(3)	12070(2)	23(1)
C(104)	13978(3)	9035(3)	9802(2)	21(1)
C(61)	10811(3)	6360(3)	9323(2)	27(1)
C(82)	9615(3)	3694(3)	8138(2)	26(1)
C(51)	8388(3)	6108(3)	9524(2)	27(1)
C(401)	9026(3)	7107(3)	7700(2)	26(1)
C(305)	10360(3)	6208(3)	9658(2)	29(1)
C(405)	9167(3)	5737(3)	7773(2)	22(1)
C(404)	9160(3)	5680(4)	7304(2)	29(1)
C(62)	11973(3)	6303(4)	9254(2)	28(1)
C(301)	9203(3)	6103(3)	9751(2)	28(1)
C(201)	16022(3)	9081(3)	12146(2)	21(1)
C(71)	9040(3)	7899(3)	7947(2)	25(1)
C(72)	9335(4)	8547(3)	8660(2)	31(1)
C(204)	15771(3)	7686(3)	12536(2)	29(1)
C(42)	15639(3)	6464(3)	11051(2)	27(1)
C(52)	7450(4)	6043(4)	8799(2)	33(1)
C(304)	10686(4)	6027(4)	10132(2)	39(2)
C(103)	14333(3)	9185(3)	9467(2)	23(1)
C(203)	15893(3)	8365(4)	12811(2)	31(1)
C(202)	16021(3)	9066(3)	12611(2)	26(1)
C(45)	16964(3)	6332(4)	11250(2)	31(1)

C(403)	9057(3)	6356(4)	7032(2)	31(1)
C(23)	12521(4)	9877(4)	10721(2)	37(2)
C(302)	9489(4)	5916(3)	10221(2)	32(1)
C(13)	17085(4)	7478(4)	10108(2)	34(1)
C(35)	16666(4)	12530(3)	12032(2)	34(1)
C(402)	8991(3)	7083(4)	7231(2)	29(1)
C(15)	18333(3)	7645(4)	10658(2)	37(1)
C(303)	10245(4)	5879(4)	10414(2)	36(1)
C(43)	16132(4)	5363(3)	10708(2)	32(1)
C(73)	10506(3)	8845(4)	8512(2)	36(1)
C(75)	9975(4)	9785(4)	8967(2)	38(2)
C(33)	15802(4)	11754(4)	12340(2)	37(2)
C(74)	10464(4)	9316(4)	8070(2)	40(2)
C(25)	11905(4)	8865(4)	11090(2)	39(2)
C(24)	13106(4)	10316(4)	11099(3)	47(2)
C(46)	17261(3)	5957(4)	11727(2)	37(2)
C(65)	12453(4)	7461(4)	9736(2)	41(2)
C(26)	11204(4)	8597(5)	10740(3)	53(2)
C(53)	6287(4)	5313(5)	8574(2)	52(2)
C(14)	17240(5)	7749(4)	9658(2)	55(2)
C(76)	10368(5)	9664(4)	9488(2)	53(2)
C(66)	11940(5)	8144(4)	9528(3)	57(2)
C(34)	15061(4)	11681(5)	11972(3)	52(2)
C(63)	13062(5)	7000(4)	9151(3)	51(2)
C(36)	17250(4)	12852(4)	12453(3)	51(2)
C(85)	9397(4)	2251(4)	8209(3)	48(2)
C(83)	8477(5)	3113(5)	7651(4)	78(3)
C(86)	9806(6)	1759(4)	7942(3)	66(2)
C(64)	13805(5)	6779(5)	9472(4)	71(3)
C(44)	16060(6)	5562(5)	10202(3)	75(3)
C(16)	18811(4)	8268(5)	10537(4)	67(2)
C(84)	7908(6)	3326(8)	7898(6)	126(5)
C(54)	6180(7)	4795(7)	8123(3)	94(4)
Hg(1)	15836(1)	8475(1)	11123(1)	20(1)
Hg(2)	9105(1)	6532(1)	8711(1)	24(1)
Au(4)	11121(1)	4699(1)	8707(1)	25(1)
Au(1)	17528(1)	9844(1)	11529(1)	27(1)

Au(2)	13921(1)	6932(1)	10913(1)	30(1)
Au(3)	7849(1)	7787(1)	8652(1)	38(1)
S(2)	12932(1)	7569(1)	11025(1)	27(1)
S(3)	17349(1)	11104(1)	11749(1)	32(1)
S(6)	12013(1)	5637(1)	8818(1)	30(1)
O(10)	8530(3)	107(3)	7960(2)	50(1)
C(10)	7766(4)	224(5)	7737(3)	62(2)
C(30)	6079(7)	4612(5)	2189(3)	96(4)
O(30)	5600(5)	4816(3)	1737(2)	93(3)
O(20)	4815(5)	6555(5)	8734(3)	117(3)
C(20)	5458(6)	6703(8)	9084(4)	105(4)

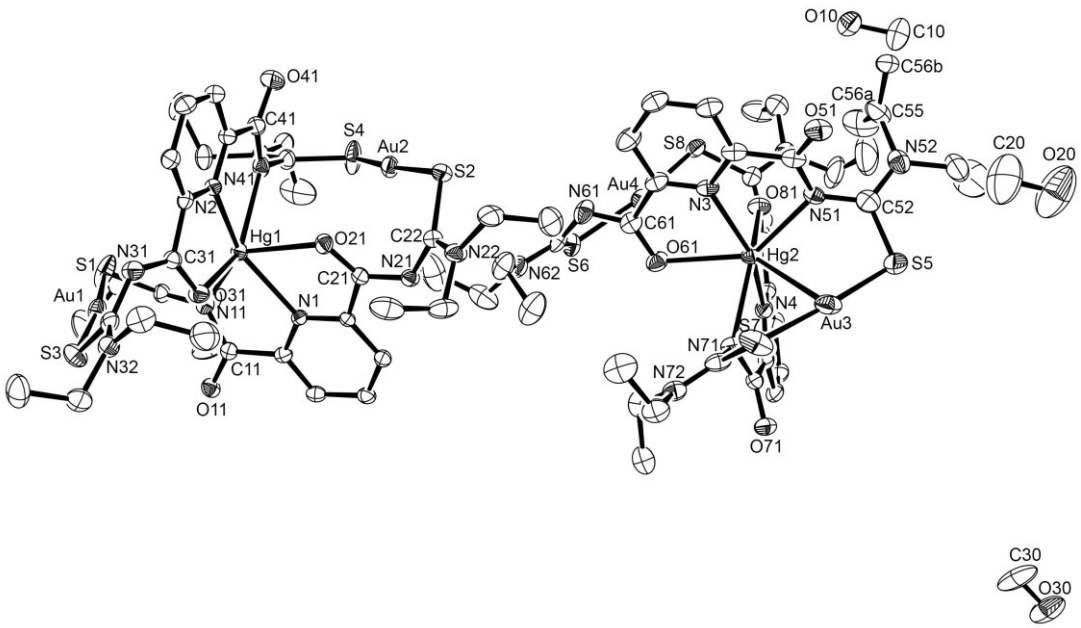

Figure A42: Ellipsoid plot of [Hg{Au(L4-κS)}$_2$] · 1.5MeOH. Thermal ellipsoids are at 50 % of probability. The hydrogen atoms have been omitted for clarity.

$[Ni\{Au(L4\text{-}\kappa S)\}_2] \cdot 0.5CH_2Cl_2 \cdot 1.5H_2O$

Table A85: Crystal data and structure refinement for $[Ni\{Au(L4\text{-}\kappa S)\}_2] \cdot 0.5CH_2Cl_2 \cdot 1.5H_2O$.

Empirical formula	$C_{34.5}H_{50}Au_2ClN_{10}Ni_1O_{5.5}S_4$	
Formula weight	1309.17	
Temperature	100(2) K	
Wavelength	0.71073 Å	
Crystal system	Monoclinic	
Space group	$P2_1/c$	
Unit cell dimensions	a = 15.0459(5) Å	α = 90°.
	b = 22.5916(8) Å	β = 100.230(2)°.
	c = 14.2312(5) Å	γ = 90°.
Volume	4760.4(3) $Å^3$	
Z	4	
Density (calculated)	1.827 g/cm^3	
Absorption coefficient	6.821 mm^{-1}	
F(000)	2552	
Crystal size	0.24 x 0.16 x 0.04 mm^3	
Theta range for data collection	2.268 to 26.404°.	
Index ranges	-18<=h<=18, -25<=k<=28, -17<=l<=17	
Reflections collected	41698	
Independent reflections	9754 [R(int) = 0.0660]	
Completeness to theta = 25.242°	99.9 %	
Absorption correction	Semi-empirical from equivalents	
Max. and min. transmission	0.7454 and 0.5168	
Refinement method	Full-matrix least-squares on F^2	
Data / restraints / parameters	9754 / 16 / 515	
Goodness-of-fit on F^2	1.036	
Final R indices [I>2sigma(I)]	R1 = 0.0447, wR2 = 0.0917	
R indices (all data)	R1 = 0.0692, wR2 = 0.1009	
Largest diff. peak and hole	2.486 and -2.176 e · $Å^{-3}$	
Diffractometer	Bruker D8 Venture	

Table A86: Atomic coordinates (x 10^4) and equivalent isotropic displacement parameters ($Å^2$ x 10^3) for $[Ni\{Au(L4\text{-}\kappa S)\}_2] \cdot 0.5CH_2Cl_2 \cdot 1.5H_2O$. U(eq) is defined as one third of the trace of the orthogonalized U^{ij} tensor.

	x	y	z	U(eq)
Au(1)	2452(1)	6169(1)	2382(1)	24(1)
Au(2)	1883(1)	3242(1)	5880(1)	24(1)
Ni(1)	2462(1)	4724(1)	4114(1)	15(1)
S(1)	1764(1)	5454(1)	1373(2)	32(1)
S(2)	2294(1)	3693(1)	7329(1)	26(1)
S(3)	2987(1)	6934(1)	3380(2)	33(1)
S(4)	1415(1)	2614(1)	4622(2)	36(1)
O(11)	3910(3)	4562(2)	1864(4)	26(1)
O(21)	2729(3)	4554(2)	5594(3)	19(1)
O(31)	2556(3)	5637(2)	4336(3)	19(1)
O(41)	1787(3)	3896(2)	3892(4)	21(1)
N(1)	3730(4)	4470(2)	4300(4)	15(1)
N(2)	1178(4)	4958(3)	3975(4)	16(1)
N(12)	1746(4)	4293(3)	1475(4)	23(1)
N(21)	3831(4)	4096(3)	6718(4)	20(1)
N(22)	3742(5)	4218(3)	8279(5)	31(2)
N(31)	1686(4)	6481(3)	4291(5)	24(1)
N(32)	2565(5)	7228(4)	5048(6)	49(2)
N(41)	342(4)	3499(3)	3671(5)	23(1)
N(42)	139(5)	2556(3)	3105(6)	45(2)
C(101)	4172(4)	4457(3)	3566(5)	17(2)
C(201)	978(5)	5526(3)	4049(5)	20(2)
C(102)	5072(5)	4290(3)	3693(6)	24(2)
C(202)	76(5)	5708(3)	3967(5)	24(2)
C(103)	5499(5)	4126(3)	4599(6)	26(2)
C(203)	-590(5)	5282(4)	3822(5)	25(2)
C(104)	5025(5)	4115(3)	5348(5)	20(2)
C(204)	-360(5)	4689(3)	3749(5)	22(2)
C(105)	4121(4)	4295(3)	5167(5)	14(1)
C(205)	547(4)	4541(3)	3833(5)	17(2)
C(11)	3603(5)	4602(3)	2611(5)	19(2)
C(12)	2115(5)	4782(4)	1868(5)	24(2)

C(13)	2052(5)	3699(3)	1810(6)	28(2)
C(14)	2624(7)	3409(5)	1158(8)	56(1)
C(15)	955(5)	4304(4)	700(6)	36(2)
C(16)	86(7)	4382(5)	1075(8)	56(1)
C(21)	3492(4)	4313(3)	5876(5)	17(2)
C(22)	3344(5)	4043(3)	7432(5)	22(2)
C(23)	3358(7)	4146(5)	9153(7)	54(3)
C(24)	2794(7)	4682(5)	9320(8)	56(1)
C(25)	4621(6)	4523(5)	8421(7)	47(3)
C(26)	5388(7)	4092(5)	8688(8)	56(1)
C(31)	1804(5)	5908(3)	4244(5)	22(2)
C(32)	2382(5)	6860(3)	4314(6)	30(2)
C(33)	3223(7)	7721(5)	5091(10)	78(4)
C(34)	2778(7)	8289(5)	4661(8)	56(1)
C(35)	2121(7)	7153(5)	5885(8)	63(4)
C(41)	940(4)	3930(3)	3809(5)	19(2)
C(42)	592(5)	2930(4)	3740(6)	32(2)
C(43)	317(7)	1883(5)	3131(8)	54(3)
C(44)	-202(7)	1638(5)	3783(8)	56(1)
C(45)	-599(6)	2753(4)	2332(7)	40(2)
C(46)	-315(7)	2727(5)	1369(8)	56(1)
C(36A)	2560(9)	6639(7)	6571(9)	51(4)
C(36B)	3036(18)	7000(20)	6570(20)	51(4)
C(1E)	4320(20)	2672(14)	3670(20)	93(2)
Cl(1E)	4773(8)	2916(5)	2683(10)	93(2)
Cl(2E)	3427(8)	3118(5)	3858(10)	93(2)
C(1F)	3660(20)	2610(30)	3339(18)	93(2)
Cl(1F)	4469(12)	2347(8)	2698(14)	93(2)
Cl(2F)	3874(13)	2667(8)	4573(14)	93(2)
O(20)	2477(14)	5633(11)	6710(40)	290(30)
N(11)	2751(4)	4743(3)	2697(4)	20(1)
O(30)	5229(5)	3819(6)	1298(6)	114(5)

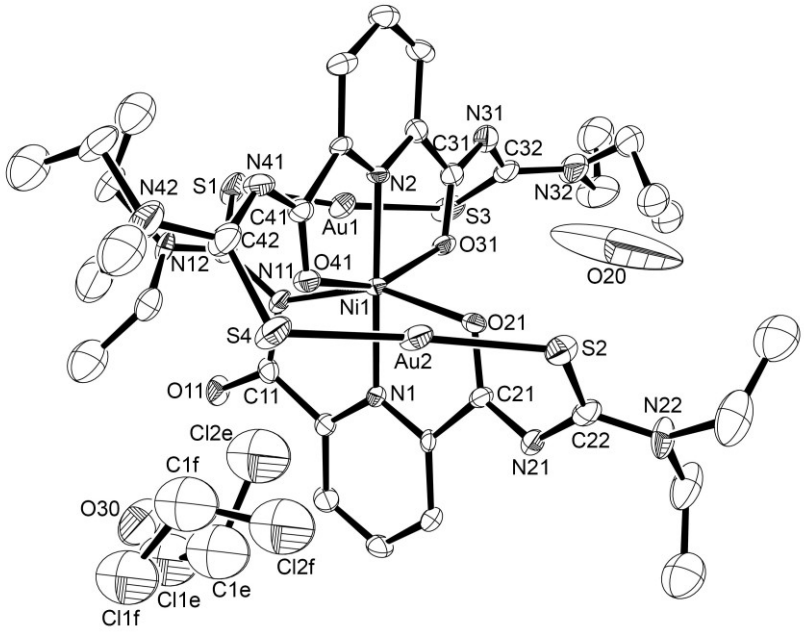

Figure A43: Ellipsoid plot of $[Ni\{Au(L4\text{-}\kappa S)\}_2] \cdot 0.5CH_2Cl_2 \cdot 1.5H_2O$. Thermal ellipsoids are at 50 % of probability. The hydrogen atoms have been omitted for clarity.